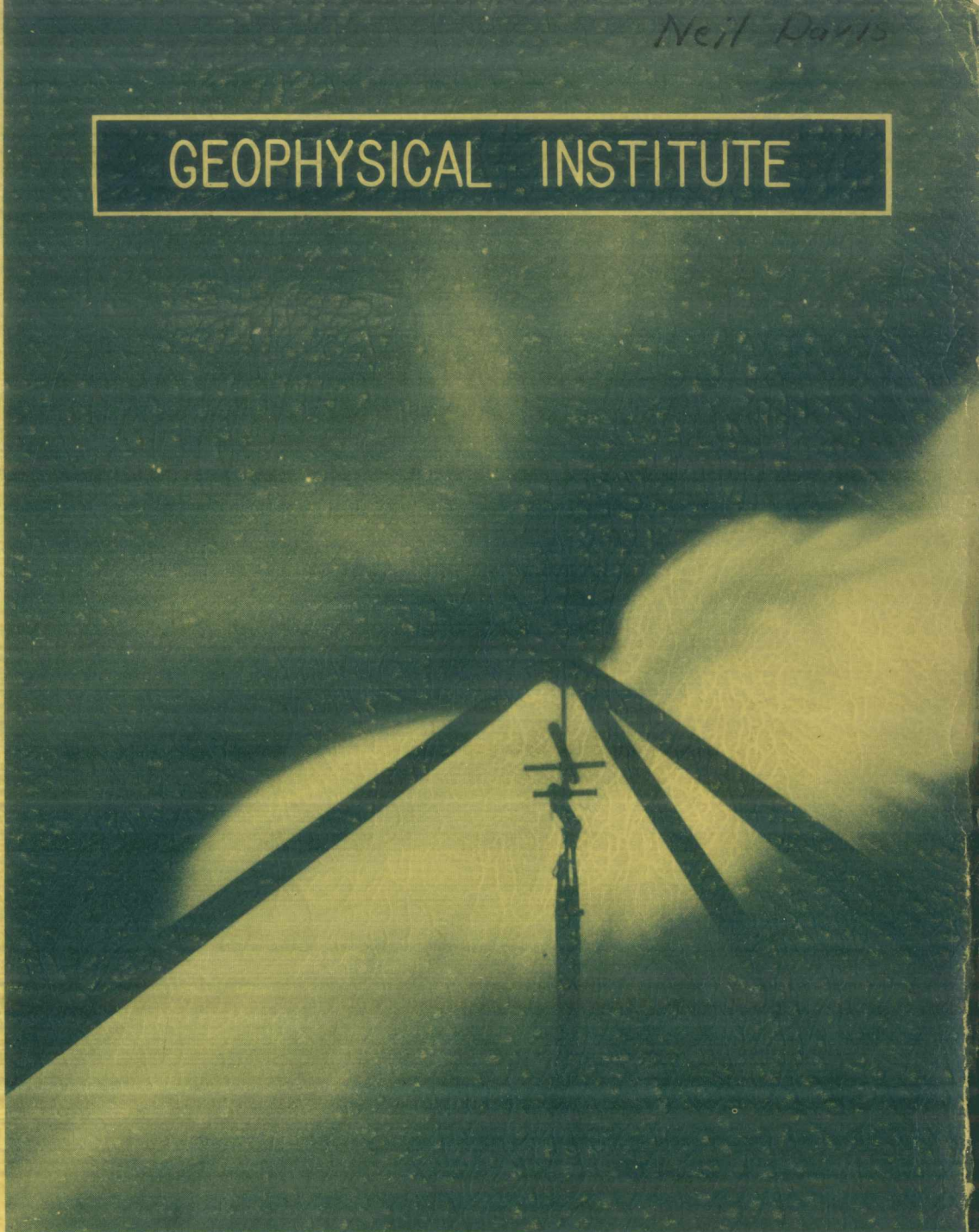R112

Neil Davis

GEOPHYSICAL INSTITUTE

UNIVERSITY
OF ALASKA

COLLEGE
ALASKA

UAG-R112

A STUDY OF MAGNETIC STORMS AND AURORAS

By

Syun-Ichi Akasofu
and
Sydney Chapman

GEOPHYSICAL INSTITUTE

of the

UNIVERSITY OF ALASKA

Scientific Report No. 7

A STUDY OF MAGNETIC STORMS AND AURORAS

by

Syun-Ichi Akasofu

Geophysical Institute, University of Alaska

and

Sydney Chapman

Geophysical Institute, University of Alaska
High Altitude Observatory, University of Colorado
Institute of Science and Technology, University of Michigan

Submission Date: Principal Investigator:

                                          C. T. Elvey
March, 1961   Director

GEOPHYSICAL INSTITUTE

of the

UNIVERSITY OF ALASKA

Scientific Report No. 7

A STUDY OF MAGNETIC STORMS AND AURORAS

by

Syun-Ichi Akasofu

Geophysical Institute, University of Alaska
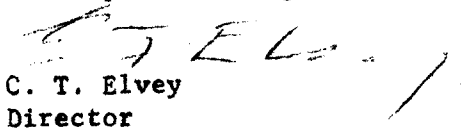
and

Sydney Chapman

Geophysical Institute, University of Alaska
High Altitude Observatory, University of Colorado
Institute of Science and Technology, University of Michigan

Submission Date: Principal Investigator:
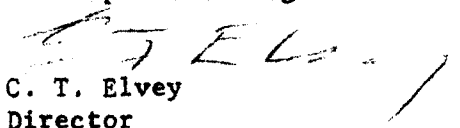
                                          C. T. Elvey
March, 1961   Director

TABLE OF CONTENTS

SUMMARY

New notations for magnetic disturbance fields are proposed, based on
the theoretical consideration of the electric current systems by which
they are produced.

A typical magnetic storm begins suddenly when the onrush of the front
of the solar gas is halted by the earth's magnetic field. This effect
(DCF field) is most markedly observed as a sudden increase of the hor-
izontal component of the earth's field (the storm sudden commencement,
abbreviated to ssc)--like a step function. In many cases, however, the
change of the field during the ssc is more complicated, and different at
different places. Such a complexity superposed on the simple increase
(DCF) is ascribed to a complicated current system generated in the polar
ionosphere (DP current). It is found that the changes of electromagnetic
conditions in the polar regions are communicated, without delay, to lower
latitudes, even down to the equatorial regions. It is inferred that the
equatorial jet is affected by such a change and produces the abnormal
enhancement of ssc along the magnetic dip equator.

From the extensive analysis of several magnetic storms that occurred
during the IGY and IGC, it is suggested that the capture of the solar
particles in the outer geomagnetic field occurs when irregularities
(containing tangled magnetic fields and high energy protons) embedded in
the solar stream, impinge on the earth. Thus the development of a magnet-
ic storm depends on the distribution of such irregularities in the stream.
The motions and resulting currents and magnetic fields of such "trapped"
solar particles are studied in detail for a special model. It is inferred
that a large decrease (DR field) must follow the initial increase; it is

ascribed to the ring current produced by such motion of solar protons of energy of order 500 Kev. It is proposed that during the storm there appears a transient 'storm-time' belt well outside the outer radiation belt.

It is predicted that the earth's magnetic field is reversed in limited regions when the ring current is appreciably enhanced. This involves the formation of neutral lines there. These may be of two kinds, called X lines or 0 lines according as they are crossed or encircled by magnetic lines of force. These may be entirely separated or may be joined to form a loop, called an OX loop. It is shown that one of them, the X line, which is connected with the auroral ionosphere by the lines of force, could be the proximate source of the particles that produce the aurora polaris. By postulating the existence of such X-type neutral lines at about 6 earth radii, an explanation is obtained of the detailed morphology of the aurora. This includes the auroral zones and their changes, the nighttime peak occurrence of auroras, their thin ribbon-like structure and their multiplicity, their diffuse and active forms and the transition between them (break-up) the required electron and proton flux, and the ray and wavy structures.

Among the most important phenomena associated with the sudden change of the aurora from the diffuse to the active form are the simultaneous appearance of the auroral electrojet and the resulting polar magnetic disturbances (DP sub-storms). Several typical DP sub-storms are studied in detail. It is concluded that a westward auroral jet is produced by a southward electric field. It is shown that an instability of the sheet-beam issuing from along the X-type neutral line can produce a southward

electric field of the required intensity. The southward electric field produces an eastward motion of the electrons in the ionosphere. This may be identified with the eastward motion of an active aurora and with the westward auroral electrojet.

Besides such large changes of the field, there often appear various quasi-sinusoidal changes of the field, much less intense. They are supposed to be hydromagnetic waves, some of which are generated in the outer atmosphere and propagated through the ionosphere, where a certain amount of their energy is dissipated. It is concluded however that such a dissipation is not sufficient to produce any appreciable heating of the ionosphere.

CHAPTER I

THE ELECTROMAGNETIC ENVIRONMENT OF THE EARTH

1.1 THE SOLAR SYSTEM IN THE GALAXY

The possible existence of a magnetic field and its importance in space far distant from the earth has been inferred from several kinds of evidence. The polarization of star light provides a useful tool for the exploration of the magnetic field in the spiral arms of the Galaxy (Hiltner 1956, Shain 1956). The luminosity in some nebulae such as the Crab Nebula and M87 shows also a marked polarization, from which the configuration of the magnetic field in these nebulae has been determined (Hiltner 1957, 1959). Such nebulae strongly emit synchrotron radio waves produced by high energy electrons, from which the existence of a magnetic field is also inferred (Oort and Walraven 1956).

The existence of such large scale magnetic fields in the spiral arms of the Galaxy has also been conjectured from the study of cosmic ray particles, their origin and propagation through the interstellar space (Fermi and Chandrasekhar 1953, Fermi 1954, Morrison 1957, Parker 1958). It is believed that the field lines are nearly parallel to the spiral arms. The extensive radio study of the 21 cm emission from neutral hydrogen in space shows that the sun and its planets are embedded in one such spiral arm of the Galaxy (Oort et al. 1958). It is not known whether the interplanetary space is permeated by the galactic magnetic field or whether the space excludes such field from it. It is true however that primary cosmic ray particles produced somewhere in the Galaxy travel through the interplanetary space and some of them are caught by the earth's magnetic field.

1.2 THE SUN AND THE INTERPLANETARY SPACE

The solar general (dipole-like) magnetic field of order a few gauss has recently been extensively studied by Babcock and Babcock (1955). The existence of such a field in the solar corona has also been inferred from the eclipse observations of the coronal streamers (cf. Van de Hulst 1950). Babcock (1959) reported that the direction of the axis of the field has recently been reversed. Sunspot groups in a certain stage consist of a pair of spots of opposite polarity. The field intensity is much larger than that of the general field. A typical solar flare that produces magnetic storms and auroras occurs most often in a spot-group with complicated polarity. Besides such 'bi-polar' or multi-polar regions, there are regions in which the magnetic polarity has only one sign--'uni-polar' regions. It has been inferred that it is these regions that produce persistent solar streams. Such streams are believed to produce the 27-day recurrence storms.

The magnetic field in interplanetary space has been discussed mainly by cosmic ray physicists seeking to explain the propagation of solar cosmic ray particles through interplanetary space. They also try to explain the Forbush decrease during magnetic storms by changes of electromagnetic conditions in the space. (cf. Davis 1955, Parker 1956, Mayer, Parker and Simpson 1956, Elliot 1960). One of the space probes Pioneer V, launched on 11 March 1960, seemed to detect a constant magnetic field of order 2.7 to 3.2 gammas in a part of the inner solar system (Coleman et al. 1960). How this field is connected with the galactic field in the spiral arm or with the solar general magnetic field is not yet definitely known.

The interplanetary space is filled by   rarified ionized hydrogen

gas and cosmic dust. The gas is somewhat concentrated towards the

ecliptic plane. The electrons and dust scatter the solar radiation and

produce a diffuse polarized luminosity around the sun along the ecliptic

plane--the zodiacal light. The electron density has been obtained from

the polarization of the zodiacal light. It is now believed that the

electron density obtained by Siedentopf et al. (1953) was too large and

that it is of order 100 electrons/cc or less, near the earth's orbit.

The observations seem to suggest a rather continuous change of the

electron density from the solar corona to the interplanetary space.

However the physical state of this gas system is still a highly con-

troversial matter (Chapman 1957a,b; 1961a,b; Parker 1958, 1960;

Chamberlain 1960; Shklovski 1958).

1.3 THE OUTER ATMOSPHERE, THE VAN ALLEN BELTS AND THE IONOSPHERE

Near the earth the interplanetary gas merges with the outer part of

the earth's atmosphere. There may be no clear boundary between them.

Ionized hydrogen is also probably the most important constituent in the

outer atmosphere. Several attempts have been made to determine the

electron density in this region (Storey 1953, Allcock 1959, Johnson 1959,

Pope 1959). The concentration of neutral hydrogen increases towards the

earth. The importance of this constituent there was early pointed out

by Chapman (1958b). Such neutral hydrogen scatters solar L_α radia-

tion. Kupperian et al. (1959) detected this radiation in the night sky

by rockets.

6

During the last few years the radiation belts that contain high energy particles have been explored by USA and USSR satellites. There are two such belts with maxima located at about 1.5 and 3.5 earth radii respectively. It has been shown that the outer belt undergoes considerable changes and that it is controlled by the solar activity.

The lower part of the ionized atmosphere is called the ionosphere. The ionosphere consists of three main layers, E, F1 and F2. They are produced by ultraviolet radiation and X-radiation. It is now believed that the F2 layer is a 'tail' of the F1 layer. The electrodynamic process in the ionosphere is complicated because of the existence of far larger numbers of neutral gas particles than ionized ones. One of the peculiar phenomena connected with this complexity is the large electric conductivity in the E region (Hirono 1952, Baker and Martyn 1953, Fejer 1953). Dynamo action in this region produces the solar quiet day daily variation Sq and the lunar daily variation L.

Solar particles emitted from regions where an intense solar flare is taking place, and from uni-polar regions, considerably disturb the earth's magnetic field in the outer atmosphere, the Van Allen belts and the ionosphere. Such interaction has been observed on the earth's surface as magnetic storms, aurora polaris, ionospheric storms and other associated geophysical phenomena. This paper is mainly concerned with such interactions between the solar gas and the earth's outer atmosphere and magnetic field.

1.4 THE EARTH'S PERMANENT MAGNETIC FIELD

Hydromagnetic studies of the motions in the earth's core promise to explain the production of the earth's magnetic field. Elsasser (1946) was the first to formulate this problem. Later it has been discussed by Bullard (1949), Parker (1955), Bullard and Gellman (1954) and others. They have suggested that complicated couplings between the motion of the liquid in the core and a dipole field could maintain the original dipole magnetic field. Some irregular changing motions in the core are believed to produce the secular magnetic variations.

1.5 INTRODUCTION TO GEOMAGNETIC STORMS AND AURORAS

Solar streamers and clouds of neutral ionized gas impinge on the earth from time to time. The geomagnetic field resists their advance and carves a hollow in them. The "vertex" of the hollow is on the sunward side of the earth. On the dark side the hollow may be open, or if it has an end, this will be far away. Near the surface of the hollow the positive and negative charges are differently deflected, backwards or sideways (Chapman and Ferraro 1931). Their combined motions correspond to electric current flow on the surface of the hollow, mostly on the sunward side. The current flow is substantially confined to a thin layer near the surface.

These are the opening events in magnetic storms. The onrush of the front of the solar stream may be very rapidly halted--within a minute or so. During this time electric currents are set up near the surface of the hollow. Their magnetic field is observed as a sudden increase of the horizontal component of the earth's field. Great magnetic storms typically begin with such a sudden commencement.

However, in ways not yet understood, some of the solar gas is captured and becomes "trapped" in the geomagnetic field. The trapped particles oscillate rapidly to and fro between "mirror" points in fairly high northern and southern latitudes. At the same time they drift round the earth, and produce what is called the (geomagnetic) ring current. Its growth is manifested by a decrease of the horizontal component of the earth's field.

The ring current at times may considerably distort the earth's normal dipole field at about 6 earth radii from the earth's center, where the solar particles may mostly be captured. When the ring current is considerably enhanced it may reverse the direction of the earth's field in certain limited regions, and produce neutral lines, namely, lines along which the field intensity is zero. These lines are of two different kinds, which are called respectively X-type and O-type. The X-type lines are so called because the lines of magnetic force cross on such lines, whereas the O-type lines are encircled by the lines of force. The neutral lines must lie in or close to the equatorial plane. We think that a narrow strip close to an X-type neutral line is the region from which come the particles that enter the atmosphere and produce auroras. When there is no electric field along the neutral line, high energy particles in the outer radiation belt travel from the strip into the auroral ionosphere and produce a diffuse arc. Local capture of solar gas in the belt may produce an eastward electric field as it spreads around the earth. The eastward electric field accelerates electrons, both those of high energy, members of the outer belt, and also the low energy ambient electrons present there. The result may be a large increase in the

number and flux of high energy particles into the atmosphere, and an active aurora. The acceleration involves an eastward current along the X-type neutral line. Such a line current may not be stable and may cause the neutral line to become wavy; this will produce the folded or wavy structure of active auroral curtains.

An instability in the intense sheet-beam issuing from near the X-type neutral line produces a charge separation and an equatorward electric field. When such a polarization beam penetrates the auroral ionosphere, it drives a strong westward electric current-- called an auroral electrojet. In the auroral zone the jet thus created produces a large negative disturbance of the horizontal component-- a prominent feature of many polar magnetic disturbances.

1.6 THE ANALYSIS OF THE EARTH'S FIELD

1.61 Subdivision of the field

It is convenient to adopt symbols for magnetic fields as wholes (cf. Chapman and Bartels 1940, pp. 6-8). Thus let F denote the earth's field at time t. It is specified by the intensity F at each point at that time. The mean field $\bar{F}$ over an interval of one or more complete years centered at the time t is denoted by M. It is called the main field, at that time. Its intensity at any point is the (vector) mean of F at that point over the said time interval.

Electric currents in the ionosphere, and associated induced earth currents, generate fields denoted by Sq and L, which manifest themselves as quiet-day solar and lunar daily magnetic variations. At a time t of complete magnetic calm, the field F is made up wholly by these three

10

fields, M, Sq and L. Symbolically, at such a time,

$$F = M + Sq + L \qquad\qquad (1)$$

In general, however, the field F has a part generated by external currents (and their associated induced earth currents) additional to the currents that produce the Sq and L fields. This additional part of F is denoted by D, and called the disturbance field. Thus, in general,

$$F = M + Sq + L + D \qquad\qquad (2)$$

or alternatively

$$D = F - M - Sq - L \qquad\qquad (3)$$

These definitions are ideal in the sense that we are not able with certainty to determine the exact values of the fields M, Sq and L at every place and time. At places where the earth's field is continuously recorded, we know F at all times. From the study of the variations of F on days that from a magnetic standpoint are very quiet, we learn the nature of the Sq and L fields and their seasonal and sunspot-cycle variations. But these fields also manifest day-to-day variations that are at present unpredictable. Subject to some uncertainty on this account, we can estimate the value of the fields Sq and L at any time, whether at that time the field F is quiet or disturbed. If disturbed, then the D field at that point and time is given by (3), subject to the stated uncertainty as to Sq and L.

11

1.62 Geometrical subdivisions

Chapman (1952) has made a geometrical analysis of the D field on idealized lines, associated with the conception that the D field is intimately related to the dipole component of the field M. This component is determined by spherical harmonic analysis of the field M, and it has an axis that is called the geomagnetic axis. Latitudes and longitudes defined relative to this axis (and a chosen meridian plane through it) are called geomagnetic (gm) latitude and longitude. Where latitudes and longitudes are referred to in this section, it is to be understood that they are geomagnetic and not geographic.

Let X, Y, Z denote the components of the D field at any point and time, along the directions of gm N, E and the downward vertical. Let $X(\phi)$, $Y(\phi)$, $Z(\phi)$ denote the mean values of X, Y, Z round the circle of latitude ϕ at the time t. The field whose components at all points along the circle of latitude ϕ have the values $X(\phi)$, $Y(\phi)$, $Z(\phi)$ is denoted by $\overset{o}{D}$. By definition it is symmetrical about the gm axis. It is a function of gm latitude and time. The field obtained by subtracting this field $\overset{o}{D}$ from D is denoted by DS. It is called the asymmetric part of the D field. Thus

$$DS = D - \overset{o}{D} \tag{4}$$

The field DS is a function of time t and position. For points at the earth's surface it is convenient to regard the position as specified by the latitude ϕ and the longitude relative to the (gm) meridian opposite to that through the sun. This longitude is the gm local time, reckoned from gm midnight. By definition, the mean value of each element of the field DS (to N, E or vertical), round each parallel of latitude, is zero.

12

If a magnetic storm suddenly begins from an instant of magnetic calm, time reckoned from this instant is called the storm-time. The subsequent time variation of the field $\overset{o}{D}$ at any point P is called the storm-time variation of the field D, and is denoted by Dst. It is of course manifested in each element. The whole variation of an element at P is the sum of the Dst variation and of the variation of that element of the DS field at P; this value depends on the changing local-time longitude of P along its circle of latitude, and on the changes of the DS field.

The Dst and DS fields have so far been studied mainly at low and middle latitudes, and by averaging over numerous magnetic storms. It is thus found that in those regions the main element of the Dst field is the N component. It undergoes a characteristic storm-time variation: there is first an increase, followed later by a larger and more prolonged decrease. The vertical force has much smaller inverse changes, that is, first a decrease, then an increase. After this second, main, phase of the Dst variation has reached its peak, there is a gradual recovery towards the normal quiet-day (zero) value of the Dst field. The DS field also waxes and wanes from and to its zero quiet-time value. On the average it has a fairly simple form, its variation round any parallel of latitude being approximately a simple sine function in each element. But the orientation round the parallels changes with the passage of storm-time. In high latitudes the DS field is the main part of the D field, in low latitudes the intensity of the Dst field is comparable with that of the DS field, and sometimes it is the greater of the two.

The D field during an individual magnetic storm, if registered at an adequate number of observatories well distributed over the earth, can be

13

divided into its Dst and DS parts. This is a purely geometrical divi-
sion which has proved useful in the study of magnetic fields in general.

1.63 Physical subdivisions

Akasofu and Chapman (1961) have defined another kind of division of

the D field, based on physical considerations. These are associated

with theoretical ideas as to the electric current systems by which the

D field is produced. Three main parts are distinguished. They are

denoted by DCF, DR and DP. The letters have the following significance:

D for disturbance; CF for corpuscular flux; R for ring current; P for

polar. The definitions are as follows:

The DCF field is produced by electric currents flowing near the

surface of the hollow carved by the geomagnetic field in the solar stream

or cloud that generates the magnetic storm. The current flows as long

as the corpuscular flux continues. It is caused by relative motion of the

electrons and protons near the hollow surface, as they are turned back-

wards or sideways by the magnetic field. The main effect of the DCF

field at the earth's surface is to increase H in low and middle lat-

itudes--more on the dayside than on the nightside of the earth.

The DR field is produced by enhanced westward electric current round

the earth during the storm; this current is associated with the motions

of energetic particles in the outer geomagnetic field. The main effect

of the DR field at the earth's surface during storms is to reduce H in

low and middle latitudes. We think that a new 'storm-time belt' appears

at about 6 earth radii during the storm, well beyond the radius (about

3.5a) at which the normal outer Van Allen belt has its maximum intensity.

14

The DCF and DR currents flow at distances of a few earth radii, far above the main terrestrial ionosphere.

The DP field is produced by currents flowing in the ionosphere. They are driven by electromotive forces in the auroral zones. Thence they spread over the main region of the earth between the zones, and over the enclosed polar caps. This DP field has a different time scale from that of the magnetic storm; it may wax and wane more than once during a storm. Each such event, which Birkeland (1908) called a polar elementary storm, is here called a DP sub-storm.

There may be a fourth addition to the pre-existing fields during the storm. The solar gas may carry with it a magnetic field transported away from the sun. This field may be denoted by DSM (Disturbing Solar Magnetism). As yet very little is known about such fields, although one of the space probes seemed to detect such a field (Coleman et al. 1960).

Thus, in all, the disturbing field D during a magnetic storm may be divided into the following four main parts.

$$D = DCF + DP + DR + DSM.$$

Both the Dst and DS fields include a part of the DCF, DP and also DR fields. The magnitude of the DCF field may not be the same on the day side and the night side, so that DCF contributes a small part of DS. A part of Dst is contributed by the DP field, because westward auroral electrojets and their associated currents in middle and low latitudes are usually larger than the eastward ones. The asymmetry of the ring current relative to the axis, if any, may contribute to the DS field. But as a first approximation we may write

(a) low and middle latitudes (gm. lat. from 0° to $\pm$ 60°):

$$DCF \quad + \quad DR \approx Dst$$

$$DP \sim DS$$

(b) high latitudes (gm. lat. above $\pm$ 60°):

$$DP \approx D$$

CHAPTER II

THE SUDDEN COMMENCEMENT OF MAGNETIC STORMS[*]

2.1 INTRODUCTION

The sudden onset of many geomagnetic storms is one of the many striking phenomena of the earth's magnetism. On some magnetograms it resembles what is known to mathematicians as a step function, though of course the change is not instantaneous. But this is not the only kind of sudden commencement. Sometimes the initial changes are of the opposite sign. Some of them show a small initial change in one direction followed by a larger opposite change.

A storm that began with a rather simple ssc occurred during the IGY, on September 29, 1957. Fig. 2.1 shows the H variations during the first three hours of this storm at 24 observatories in low latitudes. The time base is the same for all the records, but they are shown with different force scales. They are divided into five groups, for sets of observatories in different longitude sectors. All these records show an initial increase of H, but the amount differs from station to station. At many the amount is 20 to 30 γ. But at Koror it is much greater, about 80 γ.

Fig. 2.2 shows corresponding records for the declination D as well as for H, for 37 stations in higher latitudes, including (lower right) three in the Antarctic. For many stations in middle latitudes these records likewise show a simple ssc increase of H. But in higher latitudes the ssc is more complex. Sometimes there is an initial decrease,

---

[*] Part of this chapter covers the same ground as the paper: Akasofu and Chapman (1961c).

17

rapidly succeeded by a net increase.

Figs. 2.3a and b show more clearly the H and D variations during the first three hours of this storm at Fredericksburg (gm. lat. $49°.6$) and Big Delta (gm. lat. $64°.4$).

A new notation[**] is proposed for the various types of sudden commencement, to replace the current notations (ssc, ssc[*], reversed ssc, reversed ssc[*]). Sudden commencements in general we would denote by Sc; four different types we would denote by Sc(+), Sc(-+), Sc(-), Sc(+-), indicating the sign of the change (s) in H, and also their order, when there are changes of more than one sign. We may also notice yet another type of Sc, denoted by Sc(++), which shows two distinguishable successive increases of H. An Sc for a particular magnetic storm may appear in one form, e.g., Sc(+), in some regions, and elsewhere in other forms, e.g., Sc(-+) or Sc(+-).

It is an essential part of the definition of an Sc that it is followed by increased magnetic activity with storm characteristics, for a sufficiently long period of storminess (IAGA 1957).

Other sudden magnetic changes occur, which in some respects resemble Sc's, but are not followed by magnetic storms, or at least by easily recognizable storms. However, Yamaguchi (1958) showed clearly that, on the average, these are followed by a storm time variation Dst, though its

---

[**] This proposal is intended to relate only to discussions of the phenomena, and is not intended to suggest any change in the usages of observatories in their reports to the permanent service.

range is much less than that in the usual storm. Such changes are called

sudden impulses, and denoted by Si (Ferraro, Parkinson and Unthank 1951).

The notation for Sc cannot be immediately extended to such Si changes.

In low latitudes the usual type of Sc is Sc(+). For example,

Chakrabarty (1951), who examined about 800 sudden changes at Alibag

($9\overset{o}{.}5$ N gm. lat.), found none of type Sc(-+), and not more than 28 of

Sc(-). He appears not to have distinguished between Sc and Si, so that

his results apply to (Sc + Si).

The dual type of Sc becomes more frequent in higher latitudes.

Matsushita (1957) examined 44 Sc's at six observatories in geomagnetic

latitudes ranging from 21°N to 68°N gm. lat.; the distribution of their

types in the higher latitudes was as follows:

Type of Sc	Sc(+)	Sc(-+)	Sc(+-)
Number	9	21	14

Watson and McIntosh (1950) found that among 340 Sc's observed at Lerwick

($62\overset{o}{.}5$ N gm. lat.) only 65 were Sc(+) and 162 were Sc(-+).

2.2 STUDIES OF Sc AND Si AT INDIVIDUAL OBSERVATORIES

As with other types of transient geomagnetic variation, the sudden

changes--Sc and Si--should be studied in various ways at individual

observatories with records over a sufficiently long period. Several

workers, following Moos (1910) for Bombay ($9\overset{o}{.}5$ N gm. lat.), have examined

the daily variation of frequency of sudden magnetic changes. The earlier

studies did not distinguish between Sc and Si. A forenoon minimum and

afternoon maximum of frequency were found by Rodes (1932) from 218 cases

(1905-31) at Ebro ($43\overset{o}{.}8$ N gm. lat.), by McNish (1933) from 151 cases

(1919-30) at Watheroo (41°7 S gm. lat.), and by Newton (1948) from 681

cases (1874-1944) at Greenwich (54°2 N gm. lat.); see also Fig. 3

(broken curve). Ferraro, Parkinson and Unthank (1951) first analyzed the

Sc and Si data separately, from the following six observatories, for the

period 1926-46, common to all six.

	gm. lat.			gm. lat.
Cheltenham	50° N		Honolulu	21° N
Tucson	40° N		Huancayo	1° S
San Juan	30° N		Watheroo	42° S

No sudden change was included unless it was shown by at least one station

in two elements. Their data included 141 Sc's and 381 Si's. As

Chakrabarty found at Alibag, Sc(-) did not appear in the San Juan records,

and only 13 cases in all were found (8 at Watheroo, 2 at Honolulu, 1

each at the other three stations). They found a slight tendency for Sc's

to be most frequent at about 13^h local time, and least frequent at about

5^h; but the daily variation of frequency was small; relative to the mean

frequency taken as unity, the daily variation was expressed thus:

$$1 - 0.007 \cos (\theta - 63°) + 0.002 \cos 2 (\theta - 7°),$$

where $\theta = 15(t + 1/2)$.

The Si's, on the other hand, showed a more marked daily variation,

expressed thus, in the mean for the six stations:

$$1 + 0.008 \cos (\theta + 43°1) + 0.17 \cos 2 (\theta - 34°).$$

The probable errors for the two amplitudes are 0.04, so that, at most,

only the semidiurnal variation can be considered reliable. As Si's are

more numerous than Sc's, this variation will appear in combined statistics

for Sc and Si taken together. Nevertheless this variation is only small, relative to the mean. The difference between the daily variations of Sc and Si may indicate another real distinction between these two kinds of sudden change. But the reliability of statistical conclusions on the daily (and seasonal) variation of frequencies of Si's is rendered doubtful because Si's can be clearly recognized only during quiet periods. Hence it is necessary to consider how the daily (and seasonal) variation of active periods might influence the conclusions regarding Si's.

Ferraro, Parkinson and Unthank also examined the daily frequency variation for Sc(-+) and Si(-+) at five of their stations (Honolulu being excluded because it had too few cases). They found that for the higher geomagnetic latitudes (30° to 50°), both Sc(-+) and Si(-+) are most frequent from noon to 19^h; this was confirmed by Nagata (1952).

Ferraro and Parkinson (1950) found also that the ratio of the number of Sc(-+) to the total number of Sc is about the same as the corresponding ratio for Si. A more remarkable result was that these ratios both showed a marked dependence on geomagnetic longitude. This conclusion, as Jackson (1950) suggested, is not yet certainly established. The question calls for further examination at other observatories.

The yearly frequency variation of Sc and Si has been examined for Greenwich by Newton (1948) for both types together, and for the separate types at Honolulu by Ferraro et al. (1951). The Honolulu Sc's show marked equinoctial maxima of frequency (like those for magnetic storms in general). The Si's show no marked yearly variation either of frequency or average amplitude, and this agrees with the (Sc + Si) results (doubtless mainly Si) for Greenwich. But many Si's may go unrecognized, more

particularly during disturbed equinoctial periods.

The combined (Sc + Si) frequency for each of the six stations considered by Ferraro et al. (1951) shows a clear variation with the sunspot cycle.

There is need for further studies of this kind for other observatories with long series of records--and also studies of the inter-relation of Sc's and Si's with other phenomena, ionospheric, auroral, etc., such as those by Matsushita (1957) and by Thomas and Robbins (1958), who considered the ionospheric disturbances associated with Si.

In addition to studies of the frequency of the sudden changes, important results have been obtained as regards their amplitude. At Huancayo, almost on the magnetic equator, the Sc amplitude shows a marked daily variation (Sugiura (1953)), which is reminiscent of the abnormal enhancement of Sq (H) at this station; see Ferraro, Parkinson and Unthank (1951), Sugiura (1953), Forbush and Vestine (1955). The last paper also showed that the initial storm phase (and not only the Sc) is enhanced at Huancayo. Ferraro (1954) found that the other five stations (see above) considered by him and his colleagues in 1951 did not show the Sc daytime enhancement; in fact there seemed to be a weak daily minimum of amplitude at about 8^h local time. Jackson (1952, p. 163) concluded that the structure of the Sc at this hour is radically different from Sc(+), and is not merely Sc(+-); also that the form is not what one might expect from a simple process of ionospheric screening, which would have the effect of slowing down the rate of change; and that the initial quick stroke, as well as the oscillations found to be associated with these "8^h" Sc's, may be a secondary effect which has its origin in currents which are set up in the ionosphere at the time.

2.3 MORPHOLOGICAL STUDIES

For a proper understanding of the sudden changes Sc and Si, another--morphological--type of study is even more necessary than the studies at individual observatories. A morphological study is one concerned with the determination and representation of the magnetic field vector over the earth's surface as a function of both time and position. This involves all three magnetic elements. The effectiveness of morphological studies depends on the number and world distribution of the observatories that record the kind of phenomenon under consideration. The more locally differentiated is its distribution, the closer must be the network of observatories.

The general morphology of magnetic storms has been studied by Moos (1910), Chapman (1919, 1935, 1956a), Vestine et al. (1947), Sugiura and Chapman (1959) and others. The average variations are generally determined in two parts, denoted by Dst and DS[*]. The additional D field, present during a storm, is a function of storm time--reckoned from the storm commencement--and of position. In each element, at each instant of storm time, Dst denotes the mean value of the storm field round a parallel of geomagnetic latitudes; thus Dst is a function of t and of geomagnetic latitude. It represents the part of the field that is symmetrical around the geomagnetic axis. The difference between the whole field D, and its part Dst, is denoted by DS; it is a function of t, of geomagnetic latitude, and of geomagnetic local time (or geomagnetic longitude relative to the geomagnetic midnight meridian at that instant

---

[*] From our physical analysis of magnetic storms, we may regard DS as the statistical result of DP sub-storms (see §1.5)

of storm time). The parts Dst and DS have been determined for the
average of many magnetic storms of similar intensity, for groups of
storms of different intensity, at different seasons. The material used
was the hourly values of the magnetic elements published by the magnetic
observatories.

Such values cannot suffice for the study of the morphology of sudden
brief changes such as Sc and Si; it is necessary to refer directly to the
magnetograms. Nevertheless, on this shorter time scale, it is convenient
to divide up the Sc or Si field into the two parts Dst and DS. In order
to be sure that these two parts are accurately determined, for the same
instants in different parts of the earth, it is clear that the timing of
the records at each observatory used must be accurate to a small fraction
of the duration of these sudden changes.

2.4 SIMULTANEITY AND TIME ACCURACY

If everywhere over the earth an Sc or Si were simple, namely a
sudden increase in H (and decrease in V), the first important question
that would arise is "how nearly simultaneous is it over the earth?". In
other cases, when the sudden change is not simple, morphological study
requires a knowledge of the vector distribution of its field over the
earth at a succession of instants, accurately timed. The accuracy of
time estimation depends partly on the time scale of the record and its
absolute synchronization, and partly on the actual rate of the magnetic
change. Early studies of Adams (1892) and Ellis (1892) showed that Sc's
may be simultaneous over the earth to within a few minutes. Bauer (1910)
studied this question of simultaneity, and inferred that the Sc has a

24

time of propagation round the earth of order 3 or 4 minutes. His results were critically discussed by Chree (1910), Angenheister (1913) and Chapman (1918). They concluded that the observations did not provide a safe basis for the determination of propagation speeds-- instead they indicated the relative inaccuracy of the records. Chapman suggested that the time differences of the Sc between different stations might depend on simple geometrical considerations involving the aspect of the earth as viewed from the sun. He envisaged the envelopment of the earth in a stream issuing radially from the rotating sun. This suggested a possible minimum range of the times of Sc at different places, of order 30 seconds, the time being earliest near the sunset meridian and latest near the dawn meridian. The data were not accurate enough to confirm or overthrow this simple conception.

Gerard (1959) has recently made a more accurate study of the times of Sc(+) and Sc(-+). He found that the time differences, in either case, range only up to a few seconds, and concluded that the sun controls the hemisphere in which the Sc first appears. However, his time differences seem to be of the order of the timing accuracy, so that there is need to check his conclusions as to the time distribution relative to the aspect of the earth seen from the sun, using still more accurate data. The IGY saw a general improvement in timing and recording techniques, and many stations provided quick-run magnetograms. But a timing accuracy of 1 or 2 seconds is desirable. Campbell (1959) used methods giving this accuracy. It would be valuable for this purpose to have Sc records from Huancayo and from other low-latitude stations, Pacific and African,

25

Indian and Australian, with open time scales, and synchronized by
registration of WWV signals.

2.5 MORPHOLOGICAL REPRESENTATION BY CURRENT SYSTEMS IN CONCENTRIC SPHERICAL SHEETS

The transient magnetic changes at the earth's surface can be
analyzed into parts that originate respectively above and below the
surface. In all cases the major part is of external origin, and the
part of internal origin is reasonably explained as due to electromagnetic
induction by the primary external part. Hence the main interest centers
on this external part.

From a knowledge of the distribution of this external changing
field over the earth, as a function of time and position, its magnetic
potential can be determined. From this it is possible to determine a
current system, flowing in a spherical sheet concentric with the earth,
that _could_ produce the said field. But this may or may not be the
current system that _does_ produce the field; and even if the system does
flow in a concentric layer, the surface magnetic data cannot determine
the radius of the current sheet. In any case, however, such a current
representation is valuable and interesting, because it provides a
convenient graphical scalar synopsis of the field morphology.

In the case of the external storm field D, _average_ current systems
for the middle belt of the earth have been determined that represent its
parts Dst and DS, and the combined total field, throughout the average
storm. World-wide or partial current systems associated with a number
of individual magnetic storms have also been given, by McNish and
Johnston (1939) and Vestine (1940), and also for bays (Fukushima 1953).

26

The D field at its sudden commencement has been likewise examined by several writers. Nagata (1952) and Nagata and Abe (1955) studied Sc's of the type Sc(-+). Further and more comprehensive studies were made by Oguti (1956) and Obayashi and Jacobs (1957). The Dst part of the current of the Sc field is eastward, opposite to that for the main storm phase in which H is below normal. The DS currents for the Sc field are similar in some respects to those observed during the initial and main storm phases; that is to say, the current system shows a nearly parallel flow over the polar cap centered on the geomagnetic pole, with lateral eastward and westward return flow. The orientation of the DS field around the geomagnetic axis fluctuates during the main course of a storm, with little change in its general form, but much less rapidly than during the Sc.

Obayashi and Jacobs (1957) showed that at the earlier instant the Dst part seems to be inconspicuous and the current system is almost wholly of Sc DS type, and is practically confined to higher latitudes; then follows the main Sc movement, which shows an eastward Dst current in low latitudes and a DS current system in higher latitudes; this is nearly oppositely directed to that shown for the earlier Sc epoch. Oguti (1956) independently found similar changes; he stated that the DS part of the current system may rapidly rotate clockwise, during an Sc which in high latitudes appears as an Sc(-+).

The DS part of the Sc field, most intense in high latitudes, and changing in orientation (at least in some cases) during the Sc, accounts for the greater complexity of Sc's in higher latitudes than in low (where

27

in general the simpler Dst part is paramount).

Vestine (1940) first gave current diagrams for successive epochs of several magnetic storms (from data obtained during the second International Polar Year). His diagrams referred to hourly means of the disturbance field. Hence his diagrams for the _initial phase_ of two magnetic storms (1932, October 14, and 1933, April 30), though highly interesting, do not refer to the brief Sc field of these storms.

2.6 THE TRUE FORM AND LOCATION OF THE Sc CURRENTS

As stated in §2.5, the current systems illustrated for the Sc field and the field of the later phases of a magnetic storm are convenient representations of the field morphology, but do not necessarily represent the true form and location of the external currents. The polar part of these current systems DP is, however, generally believed to be located in the atmosphere at auroral levels (that is, in the lower ionosphere). There the atmosphere is known to be strongly ionized during most of the initial and main phases of magnetic disturbances, especially along the auroral zones. The strongest currents in high latitudes flow along these zones, partly eastward, partly westward.

In lower latitudes, except near the magnetic equator (as at Huancayo), DCF is the major part. The small difference of current intensity between the day and night hemispheres—despite the great difference in the ionization of the atmosphere over the two regions—is one main reason for the view, held by a number of workers, that these DCF currents flow mainly outside the ionosphere (as this term is usually understood). The Huancayo daytime enhancement of Sc (H) indicates, however, a notable

28

current flow along the daytime equatorial electrojet which is part of the Sq current system.

It is shown later (§ 5) that the DP current in the auroral zone will set up a polarization field at its eastern and western ends and this will cause the electric current curcuit to be completed in lower latitudes. We infer that the equatorial enhancement of Sc (H) is due to the enhancement of the equatorial electrojet resulting from the DP polarization field. Fig. 2.4 shows an example of the enhancement of the equatorial jet at Huancayo (gm. lat. -0°6 S, long. 353°8) during the 29 September 1957 storm. Large irregularities superposed on the DR decrease (see § 3.6 Fig. 3.10) correspond to large DP sub-storms in the auroral zone. The Huancayo trace may be contrasted with the Pilar trace (Pilar, gm. lat. -20°3S,long. 4°6) on the same day (Fig. 2.4b). It is clear that the DP currents were abnormally enhanced in the ionosphere along the magnetic equator.

Rocket and satellite observations can help to solve some of the uncertainties as to the form and location of the external electric current systems during magnetic storms, both for Sc's and for the later phases. By magnetic recording along its path, a rocket or satellite can show when it traverses regions of electric current flow. Naturally it may be expected that the results will mainly refer to the main phases of storms, rather than to Sc's, on account of the short duration of Sc's (Cahill 1959).

Further light on the nature of the external storm current systems, especially of Sc's, may be sought also from theories of magnetic storm production.

2.7 A THEORY OF THE Sc OF GEOMAGNETIC STORMS

The first fairly plausible theory of the sudden commencement of a
magnetic storm was given in 1931 by Chapman and Ferraro. It was part of
an attempt to infer the course of events, supposing that the sun ejects
a stream of neutral ionized gas towards the earth. This hypothesis was
suggested by Lindemann (1919), to overcome Schuster's objection (1911)
to earlier theories, like those of Birkeland (1913) and Stormer (cf.
1955), which assumed a solar stream of charged particles all of the same
sign.

Chapman and Ferraro tacitly treated the solar stream as uniform in
density and speed, and traversing empty space between the sun and the
earth. They inferred that the stream would be retarded by the geo-
magnetic field, which would produce a hollow in the stream. At first
they treated the stream as having initially a plane front perpendicular
to the velocity of the gas, and parallel to the geomagnetic axis. They
inferred that an electric current system would be induced in a thin
front layer of the stream. This system would increase the geomagnetic
field intensity within the hollow. But to north and south of the geo-
magnetic equatorial plane there would be focal points round which the
electric current would flow. Everywhere except at these points the
geomagnetic force on the currents would retard the stream surface; but
the gas could flow freely through the focal points. It was guessed that
"horns" of gas would extend from these focal areas, perhaps approximately
along geomagnetic lines of force, and flow into the earth's atmosphere
somewhere in the auroral zone.

The shape of the hollow, and the detailed course of events, could

30

not be calculated because of the complexity of the problem. But

illustrative idealized problems were solved (note especially Chapman and

Ferraro 1940 and Ferraro 1952), that seemed to indicate some probable

features of the actual geomagnetic storm commencement.

The determining characteristic of the stream was found to be its

energy density ϵ just before the stream became affected by the geo-

magnetic field. This is the initial kinetic energy of the gas per unit

volume--the gas being composed of protons and electrons in equal number.

Let fa denote the distance from the earth's center 0 to the point C of

closest approach of the stream towards the earth; here a denotes the

earth's radius. The point C (the "vertex" of the hollow) will lie on the

line joining the sun S to the earth's center 0. It was found that

approximately

$$f = \left[\frac{H_o^2}{8\pi\epsilon} \right]^{1/6} \tag{1}$$

where H_o denotes the earth's equatorial surface magnetic intensity (0.3

gauss). This is a consequence of the simple approximate relation

$\epsilon = H^2/8\pi$, where H denotes the geomagnetic field at C. Thus f varies

inversely as the one-sixth power of ϵ, so that a great range of ϵ, for

example in a ratio of 3^6 or 729, corresponds only to a threefold range of

f. The corresponding magnetic disturbance at the earth's center 0 may be

inferred from the approximate Chapman-Ferraro conception of an image

dipole for the field of the electric currents induced in the stream front

(Fig. 8, Chapman and Bartels, p. 861); it is northward, and of amount,

$$H_o/8 \ f^3 \quad \text{or} \quad (\pi_\iota/32)^{1/2} ,$$

varying as $\epsilon^{1/2}$.

Thus, for a sudden commencement of moderate magnitude, in which the external part of the initial increase (only slightly more than half the total increase) is 10 γ, f would be approximately 7.2. For twice this initial increase, f would be approximately 5.7, and for a very intense Sc, showing an initial increase of 420γ[*], of which 225 γ was of external origin, f would be approximately 2.56. Such considerations given by Chapman and Ferraro indicated the scale of the hollow space and of the electric current distribution round the earth, during the earliest stage of storms of different intensities, from mild to very great. This scale was far smaller than that previously envisaged, in Störmer's theory.

In their theory of the initial impact of the solar stream upon the geomagnetic field, it was clearly shown how abruptly the stream front was stopped at the distance fa, where f depends on the energy density ϵ of the stream. Owing to the nature of the relation (1), a hundredfold increase in ϵ would diminish f by less than half, and the initial Sc would vary tenfold. Moreover, the change of the field near the earth would be very rapid, increasing to its full amount from a tenth of this value in a time less than two minutes. This estimate assumes a stream

---

[*] This was the value at Hermanus Observatory (33°3 S gm. lat.) at the second Sc on February 11, 1958, at $01^h59^m30^s$ UT; this followed the first Sc that day after 34 minutes. The associated flare was observed on February 9 at 21^h08^m UT. The travel time was 28^h52^m and the corresponding speed was 1.46×10^8 cm/sec. The above formulae give f = 2.56, $\epsilon = 1.3 \times 10^{-5}$ erg/cc, and for the number density of the stream protons or electrons, about 750/cc.

speed of 1000 km/sec, which is of the order indicated by the travel time

from the sun (in cases where the initiation of the stream can be

associated with an identifiable solar event, such as a flare or radio

burst). The undisturbed number density of the stream, just outside the

geomagnetic influence, is then of order 28/cc for $f = 5$.

The particles at the front of the stream, near the line OS, would

be turned back, those further from OS would be deflected sideways. Near

the vertex C of the hollow, the initial kinetic energy of the protons

and electrons would be much reduced (the balance of their energy going

into the disturbed magnetic field). Their remaining energy would be

much greater for the electrons than for the protons. Other particles

coming on from behind would pass through the earlier particles flowing

backwards, before their motion also was reflected or deflected. The main

change of the motion would be concentrated in a thin front layer of the

stream, whose density would be increased. This thin layer might be

called a shock front, but this term is perhaps better not used, because

it could be taken to imply a closer analogy with shock waves in

ballistics than is actually the case.

The treatment of the stream as being of uniform density and speed

is of course an idealization, permissible in a first attack on such a

problem. In actual solar streams there will be non-uniformities of

density, a spread of forward speeds, and irregularities in the form of

the front "surface". During the travel from the sun the speeds will to

some extent sort themselves out (if the stream carries away no magnetic

field from the sun). Thus the faster particles arrive first, with a

reduced spread of speeds. A small spread would only slightly affect the

33

abruptness of the stream stoppage and of the resulting sudden storm commencement (see also § 2.8).

In their discussion of the sudden commencement, Chapman and Ferraro mainly considered the disturbance of the geomagnetic field by the surface electric currents at the front of the stream when the front is at a distance of a few earth radii from the earth's center O. These may be called the corpuscular flux (or DCF) currents. These would produce a disturbance of rather simple form, of plain Sc(+) type.

2.8 TRANSMISSION OF THE AGENT FROM THE SUN TO THE REGION JUST OUTSIDE THE GEOMAGNETIC FIELD

During the decade that included the studies of geomagnetic storm theory by Chapman and Ferraro (1931-1940), it was natural to ignore the presence of any interplanetary gas. This was actively studied later, from observations of the zodiacal light (Siedentopf et al. 1953) and of the outer solar corona (Blackwell 1955, 1956; Hewish 1955, 1958, and others). This led to varied speculations (Biermann 1957, Chapman 1957, 1959).

Here our special concern is with the influence of the interplanetary gas on the transmission to the earth of solar influences connected with eruptions and solar flares. Three main possibilities have been considered:

(1) A blast wave travels from the sun, without mass transport.

(2) Ejected solar matter collides with the interplanetary gas, and pushes it forward.

(3) Ejected solar matter interpenetrates the interplanetary gas.

All these three possibilities have been discussed, in many cases using the terms shock wave or shock front. But there are important differences between them.

(1) The first case was discussed by Gold (1955) in 1953, and later by Jennison (1955). At a symposium on gas dynamics, Gold remarked that for a geomagnetic Sc to be produced by a solar stream that is unimpeded until it nears the earth, the stream must have a quite unreasonably small velocity dispersion. "Even the purely thermal velocity dispersion would cause a time of build-up of more than one half hour, ... A much more reasonable interpretation of the phenomenon would be the arrival of a

35

highly supersonic shock wave with the characteristic sharp wave front".

(2) The second case was discussed by Singer (1957) and Akasofu (1957), who supposed that a shock wave might develop at the front of the solar stream, and that both the stream and the shock front would advance toward the earth, with slightly different speeds.

(3) Parker (1959) has considered the case of interpenetration, and has discussed the stream front and the plasma oscillations that will occur. In these oscillations there is a continual interchange between relative kinetic energy and electrostatic potential energy. Interaction with the oscillating electric field may almost fully preserve the initial velocity distribution of the stream protons, Maxwellian or otherwise, without direct collisions. The 'relaxation time' will be of the same order of magnitude as the ion plasma oscillation (for the number density of 100/cc, it is less than 10^{-4} sec, cf. Parker 1959). The range of the relative oscillations of ions of different speeds will be of order 10 to 20 meters.

The generally accepted view is that solar matter not only reaches the outer region of the geomagnetic field, but also enters the earth's ionosphere in auroral regions; the protons observed by Vegard (1939, 1940), Gartlein (1950) and Meinel (1950) are usually interpreted as being of solar origin, though it has not been absolutely demonstrated that they must come from the sun.

The blast wave and collision wave hypotheses (1, 2) are rendered unlikely by reason of the large mean free paths in the stream and in the interplanetary gas. As regards Gold's objection based on velocity dispersion, particles of different speeds will, to some extent, sort themselves out during the travel of the solar matter to the earth. Moreover,

there is solar evidence that the ejected matter includes two distinct emissions, in which the dispersion of the particles that produce storms may be small (Wild, 1955, p. 661; 1957, p. 321). They come from type II bursts; the other type, III, may produce solar cosmic rays but no magnetic disturbance.

Opinions differ as to whether, as Biermann (1957) suggested, there is a continual though non-uniform ejection (the "solar wind") from all over the sun (Parker, 1958b). Instead the emission may be mainly in the form of clouds ejected from flare regions, and continued though perhaps intermittent streams from M regions (Babcock and Babcock 1955). Biermann's conception might imply that there is no static or nearly static interplanetary gas. The alternative conception would allow that there may be. But if such a nearly static gas exists, its temperature and density are as yet not well enough known to allow certain deductions as to the interaction between it and the ejected solar gas. Further information from satellite and cosmic ray studies is very desireable.

As regards a magnetic field in the solar gas, several writers (Alfvén 1956, Parker 1958b) have suggested that the stream or wind stretches out magnetic lines of force anchored in the sun, so that the gas flow is along or nearly along the lines of force. This would seem to imply that the electric field associated with the stream motion is absent or small.

2.9 TRANSMISSION OF THE Sc FROM THE INNER BOUNDARY OF THE SOLAR STREAM FRONT TO THE EARTH'S SURFACE

The Chapman-Ferraro studies of magnetic storms indicated that a solar stream would cause important field changes at a distance of a few earth

37

radii from the earth's center. At that time it was natural to regard the space where these phenomena occur as being empty. Hence those authors took no account of any residual gas in the region of the stream retardation and of the growth of the supposed ring-current. They regarded the field changes as being propagated with the speed of light in vacuo towards the earth's surface, until the ionosphere was reached. There electric currents would be induced that would partly shield the earth's surface from the primary field changes. The non-uniform ionization and electric conductivity of the ionosphere would somewhat modify the form of the field transmitted to the earth's surface (Ashour and Price 1948; Sugiura 1950).

In 1954, Storey's theory of whistlers gave the first strong evidence of the presence of ionized gas out to distances of a few earth radii. Later it became recognized that the earth's outer atmosphere will consist mainly of atomic hydrogen, and that this will extend out to at least a few earth radii. Associated speculations were developed, about the temperature of the interplanetary gas and the possible ionization of the upper layers of this atomic hydrogen (Chapman 1957b).

One result of this enhanced interest was a controversy over the transmission of the outer geomagnetic storm field changes to the lower ionosphere and the earth's surface. Parker (1956), who has contributed greatly to our understanding of many difficult problems in this field, argued that the ionized gas intervening between the earth and the region where field changes are generated would shield the earth from the Dst decrease of the horizontal field--the transmission requiring months or even years. Hines (1957) and Hines and Storey (1958) gave counter

38

arguments, in favor of rapid transmission through the outer ionized atmosphere, by hydromagnetic waves. This view is now adopted also by Dessler and Parker (1959) and by Piddington (1959). Estimates of the speed of such waves over most of the path range around 1000 km/sec, so that passage over a distance of, say, 5 earth radii, or about 30000 km, would require a time of order 1/2 minute, and a little longer (about 10 seconds) to reach the dark side of the earth (Green et al, 1959; Francis et al, 1959); these times are less than those earlier estimated by Dessler, (1958a). The inferred time difference of transmission to different parts of the earth would thus appear to be of order one minute-- rather more than seems indicated by magnetic storm data. However, the transmission of hydromagnetic waves through a non-uniform partly ionized gas can be complex, and as regards Sc the results are not yet clear.

Dessler and Parker (1959) and also Piddington (1959) conclude that during an Sc the field-changes produced by the retardation of the solar stream are transmitted downwards by hydromagnetic waves to the ionosphere. They refer to the suggestion by Forbush and Vestine (1955) "that important sources of the field of geomagnetic storms were located in the atmosphere" (by atmosphere they mean the region below about 1000 km.). Dessler and Parker (1959) conclude that "the surface magnetic observations may be interpreted as ionospheric current systems". Piddington (1959) concludes that "the currents directly responsible for all geomagnetic disturbances must flow below about 1000 km". He gives a simplified picture of the atmosphere as consisting mainly of two regions (with a transitional layer between them):

(1) Up to a few hundred km the medium behaves as a rigid conductor and dispersive medium for waves of all periods between 1 and 10^4 seconds;

(2) Above 1000 km magnetic disturbances travel as hydromagnetic waves in the plasma (ions and electrons) alone. Losses in this region are small, but transmission is likely to be complicated by refraction, partial reflection and (for the extraordinary wave) by anisotropy.

Recently Dessler et al. (1960) inferred Sc rise times of several minutes, regardless of how abrupt may be the impact of the solar stream on the earth's outer atmosphere. Their reasoning was based on the variation in hydromagnetic transit times from different points on the front of the solar stream, to a point on the earth's surface. They based their calculation on Fermat's principle (ray-path theory). However, the ray-path treatment cannot be applied here, because the velocity of hydromagnetic waves in the outer atmosphere varies so greatly (from 100 km/sec to 6000 km/sec in a distance of about 3000 km) within one wave length λ (λ = 6000 km for 1 c/sec waves at 3000 km height above the ground). The wave treatment must be used. Ferraro (1952) has shown that the impact of solar streams on the outer atmosphere cannot be abrupt, and that the retardation of the solar stream near the earth can account for the observed rise time of order two minutes.

Our own view is that currents of the type that produce the Sc(+) continue to flow during the early hours of a storm, that is, as long as the stream is impinging on the earth's field and being reflected back or pushed sideways so as to travel on beyond the earth. Temporary initial hydromagnetic wave effects may occur in the ionosphere, involving some transient current flow in the E layer; but the main Dst effect in the first

phase comes from currents at the inner surface of the stream. These currents probably continue to flow during at least part of the development of the main phase. During this period the observed Dst magnetic changes are a superposition of effects due to currents at the inner stream surface and ring currents in the Van Allen belt.

At present the details of these processes remain obscure, and affect important questions relating to the distribution of electric currents and energy in the space round the earth.

2.10 THE SUDDEN COMMENCEMENT DP CURRENTS

The conception of a storm Sc attained as the result of observational and theoretical studies may perhaps be described as follows. The Sc field at the earth's surface is partly formed by the initial retardation of a solar cloud or stream at a distance of a few earth radii; this field change is transmitted in some way from that region, through the outer atmosphere and the ionosphere, to the earth's surface. Another major part of the Sc field, comprising most of the DP part, is due to a current system generated in our atmosphere, mainly in polar latitudes; but these currents also extend over a large part of the earth.

In order to explain this second electric current system, dynamo action has been proposed as an explanation, by Wulf (1945, 1953), Vestine (1954) and Obayashi and Jacobs (1957). But by detailed analysis of the current system and the probable dynamo-induced emf's, Maeda (1957, 1959) concluded that dynamo action was inadequate. Other evidence adverse to the conclusion that dynamo action is the main cause is provided by the rapidity of change of the DP currents during an Sc, as reported by Oguti (1956).

41

It seems scarcely possible that the winds responsible for dynamo emf's could change, over a wide area, during the brief interval occupied by an Sc (less than three minutes), so rapidly as to reverse the current system, or rotate it through a large angle. Hence some more direct source of emf, related to the changing intensity and location of influx into the auroral ionosphere, seems to be needed.

The emf's supposed to be generated in the polar regions impel electric current flow over a large part of the earth. It may be that during the day hours at Huancayo some of this current system flows preferentially along the narrow electrojet belt of high electrical conductivity that lies above the magnetic equator. This effect, suggested by Forbush and Vestine (1955, p. 315) and Piddington (1959), may provide an explanation of the large daytime enhancement of the Sc at Huancayo.

Geomagnetic longitude
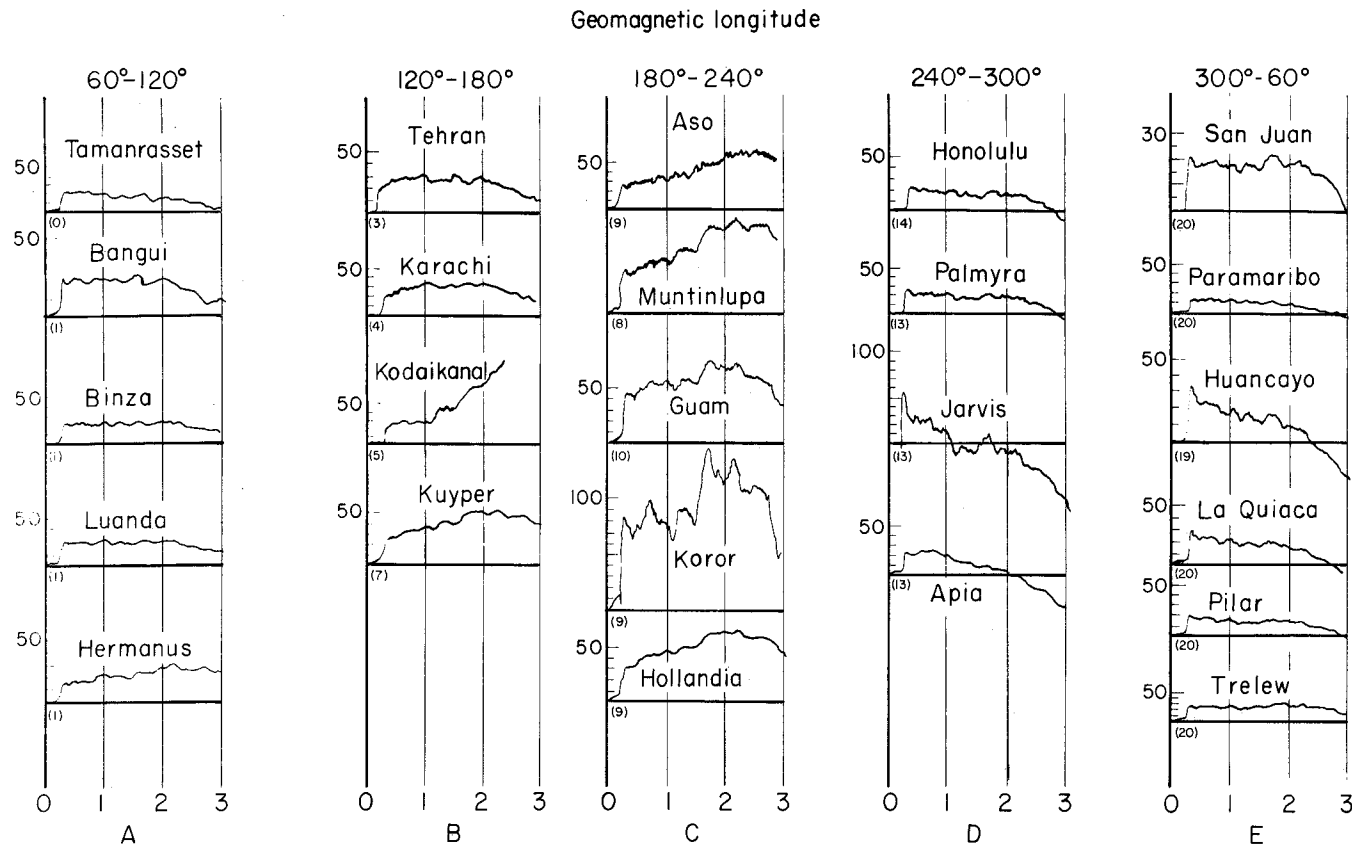
Fig.2.1. The H component magnetograms during the first three hours of the 29 September 1957 storm at 24 observatories in low latitudes. The ssc occurred at 00^{h}16^m GMT 29 September 1957.
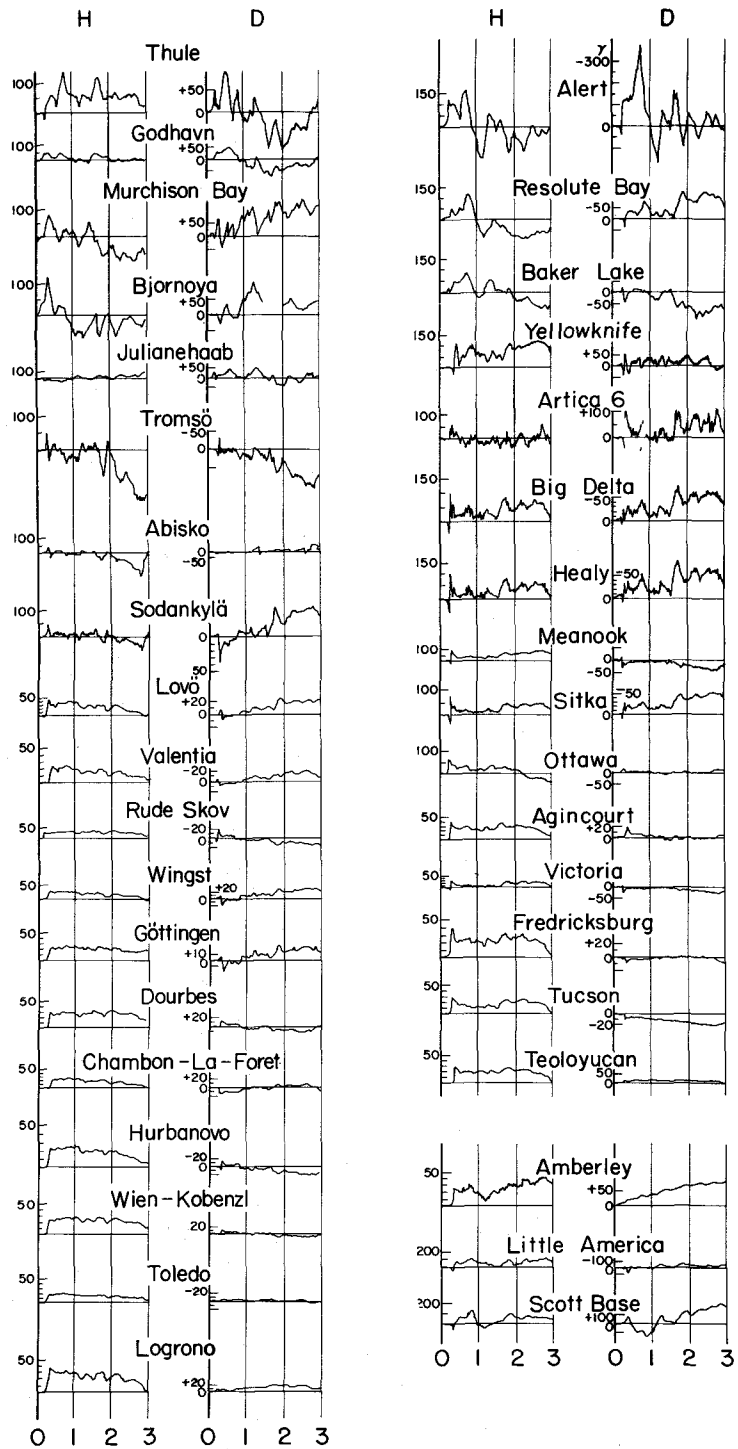
Fig. 2.2. The H and D magnetograms during the first three hours of the 29 September 1957 storm for 37 observatories in high latitudes.

FREDRICKSBURG (MD.)

SEPT. 29, 1957
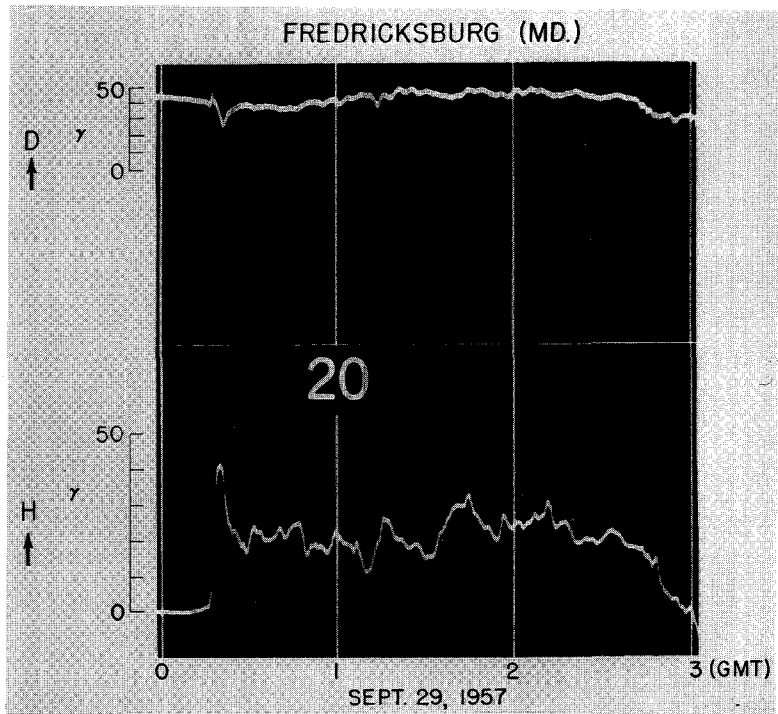
Fig.2.3a. The H and D magnetograms during the first three hours of the 29
September 1957 storm at Fredricksburg (gm.lat. 49⁰6N).

BIG DELTA (ALASKA)

SEPT. 29, 1957
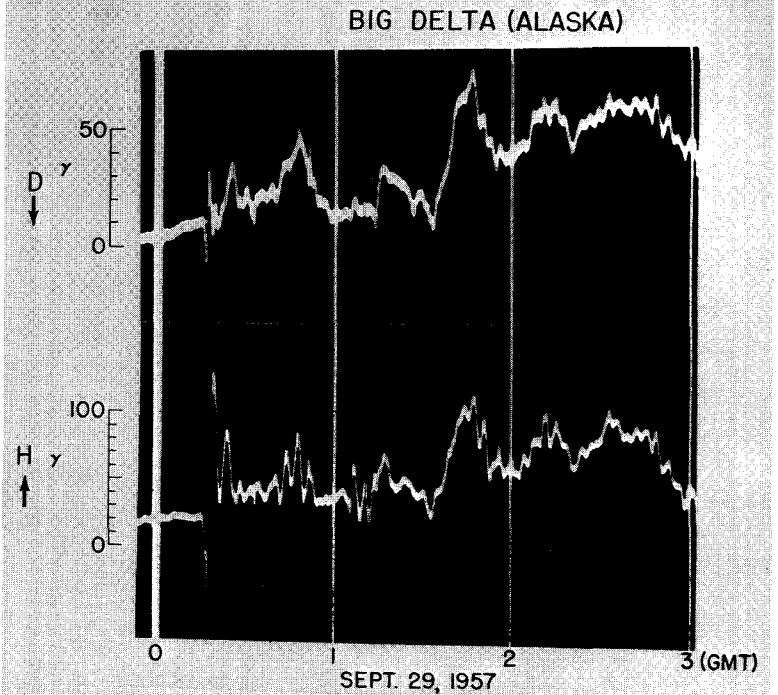
Fig.2.3b. The H and D magnetograms during the first three hours of the 29
September 1957 storm at Big Delta (gm.lat. 64⁰4N).

HUANCAYO
gm. lat. $-0°.6$, long. $353°.8$

H component
——— SEPT. 29 1957
·········· SEPT. 28 1957

SC

γ

GMT

PILAR
gm. lat. $-20°.3$, long. $4°.6$

H component
SEPT. 29 1957

SC

γ

GMT

Fig. 2.4. The horizontal component magnetograms from Huancayo
(Peru) and Pilar (Argentina) for the 29 September 1957
storm.

CHAPTER III

THE RING CURRENT, GEOMAGNETIC DISTURBANCE, AND THE VAN ALLEN RADIATION BELTS*

3.1 INTRODUCTION

Two major average features of geomagnetic storms are an initial increase of the horizontal magnetic force at the earth's surface, followed by a larger and more prolonged decrease. Many years ago Schmidt (1917) discussed the decrease. He ascribed it to the influence of a westward electric current that encircles the earth: this is now generally called the (geomagnetic) ring current. He concluded that it must wax and wane as magnetic disturbance increases or decreases. But from a study of the monthly means of the horizontal component (at Potsdam) he suggested that the current never dies away completely--hence that it is a permanent companion of the earth.
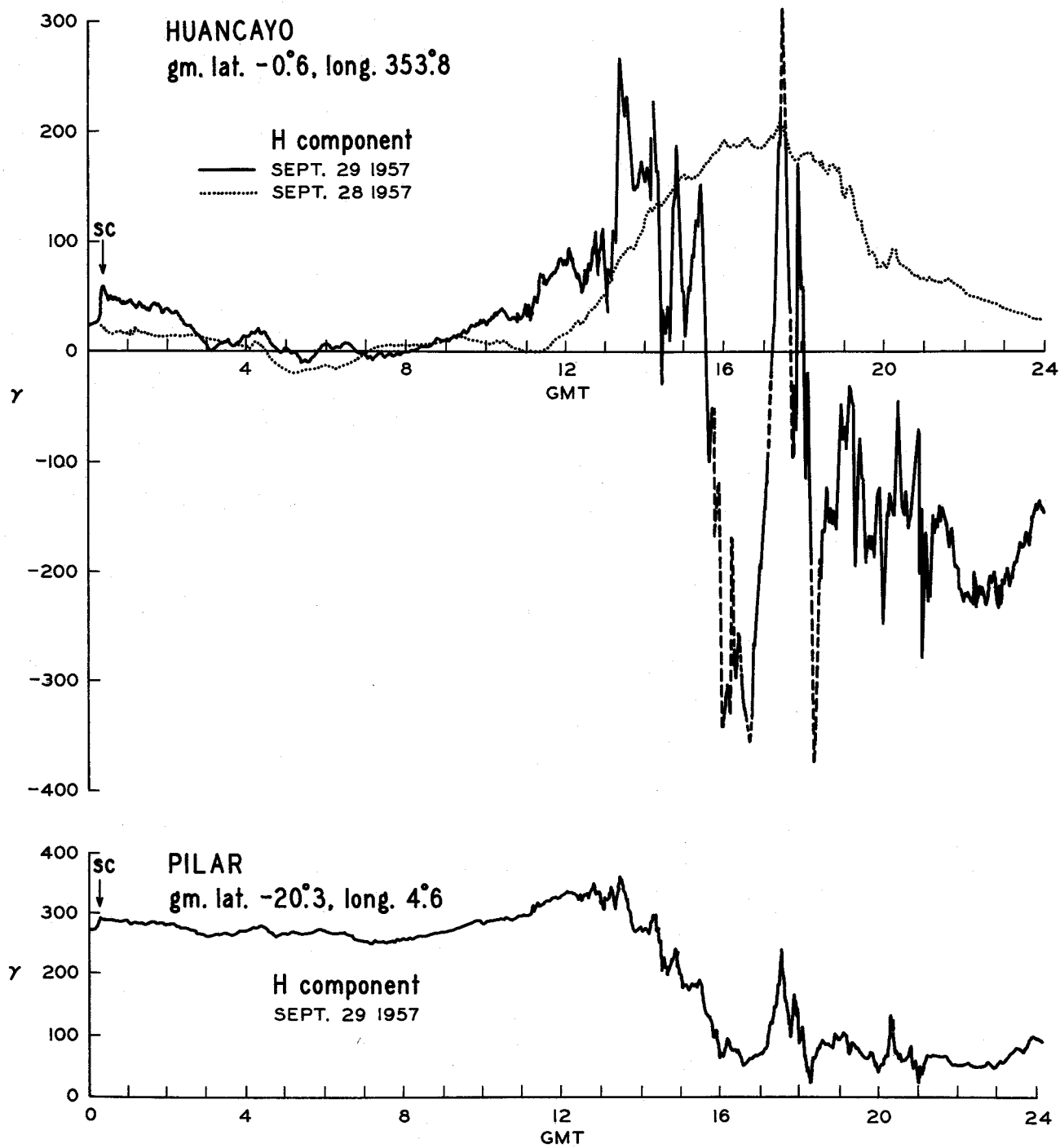
Like most students of geomagnetic disturbance, Schmidt attributed magnetic storms to the influence of corpuscular streams or clouds from the sun. The clear implication of his conclusions was that some of the solar matter that affects the earth remains in our vicinity for a considerable period. In the phraseology now common, the solar material is partly trapped by the earth's magnetic field, and one consequence is the enhancement of the ring current and its geomagnetic effects. Schmidt did not consider the scale or location of the current.

Chapman and Ferraro (1931a, 1931b, 1933, 1940) and Ferraro (1952) attempted to infer by mathematical deduction the consequences of the impact of a neutral ionized solar stream upon the earth. Their theory discussed an idealized "model", which in more than one respect left out

---

*Part of this Chapter covers the same ground as the paper: Akasofu and Chapman (1961b).

43

significant features of the actual situation. Their inferences, although imperfect and incomplete, seemed and still seem to indicate the essential mechanism of the first phase of magnetic storms, and the scale of the penetration of the solar gas. The deflection of the gas particles by the geomagnetic field, by which much of the gas is continuously reflected or scattered away from the earth, produces the first phase of the storm. It seemed clear, however, that some of the gas finds its way into the earth's atmosphere in high latitudes (and there produces auroras), and also that some is retained in the field for a time, in the form of a ring current. They were unable to explain or delineate the motions of these two sub-groups of the solar particles. However, postulating (like Schmidt) the existence of the ring current, on the basis of the geomagnetic evidence, they discussed the equilibrium, stability and decay of the current. The model current ring in their discussion was toroidal, with protons and electrons simply circulating round the geomagnetic axis, with slightly different speeds--the motion of the protons, at least, being westward. Some of the particles near the surface of the toroid would not be in equilibrium: they would leak away, spiralling round the lines of force into the auroral zones.

Singer (1957) proposed a different conception of the trapped component of the solar gas. Instead of a toroidal form, and simple circular motion for most of the particles of the gas, he inferred that the gas would have the form and motions not long afterwards indicated by satellite and cosmic rocket exploration (Van Allen and Frank 1959: Vernov et al. 1959). The particles oscillate rapidly to and fro between "mirror" points in fairly high northern and southern latitudes. At the same time they circle

round the local magnetic lines, and also drift round the earth--the

protons westward, the electrons eastward. Singer concluded that a part

of these motions of the particles of the belt necessarily corresponds to

a ring current round the earth. Thus any temporary enhancement of the

belt would decrease the magnetic field at the earth's surface, as

observed during the main phase of a magnetic storm. Recently the ring

current problem has been further studied by Dessler and Parker (1959).

The present paper continues and extends these discussions. Since it

was written, Professor Singer has sent us a paper by J. Apel on the

same subject; this is not yet published. There is now general agreement

on the equations of the problem, but all these papers attempt only a first

step towards its solution, in that they consider the motion of the par-

ticles as being controlled only by the dipole field--ignoring the per-

turbation of the field by the radiation belts.

Another important problem that is not yet solved is the manner in

which the solar particles become trapped by the geomagnetic field.

Dessler and Parker (1959) attribute this to instability at the surface

of the hollow carved in the stream by the geomagnetic field. They think

that portions of the solar gas will penetrate the geomagnetic field and

break up and diffuse in the field. In $\S$ 3.6 we show that the capture

seems to occur to very different degrees in different storms.

Meanwhile extensive satellite observations bearing on these questions have been made, during periods that included some magnetic storms. These observations refer partly to the constitution of the belts, and partly to the variation of the magnetic field in and beyond the region of the belts. It appears that the outer, main, radiation belt at times suffers marked depletion during the main phase of a storm (Rothwell and McIlwain 1960; Arnoldy et al. 1960; Van Allen and Lin 1960). This contrasts with their expected enhancement. The depletion concerns protons of energy 30 Mev or more, and electrons of energy 30 Kev or more: so far particles of less energy are undetected.

The earth's magnetic field far away from the earth beyond 5 earth radii has also been explored by satellites. Sonett et al. (1960) found little sign of the existence of the ring current in the central region of the outer belt, but clear evidence of it beyond 5 earth radii. From the study of the multiple structure of auroral arcs, Akasofu and Chapman (1961) have inferred that during a storm the ring current may consist of an irregular distribution of current located mainly between 5 and 8 earth radii.

This suggests that the main part of the outer radiation belt is not the seat of the main ring current, but that during a storm a new 'storm-time belt' appears at about 6 earth radii, presumably by injection of solar particles there. It may be convenient to refer to the standard inner and outer Van Allen belts by the symbols V_1 and V_2 respectively. If so, the suggested new storm-time belt may be denoted by V_3.

In the first part of this chapter (§§ 3.1-3.5) we discuss the motions of trapped particles in the outer geomagnetic field, and the currents

46

produced by these motions. We derive the general equations for the intensity of the ring current and for the magnetic field at the earth's center produced by the current. We then give several numerical examples to indicate how our equations can be applied to the outer radiation belt and to our suggested storm-time belt. In this part we correct and supplement Akasofu's earlier paper.

In the second part (§3.6) we analyse several magnetic storms that occurred during the IGY and IGC 1959, and discuss the development of the ring current during these storms.

3.11 Notation (general)

The following general notation is used in this chapter:

a = the earth's radius;

r = the radial distance from the earth's center 0 to a point P;

m = the mass of a trapped particle;

e = its charge, in esu;

$\underline{w}$ = its velocity;

w = its speed;

$\mathcal{E}$ = its energy, in Kev, namely $\frac{1}{2}mw^2 / 1.602 \times 10^{-9}$;

n = the number density of the particles;

$\underline{H}$ = the magnetic vector, of magnitude H;

$\underline{h}$ = the unit vector along $\underline{H}$, so that $\underline{H} = H\underline{h}$;

p_m = the magnetic pressure, namely $H^2/8\pi$;

θ = the angle, called the pitch angle, between $\underline{w}$ and $\underline{H}$;

w_s = the component of $\underline{w}$ along $\underline{H}$, so that $w_s = w \cos \theta$;

w_n = the component of $\underline{w}$ normal to $\underline{H}$, so that $w_n = w \sin \theta$;

p_s = the pressure of the gas along $\underline{H}$; it is the sum of mw_s^2 over all the

particles per unit volume;

p_n = the pressure of the gas normal to H; it is the sum of $\frac{1}{2}mw_n^2$ over all

the particles per unit volume.

3.12 Geometrical formulae relative to a dipole field

Here and later in this chapter the terms axis, latitude, longitude, equator, equatorial or meridian plane will refer to a dipole field, namely, in general, to the geomagnetic dipole field. The subscript e will signify reference to the equatorial plane.

The position of any point P may be specified by the usual spherical polar coordinates r, ϕ, $\emptyset$, where ϕ and $\emptyset$ denote the latitude and longitude. But in this paper, whenever a dipole field is being considered, the position will generally be specified by r_e, ϕ, $\emptyset$, where r_e denotes the radial coordinate of the related point P_e where the line of force through P cuts the equatorial plane. The equation of this line is

$$r = r_e \cos^2 \phi; \tag{1}$$

this will often be referred to as the line (of force) r_e.

With each point P we associate two unit vectors $\underline{j}$, $\underline{k}$, which with $\underline{h}$ form a right-handed orthogonal unit vector triad $\underline{h}$, $\underline{j}$, $\underline{k}$. The definitions of $\underline{j}$ and $\underline{k}$ are:

$\underline{k}$ = the eastward unit vector normal to the meridian plane through P.

$\underline{j}$ = the unit vector $\underline{k} \times \underline{h}$; it is outward from the origin, but not

radially outward.

Let P' be a point adjacent to P with coordinates differing by dr_e, $d\phi$, $d\emptyset$ from those of P, namely r_e, ϕ, $\emptyset$. The vector element PP' or $\underline{ds}$ can be specified as follows relative to the vector triad $\underline{h}$, $\underline{j}$, $\underline{k}$:

$$\underline{ds} = \underline{h} \, h_1 d\phi + \underline{j} \, h_2 \, dr_e + \underline{k} \, h_3 \, d\emptyset$$

Here h_1, h_2 and h_3 can be thus specified in terms of r_e, ϕ, $\emptyset$:

$$h_1 = r_e (1 + 3 \sin^2 \phi)^{1/2} \cos \phi \qquad\qquad (2)$$

$$h_2 = \cos^3 \phi / (1 + 3 \sin^2 \phi)^{1/2} \qquad\qquad (3)$$

$$h_3 = r_e \cos^3 \phi \qquad\qquad (4)$$

Hence an element of area dS_3 in the meridian plane through P, bounded by the lines of force r_e, $r_e + dr_e$ and the radii with latitudes ϕ, $\phi + d\phi$, is given by

$$dS_3 = h_1 \, h_2 \, dr_e \, d\phi$$
$$= r_e \cos^4 \phi \, dr_e \, d\phi \qquad\qquad (5)$$

This surface element is normal to $\underline{k}$. The surface element dS_1 normal to $\underline{h}$ is similarly given by

$$dS_1 = h_2 \, h_3 \, dr_e \, d\emptyset$$

or

$$\left\{ r_e \cos^6 \phi / (1 + 3 \sin^2 \phi)^{1/2} \right\} dr_e \, d\emptyset$$

Since the tubes of magnetic force are of constant strength, it follows

49

that

$$H\, h_2\, h_3 = (H\, h_2\, h_3)_e.$$

Hence

$$H_e/H = h_2 \cos^3 \phi \tag{6}$$

The field intensity H_e in the equatorial plane is given by

$$H_e = a^3 H_o / r_e^3 \tag{7}$$

Here H_o denotes the value of H_e at the equator at the earth's surface. It is taken to be 0.32 gauss ($= 3.2 \times 10^4 \gamma$).

A volume element dV at P can similarly be expressed by

$$dV = h_1\, h_2\, h_3\, dr_e\, d\phi\, d\emptyset$$

$$= r_e^2 \cos^7 \phi\, dr_e\, d\phi\, d\emptyset \tag{8}$$

The total area in the meridian plane enclosed by the line of force r_e is given by

$$S = \iint dS_3 = \int_0^{r_e} \int_{-\pi/2}^{\pi/2} r_e \cos^4 \phi\, dr_e\, d\phi$$

$$= \frac{3}{16} \pi r_e^2 \tag{9}$$

Similarly the volume V enclosed by the surface formed by revolving the line of force r_e about the axis is given by

$$V = \iiint dV = 2\pi \int_0^{r_e} \int_{-\pi/2}^{\pi/2} r_e^2 \cos^7 \phi\, dr_e\, d\phi = \frac{64}{105} \pi r_e^3 \tag{10}$$

50

For later use we calculate the gradient of a scalar function Q in our coordinate system. It is given by

$$\nabla Q = \underline{h} \, \frac{1}{h_1} \, \frac{\partial Q}{\partial \phi} + \underline{j} \, \frac{1}{h_2} \, \frac{\partial Q}{\partial r_e} + \underline{k} \, \frac{1}{h_3} \, \frac{\partial Q}{\partial \phi} \qquad (11)$$

If the system is axially symmetric, the last term in (11) is zero. In such a case, it follows that

$$\underline{h} \times \nabla Q = \frac{1}{h_2} \, \frac{\partial Q}{\partial r_e} \, \underline{k} \qquad (12)$$

It is also convenient to note that

$$(\underline{H} \cdot \nabla) \, \underline{H} = - H^2 \underline{j} \, / \, R_c \qquad (13)$$

where R_c denotes the length of the radius of curvature of the line r_e at P;

R_c is given by

$$\frac{1}{R_c} = \frac{3(1 + \sin^2 \phi)}{r_e \cos \phi \, (1 + 3 \sin^2 \phi)^{3/2}} \qquad (14)$$

3.2 THE MOTION OF CHARGED PARTICLES IN THE EARTH'S DIPOLE MAGNETIC FIELD

The speed gained by a particle in free fall under gravity, from infinity to a distance of 6 earth radii from the earth's center, is 5 km/sec, and the energy is about 0.1 ev. For fall from infinity to the earth's surface the corresponding quantities are respectively 11 km/sec and 0.65 ev. For the energetic particles of the Van Allen belts these

speeds and energies are insignificant. Table 3.1 shows for a proton of energy 480 Kev moving in the equatorial plane, at r_e = a (the earth's surface) and r_e = 6a, the gravitational force f_g and the electromagnetic force f_{em}. It gives also their ratio f_g/f_{em}. Clearly in considering the motion of the energetic particles of the belt we can ignore gravity. Then, in the absence of electric fields, the particle speed w is constant.

Table 3.1

Gravitational and Electromagnetic Forces on a Proton of Energy 480 Kev,
Moving in the Equatorial Plane, at r_e = a and r_e = 6a.

	r_e = a	r_e = 6a
$f_g = GM_E \, m/ \, r_e^2$ (dyne)	1.64×10^{-21}	4.54×10^{-23}
$f_{em} = (e/c) \, \underline{w} \times \underline{H}$ (dyne)	4.90×10^{-12}	2.28×10^{-14}
The ratio f_{em}/f_g	3×10^9	5×10^8

The following numerical values were used in calculating the quantities given in Table 3.1: G = the constant of gravitation = 6.67×10^{-8} dyne $cm^2 g^{-2}$; M_E = the earth's mass = 5.98×10^{27} g; m = the mass of a proton = 1.67×10^{-27} g; w = the speed of a 480 Kev proton = 9.57×10^8 cm/sec; H = the intensity of the earth's field, namely 0.32 gauss at r_e = a and 1.48×10^{-3} gauss at r_e = 6a.

Chapman and Ferraro (1931a), early workers in the field of plasma motions in and across magnetic fields, studied some interesting model

problems of a specially simple character. To these they gave the names
"infinite plane slab" (Chapman and Ferraro 1931a), "infinite cylinder"
(Chapman and Ferraro 1931a), "toroidal ring current" (Chapman and Ferraro
1933), "cylindrical sheet" (Chapman and Ferraro 1940) and "successive
sheets" (Ferraro 1952). A feature common to all their problems was the
absence, except peripherally, of detailed circular motion around the
lines of force. This, however, as was remarked especially by Alfvén
(1950) and Singer (1957), is a prominent characteristic of the motions
of the particles in a dipole field, as in the Van Allen belts.

As was shown by Alfvén (1950), the motion of a charged particle in
a magnetic field can in certain circumstances be analyzed into (a) the
motion of a "guiding center" associated with the particle (this motion
being partly along and partly across the lines of force), and (b) nearly
circular motion round the lines of force, relative to the guiding center.
The motion of the guiding center perpendicular to the lines of force is
often called a drift. The total electric current and the magnetic field
produced by a typical moving charge results from all three parts of the
motion--along the lines of force, the drift transverse to them, and the
circular motion round the lines. The magnetic field due to the circular
motion can be regarded as a consequence of diamagnetism.

The guiding center approximation is valid (i) when the average
radius of gyration is much smaller than the scale length of the system
considered and (ii) when the period of gyration is much shorter than the
other scale times associated with the phenomenon. Chapman (1961c) defines
the scale length and the scale time. In the earth's undisturbed dipole
field the scale length is of order 8000 km, and the scale time may be of

order 10^4 sec in our ring current problem. We show in Table 3.2 the radius of gyration R and the period of gyration T for typical energetic particles in the radiation belts. Clearly both conditions (i) and (ii) are satisfied for such particles.

The motions of the trapped particles in the outer geomagnetic field can accordingly be analysed into (a) a rapid oscillation of the particles along the lines of force between two mirror points, one (M) located in the northern and the other (M') in the southern hemisphere, (b) a slower eastward or westward drift motion, and (c) the circular gyrational motion round the lines of force. Some illustrative numerical data relating to these three motions n the earth's undisturbed (dipole) field are given in Table 3.2.

3.21 The three motions in a dipole field

(a) Oscillation between the two mirror points

In the rapid oscillation of a trapped particle between M and M', the magnetic moment is invariant; it is given by

$$\mu = \frac{\frac{1}{2} m w_n^2}{H} = \frac{\frac{1}{2} m w^2}{H_m} \tag{15}$$

Here H_m denotes the value of H at the mirror point s, where $w_s = 0$, $w_n = w$. Thus the particle is reflected at the point where

$$H_m = \frac{w^2}{w_{ne}^2} H_e \tag{16}$$

Because of the relation $w_{ne} = w \sin \theta_e$, the equation (16) may be rewritten as

$$H_m = \frac{H_e}{\sin^2 \theta_e} \tag{17}$$

54

The time T_o required for one complete oscillation between the two mirror points (from P_e to M, thence through P_e to M' and back to P_e) is given by

$$T_o = 4\, \ell/w \tag{18}$$

Here ℓ denotes the arc length of the _spiral_ path of the particle from P_e to M or M'. Its value has been calculated by Wentworth et al. (1959; their Fig. 2). For the case $w_{ne}/w = \sin \theta_e = 0.1$, ℓ is approximately given by

$$\ell = 1.25\, r_e \tag{19}$$

In calculating the data of Table 3.2, the distance r_e is taken to be 6a. The field intensity H_e at 6a is about 148 γ . Thus (17) shows that a particle for which $\sin \theta_e$ is 0.1 will be reflected at a point M where the field intensity on the line of force crossing the equatorial plane at 6 earth radii is 14800 γ . In this case M is 3190 km above the ground. The corresponding mirror latitude ϕ_o is approximately 60°. For such a particle, according to (19),

$$\ell = 7.50\ a \tag{20}$$

and

$$T_o = 30\ a/w = 1.91 \times 10^{10}/w \quad \text{sec} \tag{21}$$

if w is expressed in cm/sec. Note that for a particle that crosses the equatorial plane at a given distance r_e the latitude ϕ_o and height Z_o of its mirror points depend only on its pitch angle θ_e, _not on its speed_ w.

Fig. 3.1 shows how Z_o depends on θ_e, for $r_e = 6a$.

(b) The slow east-west drift motion

During the oscillations between the mirror points, the protons drift westward and the electrons drift eastward. The guiding centers move on a surface of revolution containing the lines of force r_e.

The drift motion results from two causes, (a) the inhomogeneity of the earth's field and (b) the centrifugal force associated with the motion along the curved lines of force. The corresponding parts u_1 and u_2 of the drift velocities are respectively given (cf. Parker 1957) by the general formulae

$$\underline{u}_1 = (\tfrac{1}{2} mw_n^2 \; c/eH^4) \; \underline{H} \times \nabla H^2/2 \tag{22}$$

$$\underline{u}_2 = (mw_s^2 \; c/eH^4) \; \underline{H} \times (\underline{H} \cdot \nabla) \; \underline{H} \tag{23}$$

For the earth's dipole field, these two equations may be transformed to

$$\underline{u}_1 = -\underline{k} \; \frac{mc}{eH} \; \frac{\tfrac{1}{2}w_n^2}{R_c} \tag{24}$$

$$u_2 = -\underline{k} \; \frac{mc}{eH} \; \frac{w_s^2}{R_c} \tag{25}$$

and R_c is given by (14). It may be noticed that both equations involve the charge e, and that protons drift westwards (in the $-\underline{k}$ direction) and electrons (for which e is negative) drift eastwards.

During each complete oscillation between the two mirror points the particle has a longitudinal displacement $\delta\lambda$ resulting from the above two drift motions. It is given (Alfvén 1950, p. 28) by

$$\delta\lambda = 4 \left(\frac{r_e}{C_{st}} \right)^2 \; I_1 \; (\phi_o) \tag{26}$$

56

Here C_{st} denotes Störmer's unit length (Störmer 1955, p. 217) given by

$$C_{st} = \left(\frac{Me}{cmw}\right)^{1/2} = \left(\frac{M}{R_M}\right)^{1/2} \tag{27}$$

Here M denotes the dipole moment of the earth (8.1×10^{25} gauss cm), and

$$R_M = mwc/e \tag{28}$$

R_M is called the magnetic rigidity of the charged particle. This length C_{st} was introduced by Störmer in his calculations of the paths of <u>single</u> particles entering the earth's magnetic field from outside, or trapped in the field.

Also I_1 is the integral

$$I_1 (\phi_o) = \int_0^{\phi_o} \frac{h_3}{R_c} \frac{1 - \frac{1}{2} H/H_m}{(1 - H/H_m)^{1/2}} \, d\phi \tag{29}$$

The first factor in the integrand, by (4) and (14), has the value

$$\frac{3 \cos^2 \phi \,(1 + \sin^2 \phi)}{(1 + 3 \sin^2 \phi)^{3/2}} \tag{30}$$

and in the second factor of (29), H/H_m or its equivalent $(H/H_e)/(H_m/H_e)$ can be calculated as a ratio of functions of ϕ and ϕ_o from (6). The integral $I_1 (\phi_o)$, an angle, has been evaluated by Alfvén (1950, p. 29) for a series of values of the mirror latitudes ϕ_o. When ϕ_o exceeds 45°, $I_1 (\phi_o)$ is nearly independent of ϕ_o, with the approximate value 76°. Thus in that case the longitudinal displacement per complete oscillation is given by

$$\delta\lambda = 4 \times 76^o \left(\frac{r_e}{C_{st}}\right)^2 \tag{31}$$

The number of oscillations made by the particle per revolution is $(360°/\delta\lambda)$. The time T_R required for one revolution is given by

$$T_R = (360°/\delta\lambda)\, T_o \tag{32}$$

(c) Gyration

The radius R and the period T of the gyration of the particle are given by

$$R = \frac{cmw_n}{eH} \tag{33}$$

$$T = \frac{2\pi\, cm}{eH} \tag{34}$$

Table 3.2 illustrates these formulae numerically, for protons and electrons that cross the equatorial plane at $r_e = 6a$ with a pitch angle $\theta_e = \sin^{-1} 0.1$; the latitude of the mirror points for these particles is approximately $60°$. Various energies are considered, corresponding to a series of values of the magnetic rigidity R_M that are included in a Table given by Störmer (loc. cit., p. 294, Table 1).

Table 3.2

Numerical particulars relating to the gyratory, oscillatory and drift motions of electrons and protons of various energies, that cross the equatorial plane with pitch angle $\theta_e = \sin^{-1} 0.1$, and are associated with the lines of force $r_e = 6a$ of the earth's dipole field.

In this Table a number expressed as X^y signifies $X \times 10^y$.

R_M = the magnetic rigidity (28),

w = the speed,

E = the energy,

58

C_{st} = Störmer length unit (27),

R = the radius of gyration at r_e = 6a (33),

T = the period of gyration at r_e = 6a (34),

$\delta\lambda$ = the longitudinal displacement per oscillation (31),

$360^{\circ}/\delta\lambda$ = the number of oscillations per revolution,

T_o = the time of oscillation (21),

T_R = the time of revolution (32).

$HV = 3.95$

	R_M	w (cm/sec)	E (Kev)	C_{st} (km)
	1^2	1.76^7	0.879	9.00^6
	3^2	5.20^8	7.85	5.20^6
	6^2	9.95^9	30.7	3.67^6
Electrons*	1^3	1.52^{10}	81.4	2.85^6
	5^3	2.84^{10}	1.07^3	1.27^6
	1^4	2.96^{10}	2.53^3	9.00^5
	5^3	4.79^7	2.0	1.27^6
	1^4	9.58^7	4.79	9.00^5
	3^4	2.87^8	43.1	5.20^5
Protons	6^4	5.75^8	172	3.67^5
	1^5	9.57^8	479	2.85^5
	1^6	9.13^9	4.79^3	9.00^4

* The relativistic correction is

R (km)	T (sec)	$\delta\lambda$ (°)	$360°/\delta\lambda$	T_o (sec)	T_R	
6.76^{-2}	2.42^{-4}	0.0055	65455	1.09^{3}	764	days
2.03^{-1}	2.46^{-4}	0.0185	19459	36.7	8.3	days
4.06^{-1}	2.57^{-4}	0.0356	10121	1.92	5.4	hours
6.76^{-1}	2.81^{-4}	0.0578	6233	1.27	2.2	hours
3.38	7.48^{-4}	0.2845	1265	0.673	14.2	minutes
6.76	1.44^{-3}	0.5673	635	0.645	6.8	minutes
3.38	0.433	0.2845	1265	3.99^{2}	6.6	days
6.76	0.433	0.5673	635	1.99^{2}	35	hours
2.03^{1}	"	1.712	210	66.6	3.9	hours
4.06^{1}	"	3.429	105	33.2	58	minutes
6.76^{1}	"	5.688	63.3	20.0	21	minutes
6.44^{2}	"	57.06	6.3	2.09	16	seconds

made for high energy electrons, in calculating R and T.

For protons of energy greater than 10 Mev, the time of revolution T_R becomes comparable with the time of oscillation T_o. In this case the guiding center approximation ceases to be valid; the radius of gyratory motion becomes comparable with the radius of the earth.

3.3 ELECTRIC CURRENTS IN AN IONIZED GAS: GENERAL FORMULAE

3.31 Volume current

All three motions (a), (b) and (c) discussed in § 2 may produce electric currents. The current associated with the oscillatory motion (a) of the charged particles, along $\underline{H}$, is given by the formula appropriate when the magnetic field is absent, namely

$$i = \sum enw_s \tag{35}$$

Here the summation includes both electrons and protons.

Parker (1957), in the paper mentioned earlier, gave expressions for the __volume__ current densities $\underline{i}_D$ and $\underline{i}_L$ arising respectively from (b) and (c). For $\underline{i}_D$ he gave the formula

$$\underline{i}_D = en\,(\underline{u}_1 + \underline{u}_2) = \frac{c}{8\pi\,p_m}\,\underline{H}x\left\{\tfrac{1}{2}(p_n/p_m)\,\nabla p_m + (p_s/p_m)(\underline{H}\cdot\nabla)\underline{H}/8\pi\right\} \tag{36}$$

(his equation 21), in accordance with (22) and 23).

The part $\underline{i}_L$, due to the gyration, is given by his equation 19,

$$\underline{i}_L = \frac{c}{8\pi\,p_m}\,\underline{H}x\left\{\nabla p_n - \tfrac{1}{2}(p_n/p_m)\,\nabla p_m - (p_n/p_m)(\underline{H}\cdot\nabla)\,H/8\pi\right\} \tag{37*}$$

* By oversight in the typescript, Akasofu (1960) omitted the factor (p_n/p_m) of the third term in the bracket in (37), but his calculations took account of this term.

The three current components (35), (36) and (37) correspond to the particle motions when there is no electric field. If conditions are changing, and an electric field $\underline{E}$ is present, the particles will have an additional velocity $\underline{v}$ given by

$$\underline{v} = c \, \underline{E} \times \underline{H} / \, H^2 \tag{38}$$

Consequently there will then be a fourth contribution, $\underline{i}_p$ to the current. This is given by Parker (1957) in the form (correcting a misprint in the original):

$$\underline{i}_p = (mnc/H^2) \, \underline{H} \times (d\underline{v}/dt) \tag{39}$$

Like (36) and 37), this is perpenicular to $\underline{H}$.

Thus the total volume current $\underline{i}$ in an ionized gas is the combination of (35) along $\underline{H}$ and the sum $\underline{i}$ of the above three currents perpendicular to $\underline{H}$:

$$\underline{i} = \underline{i}_D + \underline{i}_L + \underline{i}_P \tag{40}$$

$$= \frac{c}{8\pi \, p_m} \, \underline{H} \times \left((p_s - p_n)(\underline{H} \cdot \nabla) \, \underline{H}/8\pi \, p_m + \nabla p_n \right) + (mnc/H^2) \, \underline{H} \times (d\underline{v}/dt)$$

Part of the current resulting from the drift velocity $\underline{u}_1$ namely that associated with the bracketted term $\frac{1}{2}(p_n/p_m) \nabla p_m$ in (36), is everywhere exactly cancelled by a part of $\underline{i}_L$ namely that associated with the second bracketted term in (37).

3.32 Surface current

When an ionized gas is sharply bounded, there is, in general, besides the volume current described in § 3.31, a current in the boundary surface of the gas. Suppose that in a uniform magnetic field H, there is a uniform distribution of neutral ionized gas in a cylinder whose axis, along $\underline{H}$, is taken as the z axis of a coordinate system (r, $\emptyset$, z). Suppose that the particles all have the same speed w, with no component along $\underline{H}$. Then they will gyrate in planes perpendicular to the z axis. Suppose also that the particles have no collisions. Each gyrating particle acts like a magnet of moment μ . Thus the whole gas is equivalent to a uniform distribution of magnetization of intensity $\underline{I}$, in the sense opposite to $\underline{H}$, given by $\underline{I} = - n\mu\,\underline{h}$. Here n denotes the total number density of the particles, positive and negative.

The magnetic field $\delta\,\underline{H}$ produced by such a magnetized body is given by

$$\delta\,\underline{H} = - \text{ grad } \Omega \tag{41}$$

where Ω denotes the magnetic potential. This is given by Poisson's formula

$$\Omega = \iiint \frac{- \text{div } \underline{\underline{I}}}{r}\, dV + \iint \frac{\underline{I} \cdot \underline{v}}{r}\, dS \tag{42}$$

63

where dV and dS respectively denote an element of the volume and of the surface of the cylinder, and $\underline{V}$ denotes the unit vector directed along the outward normal to the surface element dS. Thus the magnetic field of the gas at outside points is the same as that due to a volume distribution of magnetic matter of density - div $\underline{I}$ and a surface distribution of density $\underline{I} . \underline{V}$.

Alternatively $\underline{H}$ may be expressed by $\underline{H} = \underline{B} - 4\pi\underline{I}$ and $\underline{B} = \text{curl } \underline{A}$, in terms of the magnetic vector potential $\underline{A}$ given (cf. Stratton 1941, p. 242, equation 4; Ferraro 1954, p. 253, equation 9.47) by

$$\underline{A} = c \iiint \frac{\text{curl } \underline{I}}{r} \, dV + c \iint \frac{\underline{I} \times \underline{V}}{r} \, dS \qquad (43)$$

This results from another vector transformation of Poisson type. It indicates that the magnetic field produced at outside points by the gas is the same as that due to a volume current density given by

$$c \text{ curl } \underline{I} = c \text{ curl } (- n\mu\underline{h}) = - \frac{1}{2} cm w_n^2 \text{ curl } (n/H) \qquad (44)$$

and a surface current distribution given by

$$c \underline{I} \times \underline{V} \qquad (45)$$

It is easily shown that (44) is equivalent to the volume current $\underline{i}_L$. The current (45) is the surface current above mentioned.

In the above illustrative case of a uniform magnetic field $\underline{H}$ and a uniform density distribution n throughout an infinite cylinder of circular cross section, the volume current is zero (since curl $\underline{I} = 0$), but there is a surface current of intensity given by

$$cI = - cn\mu \underline{h} = - \frac{1}{2} cmw_n^2 n/H = - cp_n/H \tag{46}$$

It is the negative $\emptyset$ direction.

However, if the sharply bounded <u>surface</u> is replaced by a thin boundary <u>layer</u>, in which the density n (or the pressure p_n) falls off rapidly to zero, the above surface current intensity is replaced by a volume current intensity in this layer. The effective volume density is due to ∇p_n, the first term in the bracket on the right hand side of (37). Thus it is given by

$$\frac{c}{8\pi\, p_m} \underline{H} \times \nabla p_n$$

The magnitude of this layer current is $- c \nabla\, p_n/H$; integration of this through the thin layer yields the same current as (46).

In the case of the Van Allen belts there will not be any sharp boundary of the ionized gas. Thus the volume currents alone need consideration.

3.4 THE STEADY RING CURRENT IN A DIPOLE FIELD

We now consider a special case of the volume current, which is given by (40) for a magnetic field of any form (subject only to the validity of the guiding center approximation). The special case relates to a steady unchanging system of particles, symmetrical round the axis, in the geomagnetic dipole field. Thus we omit the last term in (40), and use equations (12) and (13), so transforming (40) to

$$\underline{i} = - i\underline{k} \tag{47}$$

where

$$i = (c/H\ R_c)(p_s - p_n) - (c/H\ h_2)(\partial p_n / \partial r_e) \qquad (48)$$

In (47) a positive term in i denotes a westward contribution to the current density $\underline{i}$, and a negative term denotes an eastward contribution. The values of R_c and h_2 are given by (14) and (3).

In Akasofu (1960a) the ∇p_n term in (40)--corresponding to the second term in (48)--was briefly discussed and finally neglected. Also, writing $\underline{i} = ne\underline{V}$, the velocity $\underline{V}$ was loosely referred to as a drift velocity. These faults were justly criticized by Parker, Dessler and Johnson (1960, Private communication). The pressure gradient term is important, and $\underline{V}$ may more appropriately be called the mass transport velocity, according to the definition by Parker (1957, p. 929, equation 47).

Both terms in (48) depend on the pressure of the gas formed by the particles. This in turn depends on the number and velocity distribution of the particles. Owing to the continual gyration of the particles round the lines of force, the velocity distribution function will depend only on the speed w and the pitch angle θ, but not on the azimuth of $\underline{w}$ relative to the vector $\underline{h}$. Let F (w, θ) dw dθ denote the number density of the particles whose speeds lie between w and w + dw, and whose pitch angles lie between θ and θ + dθ. There will be such a function for each type of particle present. Thus

$$P_s = \sum \iint mw_s^2 \, F(w, \theta) \, dw \, d\theta = \sum \iint mw^2 \, F(w, \theta) \cos^2 \theta \, dw \, d\theta$$

$$P_n = \sum \iint \tfrac{1}{2} mw_n^2 \, F(w, \theta) \, dw \, d\theta = \sum \iint \tfrac{1}{2} mw^2 \, F(w, \theta) \sin^2 \theta \, dw \, d\theta$$

where the summation includes terms for each kind of particle, indicated by the addition of subscripts 1, 2, ...; m, w, F will all have such subscripts in each term.

For the present we shall consider particles of one type only, with speeds lying between $w + dw$. For brevity the symbols $\sum$ and $\int \ldots dw$ will be omitted from our equations. Expressions thus abbreviated will be denoted by an asterisk, thus:

$$p_s^* = mw^2 \int_0^\pi F(w, \theta) \cos^2 \theta \, d\theta, \quad p_n^* = \tfrac{1}{2} mw^2 \int^\pi F(w, \theta) \sin^2 \theta \, d\theta \tag{51}$$

This equation gives only one "item" of p_s and p_n. To obtain the complete value from such an item-expression we must integrate with respect to w and sum over all the types of particle present. These conventions will be applied not only to p_s and p_n but to all quantities derived from them or from $F(w, \theta)$. For example, the corresponding item of number density is given by

$$n^* = \int_0^\pi F(w, \theta) \, d\theta \tag{52}$$

The function $F(w, \theta)$ will in general depend not only on the variables explicitly indicated in its notation, but also on the position of the point P to which it relates. Thus it is also a function

of r_e and ϕ, but not of $\emptyset$, according to our condition of symmetry about the dipole axis. Owing to the relation of the motion of the particles to the magnetic field, F cannot be an arbitrary function of r_e and ϕ. Parker (1957) has discussed the relation between the form of F as a function of position, for points along any line of force in a general magnetic field. He showed that the relation is especially simple if F involves θ only by a factor $\sin^{\alpha+1}\theta$. If F is thus related to θ at one point of a line of force, it has the same relation at all points along the line. But in general the cofactor of $\sin^{\alpha+1}\theta$ in $F(w, \theta)$ will vary along the line, proportionately to $H^{-1/2\,\alpha}$.

3.41 Special pitch-angle distribution

Applying this general result to the dipole field here considered, the relation between the values of n^* at a general point P and at its associated equatorial point P_e on the line of force r_e is given by

$$n^* (r_e, \phi) = n^* (r_e) (H_e/H)^{1/2\,\alpha} \qquad (53)$$

For the last factor see (6).

The relation (52) between n^* and F when F has this special form of dependence on θ is

$$F (w, \theta) = n^* A (\alpha) \sin^{\alpha+1}\theta \qquad (54)$$

where

$$A(\alpha) = \Gamma(\alpha + 2) \,/\, 2^{\alpha+1} \left\{ \Gamma(\tfrac{1}{2}\alpha + 1) \right\}^2 \qquad (55)$$

The expression (54) applies to any point, such as P and P_e; the appropriate values of n^*, related as in (53), must be used in each case.

68

Inserting the special expression given by (54) in (51) we have

$$p_n^* = 2mw^2 B(\alpha)n^*, \quad p_s^* = mw^2 \left\{1 - 4B(\alpha)\right\} n^* \tag{56}$$

where

$$B(\alpha) = (\alpha + 2)/ 4(\alpha + 3) \tag{57}$$

Table 3.3 gives values of $B(\alpha)$ for various values of α.

Table 3.3

The Values of $B(\alpha)$ for Various Values of α

α	- 0.9	- 0.5	0	1	2
$B(\alpha)$	0.1310	0.1503	1/6	0.1878	1/5

Hence, from (48), using (53) and (56), i^* is obtained thus:

$$i^* = \frac{mcw^2}{H}\left[\frac{H_e}{H}\right]^{1/2}\left[n^*(r_e)\frac{\left\{1 - 6B(\alpha)\right\}}{R_c} - \frac{dn^*(r_e)}{dr_e}\frac{2B(\alpha)}{h_2}\right] \tag{58}$$

By means of equations (3), (6), (7) and (14), this may be transformed to

$$i^* = \frac{m\,w^2}{H_o a3}\left[n^*(r_e)\,r_e^2\,D_1(\phi, \alpha) - \frac{dn^*(r_e)}{dr_e}\,r_e^3\,F_1(\phi, \alpha)\right] \tag{59}$$

which is valid for the particular pitch-angle distribution (54).

Here

$$D_i(\phi, \alpha) = \frac{3\{1 - 6B(\alpha)\} (\cos \phi)^{5 + 3\alpha}}{(1 + 3 \sin^2 \phi)^{2 + 1/4\alpha}} \qquad (60)$$

and

$$F_i(\phi, \alpha) = \frac{2B(\alpha) (\cos \phi)^{3\alpha + 3}}{(1 + 3 \sin^2 \phi)^{1/4\alpha}} \qquad (61)$$

The complete value of i at any point P is given by

$$i = \int i^* \, dw \qquad (62)$$

integrated over all values of w and summed over all kinds of particle.

3.411 The case $\alpha = 0$; uniform distribution of velocity direction

When $\alpha = 0$ the pitch-angle distribution (54) corresponds to a uniform distribution of velocity direction. This is because $F(w, \theta)$ is then proportional to the zonal area of a sphere of radius w (in the velocity space) lying between the polar angles θ and $\theta + d\theta$. Moreover in this case, by (53), n^* has the same value all along any line of force, and by (59) the first term in i^* is everywhere zero. Thus (59) reduces to

$$i^* = -\frac{mcw^2}{H_o a^3} \frac{dn^*(r_e)}{dr_e} r_e^3 F_1(\phi, \alpha) \quad (\alpha = 1) \qquad (63)$$

This current is part of the current equivalent to the diamagnetism.

3.412 $\alpha \neq 0$

When $\alpha \neq 0$, the velocity-distribution is non-uniform. The density of velocity points on the sphere of radius w is proportional to

$F(w, \theta)/\sin \theta$. Fig. 3.2 illustrates this density as a function of θ for a few values of α. The curves are normalized to give the same mean density in each case. For $\alpha > 0$ the larger pitch angles are in excess, for $\alpha < 0$, the smaller pitch angles.

As H increases away from the equator along any line of force, (53) signifies that if $\alpha > 0$ the number density n^* decreases polewards, whereas for $\alpha < 0$ it increases polewards.

For $\alpha > 0$ the first part of i^* in (59) is negative, corresponding to an eastward flow; for $\alpha < 0$ this part is positive, therefore westward.

For all values of α, the sign of the second part of i^* in (59) is negative (eastward) when $n^*(r_e)$ is increasing outwards, and positive (westward) where $n^*(r_e)$ is decreasing outward. If $n^*(r_e)$ increases outwards to a single maximum at $r_e = r_{eo}$, and then declines to zero as r_e further increases, the second part of i^* is eastward for $r_e < r_{eo}$, and westward for $r_e > r_{eo}$. If the distribution of $n^*(r_e)$ is less simple, the distribution of this part of i^* will be more complicated.

3.42 A special number-density distribution

Our discussion will now be further specialized by taking the function $n^*(r_e)$ to have the following form:

$$n^*(r_e) = n_o^* e^{-q^2 x^2} \tag{64}$$

where

$$x = r_e - r_{eo} \tag{65}$$

Thus n^* has its maximum at $x = 0$, $r_e = r_{eo}$.

Taking the earth's radius a as the unit of length we write

$$r_e = fa, \qquad r_{eo} = f_o a \qquad\qquad (66)$$

$$q = g/a \qquad\qquad (67)$$

$$x = (f - f_o)a = za \qquad\qquad (68)$$

The values of g (or q) determine how the particles are distributed relative to the center line of the belt, $r_e = r_{eo}$. The greater the value of g, the less the effective width of the belt, and the greater the gradient of the number density distribution $dn^*(r_e)/dr_e$, so that the number density decreases more steeply inwards and outwards from the center line of the belt. Table 3.4 gives the number density for several values of g at a distance $x = \pm$ a from the center of the belt.

Table 3.4

Values of g and the Corresponding Density at a Distance $x = \pm$ a

from the Center of the Belt

g	1.517	2.145	2.625
n at $x = \pm$ a from the center	$n_o/10$	$n_o/100$	$n_o/1000$

A Gaussian distribution (64) with g = - 1.52 fits the middle part (from r_e = 3.5a to r_e = 4.5a) of V_2, the outer Van Allen belt (cf. Van Allen and Frank 1959).

3.421 The current intensity distribution

The special density distribution given by (53) and (64) leads to the following distribution of current intensity, using (59):

$$i^* = i_o^* \left\{ C_i(g, f_o, z) \, D_i(\phi, \alpha) + E_i(g, f_o, z) \, F_i(\phi, \alpha) \right\} \qquad (69)$$

where

$$i_o^* = n_o^* \, mcw^2/H_o a \qquad (70)$$

$$C_i(g, f_o, z) = (f_o + z)^2 \, e^{-g^2 z^2} \qquad (71)$$

$$E_i(g, f_o, z) = 2 \, g^2 z (f_o + z)^3 \, e^{-g^2 z^2} \qquad (72)$$

For illustration the two parts of i^* have been calculated for many points in the meridian plane, for a hypothetical V_3 belt (§3.73), corresponding to the following values of f_o, α and g:

$$f_o = 6, \quad \alpha = -\frac{1}{2}, \quad g = 1.517 \qquad (73)$$

As shown in Table 3.4, this value of g corresponds to a reduction of the density by a factor 10 at the distances $\pm$ a from the center line of the belt. The calculated values of i^* have been used in drawing the current contour lines, or lines of constant current intensity, shown in Fig. 3.3a, 3.3b and 3.3c. Figs. 3.3a and 3.3b relate to the first and second parts of i^* in (69), and Fig. 3.3c relates to i^* itself. The contour lines are numbered in terms of the value i^+ at the center line of the belt, $r_e = r_{eo}$ (or $z = 0$) and $\phi = 0$;

$$i^+ = 3f_o^2 \left\{ 1 - 6B(\alpha) \right\} i_o^*$$

$$= 1.56 \times 10^3 \; n_o^* \; mw^2 \; esu$$

$$\doteq 1.61 \times 10^{-15} \; n_o^* \; \mathcal{E} \; amperes$$

where $\mathcal{E}$ denotes the kinetic energy of the particle expressed in Kev.

As already stated (§ 3.412), in the present case ($\alpha < 0$) the first part of i^* (Fig. 3.3a) is everywhere westward. The second part is east-ward on the inner side of the belt and westward on the outer side (Fig. 3.3b). The resultant current i^* is more westward than eastward, but it is eastward, in the equatorial plane, within a radius slightly less than r_{eo}. The maximum westward intensity in this plane slightly exceeds $12i^+$, at about 6.5a; the maximum eastward intensity is rather more than $6i^+$, at about 5.6a.

3.43 The total ring current

The total ring current J^* corresponding to i^* is given by

$$J^* = \iint i^* \; dS_3 = \iint i^* \; r_e \cos^4 \phi \; dr_e \; d\phi$$

using (5). Inserting (59), this equation may be rewritten thus:

$$(74)$$

$$J^* = \frac{mcw^2}{H_o a^3} \iint \left[n^*(r_e) \; r_e^3 \; D_J(\phi, \alpha) - \frac{dn^*(r_e)}{dr_e} \; r_e^4 \; F_J(\phi, \alpha) \right] dr_e \; d\phi$$

where

$$D_J(\phi, \alpha) = D_i(\phi, \alpha) \cos^4 \phi = \frac{3 \left\{ 1 - 6B(\alpha) \right\} (\cos \phi)^{9 + 3\alpha}}{(1 + 3 \sin^2 \phi)^{2 + 1/4 \alpha}} \qquad (75)$$

$$F_J(\phi, \alpha) = F_i(\phi, \alpha) \cos^4 \phi = \frac{2B(\alpha) (\cos \phi)^{3\alpha + 7}}{(1 + 3 \sin^2 \phi)^{1/4 \alpha}} \qquad (76)$$

In order to integrate the above equation, it must be realized that the extent of the belt is limited by the solid earth and also by the dense lower atmosphere, although we do not discuss the latter effect in this paper. The meridian cross section of the volume occupied by the particles will be bounded by a closed curve which is symmetrical with respect to the equatorial radius (the curve $Ar_2 A'r_1$ in Fig. 3.4). Let $\pm \phi(r_e)$ denote the latitudes of the points A and A' where the line of force r_e meets the curve, and r_1 and r_2 denote the values of r_e where the curve crosses the equatorial plane. Thus the limits of the integration with respect to ϕ must be $\pm \phi(r_e)$, and those with respect to r_e must be r_1 and r_2. Rewriting (74), we have

$$J^* = \frac{2mcw^2}{H_o a^3} \left[\int_{r_1}^{r_2} n^*(r_e)\, r_e^3\, I_D(r_e,\alpha)\, dr_e - \int_{r_1}^{r_2} \frac{dn^*(r_e)}{dr_e}\, r_e^4\, I_F(r_e,\alpha)\, dr_e \right] \tag{77}$$

where

$$I_D(r_e,\alpha) = I_D\left\{\phi(r_e),\alpha\right\} \tag{78}$$

and

$$I_D(\phi,\alpha) = \int_0^\phi D_J(\phi,\alpha)\, d\phi \tag{78'}$$

and also

$$I_F(r_e,\alpha) = I_F\left\{\phi(r_e),\alpha\right\} \tag{79}$$

and

$$I_F(\phi,\alpha) = \int_0^\phi F_J(\phi,\alpha)\, d\phi \tag{80}$$

Figs. 3.5 and 3.6 show $I_D(\phi,\alpha)$ and $I_F(\phi,\alpha)$ respectively as functions of ϕ for various values of α. As ϕ increases from 0 to $\pi/2$, $I_D(\phi,\alpha)$ and $I_F(\phi,\alpha)$ increase from 0 to $I_D(\pi/2,\alpha)$ and $I_F(\pi/2,\alpha)$

respectively. For each value of α, the variations of I_D and I_F are small beyond certain values of ϕ. Table 3.5 gives $I_D(\pi/2, \alpha)$ and $I_F(\pi/2, \alpha)$ for several values of α and the latitudes ϕ at which they attain approximately 99% and 90% of the maximum values (for $\phi = \pi/2$).

Table 3.5

Values of $I_D(\pi/2, \alpha)$ and $I_F(\pi/2, \alpha)$ for Several Values of α, and the latitudes at which they attain approximately 99% and 90% of the above values

α =	- 0.9	- 0.5	0	1	2
I_D	0.2256	0.0966	0	-0.1028	-0.1472
ϕ (99%)	45°	42°		34°	31°
ϕ (90%)	23°	26°		20°	19°
I_F	0.1617	0.1593	0.1523	0.1383	0.1262
ϕ (99%)	61°	56°	50°	42°	37°
ϕ (90%)	42°	37°	34°	28°	26°

In connection with the radiation belt, we will consider values of r_1, the lower limit of r_e in (77), not less than 2.5a. The lines of force $r_e \geqslant 2a$ meet the earth's surface at $\phi \geqslant 45°$. For the values of ϕ likely to be of physical interest in this problem, we may without significant error substitute $I_D(\pi/2, \alpha)$ for $I_D(r_e, \alpha)$ and $I_F(\pi/2, \alpha)$ for $I_F(r_e, \alpha)$. Thus (77) becomes

$$J^* = \frac{2mcw^2}{H_o a^3} \left[I_D(\pi/2, \alpha) \int_{r_1}^{r_2} n^*(r_e) \, r_e^3 \, dr_e - I_F(\pi/2, \alpha) \int_{r_1}^{r_2} \frac{dn^*(r_e)}{dr_e} \, r_e^4 \, dr_e \right] \tag{81}$$

3.431 The total current for the special number density distribution (64)

The special density distribution given by (53) and (64) leads to the following total current:

$$J^* = \frac{2mcw^2 n_o^* a}{H_o} \left[I_D(\pi/2, \alpha) \int_{r_1'}^{r_2'} C_J(g, f_o, z) \, dz + I_F(\pi/2, \alpha) \int_{r_1'}^{r_2'} E_J(g, f_o, z) \, dz \right] \tag{82}$$

using (66), (67) and (68). Here

$$C_J(g, f_o, z) = (f_o + z) \, C_i(g, f_o, z) = (f_o + z)^3 \, e^{-g^2 z^2} \tag{83}$$

$$E_J(g, f_o, z) = (f_o + z) \, E_i(g, f_o, z) = 2g^2 z (f_o + z)^4 \, e^{-g^2 z^2} \tag{84}$$

Also we change the limits of the integration with respect to z, from r_1' and r_2' respectively to $-\infty$ and ∞. For the range of g in Table 3.4 this may be a reasonable first approximation (about 99.9%). Thus (82) becomes

$$J^* = \frac{2mcw^2 \, n_o^* a (\pi)^{1/2}}{H_o} \left(\frac{f_o^3}{g} + \frac{3f_o}{2g^3} \right) \left[I_D(\pi/2, \alpha) + 4I_F(\pi/2, \alpha) \right]$$

$$\tag{85}$$

$$= 88.20 \, n_o^* \, \in (Kev) \left(\frac{f_o^3}{g} + \frac{3f_o}{2g^3} \right) \left[I_D(\pi/2, \alpha) + 4I_F(\pi/2, \alpha) \right] \text{ amperes}$$

The values of $\left\{ (f_o^3/g) + (3f_o/2g^3) \right\}$ are tabulated in Table 3.6 for various values of f_o and g.

Table 3.6

Values of $\left\{(f_o^3/g) + (3f_o/2g^3)\right\}$ for Various Values of f_o and g

$g \backslash f_o$	3.5	4	5	6	7	8	9	10
1.517	29.77	43.91	84.55	145.0	229.1	340.9	484.5	663.5
2.145	20.52	30.45	59.04	101.6	161.0	239.9	341.3	467.7
2.625	16.63	24.71	48.03	82.79	131.3	195.7	278.4	381.8

The values of $I_D(\pi/2, \alpha) + 4I_F(\pi/2, \alpha)$ are also given in Table 3.7 for several values of α.

Table 3.7

Values of $\left[I_D(\pi/2, \alpha) + 4I_F(\pi/2, \alpha)\right]$ for several values of α

α	-0.9	-0.5	0	1	2
$\left[I_D + 4I_F\right]$	0.8724	0.7338	0.6092	0.4504	0.3576

For our model belt (73), we find that

$$J^* = 9.38 \times 10^3 \, n_o^* \, \in \text{ amperes} \tag{86}$$

In the outer radiation belt (V_2) we may adopt

$$f_o = 3.5, \quad g = 1.517. \tag{87}$$

Hence for $\alpha = 1$,

$$\left[I_D + 4I_F\right] = 0.4504$$

and

$$J^* = 1.18 \times 10^3 \, n_o^* \, \in \text{amperes} \tag{88}$$

This result is less than the value given by (86), mainly because of the smaller cross section. In § 3.522 we discuss the energy spectrum of the particles in the V_2 belt and the value of α .

3.5 THE MAGNETIC FIELD PRODUCED BY THE RING CURRENT

Let H^*_ω and H^*_z denote respectively the components of the magnetic field of the ring current, parallel and perpendicular to the equatorial plane, at a point (r_{e1}, ϕ_1). Let δH^*_ω and δH^*_z denote the contributions to these components, made by the part of the ring current i^* that flows across the section dS_3 at (r_{e2}, ϕ_2). They are given (cf. Stratton 1941, p. 263) by

$$\delta H^*_\omega = - \frac{2 \, i^* \, dS_3}{c} \frac{\zeta}{\omega \left[(\xi + \omega)^2 + \zeta^2 \right]^{1/2}} \left[-K + \frac{\xi^2 + \omega^2 + \zeta^2}{(\xi - \omega)^2 + \zeta^2} \, E \right] \quad (89a)$$

and

$$\delta H^*_z = - \frac{2 \, i^* \, dS_3}{c} \frac{1}{\left[(\xi + \omega)^2 + \zeta^2 \right]^{1/2}} \left[K + \frac{\xi^2 - \omega^2 - \zeta^2}{(\xi - \omega)^2 + \zeta^2} \, E \right] \quad (89b)$$

Here

$$\omega = r_{e1} \cos^3 \phi_1$$

$$\zeta = r_{e1} \cos^2 \phi_1 \sin \phi_1 - r_{e2} \cos^2 \phi_2 \sin \phi_2 \quad (90)$$

$$\xi = r_{e2} \cos^3 \phi_2$$

and $K (k^2)$ and $E (k^2)$ are the complete elliptic integrals of the first and second kinds for

$$k^2 = \frac{4 \, \xi \, \omega}{(\xi + \omega)^2 + \zeta^2} \quad (91)$$

79

The complete values of H_ω and H_z are obtained by integrating (89a) and (89b) over the meridian cross section of the belt and then by summing as follows:

$$H_\omega = \int H_\omega^* dw$$

$$Hz = \int H_z^* dw$$

(92)

3.51 The magnetic field along an equatorial radius

In order to see how our model ring current fits the magnetic observations made by satellites, H_ω and H_z must be calculated for points along the path of satellites. Here the calculation is made only for points along the equatorial radius, where

$$\phi_1 = 0$$

and

$$\omega = r_{e1}$$

$$\zeta = - r_{e2} \cos^2 \phi_2 \sin \phi_2$$

$$\xi = r_{e2} \cos^3 \phi_2$$

The component H_ω^* vanishes because of the symmetry of the cross section of the belt with respect to the equatorial plane. Thus

(93)*

$$H_z^* = - \frac{2}{c} \iint \frac{i^*}{\left[(\xi + r_{e1})^2 + \zeta^2 \right]^{1/2}} \left[K + \frac{\xi^2 - r_{e1}^2 - \zeta^2}{(\xi - r_{e1})^2 + \zeta^2} E \right] r_{e2} \cos^4 \phi \, dr_{e2} d\phi_2$$

---

* For the numerical integration of (93) and the comparison with the satellite observation, see Appendix II ,p.107a .

3.52 The magnetic field at the earth's center

When the point (r_{e1}, ϕ_1) is located at the earth's center, (93) reduces to

$$H_{zc}^* = -\frac{2\pi}{c} \iint \frac{i^* \, dS_3}{r_e} \tag{94}$$

where

$$r_{e1} = 0 \text{ and } \phi_1 = 0$$

$$\omega = 0$$

$$\zeta = -r_{e2} \cos^2 \phi_2 \sin \phi_2$$

$$\xi = r_{e2} \cos^3 \phi_2 \tag{95}$$

$$E \, (k^2 = 0) = K \, (k^2 = 0) = \pi/2$$

Using (81) and (94), we have

$$\tag{96}$$

$$H_{zc}^* = \frac{2mcw^2}{H_o a^3} \left[I_D(\pi/2, \alpha) \int_{r_1}^{r_2} n^*(r_e) \, r_e^2 \, dr_e - I_F(\pi/2, \alpha) \int_{r_1}^{r_2} \frac{dn^*(r_e)}{dr_e} \, r_e^3 \, dr_e \right]$$

3.521 The magnetic field at the earth's center for the special number density distribution (64)

If we adopt a Gaussian number density distribution along an equatorial radius as given by (64), (96) can be transformed to:

$$\tag{97}$$

$$H_{zc}^* = \frac{2mcw^2 \, n_o^*}{H_o} \left[I_D(\pi/2, \alpha) \int_{r_1'}^{r_2'} C_i(g, f_o, z) \, dz + I_F(\pi/2, \alpha) \int_{r_1'}^{r_2'} F_i(g, f_o, z) \, dz \right]$$

where $C_i(g, f_o, z)$ and $F_i(g, f_o, z)$ are respectively given by (71) and (72).

Taking the same upper and lower limits of integration to be $\pm \infty$, as for (82), (97) becomes

$$(98)$$

$$H^*_{zc} = - \frac{4(\pi)^{3/2}{}_{mw}{}^2\, n^*_o}{H_o} \left(\frac{f^2_o}{g} + \frac{1}{2g^3} \right) \left[I_D\,(\pi/2, \alpha) + 3I_F(\pi/2, \alpha) \right]$$

$$= - 2.23 \times 10^{-2} n^*_o \epsilon \left(\frac{f^2_o}{g} + \frac{1}{2g^3} \right) \left[I_D\,(\pi/2, \alpha) + 3I_R(\pi/2, \alpha) \right] \quad (\text{in } \%)$$

The values of $\left\{ (f^2_o/g) + (1/2g^3) \right\}$ and $\left\{ I_D(\pi/2, \alpha) + 3I_F(\pi/2, \alpha) \right\}$ are tabulated respectively in Table 3.8 and Table 3.9.

Table 3.8

Values of $\left\{ (f^2_o/g) + (1/2g^3) \right\}$ for Various Values of f and g

g \ f_o	3.5	4	5	6	7	8	9	10
1.517	8.218	10.69	16.62	23.87	32.44	42.33	53.53	66.06
2.145	5.762	7.510	11.71	16.83	22.89	29.89	37.81	46.67
2.625	4.695	6.123	9.552	13.74	18.70	24.41	30.89	38.13

Table 3.9

Values of $\left\{ I_D(\pi/2, \alpha) + 3I_F(\pi/2, \alpha) \right\}$ for Several Values of α

α	- 0.9	- 0.5	0	1	2
$I_D + 3I_F$	0.7107	0.5745	0.4569	0.3121	0.2314

For our model V_3 belt (73), the result is

$$H^*_{zc} = - 0.306\, n^*_o \in \gamma \tag{99}$$

3.522 The magnetic field H_{zc} produced by the particles
with a special energy spectrum in the outer radiation belt V_2

For the V_2 belt (87), the field intensity H^*_{zc} is given by

$$H^*_{zc} = - 0.1833 \left[I_D(\pi/2, \alpha) + 3 I_F(\pi/2, \alpha) \right] n^*_o \in \gamma \tag{100}$$

In a steady state, the value of α in the V_2 belt may be positive. The
particles with a small pitch-angle have their mirror points in the dense
atmosphere and they will be absorbed during the oscillatory motion be-
tween the mirror points. For illustration, for α we adopt the value 1.
Then (100) becomes

$$H^*_{zc} = - 0.0572\, n^*_o \in \gamma \tag{101}$$

The complete value of H_{zc} is then given by

$$H_{zc} = \int H^*_{zc}\, dw = - 0.0572 \int n^*_o \in d\in \tag{102}$$

In order to calculate H_{zc} we must know the energy spectrum of the
particles in the belt. Van Allen (1959) summarized all the information
available as follows:

	Energy	Flux
Electrons	$\in > \quad 20$ Kev	$\sim 1 \times 10^{11}/cm^2$ sec
	$\in > \quad 200$ Kev	$\leq 1 \times 10^8/cm^2$ sec
Protons	$\in > \quad 60$ Mev	$\leq 10^2/cm^2$ sec
	$\in < \quad 30$ Mev	no significant information

83

It seems that at present we do not know the energy spectrum of the particles in the V_2 belt. For illustration, we assume a Maxwellian type velocity-distribution (cf. Chapman and Cowling 1953, p. 72):

$$n_o^* = \left(\frac{2}{\pi}\right)^{1/2} n_o \left[\frac{m}{kT}\right]^{3/2} w^2 \, e^{-mw^2/2kT} \, dw \tag{103}$$

where k denotes the Boltzmann constant and T the temperature.

In terms of energy ϵ ($= \frac{1}{2}mw^2$), (103) may be rewritten as

$$n_o^* = \frac{n_o}{(2\pi)^{1/2}} \left[\frac{1}{\epsilon_m}\right]^{3/2} e^{-\epsilon/2\epsilon_m} \epsilon^{1/2} \, d\epsilon \tag{104}$$

where ϵ_m denotes the energy for which n_o^* has the maximum value. Note that n_o, the total number density at r_{eo}, satisfies the equation

$$n_o = \int n_o^* \, dw = \int_o^\infty \frac{n_o}{(2\pi)^{1/2}} \left[\frac{1}{\epsilon_m}\right]^{3/2} e^{-\epsilon/2\epsilon_m} \epsilon^{1/2} \, d\epsilon \tag{105}$$

Using (104), we have

$$\int n_o^* \epsilon \, d\epsilon = \int_o^\infty \frac{n_o}{(2\pi)^{1/2}} \left[\frac{1}{\epsilon_m}\right]^{3/2} e^{-\epsilon/2\epsilon_m} \epsilon^{3/2} \, d\epsilon \tag{106}$$
$$= 3n_o \epsilon_m$$

Thus, (102) and (106) lead to the following important equation,

$$H_{zc} = -0.172 \, n_o \epsilon_m \, \gamma \tag{107}$$

Neither for electrons nor protons is there at present any available information on n_o and ϵ_m. It is not known whether the value of ϵ_m is above or below the instrumental cut-off. For electrons, however, we may tentatively adopt the values $n_o = 20/cc$ and $\epsilon_m = 10$ Kev (just below the

instrumental cut-off). Then the magnetic field produced by the electrons in the V_2 belt is given by

$$H_{zc} = - 34.4 \; \gamma \tag{108}$$

At present it seems impossible to judge how much the protons in the belt add to the combined H_{zc}.

Equation (108) suggests that the reduction of the horizontal component of the field at the earth's surface resulting from the existence of the outer radiation belt may be of order 1/1000 of the normal intensity H_o. This inference is valid under the following conditions:

(a) the actual pitch-angle distribution is given by (54) with $\alpha = 1$,

(b) the density distribution is Gaussian, given by (64) with $g = 1.517$,

(c) the energy spectrum is of Maxwellian type (104) with $n_o = 10/cc$ and $\xi_m = 10$ Kev,

(d) the proton contribution is of similar or less magnitude.

If such a V_2 belt completely vanished, the field intensity at the earth's surface would be increased by about 34 γ .

3.54 The total number of particles

It is of interest to express (98) in terms of the total number N of particles in the belt. The total number N is given by

$$N = \iiint n(r_e, \phi) \; dV = \iiint n(r_e, \phi) \; r_e^2 \cos^7 \phi \; dr_e \; d\phi \; d\emptyset \tag{109}$$

using (8). Substituting our special type of number density distribution (53), corresponding to the $\sin^\alpha \theta$ pitch-angle distribution, we obtain

$$N^* = 2\pi \int_{r_1}^{r_2} \int_{-\phi(r_e)}^{\phi(r_e)} n^*(r_e) \, r_e^2 \cos^7 \phi \left[\frac{\cos^6 \phi}{(1 + 3 \sin^2\phi)^{1/2}} \right]^{1/2} dr_e \, d\phi$$

$$= 4\pi \frac{I_F(\pi/2, \alpha)}{(2B(\alpha))} \int_{r_1}^{r_2} n^*(r_e) \, r_e^2 \, dr_e \tag{110}$$

where $I_F(\pi/2, \alpha)$ is given by (80).

Introducing a Gaussian number density distribution (64) along an equatorial radius, (110) is transformed to:

$$N^* = \frac{4(\pi)^{3/2} a^3 n_0^* I_F(\pi/2, \alpha)}{2B(\alpha)} \left(\frac{f_0^2}{g} + \frac{1}{2g^3} \right)$$

$$= 5.780 \times 10^{27} \left(\frac{f_0^2}{g} + \frac{1}{2g^3} \right) \frac{I_F(\pi/2, \alpha)}{2B(\alpha)} n_0^* \tag{111}$$

The factor $\left\{ (f_0^2/g) + (1/2g^3) \right\}$ is given in Table 3.8, and $I_F(\pi/2, \alpha)/2B(\alpha)$ is given in Table 3.10 for several values of α.

Table 3.10

Values of $I_F(\pi/2, \alpha)/2B(\alpha)$ for Several Values of α

α	-0.9	-0.5	0	1	2
$\dfrac{I_F(\pi/2, \alpha)}{2B(\alpha)}$	0.6170	0.5300	0.4570	0.3683	0.3154

In our model V_3 belt (73),

$$N^* = 7.31 \times 10^{28} \, n_0^* \tag{112}$$

and in the V_2 belt ((87) with $\alpha = 1$), it is given by

$$N^* = 1.75 \times 10^{28} \, n_o^*$$ (113)

It may be noticed that

$$N = \int N^* \, dw = 1.75 \times 10^{28} \int n_o^* \, dw = 1.75 \times 10^{28} \, n_o$$ (114)

3.541 The magnetic field at the earth's center produced by the

ring current in terms of the total number of the particles

Inserting n_o^* from (111) into (98), we have

$$H_z^* = -7.716 \times 10^{-30} B(\alpha) \left[\frac{I_D(\pi/2, \alpha)}{I_F(\pi/2, \alpha)} + 3 \right] N^* \epsilon$$ (115)

The values of $B(\alpha) \left\{ \left[I_D(\pi/2, \alpha) / I_F(\pi/2, \alpha) \right] + 3 \right\}$ are given in

Table 3.11 for several values of α .

Table 3.11

Values of $B(\alpha) \left\{ \left[I_D(\pi/2, \alpha) / I_F(\pi/2, \alpha) \right] + 3 \right\}$

for Several Values of α

α	-0.9	-0.5	0	1	2
$B(\alpha) \left[\dfrac{I_D(\pi/2, \alpha)}{I_F(\pi/2, \alpha)} + 3 \right]$	0.5757	0.5420	0.5001	0.4239	0.3668

In our model V_3 belt (73),

$$H_{zc}^* = -4.182 \times 10^{-30} N^* \epsilon \, \gamma$$ (116)

and in the V_2 belt ((87) with $\alpha = 1$), it is given by

$$H^*_{zc} = - 3.27 \times 10^{-30} \, N^* \in \gamma \qquad (117)$$

The complete value of H_{zc} is then given by

$$H_{zc} = \int H^*_{zc} \, dw = - 3.27 \times 10^{-30} \int N^* \in d\in \gamma$$

$$= - 9.81 \times 10^{-30} \, N \in_m \gamma \qquad (118)$$

Therefore if both H_{zc} and $\in_m$ are obtained, it is possible to calculate the total number in our model V_2 belt.

3.6 THE MAIN PHASE OF MAGNETIC STORMS

In this section we discuss the main phase of several magnetic storms that occurred during the IGY and IGC 1959. We show how the development of the main phase differs from one storm to another, and we discuss the injection of solar particles into the region of the ring current.

It is interesting to consider first the variation of the monthly mean values of H during the IGY, in the same way as Schmidt (1917), who used the Potsdam H data from 1904 to 1910 (Chapman and Bartels 1940, p. 293). A station like Potsdam, in geomagnetic latitude $52°5$ N, is much affected by polar magnetic disturbances. Hence it is preferable to use H data for a station in a low geomagnetic latitude, where the effect of polar disturbances is less, and the ring current influence is greatest. We have used the data for Koror (gm. lat. $3°3$ S; dip angle $+ 0° 48'$).

Fig. 3.7 shows the monthly mean values of the horizontal component
at Koror observatory during the IGY. The Koror mean value of H obtained
from quiet days during the IGY is 37,860 γ. The monthly mean values
(for all days) during the IGY were below this mean except for November
1958. The largest decrease of H occurred in September 1957, and the
second largest in July 1958. For September 1957 the deviation from the
IGY quiet-day mean was 60 γ.

Fig. 3.8 shows for the period from 1957 August 25 to October 10 the
changes of the daily mean values of the H component at Koror. Clearly
the large September 1957 decrease of monthly mean H in Fig. 3.7 resulted
from the appearance of several large but brief magnetic disturbances.
Fig. 3.8 shows by arrows the sudden commencements of the nine storms for
that month (Geomagnetic and Solar Data 1958). The large impulsive
decreases that began on September 2, 12 and 21 resulted from the super-
position of two or three successive storms, involving the superposition
of successive ring currents. After the minima were reached, the H
component quickly recovered, and regained values approaching or even
exceeding the IGY mean value.

The ring current may not die away completely during a magnetically
disturbed month. As yet we have no way of knowing the value of the H
component which would correspond to the complete disappearance of the
ring current. But Fig. 3.8 suggests that the major part of the ring
current that is enhanced during magnetic storms has a rather short life,
and does not survive more than 10 days if there is no continued inject-
tion of solar particles. In the following we discuss the main phases of
several magnetic storms that occurred during the IGY and IGC 1959,

89

including the two storms of September 1957 in Fig. 3.8.

Let X_m and Y_m denote the instantaneous values of the north-south and the east-west components of the geomagnetic field at a point.

We first consider the storms of 1957 September 13 (Fig. 3.9) and 1957 September 29 (Fig. 3.10). In both cases it happened that their ssc's occurred close to Greenwich midnight, namely $00^h 47^m$ GMT, 13 September and $00^h 16^m$, 29 September, 1957. There were no significant magnetic disturbances between the Greenwich midnight and the times of their ssc's. Thus we take the base value for X_m and Y_m to be the value at Greenwich midnight in each case, and storm time is reckoned from that time. In order to show the latitude dependence of the Dst, we divide the earth's surface into four zones, bounded as follows by circles of geomagnetic latitude:

Group I   Between $\pm 5^o$

Group II   From 5° to 20° and from -5° to -20°

Group III   From 20° to 40° and from -20° to -40°

Group IV   From 40° to 60° and from -40° to -60°

Figs. 3.9 and 3.10 show the Dst (X_m) and Dst (Y_m) curves thus obtained. The contributing observatories in the four zones are listed in the Appendix.

The Dst (X_m) curves in Fig. 3.9 show a notable ssc of order 100 γ at $00^h 47^m$ GMT on September 13, 1957. We ascribe this to the DCF field. The magnetograms from the polar region (which are not given in this paper) show that the ssc was soon followed by active DP substorms. As occurs in most (if not all) great magnetic storms, the DCF field was

quickly overpowered by the DR field. This occurred about two hours

after the ssc. The Dst (X_m) curve attained its minimum at $09^h\ 00^m$, about

8 hours after the ssc. We estimate that the total DR field at the

earth's surface was at least of order 600 γ. Thus the external part of

H_{zc} was about 400 γ. The ring current began to decay quickly after 09^h,

when also the major DP disturbances ceased. Small irregularities super-

posed on the Dst (X_m) curve in Fig. 3.9 are attributed to the incomplete

elimination of the effects of DP sub-storms. Dst (Y_m) shows a small

increase of order less than 50 γ. Comparing Dst (X_m) with Dst (Y_m), it

is clear that the main DR variation was produced by a westward current.

The Dst (X_m) and Dst (Y_m) curves in Fig. 3.10 show a less marked

DCF increase at $00^h\ 16^m$ GMT on September 29, 1957. The ring current

seemed to become appreciable around 06^h, but decayed or was overcome by

the DCF field at about 12^h. A remarkable growth of the DR field began

at about $13^h\ 20^m$. It attained its maximum at 17^h. Many large DP sub-

storms are superposed on the Dst curves. They make it difficult to

determine the exact course of the DR change. It seems that the ring

current remained strong until 23^h, that is, for about 6 hours, and then

began to decay.

It is interesting to compare the Dst (X_m) curves with the H magneto-

grams (Fig. 5.6) from 12 stations along the auroral zone. These show

mainly the DP sub-storm activity. A DP sub-storm is generally intense

over only a part of the auroral zone, so that it may scarcely be indicated

by the records of observatories elsewhere. But 12 observatories well

distributed along the zone make it possible to record most large DP sub-

storms. On September 29 the auroral zone was rather quiet until 12^h,

except at about 05^h, when a small DP disturbance was recorded. Remarkable DP disturbances began at about $13^h 30^m$. Though very transient and intermittent, they remained active until the end of the day. Comparing Figs. 3.10 and 5.6, it seems that the DR and the DP activities were apparently closely correlated. Both the DR and DP activities were moderate until about $13^h 30^m$, when they suddenly became active. They continued to be active until the end of the day.

Figs. 3.11a and b show Dst (H) curves for the July 11 and the July 15 storms. They give the average variation of H derived from 12 observatories well distributed round the earth between latitudes $\pm 45^o$ (see Appendix). The difference between Dst (H) and Dst (X_m) is very small for stations whose latitudes are less than 45°. We have discussed the differences between the two storms in detail in a recent paper (Akasofu and Chapman 1960). There was little indication of large DP sub-storms in the auroral zone during the remarkable initial phase (mainly DCF) of the July 11 storm; this phase lasted for at least 7 hours. The earth was presumably within an intense solar stream during that time, but the small DR and DP activity suggests that only a small part of the solar gas was trapped during that time. Only one appreciable DP sub-storm occurred (at about $23^h 30^m$ GMT on July 11). On the other hand, the initial phase of the July 15 storm was interrupted by an abnormally large DP sub-storm about 30 minutes after the ssc. Throughout this storm both the DP sub-storms and the DR field were considerable.

Fig. 3.12 shows the College magnetograms (gm. lat. $64^o.7$ N) of the July 11 and July 15 storms. The striking contrast in the DP activity on those days is clearly seen.

Fig. 3.13a shows the Dst (H) curve for the 1959 August 16-18 storm;
the curve refers to 13 low latitude observatories (see Appendix). This
storm was characterized by prolonged DR activity and many successive
small sub-storms. These continued for about 48 hours.

The above several examples indicate that magnetic storms can develop
in different ways, particularly as regards the course and intensity of
the DCF, DR and DP sub-storm fields. The magnetic records suggest that
in some cases a considerable amount of solar gas is trapped, and in
others only a little. We think that a simple regular neutral ionized
stream, of the type hitherto mainly considered in theories of magnetic
storms, can produce the DCF field. The intensity of this field is not
necessarily correlated with the intensity of the main phase and the ring
current. The development of the main phase and of the DP sub-storms
probably depends on irregularities embedded in the solar streams emitted
from time to time from the sun. The degree of capture of solar particles
from such irregularities may control the variation of the DR field and
of the DP sub-storms.

We believe there is reason to think that when the intensity of the
ring current is sufficiently increased, the field direction may be
reversed in certain limited regions, forming neutral lines in or near
the equatorial plane, on the inner side of the ring current. Recently we
have proposed a new theory of the aurora, based on the postulated exist-
ence of such neutral lines (Akasofu and Chapman 1961a, see § 4). A
diffuse aurora may be produced by high energy electrons issuing from a
narrow strip close to the neutral line, located in the outer part of the
outer radiation belt. We showed (loc. cit.; see § 4) that the development

of the DP sub-storm coincides with the change of the aurora from the diffuse to the active form. We think that the active aurora is produced by a slight eastward electric field along the neutral line. The eastward electric field may arise from the differential motion of protons and electrons injected from irregularities in the solar stream, as mentioned above. If so, DP sub-storm activity can be interpreted as indicating injection in or near a region where there is a neutral line.

As Fig. 5.6 indicates, DP sub-storms are short-lived phenomena. In general, several large DP storms appear during a medium magnetic storm. The injection may occur when irregularities in the solar stream traverse the space around the earth. From this point of view, the injection of solar particles during the course of the storms discussed above may be summarized as follows:

September 13 storm:

The ssc was followed for about 10 hours by a number of large intermittent injections. The remarkable ring current began to develop about 2 hours after the ssc. It attained its maximum intensity at $09^h 00^m$ (about 8 hours after the ssc). The major injection ceased at about the same time, and the ring current quickly began to decay.

September 29 storm:

Large injections began about 13 hours after the ssc. A notable ring current started at about the same time. The intermittent injections lasted for about 10 hours. The ring current remained strong during that time. The injection ceased at the end of the day, and the ring current then began to decay.

94

July 11 storm:

No appreciable injection occurred for about 7 hours after the ssc. During that period the earth was enclosed by an intense regular solar stream. Only one appreciable injection occurred, at about $23^h\ 30^m$, but nothing particular later. The intensity of the ring current was very small.

July 15 storm:

The ssc was followed by a great number of large injections for about 10 hours or more. The development of the ring current was considerable.

August 16-18 storm:

The ssc was followed for about 48 hours by a large number of small injections. The DR activity was not large, but it was prolonged and remained strong for more than 48 hours.

3.7 THE RING CURRENT BELT

3.71 Depletion of the outer radiation belt during
the main phase of magnetic storms

The several examples of magnetic storms discussed above suggest that many solar particles are trapped and produce the DR field, although there is great variety in the course of the trapping, from one storm to another. In 1958, when the radiation belts were found, it was expected that the outer radiation belt would clearly show considerable solar control. It seemed likely that it would be enhanced during magnetic storms, so as to become a main seat of the westward ring current whose existence was inferred from the magnetic observations at the earth's surface.

However, recent satellite observations have indicated that the observed particles of the outer belt are sometimes markedly depleted

during the main phase of storms. Table 3.12 lists these observations.

TABLE 3.12

Some Observations of Depletion of the Radiation Belts

During Magnetic Storms

Satellite	Magnetic Storm	Reference
Explorer IV	September 3-4, 1959	Rothwell and McIlwain 1960
Explorer VI	August 16-18, 1959	Arnoldy et al. 1960
Explorer VII	March 31-April 3, 1960	Van Allen and Lin 1960

An example is given in Fig. 3.13b, which shows the counting rate at the center of the outer radiation belt (24,000 km or 3.76 radii from the earth's center), during the storm of August 16-18, 1959 (Arnoldy et al. 1960a). Pass 18, on August 17, during the main phase of the storm, showed a marked reduction of the counting rate, which fell to 2,000/sec. Then the rate increased to 18,000/sec during Pass 19, nearly at the end of the main phase. The depletion concerned protons of energy 30 Mev or more and electrons of energy 30 Kev or more; so far particles of less energy are undetected.

Information as to the magnetic field measured by the satellite is not available at present. The change in the radiation belt shown in Fig. 3.3b is quite opposite to what the magnetic records made at the earth's surface would suggest. Arnoldy et al. (1960a) showed that the counting rate decreased by a factor 1/5 during Pass 18, and then increased again by a factor 2. If the model defined by the conditions (a), (b), (c) and (d) of § 3.522 represents the V_2 belt reasonably well, and if the number density n_o changed in proportion to the counting rate, the corresponding H_{zc} values for electrons would be respectively -7 γ and

96

-68 γ (cf. equation 108). The disturbance produced by the normal radiation belt must be a permanent feature of the earth's magnetic field, so that any change must be reckoned from this value. If we estimate it to be -34 γ , then the inferred changes of H_{zc} during the storm are respectively +27 γ and -34 γ . These are less than the changes shown in Fig. 3.14a. Therefore, it seems that the large changes of the V_2 outer radiation belt found so far do not much affect the intensity of the magnetic field at the earth's surface. They are small compared with the observed DR changes during great storms. However, the field changes near and in the V_2 belt may be large enough to be detected by satellites.

3.72 The depletion of the V_2 outer radiation belt and auroral particles.

Suppose that in the equatorial plane a cloud of particles is captured from the solar stream. The particles will encircle the earth because of the motions described in § 3.2, although for a time there may arise a slight electric field tending to prevent their independent motion. The electric field however will soon be reduced, and one may expect that the particles will eventually spread around the earth, as in the Argus Experiment. Suppose also that the pitch-angle distribution is isotropic when the particles are captured. This means that the density of velocity points on the sphere of radius w is uniform (see Fig. 3.14a). From Fig. 3.1, however, we may infer that the particles with pitch-angle θ_e less than 3° have very little chance to go back from their mirror points to the equatorial plane, because they will be absorbed when they pass through the dense atmosphere. Table 3.2 shows that the time of oscillation T_o for 30 Kev electrons, which are supposed to play an important role in the excitation of auroral luminosity, is of order only 2 seconds.

Therefore, whatever the initial condition may be, the particles in the captured cloud that have small pitch-angle (and small magnetic moment μ) will be lost in a few seconds. Then the distribution of velocity points will no longer be uniform. It will have antipodal 'holes' on the surface of the "velocity sphere", round the axis $\underline{H}$ (Fig. 3.14b). In a steady state there will then be no electrons with small μ, unless there is a mechanism which continuously produces them.

In a diffuse auroral arc the flux of high energy electrons is of order 10^7 to $10^8/$ cm^2 sec. During an extremely active auroral phase the flux may become as high as $10^{11}/$ cm^2 sec. Such electrons must have an extremely small magnetic moment. Furthermore, in order to explain the 'thin-ribbon' structure of the aurora, the width of the source must be extremely narrow, namely of order 30 kilometers or less, if it is in the main normal radiation belt V_2. High-level atmospheric scattering of energetic electrons whose mirror points, if undisturbed, would be well above auroral levels, may produce a weak spray of electrons with small μ outside the visible auroral "ribbon". In fact, Meredith et al. (1955) observed by rockoons a continuous precipitation of electrons in a wide zone of latitude, including the auroral zone. This may be a 'leakage from the large reservoir', namely the V_2 belt. But this process cannot produce a curtain-like structure of the aurora.

In a recent paper giving a new theory of auroral morphology (Akasofu and Chapman 1961a; see § 4), it is inferred that the ring current may reverse the direction of the earth's field and produce neutral lines when the current is considerably enhanced. The neutral line must lie in or close to the equatorial plane.

Because of the rapid gyration and the small cyclotron radius of electrons of high energy (see Table 3.2), the only place with a width similar to the radius of gyration of such electrons is a narrow strip close to the X-type neutral line. There the guiding center approximation in not valid and the magnetic moment μ can change. The electrons that pass through this narrow strip during their oscillatory motions between the mirror points will temporarily lose their magnetic moment μ , because they do not gyrate there. When they leave this region they will have a different μ .

At a distance of 6 earth radii from the earth's center, the flux of high energy electrons, according to satellite measurements, is about one hundredth of that at the center of the V_2 belt, namely $(10^{11}/cm^2$ sec$)/100$ $= 10^9/cm^2$ sec. In order to explain the electron flux for a diffuse arc, namely 10^7 to $10^8/cm^2$ sec, the process of conversion of the magnetic moment μ must be _anisotropic_, because the fraction of electrons with pitch-angle θ_e less than 3° is only of order $\left\{ 2x \int_o^{3^o} \sin \theta / \int_o^\pi \sin \theta \right\}$ which has the value 1.31×10^{-2}.

An isotropic process can produce a flux of order no more than

$$(10^9/cm^2 \text{ sec}) \times 1.37 \times 10^{-2} = 1.37 \times 10^7/cm^2 \text{ sec}$$

Note that for an isotropic pitch-angle distribution the number density along a line of force is the same at all points. Even the center of the V_2 belt could not supply the large flux, of order $10^{11}/cm^2$ sec, required for an active aurora, for more than a few seconds.

We think that for both diffuse and active auroras the necessary reduction of magnetic moments μ can only be made in strips close to neutral lines. For active auroras we suppose that both high energy

electrons and the ambient electrons (of much lower initial energy) are accelerated by an eastward electric field along the X-type neutral line. This may be produced by a slight charge separation of particles while a captured cloud of particles is spreading around the earth, and closing to a ring, on the dark side. A substantial increase of the flux of electrons with energy of order 5 Kev, as observed by McIlwain (1960), may indicate this acceleration of low energy ambient electrons. The type B aurora, which is supposed to be produced by high energy electrons of order more than 100 Kev during an active phase, may correspond to the acceleration of high energy electrons in the V_2 belt. It may be noticed that such acceleration by an electrostatic field is most easily possible where the guiding center approximation loses its validity, as it does near an X-type neutral line (cf. Akasofu and Chapman 1961a; see § 4).

For either diffuse or active auroras, if the neutral line stays at one place for more than a few minutes, most of the electrons that pass near it may find their way into the auroral ionosphere. It is interesting to note that even the so-called quiet arcs (we prefer to call them diffuse arcs) continuously change in brightness, and always show some motion. Where the neutral line sweeps across the outer belt the number of high energy electrons will be considerably reduced. This may be the cause of the depletion of the outer belt. In fact, the depletion seems to be greatest in the outer part of the V_2 belt.

3.73 The 'storm-time V_3 belt'

3.731 The auroral zones and the 'storm-time V_3 belt'

Auroral arcs most frequently lie near the circle of geomagnetic

latitude 67° 30'. In our theory of the aurora, we infer from this that

the neutral lines are most often formed at about 6.3 earth radii. If so,

the central line of the ring current should lie a little beyond this

distance. During a magnetic storm the auroral arcs move to rather lower

latitudes, and the DR field increases. The neutral line and the ring

current then draw inwards, towards the earth. After the DR field and

the ring current begin to decay, the arcs quickly return polewards.

Therefore, we may infer that during a magnetic storm there is an

additional ring current-belt or 'storm-time belt' V_3, corresponding to

the auroral zones.

3.732 The ring current particles

The observations of the radiation belts by the counters carried by

satellites relate as yet to protons of energy higher than about 30 Mev

and electrons of energy higher than 30 Kev. We have no indication of

any enhancement of such high energy particles during storms. However,

as we have seen above, in order to produce the main phase of storms,

particles in large numbers must be captured during a storm. We infer

that the energy of the particles that mainly produce the ring current

during the storm is below the cut-off of the instruments so far carried

by satellites.

The revolution time T_R in Table 3.2 bears on this problem. Suppose

that the capture of the particles occurs in a volume rather small compared

with the dimensions of the radiation belts, e.g., in a volume comparable

with that of the solid earth. The particles will soon encircle the

earth (§ 3.72). Then, the maximum H_{zc} should occur when the cloud of

particles has completely encircled the earth and the ring is closed. This requires a time T_R. In the 1957 September 13 storm, the whole time from the ssc to the maximum phase (minimum H) was about 9 hours. This may be taken as an upper limit for T_R. The times of growth and decay of the several intermittent DP sub-storms that occurred during this interval suggest smaller values of T_R, of order one hour or even less. As yet, we do not know how the pitch-angles θ_e are distributed when the particles are captured. Table 3.2 shows for $\theta = \sin^{-1} 0.1$ the order of magnitude of T_R for electrons and protons of different energies. Clearly, 80 Kev electrons satisfy the above requirement for T_R. If they make the main contribution to the ring current, they must be enhanced during the main phase. This, however, is not the case--rather, the contrary (see Fig. 3.13). Electrons of less energy, 10 Kev or below, cannot in this way contribute much to the ring current, because of their large T_R.

Therefore, protons with energy below the instrumental cut-off seem to be the particles more likely to produce the storm-time ring current. In Table 3.2, the time T_R for protons of energy from about 50 Kev to 5 Mev meet the requirements for T_R and for the validity (except near neutral lines) of the guiding center approximation. Equation 98 shows that H_{zc}^* is directly proportional to the energy $\mathcal{E}$. In our model V_3 belt, it is given by (99):

$$H_{zc}^* = -0.306 \ n^* \ \mathcal{E} \ (\text{Kev}) \ \gamma$$

Taking the energy to be 500 Kev,

$$H_{zc}^* = -153 \ n_o^* \ \gamma$$

Thus, our model belt ($\overset{\text{S}}{\S}$ 3.421), if populated by 500 Kev protons whose number density n_o^* is 1/cc, could produce a disturbance H_{zc}^* of order 153 γ . In order to produce the same H_{zc}^* the number density n_o^* of 50 Kev particles must be 10/cc. These must, of course, be crude estimates, because such a belt of protons would greatly distort the earth's dipole field there. We hope in a later paper to discuss how these values of $n_o^* \in$ must be modified when the local distortion of the field by the ring current is taken into account in determining its magnetic field at the earth.

Using (112), the total number N for 500 Kev and 50 Kev protons for $H_{zc}^* = -153 \gamma$ is respectively of order 7.4 x 10^{28} and 7.4 x 10^{29}. Suppose that such particles are trapped during a typical DP sub-storm that lasts 2 hours (= 7.2 x 10^3 sec), and that the capture is from a cross sectional area πa^2 of the solar stream. This is small compared with the suggested frontal area presented by the V_3 belt, of order $\pi(6a)^2$. The rate of capture for 500 Kev protons during a DP sub-storm is then

$$7.4 \text{ x } 10^{28} \text{ } / \pi \text{ } a^2 \text{ x } 7.2 \text{ x } 10^3 \text{ sec } = 8.0 \text{ x } 10^6/\text{cm}^2 \text{ sec}$$

This may be compared with the flux that produces the DCF. Taking the speed to be of order 10^8 cm/sec and the number density to be 10, the DCF flux is $10^9/\text{cm}^2$ sec. The supposed rather uniform flux of particles responsible for DCF seems likely in large part to be reflected or scattered back at the surface of the solar stream (cf. Chapman and Ferraro 1940; Chapman and Kendall 1961). Thus it would not contribute to the capture. We think this occurs when irregularities (in which protons with

energy of a few hundred Kev may be involved) pass by the earth. Thus, the protons associated with these irregularities may number only 1 in 100 of the whole number density. Such irregularities may be embedded in a fairly uniform stream or cloud, and move with it. Then their velocity is of order 10^8 cm/sec. The duration of a typical DP sub-storm is about 2 hours. If this indicates the time during which the capture occurs, the length of the irregularities may be of order 7200 sec x 10^8 (cm/sec) = 7.2 x 10^6 km. This is about 1/20 of the distance between the sun and the earth. If their cross sectional radius is of order a, they will be like threads in the stream or cloud. In a typical storm we observe perhaps 5 or 6 large DP sub-storms. The development of the ring current may depend on the distribution of such irregularities along the sun-earth line.

3.8 DISCUSSION

In this section we discuss briefly several problems, not considered in this paper, which we hope to study in the future.

(a) The distortion of the earth's field due to the ring current.

Here we have discussed the motions of the particles in the earth's _dipole_ field, and the resulting ring current. Our results are valid only if the current intensity is small enough for the motions of the particles to be little affected by their own collective distortion of the magnetic field.

During the main phase of a magnetic storm, however, the ring current must greatly change the dipole field configuration in certain regions, because the field intensity produced by the ring current even at the

earth's surface in many cases exceeds the normal dipole field intensity at 5 or 6 earth radii.

Clearly the magnetic field produced by the ring current must distort the motions of the particles; in turn this will modify the current intensity and the magnetic field thus produced. The interaction between the particle motions and the resulting magnetic field is non-linear; it cannot be studied in a simple way. One approach is to begin with a weak ring current and calculate the resulting slight distortion of the earth's field, as described in this paper. A next step may be to calculate the motions of particles and the resulting magnetic field in the earth's field thus slightly distorted. By successive steps such calculations may show what is the actual field distortion and what is the degree of stability or instability of the ring current. Some other less laborious treatment of the problem may be found.

(b) The distortion of the earth's field by the DCF field.

As long as the earth is enclosed by the solar stream, the DCF field is produced by the current flowing in the surface of the hollow formed in the stream. The earth's field is 'compressed', especially on the dayside of the earth. Therefore the earth's field will not be axially symmetric. The ring current must be a distorted ring. In order to estimate this distortion, the invariant I, namely

$$I = \int_{M'}^{M} \left(1 - \frac{H}{H_m}\right)^{1/2} d\ell$$

may be used (cf. Northrop and Teller 1960).

105

(c) Non-steady state.

In this paper we have assumed a steady state. This has greatly simplified the discussion. However, a weak east-west electric field will produce current of the type i_p (equation 39), and also outward or inward motion of the particles as a whole (equation 38). Therefore the particles which started their motion on the surface of revolution of a dipole line of force that crosses the equatorial plane at, say, 6 earth radii will move towards other surfaces, because of a local east-west electric field likely to be produced during a disturbed condition such as magnetic storms. Thus clouds of particles will not return to their initial surface, and the particles of the ring current may not follow simple closed paths.

(d) The irregular distribution of the particles along the equatorial radius.

During magnetic storms the capture of solar particles in the earth's magnetic field will generally be irregular. They will have different powers of penetration, and different liability to capture. Thus there may be several maxima and minima of the number density distribution of the particles along an equatorial radius, like that revealed by Pioneer IV (Van Allen 1959; his Fig. 2). The result may be that the current system may be composed of several superposed currents of the type considered in this paper. In our auroral paper (loc. cit., 1961; see § 4), we have discussed the multiple structure of the auroral arc and ascribed it to a complicated distribution of the current at about 6 earth radii, which produces more than one neutral line there.

APPENDIX I

List of the Magnetic Observatories whose results are used in this paper. Those that contributed to Figures 12 and 13 are respectively marked by * and +.

Group I

Guam*+
Muntinlupa*+
Jarvis
Huancayo +
Koror
Bangui +

Group II

Paramaribo
Palmyra
Luanda
La Quiaca
Kuyper*
Elisabethville*
Apia*+

Group III

San Juan*+
Teoloyucan
Tehran +
Kakioka*
Tamanrasset*+
M'Bour*+
Honolulu*+
Pilar
Trelew +
Hermanus*+

Group IV

Lovo
Nurmijarvi
Stonyhurst
Ottawa
Valentia
Rude Skov
Agincourt
Wingst
Witteveen
Victoria
Göttingen
Dourbes

Casper
Chambon-la-Foret
Pruhonice
München
Wien-Kobenzl
Price
Hurbanovo
Logrono
San Miguel
Toledo
Tucson*+
Watheroo(Gnangara)

Amberley
Beloit
Burlington
Eskdalemuir
Fredericksburg
Irkutsk
Leadville
Leningrad
Moscow
Lvov
Swift Current, Canada

3.9 THE MAGNETIC FIELD IN THE EQUATORIAL PLANE

In order to calculate numerically from (93) the magnetic field H^*_z at any point in the equatorial plane, we divide the meridian cross section of the ring current into 924 elements, bounded by radii from the earth's center, and by lines of force. The radii are spaced at 2° intervals of latitude from 0° to 66°, and the lines of force cross the equatorial plane at intervals of 0.1 earth radii from 4.75a to 7.55a. The current intensity i* (see Fig. 3.3c) is assumed to be uniform in each element, and to have the value corresponding to the points whose coordinates r_e, ϕ are half way between their limiting values for each element. The numerical integration was carried out by an IBM 704 Computer at the Computing Center, University of Michigan.

In the figure, section c shows H^*_z thus computed, on a linear scale of force, in γ, corresponding to the choice 150 for the value of $n^*_o \zeta^*$.

Also, taking n^*_o to be $1/cm^3$, it shows the distribution of n, the number density, in the equatorial plane. The corresponding variation of the current density i* along an equatorial radius is shown, taking as unit 1 ampere/$(100 \text{ km})^2$. The force H^*_z has a minimum, about $-125\,\gamma$, at a radial distance just short of 6a, and a maximum, about $45\,\gamma$, at approximately 7.5a. Its value at the earth's center is about $-45\,\gamma$.

Section b of the figure shows on a logarithmic scale the distribution of the combined field, of the earth and the ring current, along the equatorial radius. Clearly the adopted model belt of trapped solar particles produces a remarkable distortion of the earth's magnetic field.

Smith, Coleman, Judge and Sonett (1960) have published a
preliminary account and discussion of the field measurements made by
the magnetometer carried on the satellite Explorer VI. They give their
measured values of H_n (the field intensity perpendicular to the spin
axis), on a logarithmic scale. Using orbital and other data, they
calculated their theoretical H_n in the normal earth's dipole field.
These two quantities, and also the undisturbed dipole intensity H, are
shown in section a of the figure. The measured H_n curve shows a large
reduction, down to a minimum value of about 15 γ, at a radial distance
of 6.2a or 6.3a. They found it possible to fit their measured results
closely to the computed H_n values for a toroidal current as follows:

Total current	5 million amperes
radius of the center line of the ring current	60000 km (9.4a)
radius of cross section	3a or less

They remark that there was no penetration of the current by
Explorer VI in the range of distance illustrated in the figure, section
a. The notable agreement between the curves in a and b suggests that
the Explorer VI results can be interpreted as indicating the presence
of a radiation belt somewhat resembling our model V_3 belt, in the region
traversed by the satellite.

It may be noticed that the present result is only a first
approximation to the solution of this non-linear problem, as discussed
in § 3.8.

Explorer VI

theoretical H_n

H theoretical

Observed H_n

(a)

Model V_3 Belt

H dipole

Combined H

(b)

density
1.0 /cm³
0.5

Current
amp/(100km)²

W

H_z^*

E

H_z^*

(c)

earth radii
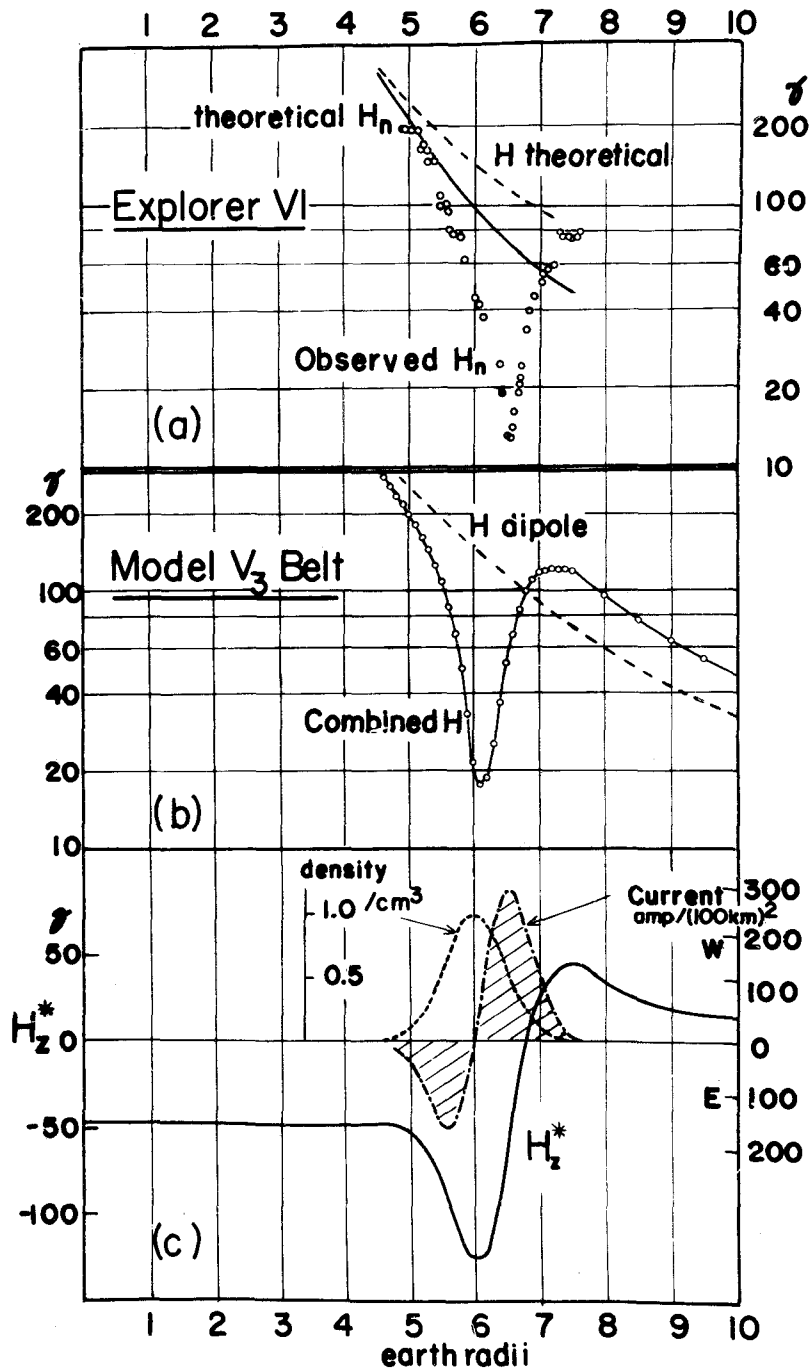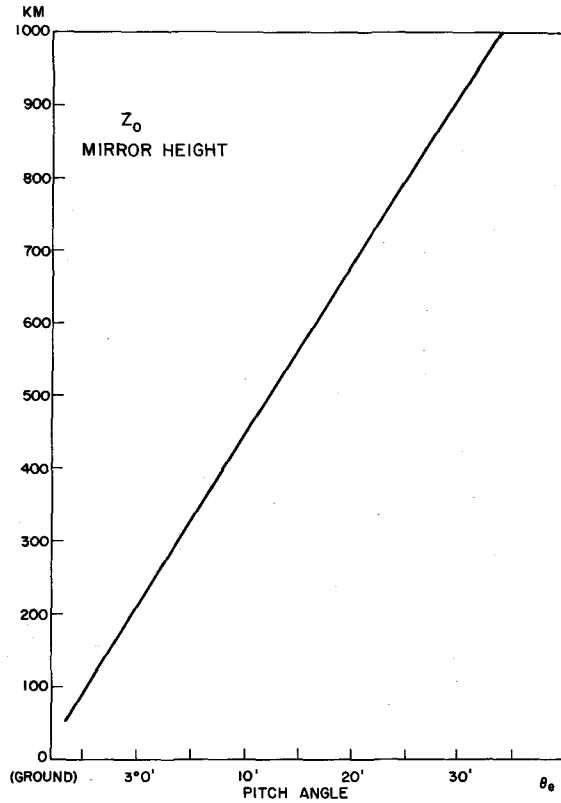
Fig.3.1. Relation between the pitch-angle θ in the equatorial plane and the height above the ground of the mirror points M,M! Note that most of the aurora must be produced by particles with equatorial pitch-angle θ_e less than 3°.
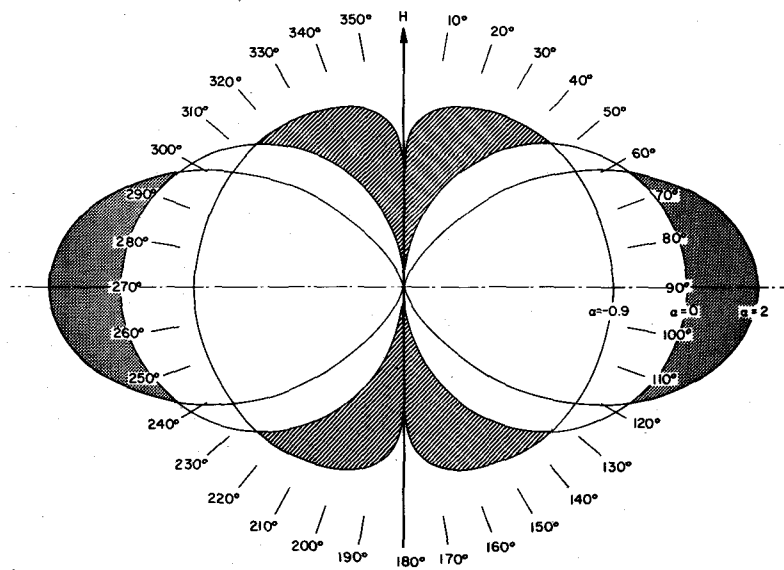
Fig.3.2. The pitch-angle distribution $F \propto \sin^{\alpha+1}\theta$ for $\alpha = 2, 0$ and -0.9. The direction $\theta = 0$ is parallel to H. The curves are normalized to give the same mean density in each case.
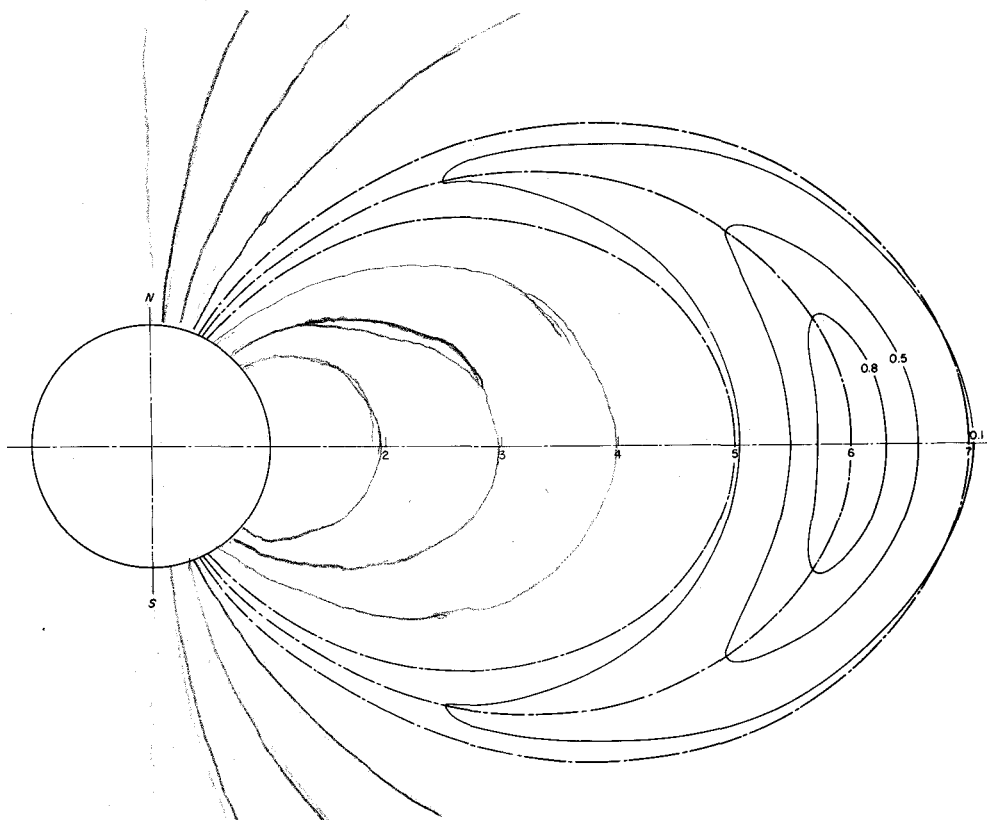
Fig. 3.3a. The proportionate current intensity distribution in the model belt V_3 (f_0=6, α= -0.5, g=1.517) representing the first term in the bracket of equation (69).
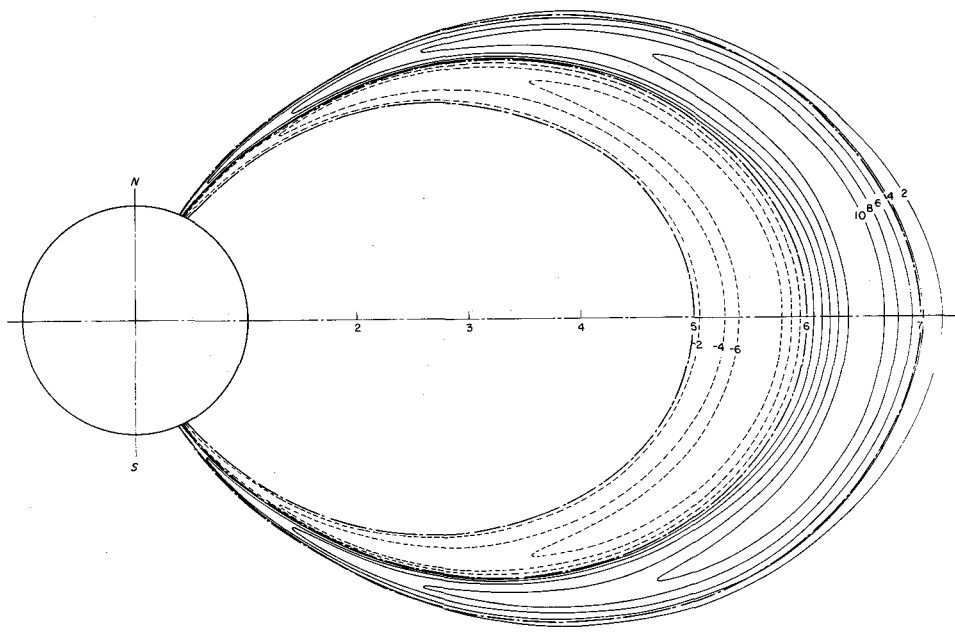
Fig. 3.3b. The proportionate current intensity distribution in the model belt V_3 (f_0=6, α=-0.5,g=1.517),representing the second term in the bracket of the equation (69).
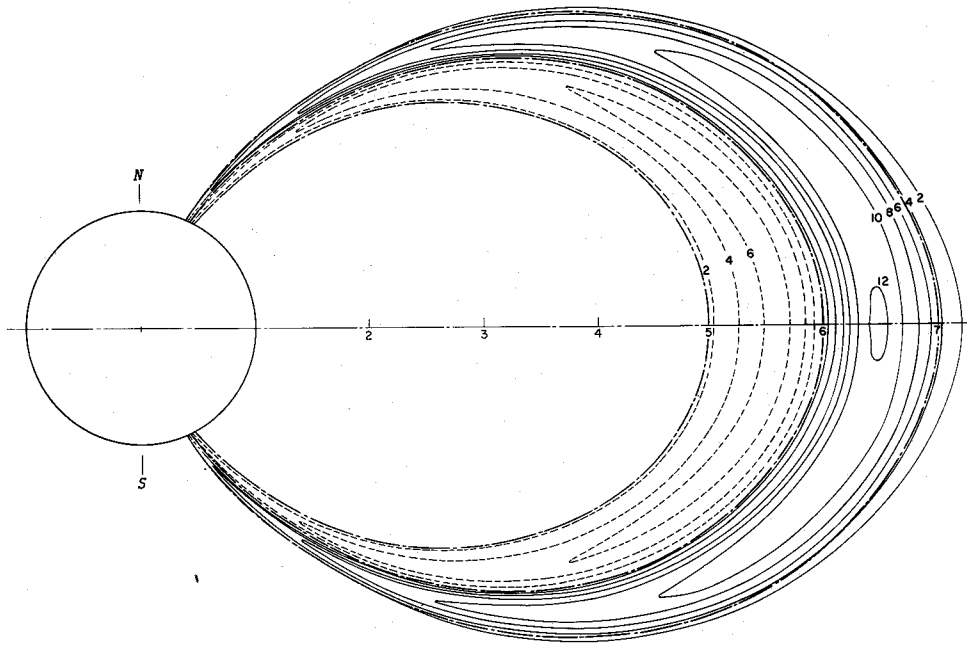
Fig.3.3c. The proportionate current intensity distribution in the model belt V_3($f_0=6$, $\alpha=-0.5$,$g=1.517$),representing the combination of the currents in Figs.3.3a and 3.3b.
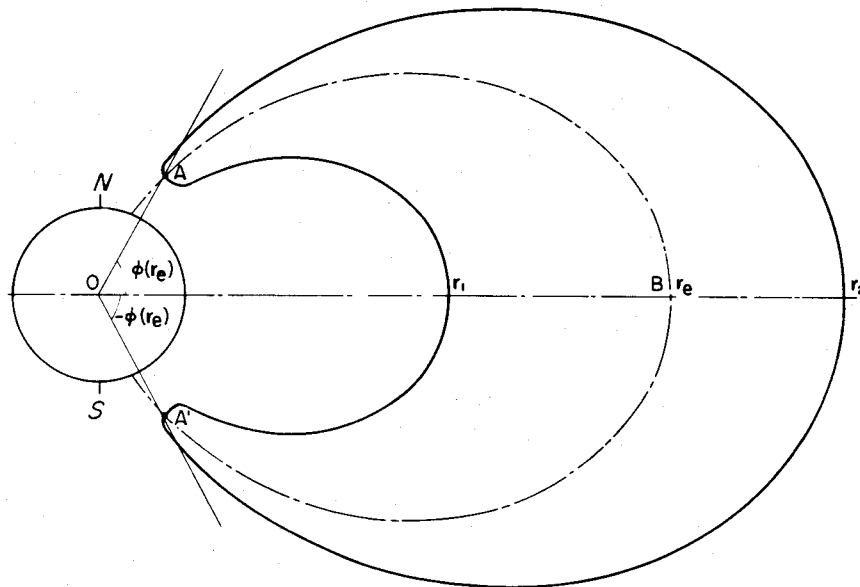
Fig.3.4. The geometry for the integrations $I_D($ ϕ, α) and $I_F($ ϕ,α). The curve $Ar_2A'r_1$ is the meridian cross section of the belt.
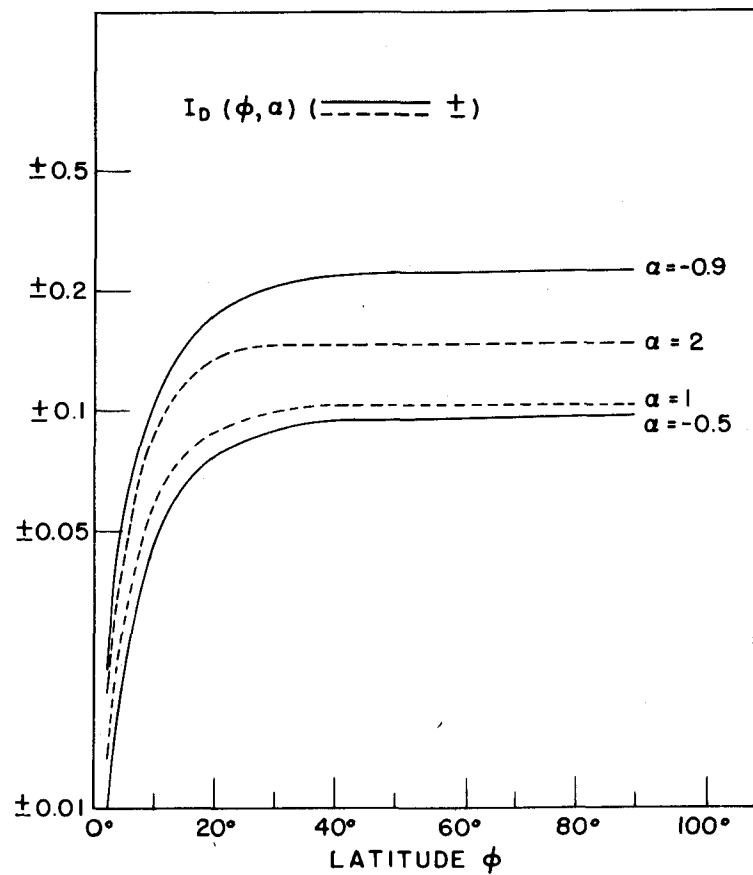
Fig.3.5. The integral $I_D(\phi, \alpha)$ as a function of ϕ for various values of α. For each values of α, the variation of I_D is small beyond a certain value of ϕ.
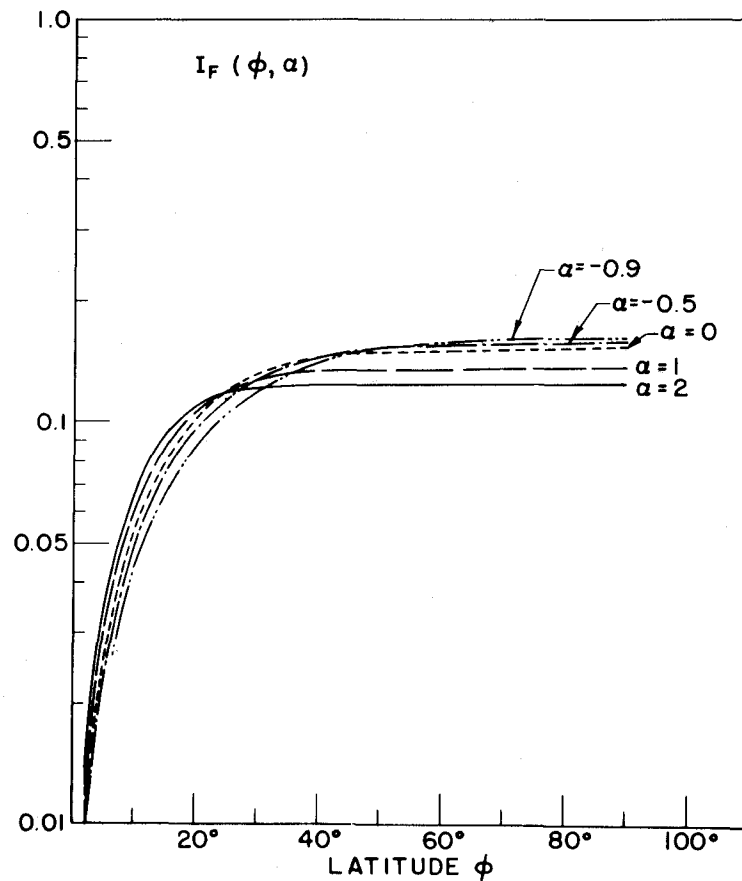
Fig.3.6. The integral $I_F(\phi, \alpha)$ as a function of ϕ for various values of α. For each value of α, the variation of I_F is small beyond a certain value of ϕ.
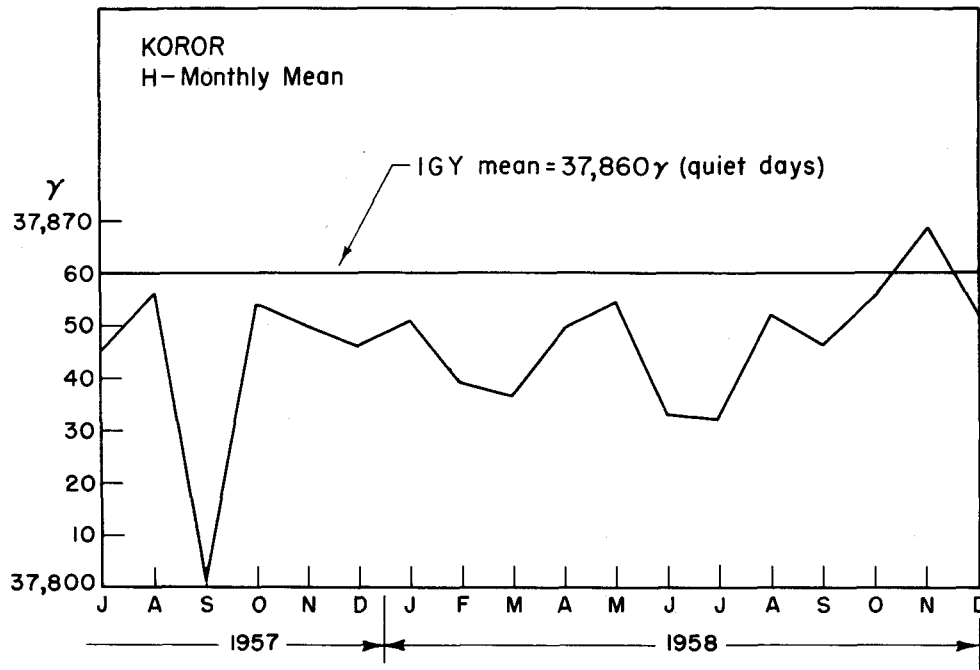
Fig.3.7. The monthly mean value of the horizontal component at Koror observatory
(gm.lat. 3°3 S, dip angle + 0° 48'). The quiet day mean value of the horizontal
component averaged over the 18 IGY months is indicated.
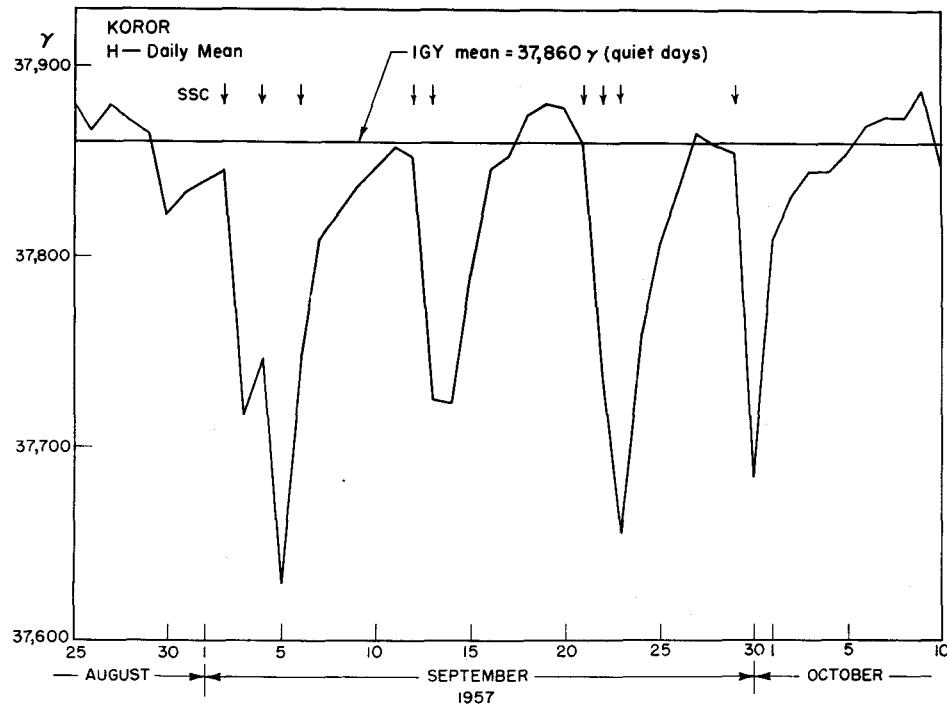
Fig.3.8. The daily mean value of the horizontal magnetic component at Koror observatory
(gm.lat.3°3 S,dip angle +0°48') from August 25 to October 10,1957.
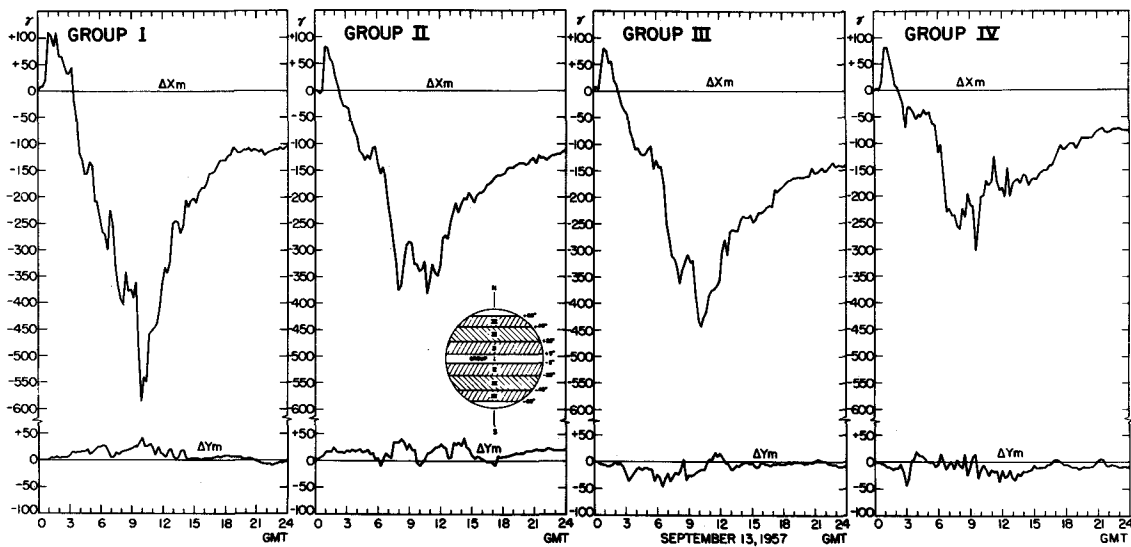
Fig.3.9 The Dst(X_m) and Dst(Y_m) curves for 13 September 1957 for four zones bounded by circles of geomagnetic latitude (indicated in the figure). The ssc occurred at $00^h 47^m$ GMT September 13,1957.
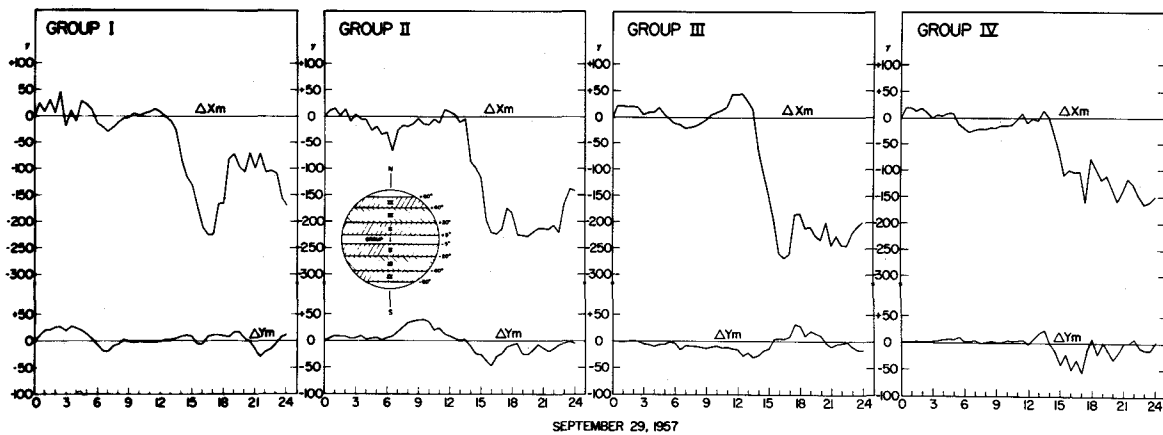
Fig.3.10. The Dst(X_m) and Dst(Y_m) curves for September 29,1957 for four zones bounded by circles of geomagnetic latitude (indicated in the figure). The ssc occurred at $00^h 16^m$ GMT on September 29,1957.
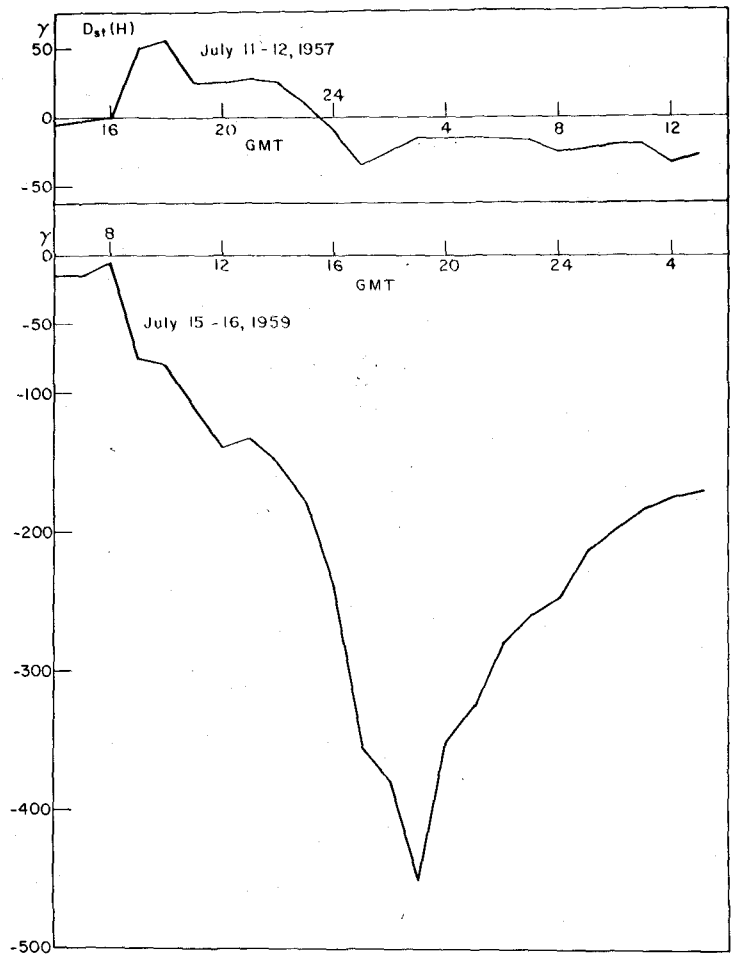
Fig.3.11. The Dst(H) curves for the July 11 and July 15,1959 storms from 12 low latitude observatories.
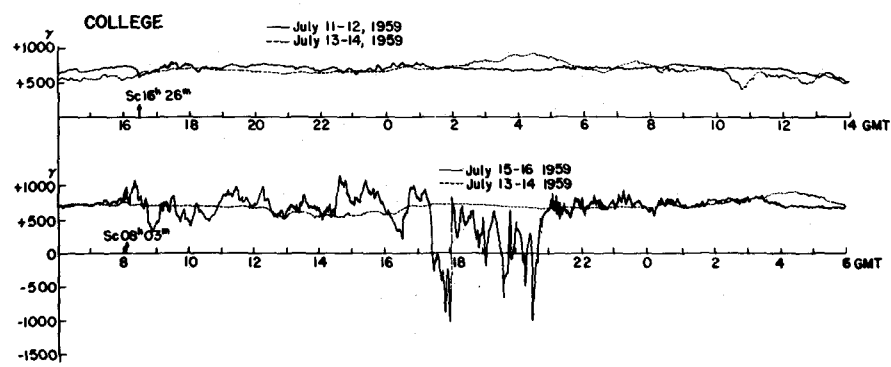
Fig.3.12. The horizontal component magnetograms from College(Alaska) for the July 11 and July 15,1959 storms; Upper,July 11-12,1959; Lower,July 15-16,1959. Dotted lines indicate the quiet day curve of July 13-14,just between the above storms.
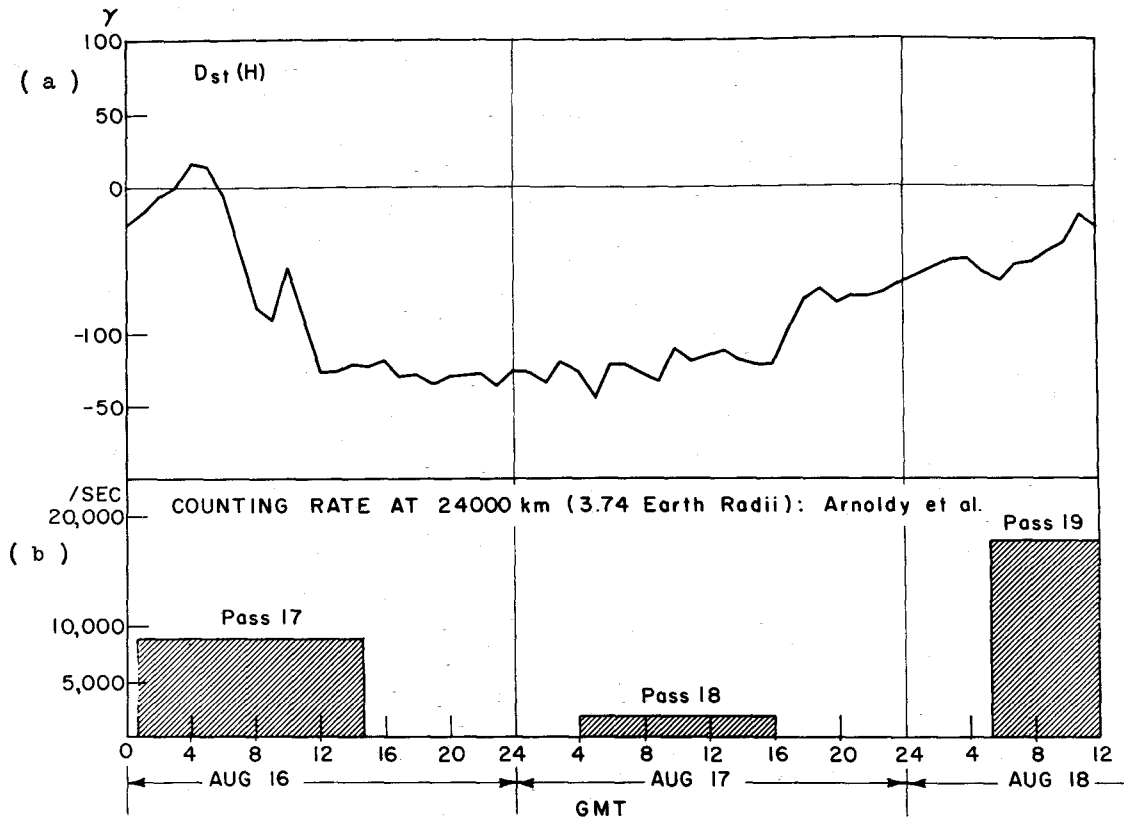
Fig.3.13. (a):The Dst(H) curve for the August 16-18,1959 storm for 13 low latitude observatories. The ssc occurred at 04h04m GMT on August 16,1959. (b): The counting rate at 24,000 km from the earth's center (3.76 earth radii),the center of the outer radiation belt,during the storm of August 16-18,1959 (Arnoldy et al.1960).
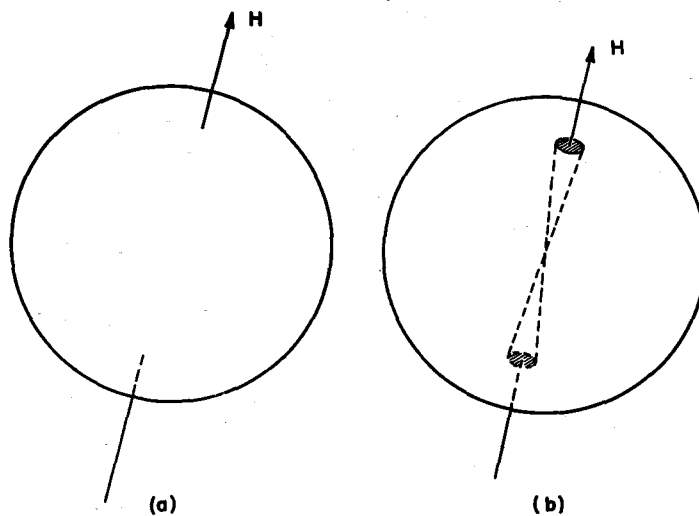
Fig.3.14. (a): The 'velocity-sphere' indicating the distribution of velocity points on the sphere of radius w. For an isotropic pitch-angle distribution (= 0),the distribution of the points is uniform. (b): The velocity sphere with antipodal "holes".

CHAPTER IV

A NEUTRAL LINE DISCHARGE THEORY OF THE AURORA POLARIS*

4.1 INTRODUCTION

The aurora polaris, which provides wonderful displays in the polar night sky, offers some of the most difficult problems in geophysics. Many partial theories have been put forward to explain one or more auroral phenomena, but all are inevitably far from complete. Störmer (1955) and Chamberlain (1958) have given good reviews of these theories. In this section, therefore, mention will be made only of such recent theories as have some relation to the new theory given in this paper.

Birkeland's <u>terrella</u> experiments led the way to the modern theories. He studied the motions of electrons in a dipole field, which later were mathematically discussed by Störmer. Störmer tried to associate the motions of solitary charged particles in the earth's field with various features of the aurora. He found that certain regions around the earth were inaccessible ("forbidden") to the particles, while others were "allowed". His theory was criticized on the ground that the mutual repulsion of the particles (all of one sign) would disperse the stream before it could reach the earth. To explain the movement of the aurora to lower latitudes during great magnetic storms, he suggested that many of the particles sweeping partly round the earth (at a distance comparable with or beyond the moon) might have a magnetic effect equivalent to that of a complete westward electric current--now generally called a ring current in this connection. However, as was pointed out by Chapman and

---

* Part of this Chapter covers the same ground as the paper: Akasofu and Chapman (1961a).

Ferraro (1933), his ring current would greatly change the earth's field in its locality, so that the calculation on which its presence was postulated would not be valid.

Chapman and Ferraro (1931a, b) were the first to infer that during magnetic storms the important interaction of solar particles with the earth's magnetic field will occur much nearer to the earth, less than 10 earth radii. The development of their magnetic storm theory was based on the hypothesis, proposed by Lindemann (1919), of a neutral ionized stream. This condition, that the number of positive and negative particles must be nearly equal, is one of the most fundamental in plasma physics. Chapman and Ferraro criticized Störmer's theory on the ground that in a stream of particles, unless they are of extremely high energy and low number density, such as cosmic-ray particles, the oppositely charged particles must affect each other's motion by their Coulomb field. They showed (1940) that if the density was low enough for the particles to travel as Störmer had calculated, it would be far too low to produce appreciable magnetic effects.

Later Alfvén (1940, 1950) advanced one of the most fundamental concepts in modern plasma physics, that of the 'guiding center'. This relates to low energy particles in a strong magnetic field. The particle gyrating in a strong field is replaced by a small magnet with moment which is invariant. Alfvén showed the usefulness of his simple 'smoothed out' version of the path of such a gyrating particle by comparing it with Störmer's complicated path. He considered the case of a particle rapidly oscillating around and along the lines of magnetic force in a dipole field, with slow drift motion in longitude.

109

Chapman and Ferraro (1931b) suggested that particles might be 'trapped' from the surface of a hollow in the solar stream, at a distance of several earth's radii beyond the earth away from the sun. This speculation remains unconfirmed and unrefuted. Singer (1957), with notable insight, identified the motion of the trapped particles with that considered by Alfvén. This led him to predict a belt of trapped particles in the earth's field, having the form of the Van Allen radiation belts, before these were discovered by the satellite researches (Van Allen and Frank 1959). The Van Allen radiation belts are associated with a varying electric ring current at several earth's radii. This ring current has been discussed by Dessler and Parker (1959) and by Akasofu (1960a).

Plasma theory predicted another important invariant of the motion of a particle in a magnetic field, besides its equivalent magnetic moment. This conception was successfully applied to the motions of the electrons of high energy (of order a few Mev) produced by the Argus Experiment (Van Allen et al., 1959). The electron shell which enclosed the earth at that time was located exactly as predicted by the second invariant law.

This led Vestine and Sibley (1959) to produce 'Calculated isochasms', which agree well with the actual isochasms first given by Fritz (1881), and revised later by Vestine (1944). This confirms that the motions of the auroral particles in the earth's field accord with the constancy of the two invariants.

However, as indicated by Chapman and Ferraro in 1931, these particles move in their collective Coulomb field. Plasma theory discusses the macroscopic behavior of auroral particles by summing the individual motions of the particles, defined by the two invariants, under the condition

110

of electrical neutrality. Any slight charge separation will produce a strong electrostatic field between them and their motions cannot be independent.

Meanwhile, quite another line of development was followed by Hoyle (1949, p. 102) and later by Dungey (1953)*. They assumed that part of the solar magnetic field is carried away by solar streams, and that at times the earth's dipole field is immersed in a rather uniform solar field. They concluded that two neutral points arise on opposite sides of the earth, and they suggested that auroral particles would there be accelerated. But it seems to us unlikely that two such neutral points would suffice to explain the complicated auroral morphology.

Alfvén (1939, 1950, 1955) and Martyn (1951) also put forward auroral theories, although they did not specifically discuss the detailed morphology of auroras. Alfvén's theory is based on the postulated presence of a general electric field enveloping the earth. The motions of the charged particles are inferred to be such as to produce a charge accumulation in the equatorial plane, whence the particles find their way towards the earth along the lines of force.

Martyn based his ideas on the hypothetical polarized ring current discussed by Chapman and Ferraro (1933), located at several earth's radii. As they indicated, charged particles are expelled from the inner and outer sides of the surface. Martyn inferred that this produces electric polarization in the ionosphere, which impels the electric current flow there.

---

*See also Dungey (1961)

111

4.11 A neutral line discharge theory of the aurora polaris

In this chapter we develop an auroral theory along new lines. Since the discovery of the Van Allen radiation belts, the outer radiation belt has been widely regarded as a kind of _reservoir_ from which the auroral particles come. However, one of the most striking characteristics of the aurora polaris--its thin ribbon-like structure--has been unexplained. The particles in the outer radiation belt, guided by the lines of force of the earth's magnetic field, penetrate the auroral ionosphere and produce the auroral luminosity. The extremely thin structure suggests that the meridian cross section of the particle-beam from the outer radiation belt must be confined between two lines of force separated by only a few hundred meters. Therefore there must be a special mechanism that releases auroral particles from the belt through an extremely narrow channel located in the large reservoir. The difficulty in explaining this can easily be realized from the fact that the width of the channel in the equatorial plane must be of the same order as the radius of gyration of high energy electrons there.

Another important problem to be solved is how to maintain the electron flux of order as high as $10^{11}/cm^2$ sec in an active aurora for at least 30 minutes or so. As has been shown in § 3.7, only a small fraction of the total flux in the equatorial plane can contribute to the auroral luminosity. A tentative estimate indicates that the flux in the equatorial plane must be of order $10^{13}/cm^2$ sec. Even at the center of the outer radiation belt, it is of order $10^{11}/cm^2$ sec. It has been suggested that there is no such large flux of high energy electrons in the solar stream, so that most particles that produce an active aurora must be accelerated in the outer radiation belt.

In a magnetic field such as the outer geomagnetic field, an electric field of moderate intensity cannot accelerate electrons there, unless the electric field is parallel to the lines of force (but such an electric field is extremely difficult to maintain). However, the acceleration is possible in a region close to the X-type neutral line (§§ 1.5, 4.2) along which the intensity of the magnetic field is zero and on which the two lines of force cross. Furthermore, the narrowness of the region is required, because otherwise the electric field will disappear in a very short time and because an active aurora has a narrower width than that of a diffuse aurora.

We suggest that the X-type neutral lines satisfy these two difficult conditions and that they are the proximate sources of the particles that produce auroral displays.

4.2 THE FORMATION OF A NEUTRAL LINE

As has been discussed in detail in § 3.8, all the calculations on the ring current shown in § 3 are strictly valid only for infinitely small current density. Actually the westward current must appreciably modify the normal field of the earth. This change affects the motion of the charged particles and so modifies the ring current itself. Consider, for illustration, the combination of a uniform magnetic field $\underline{H}$, with the field of an infinitely long straight current, perpendicular to $\underline{H}$, flowing with uniform density $\underline{i}$ in a cylindrical volume with circular cross-section. Typical field distributions have been calculated by McDonald (1954), and are shown in Fig. 4.1 for different ratios i/H.

Fig. 4.1a shows the lines of force when the volume current is zero. Fig. 4.1b shows the lines of force when the current is weak. When the

current density is sufficiently increased, a neutral line appears in the magnetic field, first on the surface of the current distribution (Fig. 4.1c). For greater current densities there are two neutral lines, one inside and one outside the cylinder, as in Fig. 4d. The inner neutral line intersects the plane of the diagram in a point marked O; there the lines of force shrink to a point. The outer neutral line intersects the plane of the diagram in a point marked X, to indicate that the line of force through it is double; this line of force has two branches that may extend to infinity.

Fig. 4.1 is drawn for a uniform current density. In the case of an actual ring current, in which the distribution of the current density may be non-uniform (and variable), the distortion may be much more than that shown in Fig. 4.1. The cylindrical current always distorts the original straight field lines so that the radius of curvature Rc is decreased. Thus the actual ring current must increase the current density, as equation (3.48) shows. Another important effect is a reduction of the intensity of the field to the left of the median plane of the cylinder (Fig. 4.1). Both effects modify the original particle motions so as to increase the current density.

Fig. 4.2 is a schematic sketch of the magnetic field configuration in a meridian half plane, when a toroidal ring current encircles the earth, strong enough to produce neutral lines in the field. These lines, which are circles with the same centre as that of the earth, intersect the plane of the diagram in the neutral points O and X (as in Fig. 4.1). The centre line of the ring current has a radius 5.5 times that of the earth.

4.21 The field intensity distribution

To a first approximation we may regard the ring current as a toroidal ring current of circular cross section. Let a, q and b denote the radii of the earth, of the center-line of the ring, and of the boundary of the cross section of the ring. The magnetic field H_R produced by the ring, in the equatorial plane, outside the ring, may approximately be given (cf. Stratton 1941, p. 263, see also equation 93 in chapter 3).

$$H_R = 2I \frac{1}{c(q + d)} (K + \frac{q^2 - d^2}{(q - d)^2} E), \quad 0 < d < (q - b). \tag{1}$$

Here I denotes the total current intensity in the ring; K (k) and E (k) are complete elliptic integrals of the first and second kinds, respectively; d denotes the distance from the center of the earth, and

$$k^2 = \frac{4qd}{(q + d)^2} \tag{2}$$

The field intensity at C the center of the earth is

$$H = \frac{2\pi I}{cq} . \qquad (d = 0) \tag{3}$$

Within the volume of the ring the field distribution may approximately change linearly along any radius. At the center of the cross section of the ring the field produced by the ring is almost zero.

The DCF field produced by the currents flowing near the surface of the hollow in the solar stream, is very roughly equal to that of a dipole with the same magnetic moment as the earth (Chapman and Ferraro 1931a). The dipole is on the line SCS' from S the sun to C the center of the

earth and beyond. Its distance from C is 2A, towards S; here A denotes

the distance from C to the vertex of the hollow. The intensity is H_{CF}.

The intensity of the compound field is $\underline{H}$, the vector sum of the

intensities $\underline{H}_M$, $\underline{H}_{CF}$, and $\underline{H}_R$. Neglecting DP, the field of the polar

currents, $\underline{H}$ will be an approximation to the field existing round the

earth during a storm. At points along the line SCS' all these fields

are parallel or anti-parallel.

Some illustrative calculations of H have been made, choosing what

seem to be reasonable values of A/a, q/a and b/a, namely

$$A/a = 6, \quad q/a = 5.5, \quad b/a = 0.5.$$

Four values of the intensity H_{Ro} of the field of the ring current at

ground level at the earth's equator are considered,

$$H_{Ro} = 50, \ 70, \ 100, \ 500 \ \gamma.$$

These cover the whole likely range of values of H_{Ro}, which of course

depends on q/a and the current strength along the ring. In Fig. 4.3 the

graphs of H for these various cases are shown, on the right for points

along CS, on the day side of the earth, and on the left, for points

along CS', on the night side. (The earth itself is omitted from the

diagram). The graph of H_{CF} is shown on the right; H_{CF} is too small to

be drawn, on the left, the dark side of the earth; if drawn, there would

be a discontinuity in the centre of the diagram, owing to the omission

of the earth's diameter. Thus on the left the graph of $(H + H_{CF})$ is

sensibly the same as curve (a), for the earth's main field alone. On

the right, at 6 earth radii, at the position of the vertex of the hollow,

H_{CF} and H_M are equal. Despite its small intensity, the DCF field pro-
duces an important difference between the values of H on the two sides
of the earth. Fig. 4.3 shows neutral points on the day side only for
rather large values of H_{Ro}, 100 γ and 500 γ. These values would
correspond, with the field of the currents induced in the earth, to about
160 γ and 800 γ decrease during the main phase of the storm (owing to
the additional field of the currents induced in the earth). The dif-
ference between the curves to the right and left should be specially
noticed in connection with the appearance of neutral lines in the field.

The deviation of the earth's external field from the expected dipole
field has recently been observed by the USSR cosmic rocket Mechta (Jan.
2, 1949) and by the US Satellite Explorer VI (Aug. 10, 24; Sept. 1, 1959;
Sonett et al. 1960). The field distribution for H_{Ro} = 50 γ seems to
agree qualitatively with their observations.

For H_{Ro} = 70 γ the direction of the composite field is reversed
near the ring on the night side meridian, but not on the day side
meridian. Fig. 4.4 shows the geometry of the X- and 0 type neutral lines
in the equatorial plane in a certain stage. They join at a point on the
surface of the ring current. Fig. 4.4 also shows the projection of the
X-type neutral line on the earth's surface, following the dipole lines
of force that intersect the X line. This projection is the locus along
which particles from the neutral line will enter the earth's atmosphere.
Their entry will be made visible by a long thin auroral arc in the east-
west direction.

For H_{Ro} = 100 γ the region of negative H, and the neutral lines, will
completely surround the earth. For H_{Ro} = 500 γ the negative region is

117

much enlarged, and one of the neutral lines (X-type) draws closer to the earth. So far we have assumed that the ring current is concentric around the earth. However, the ring may not be concentric. An exact treatment must follow the discussion given in § 3.8. As was shown there, by using the two adiabatic invariants, it is expected that the ring will be nearest to the earth on the night side hemisphere.

As also indicated there, the ring current may often be less simple than has been supposed above. It may have different parts, located between 4.5 and 7.5 earth radii.

4.3 MOTIONS OF CHARGED PARTICLES CLOSE TO A NEUTRAL LINE

4.31 Motions of charged particles in the equatorial plane

In the foregoing discussion the conditions assumed in § 3.2 were supposed to be satisfied. The first two may be written thus:

$$R/L \ll 1, \tag{4}$$

$$P/T \ll 1. \tag{5}$$

Here R and P denote the radius and period of the gyration and L and T denote the scale length and scale time. Chapman (1961c) defines the scale length L and the scale time T of a vector function $\underline{F}$ of position as follows,

$$L = F / (W:\overline{W})^{1/2} \tag{6}$$

$$1/T = d \, (\ell n \, F)/dt. \tag{7}$$

Here W and $\overline{W}$ denote $\triangle \underline{F}$ and its conjugate dyadic, respectively. In the case of a dipole field, its scale length is given by (6) as follows:

$$L = \frac{r}{3 \sqrt{2}} \; \frac{1 + 3\cos^2 \phi'}{1 + 2\cos^2 \phi'} \tag{8}$$

Here ϕ' denotes the co-latitude of the point considered and r its radial

distance from the origin. Hence L is less than r by a factor that varies

between 3.57 (for $\phi' = 0°$) to 4.24 (for $\phi' = 90°$). At 5 earth radii

from the center of the earth, in the equatorial plane, L is 7940 km.

For $H = 2.56 \times 10^{-3}$ gauss (the intensity of the earth's field at that

distance), the radius of gyration R_p for 100 Kev protons is of order

179 km, and R_e for 30 Kev electrons is 1.66 km. These are much less

than L. However, the first condition (4) is not satisfied near a neutral

point or line. We take rectangular cartesian co-ordinates such that

the neutral line coincides with the y axis (or x = z = 0) and so that all

the field lines are contained in the xz plane. Further we direct the x

and z axes in such a way that the magnetic potential ψ is expressed by

$$\psi = \psi_o \; -fxz. \tag{9}$$

Then the $\underline{H}$ field components (X,Y,Z) are

$$X = fz, \quad Y = 0, \quad Z = fx. \tag{10}$$

Here

$$f = \partial X/\partial z = \partial Z/\partial x. \tag{11}$$

Chapman (1961c) has shown that the scale length defined by (6) is

$$L = r/\sqrt{2}, \tag{12}$$

where

$$r = (x^2 + y^2)^{1/2} \tag{13}$$

Hence near the neutral line L becomes small, but R and T become large,

so that $R/L \gg 1$ and $P/T \gg 1$. Therefore the guiding center concept can

no longer be applied there, and the true paths of the particles must be

119

considered. This has been done by Åström (1956) and Parker (1957).
Here we present the analysis in a simple form.
Using (10), the equations of motion of charged particles (velocity
components (u,v,w)) near the neutral line are thus obtained. Elsewhere
in this paper w signifies the total speed of a particle; here excep-
tionally it is used for the z component of the velocity.

$$m\dot{u} = m\ddot{x} = (e/c) \ vZ = (fe/c) \ xv,$$

$$m\dot{v} = m\ddot{y} = (e/c) \ (wX - uZ) = (fe/c) \ (zw - xu), \qquad (14)$$

$$m\dot{w} = m\ddot{z} = (e/c) \ (\ - vX) = -(fe/c) \ zv.$$

We consider the motion of charges in the plane z = 0. Then the above
equations are

$$\dot{u} = \ddot{x} = (ef/mc) \ xv = Axv,$$

$$\dot{v} = \ddot{y} = (ef/mc) \ (\ - xu) = -Axu, \qquad (15)$$

$$\dot{w} = \ddot{z} = 0,$$

where

$$A = (ef/mc). \qquad (16)$$

We note that if we simultaneously change the sign of the charge, e, and
the direction of the y axis, the form of the equation remains the same.
This indicates that positive and negative particles have opposite direc-
tions of motion along the y axis. Note also that for particles of
different mass the path is the same except in scale.
The first integral is

$$u^2 + v^2 = \text{constant} = w_n^2, \qquad (17)$$

From (15) and $\dot{v} = u \ dv/dx$, v is obtained as

$$v = v_o - (1/2)Ax^2, \qquad (18)$$

where $v = v_0$ at $x = 0$ (that is, v_0 is the velocity component along the y axis when the particle crosses the neutral line).

Similarly for u:

$$u^2 = u_0^2 + Av_0 x^2 - \left(1/4\right) A^2 x^4. \tag{19}$$

Here we put $u = u_0$ at $x = 0$ (that is, u_0 is the velocity component along the x axis when the particle crosses the neutral line). We may write (19) in the form

$$u^2 = \left(1/4\right) A^2 (X_1^2 - x^2)(X_2^2 + x^2), \tag{20}$$

so that $u = 0$ at $\pm X_1$. Also

$$\int dt = \frac{2}{A} \int \frac{dx}{\left\{ (X_1^2 - x^2)(X_2^2 + x^2) \right\}^{1/2}}, \tag{21}$$

where

$$X_1^2 = \frac{2v_0}{A}\left(1 + \frac{w_n}{v_0}\right), \tag{22}$$

$$X_2^2 = -\frac{2v_0}{A}\left(1 - \frac{w_n}{v_0}\right). \tag{23}$$

Similarly

$$\int dy = \frac{2}{A} \int \frac{(v_0 - (1/2) Ax^2)\, dx}{\left\{ (X_1^2 - x^2)(X_2^2 + x^2) \right\}^{1/2}}. \tag{24}$$

The travel time τ between $x = 0$ and $x = X_1$ is then

$$\tau = \frac{2}{A} \int_0^{X_1} \frac{dx}{\left\{ (X_1^2 - x^2)(X_2^2 + x^2) \right\}^{1/2}}. \tag{25}$$

121

This can be expressed as

$$\tau = \frac{1}{\sqrt{A\,w_n}}\,E\,(k),\tag{26}$$

where $E\,(k)$ is the complete elliptic integral of the first kind, and

$$k^2 = \frac{1}{2}\,(1 + \frac{v_o}{w_n})\ .\tag{27}$$

Similarly the displacement η along the y axis during the above time interval is

$$\eta = (m\,w_n\,c/fe)^{1/2}\,\left\{E\,(k) - 2\,K\,(k)\right\},\tag{28}$$

where $K\,(k)$ is the complete elliptic integral of the second kind. Therefore the mean drift velocity of the particle $\bar{V}$ along the neutral line is

$$\bar{V} = \frac{\eta}{\tau} = w_n\,\left\{1 - \frac{2K\,(k)}{E\,(k)}\right\}\ .\tag{29}$$

For $k > 0.909$ the particle drift is in one direction, and for $k < 0.909$ it is in the opposite direction. For positive charges the former direction is positive, for electrons it is negative.

It is seen from (27) that k^2 is a function of (v_o/w_n) or $\cos \chi$, where χ denotes the angle between the neutral line and the velocity vector at a point where the path intersects the neutral line. By definition

$$-\,w_n \le v_o \le w_n\ ,$$

so that

$$0 \le k^2 \le 1\ .\tag{30}$$

122

For particles moving from a point on the neutral line with $v_o > 0$, (that is, in the positive y direction, so that $k^2 > 1/2$), the path is looped. For positively charged particles moving from the y axis in the negative direction ($v_o < 0$), so that $k^2 < 1/2$, the path is of simple wave form, and always in the negative y direction. This is the kind of motion with which we are concerned in the later part of this paper.

The paths of protons for $k^2 = 0$, 0.05, 0.1, 0.2, 0.3 and 0.4 are calculated and are shown in Fig. 4.5. The scale unit of length is $(m_p w_{np} c/ef)^{1/2}$. The electron drift velocity $\bar{V}_e$ along the neutral line is

$$\bar{V}_e = w_{ne} \left\{ \frac{2K(k)}{E(k)} - 1 \right\}, \tag{31}$$

and the scale unit of length is $(m_e w_{ne} c/fe)^{1/2}$.

The maximum width of the region in which the motion along the neutral line is uni-directional corresponds to $k^2 = 1/2$, so that

$$v_o = 0,$$

and

$$X_1 = (2w_n/A)^{1/2} = (2 m c w_n/ef)^{1/2}. \tag{32}$$

Thus for 130 Kev protons

$$X_{1p} = 3.2 \times 10^2 / \sqrt{f}, \tag{33}$$

and for 30 Kev electrons

$$X_{1e} = 3.3 \times 10 / \sqrt{f}. \tag{34}$$

Therefore the width for the electrons is about 1/10 of that for the protons.

From the above considerations, protons can drift in both the positive

123

and the negative directions. Thus the direction of the net drift and so
that of the electric current j depend on the initial condition--the
distribution function of k or k^2. However, Parker (1957, p. 933) infers
that a steady state will eventually be established. Within the width
$2X_1$ the current j is related to the gradient of the field in the
following way.

$$j_y = \frac{-c}{4\pi} \left(\frac{\partial Z}{\partial x}\right)_y .$$ (35)

4.32 Growing electric current along the neutral line

In a non-conducting gas the lines of force that meet at a point on
an X-type neutral line cross each other orthogonally. In § 4.31 it has
been shown that electric current will flow along and adjacent to an X-
type neutral line within the width $2X_1$. The angle between the two lines
of force which cross on the neutral line is thereby changed (because
$\partial Z/\partial x$ changes). The gradient of the field near the neutral line
increases, according to (35). Fig. 4.6a shows schematically the
distribution of the magnetic field intensity around the neutral line
along the x axis. As has been shown in (33) and (34), X_{1e} for 30 Kev
electrons is about 1/10 of X_{1p} for 130 Kev protons. Electrons between
X_{1p} and X_{1e} drift along the y axis with various trochoidal orbits,
according to the equation (22) in chapter 3. These electrons cannot
cross the neutral line, and their guiding centers move parallel to the y
axis (the neutral line). Several such orbits are discussed by Åström
(1956).

Dungey (1953) showed that this state will not be steady, and that the electric current will grow spontaneously. He inferred that the gradient $(\partial Z / \partial x)$ in the narrow strip around the X-type neutral line will tend to become infinite. It may be, however, that the region between $\pm X_{1p}$ has a structure similar to that of the front layer of hydromagnetic shock waves. In this transition layer various physical quantities, such as the pressure gradient Δp_n and the viscosity, will become important. They tend to reduce the high field gradient there. Petschek (1958) concluded that the thickness of the transition layer is of the same order as the radius of gyration of the protons. Therefore we may infer that X_{1p} is of order R_p just outside the narrow strip, (see Fig. 4.6a), that is,

$$X_{1p} \simeq (c \; m_p w_p / eZ = R_p .$$
(36)

Next we consider the cartesian co-ordinate system used in this section in relation to the earth's field. We take the z axis northward, antiparallel to the earth's dipole axis. In the equatorial plane we direct the positive x axis toward the earth's center. Then the positive y axis is westward, and the electric current j_y in (35) is eastward. The field intensity Z becomes H. Thus (35) may be rewritten as follows:

$$j_y = - \frac{c}{4\pi} \left(\frac{\partial H}{\partial x} \right)_y .$$
(37)

We may also take Z, in (36), to have the value of the intensity H_M of the original earth's dipole field there, namely,

$$Z = H_M .$$
(38)

125

Thus (36) is

$$X_{1p} \simeq \left(c \, m_p \, w_p / e H_M \right) . \tag{39}$$

At this point we introduce an assumption that is fundamental for the later developments in this paper. It is that an electric field may arise along the direction of the neutral line, that accelerates the spontaneous growth of the current along the line. Auroral and geomagnetic observations suggest that this electric field appears sporadically. This electric field must be eastward (in the negative y direction in Figs. 4.5, 4.6a, 4.6b). It will accelerate the particles that lie near the neutral line. The electrons (because of their smaller mass) will be more accelerated than the protons, and will move in the westward direction opposite to that of the field. They move within a strip of width $2X_{1e}$.

Therefore the electric current may be expected to increase substantially within the width $2X_{1e}$. Thus the gradient of the field is increased according to (37), and X_{1e} is reduced according to (34). Of course, even in this case, the field gradient will not be infinite. We suspect that X_{1e} becomes comparable with the radius of gyration of the electrons ($c \, m_e \, w_e / e \, H_M$). (See Fig. 4.6c).

Further the proposed electric field will cause the particles in the positive and negative x domains to draw closer to the neutral line. Outside the strip of width $2 \, X_{1e}$, in which the particles gyrate regularly around the lines of force (which there lie along the z direction), this drift is given by the first term of (3.38), namely,

$$\underline{v} = c \, \underline{E} \times \underline{H} / H^2 .$$

125

Inside this strip there is no complete gyration, and the drift will be less than $c \underline{E} \times \underline{H}/H^2$. By vector multiplication by $\underline{H}$ the above equation may be transformed to

$$\underline{E} + \underline{v} \times \underline{H}/c = 0$$

(cf. Cowling 1956a, p. 542). This indicates that a magnetic field is frozen in the plasma. Therefore there is a tendency for the particles, as they draw closer to the neutral line, to carry the lines of force with them from both sides. The concentration of particles near the neutral line is associated with an increase in the magnetic gradient $(\partial H/\partial x)$. Thus the electric field has three effects, the concentration of the particles, the steepening of the magnetic field gradient, and the acceleration of particles along the neutral line. All these effects contribute to increase the linear velocity of the particles along the neutral line.

It is shown in § 3.72 that the particles for which θ is 3° or less will quickly be lost to the outer radiation belt. Hence the distribution of velocity points will have antipodal holes on the surface of the velocity sphere, round the axis $\underline{H}$ (Fig. 3.14b). In a steady state there will be no particles in the outer radiation belt that can produce the aurora.

In order to explain the particle flux that produces the aurora, we must find a process that changes the pitch-angle distribution. The guiding center approximation must somewhere cease to be valid. The process must occur in a very narrow strip, so as to produce the thin ribbon-like structure of the aurora. Because of the rapid gyration and the small

cyclotron radius of high energy electrons, it seems that the only place where the guiding center approximation breaks down is a narrow strip close to the X-type neutral line. A group of high energy electrons crossing the strip close to the X-type neutral line will have its pitch-angle distribution changed.

Åström (1956) showed that except for $0.86 < k < 0.91$ the particle motions we have discussed are unstable in the sense that any small deviation from the equatorial plane will increase. Thus all the motions within the width $2X_1$ are unstable. The magnetic fluctuations discussed above can easily generate much instability.

Furthermore, just above and below the equatorial plane ($z = 0$) there is the X component of the magnetic field (see equation (10)). This field continuously deflects the particles upwards or downwards. The equation of motion for the particles when just above or below the equatorial plane is (see equation (14),

$$m\dot{w} = - (f\ e/c)\ zv, \tag{40}$$

or

$$\ddot{z} = \frac{1}{2}\ \frac{d\dot{z}^2}{dz} = - (f\ e/mc)\ zv \tag{41}$$

Integrating (41) we have

$$\dot{z}^2 = \dot{z}_0^2 - (f\ e/\ m\ c)\ vz^2$$

where $\dot{z}_0$ ($= w_0$) denotes the initial velocity along the z axis. We are interested in the particles drifting along the neutral line with simple wave motion (namely, particles with $k < \frac{1}{2}$). For such protons, $v < 0$, thus the right hand side of (42) is always positive. The protons, once

128

deflected from the equatorial plane, will continue to move upward or downward from the equatorial plane. Likewise the electrons also continue to move upward or downward (because $v > 0$ and $e < 0$).

We may also expect that the intense constriction of the electrons around the neutral line produces a strong electrostatic field. This is rapidly diminished by a differential motion of the background ionization along the lines of force and also by the motion of the constricted electrons themselves along the lines of force. These electrons will gain in the velocity component along the lines of force.

From the above discussion we may conclude that the region around an X-type neutral line of width $2X_1$ is the only region where the particles can be accelerated and where their velocity components w_s and w_n are inter-convertible.

In the following sections we develop the foregoing arguments in relation to auroral morphology. It seems that the major auroral phenomena can be explained as the direct or indirect result of complicated electromagnetic changes occurring in or near the equatorial plane at a distance of several earth radii from the earth's center. These changes produce associated complicated effects in the auroral atmosphere. The hypotheses proposed here and their consequences may be contrasted with Störmer's theory, in which the auroral phenomena are ascribed to solar particles coming directly from the sun, under the influence of the dipole field alone, or of this and also of the ring current.

4.4 THE AURORAL ZONES

4.41 The auroral zones

The first great compilation of all available auroral data was made

by Fritz (1881). From it he computed, for a number of stations, the average relative frequency of nights of auroral visibility, expressing it as M nights per year. Then he drew a chart showing lines of equal M. These lines he called 'isochasms'. His chart referred only to the northern hemisphere. His work was revised by Vestine (1944), who used further data accumulated up to 1942. Vestine and Snyder (1945) later made a similar map for the southern hemisphere (this has been revised recently by Bond and Jacka (1960) who used the data obtained during the ICY).

The geographical distribution of the aurora thus obtained, however, gives no indication of the space-time morphology of an individual auroral display. Davis and Kimball (1960), using data from a closely-spaced array of all-sky cameras that covered the major part of the Alaskan sky, showed that there, on the average, auroral arcs occur most often between geomagnetic latitudes 66° and 67°. They also found that new arcs most often originate between geomagnetic latitudes 66° and 69°, whence they move southward or northward.

We interpret these two facts as indicating that the neutral lines are most frequently formed in the equatorial region approximately at a distance d given by

$$d = 1/\sin^2 \phi' = 6.29 \text{ earth radii,} \tag{43}$$

where ϕ' denotes the auroral co-latitude. This is taken to be $23^{\circ}30'$. This also suggests that at such times the main part of the ring current most often lies just beyond this distance from the center of the earth. The major injection of solar particles, whose precise mechanism is not known, may occur there.

To explain this, Störmer (1955, p. 294) had to assume protons of

monochromatic energy of more than 4.8 Mev. Even if the requirement

regarding the proton energy were rendered less unlikely by the distortion

of the earth's field (Störmer ibid. pp. 340-346), it is altogether

impossible to expect that the field can guide electrons of order from

30 Kev to 100 Kev to that region. (Even electrons of energy as high as

0.3 Bev can enter only in geomagnetic latitudes higher than 77°). As

recent researches have shown (cf. Meredith et al. 1958, McIlwain 1959,

Winckler 1960), electrons of energy 30 to 100 Kev play an important role

in auroral physics. It is also against present evidence to assume that

the phenomena depend on protons of well defined monochromatic energy

4.8 Mev.

4.42 The daily variation of the auroral zones

(a) Nighttime appearance

The auroral zone defined by Fritz and others is of course derived

from nighttime observations. Radar can detect daytime auroras. It is

thus found that auroras may extend into the hours of daylight and begin

before sunset. But this seems to occur rarely. As far as the auroral

zones are concerned, one of the most important auroral features is their

occurrence chiefly at night. This can be explained by the distortion of

the earth's field by the DCF field, produced by the electric current at

the surface of the solar stream.

The "dipole" field is "compressed" and essentially doubled at the

vertex of the inner surface of the stream. But it is much less affected

on the night side of the earth. Therefore, as is suggested in § 4.21

131

and in Fig. 4.4, the ring current may often be able to reverse the undisturbed earth's field on the night side, when it cannot reverse it on the day side until the ring current is strongly enhanced. Therefore we expect that during weak and medium disturbances the neutral line or lines are usually formed only on the night side.

The argument in § 4.41 suggests that on the average the radius q of the ring is larger than 6.3 earth radii. Taking $(q/a) = 6.5$, $(b/a) = 0.5$ and $(A/a) = 6.7$, it is found that the neutral line appears at about 6 earth radii if H_{Ro}, the surface intensity of the ring at the equator, exceeds 32 γ. However, if there is a more or less permanent ring current with intensity 50 γ there, as is suggested by Sonett et al. (1960), an addition of 21 γ will suffice to produce a neutral line on the night side hemisphere. This seems quite a reasonable amount.

Thus the formation of the neutral line depends not only on the intensity of the pre-storm ring current, but also on the intensity of H_{CF} and on the position of the ring. This is further discussed in § 4.43.

It is also interesting to note that when the intensity of the ring current is enhanced the neutral line extends further towards or on to the day side of the earth. In fact, auroral displays are seen in the evening and dawn twilight at times of large magnetic disturbance.

(b) Regular daily variation of the auroral zones

Another important feature of the auroras is the regular daily progression towards the south before midnight and the recession towards the north after midnight. This has been discussed by Heppner (1954), Rees and Reid (1959) and Davis and Kimball (1960). This may also be explained by the distortion of the earth's field, as was first pointed

out by Rees and Reid (1959), and Reid and Rees (1960). However, as was

indicated in § 3.8(b), the detailed proof must await rather laborious

numerical calculation of the adiabatic invariants $\int_{m'}^{m} w_s \, d\ell = J$ for such

a distorted field.

Vestine and Sibley (1959) calculated this integral for the actual

earth's field, by taking $H_m = 0.45$ gauss and by using 48 terms of the

spherical harmonic expansion of the geomagnetic field. They drew

isolines of the integral $\int_{m'}^{m} (1-H/H_m)^{1/2} d\ell$. The close agreement with the

isochasms drawn by Fritz and Vestine suggests that the auroral particles

may be treated in the way discussed in Chapter 3. The instantaneous

position of the aurora in the polar region will be obtainable in

essentially the same way, when we can properly take into account the

distortion of the (M +DR) field by DCF.

4.43 Storm time variation of the auroral zones

(a) Equatorward shift of auroras

One of the remarkable features of large magnetic disturbances is

the shift of auroras towards the equator. Diffuse red auroras are seen

from geomagnetic latitudes as low as 30° during the largest magnetic

storms. Here, however, we are concerned with the equatorward shift of

auroras with arc structure (e.g. rayed arcs or rayed bands).

In Fig. 4.3 we have seen that when H_{Ro} is as large as 500 γ, the

neutral line advances towards the earth as far as 3.6 earth radii from

the earth's center. The corresponding geomagnetic latitude, in which we

may expect that rayed arcs and bands will appear, is $58^{\circ}11'$. This also

depends somewhat on the position of the ring current. For $(q/a) = 4$,

(b/a) = 0.5 and (A/a) = 4.5, the position of the neutral line is about 3.1 earth radii, which corresponds to 55°30' geomagnetic latitude. If we take into account the distortion of the earth's field, the neutral line may advance further towards the earth.

Fig. 7 shows an example of a rayed band. It appeared in the northern United States on the night of 23 September 1957, during one of the largest magnetic storms that occurred during the IGY. This band was seen (a) north of Pullman (gm. lat. 53°5 N) and (b) overhead at Choteau (gm. lat. 55° N). These two stations are separated from each other by about 250 miles in longitude and are about 10° south of the auroral zone. An intense X-ray burst was observed by Winckler (1960) at Minneapolis (gm. lat. 55° N), further to the east, at the same time. This time was near local dawn, but observations suggested a further extension of the rayed bands towards the east.

Barbier (1958) and Roach (1959) reported that at the same time a monochromatic 6300 Å arc detached itself from the rayed band and moved southward (see also Roach and Marovich 1959). The band also extended to the west, at least as far as Alaska (Akasofu 1960b).

(b) Day to day variation of the auroral zones

We may expect that the aurora will extend furthest towards the equator when the ring current attains its maximum intensity. Then the ring current begins to decay. The rapidity of decay first increases and then slows down. Correspondingly the neutral line will recede from the earth, and the auroral arc will return polewards. As has been seen in § 4.41, there is a daily variation of the position of the auroral zones.   Also in the northern hemisphere, the southernmost latitude of

the aurora increases from night to night, as the DR intensity becomes less and less. During this interval, we might also expect a repetition of similar auroral displays on two or three consecutive nights.

After a few nights, the aurora does not appear to progress appreciably equatorward and does not show any distinguished display; finally it disappears. This may correspond to the decay of the ring.

The life time of the neutral line depends on the nature and amount of variation of the ring current. It seems likely that the ring current constantly exists during the sun's active period, perhaps with a field of central intensity about 50 γ , although it may be too weak to produce neutral lines. Complexities arise if a new reinforcement of the ring current occurs during the decay period.

4.5 PARTICLE INJECTION ASSOCIATED WITH ARCS

4.51 Diffuse quiet arcs, single or multiple

At College, Alaska (gm. lat. 64°7 N), auroral displays begin with a rather homogeneous arc near the poleward horizon. This is only a rough description, because the aurora is far distant (> 300 km), and its details cannot be seen. When the arc advances southward, and can be seen more clearly, we often find that its brightness is continuously changing. At that stage ray structure is absent, or weak and rather diffuse. Fig. 8 shows the all-sky camera photograph taken from Fort Yukon, Alaska (gm. lat. 66°7 N) at $09^h 37^m$ GMT on 16 February 1958; the local time was $23^h 37^m$ on 15 February. The photograph shows at least five separate diffuse arcs. Two of them are south of the zenith. They extend in the geomagnetic east-west direction, approximately.

135

4.52 Auroral spectra and hydrogen emission

The most prominent and common lines and bands found in the spectra

of high latitude auroras are as follows. Atomic lines: wave-lengths

5577 (OI), 6300 (OI), 6364 (OI), 3466 (NI), 5200 (NI), 6563 (HI) (= H_α),

4861 (HI) (= H_β) Molecular bands = N_2 First Positive, N_2 Vegard-Kaplan,

N_2^+ First Negative (including 3914 and 4709), N_2^+ Meinel bands and others.

The identification of the lines and bands, and their excitation mechanisms,

have been extensively studied by various workers. The results are well

summarized in articles by Chamberlain and Meinel (1954) and by Bates

(1954, 1960).

It has been suggested at times that extra-terrestrial protons are

one of the most important agencies, direct or indirect, in producing the

auroral luminosity. Recent detailed studies have shown, however, that

the hydrogen lines appear most often in the spectra of quiet and diffuse

forms, and less often in the active forms. (cf. Romick and Elvey 1958,

Galperin 1959, Montalbetti 1959). These studies suggest that there is

no clear systematic relation between the various auroral luminosities and

the intensity of the hydrogen emission.

As a result of comparing the intensities of H_β and of 4709, Omholt

(1957) suggested that auroras are caused mainly by fast electrons rather

than by protons. Following his discussion, Bates (1960, p. 320) concluded

that protons cannot be the dominant cause of the auroral luminosity most

commonly seen in the auroral zone. The proton flux is at most $10^8/cm^2$ sec.

Usually it is much less, of order $5 \times 10^5 /cm^2$ sec. The most probable

proton energy may be of order 130 Kev (cf. Bates 1954, p. 625).

136

4.53 Rocket observations

In recent years rocket techniques for the exploration of the upper atmosphere have been extensively applied to the study of auroras. Meredith et al. (1958) showed that the energetic electron flux in a faint rayed arc was confined to the region of auroral luminosity; protons were detected over a wider area surrounding the auroras. McIlwain (1959, 1960) found that energetic electrons accounted for at least 90 per cent of the energy flux measured in the region of a diffuse auroral band penetrated by one of his rockets. These results support the conclusions derived from the spectroscopic studies.

4.54 Theory of the structure of a quiet arc

In §§ 4.31 and 4.32, we have discussed the motions of protons and electrons around the X-type neutral line. When there is no electric field along the neutral line, the width $2X_{1e}$ for 30 Kev electrons is about 1/10 of that for 100 Kev protons (see equations (33) and (34). It has been shown that the electron strip is located in the middle of the proton strip (see Fig. 4.6a). The protons and electrons in these strips are unstable, and travel to auroral levels in the atmosphere, along the lines of force through the strips.

If the strips are at 6 earth radii from the earth's center, (so that $H_M = 150 \gamma$ in equation (39)) the strip width $2X_{1p}$ and the radius of gyration R_p for 130 Kev are given by

$$2X_{1p} = 2R_p = 695 \text{ km.}$$

The distance at the auroral level between the two lines of force which

in the equatorial plane, at the distance of 6 earth radii, are separated by 695 km, is 29 km. This may correspond with the width of the layer of auroral emission of H_α and of the other lines excited by protons. In the middle part of this layer there may be a thin layer excited by electrons, which is supposed to produce the major part of the luminosity visually observed. The thickness of this inner layer is of order 3 km ($\sim 29/10$). This structure seems to agree well with the rocket observations of quiet forms of the aurora.

The fundamental form of the aurora, narrow in width but extremely long in the east-west direction, accords with Fig. 4.4, in which for a medium disturbance ($H_{Ro} = 70 \ \gamma$) the projection of the neutral line on the earth encircles nearly 3/4 of the auroral zone.

We suggest that in this way high energy protons and electrons in the outer radiation belt are discharged through the X-type neutral line into the auroral ionosphere and produce a diffuse aurora.

4.55 Multiplicity of arcs and the outer geomagnetic field

As Elvey remarks (1957), the aurora in the simplest case consists of only one arc, but in many cases it is multiple, consisting of many arcs. The arcs are, in general, nearly parallel to each other. An example is shown in Fig. 4.9 (Elvey 1957, his figure 5). Another example is also seen in Fig. 4.8.

This suggests, according to our hypothesis, that the outer geomagnetic field at the time of a magnetic storm is not at all simple. The irregular and intermittent injection of solar particles into the geomagnetic field may produce several current layers there. This would

complicate the field distribution, and may produce several neutral lines. Table 4.1 shows the approximate geomagnetic latitudes of the arcs of Fig. 4.9 and the corresponding positions of neutral lines in the equatorial plane, calculated from (43).

Fig. 4.10a shows schematically the intensity of the disturbed magnetic field along an equatorial radius from the earth, in the midnight meridian plane, during a magnetic storm. Fig. 4.10b shows the magnetic field lines in the midnight meridian plane. Protons and electrons travel along the lines from the X-type neutral lines a,b,c,d,e and produce parallel auroral arcs in the auroral ionosphere, as indicated in the diagram. Fig. 4.10c shows the five loops formed by the X-type neutral lines a,b,c,d,e of Fig. 4.10a and b and by the associated 0-type neutral lines (shown by broken lines).

TABLE 4.1

Positions of the arcs in figure 11 and of the corresponding X-type neutral lines

Arc	Position (geomagnetic lat.)	Distance from the earth's center (earth radii)
a	68°06'	7.2
b	67°06'	6.6
c	65°24'	5.8
d	64°54'	5.6
e	64°12'	5.3
f	63°18'	5.0
g	62°42'	4.7
h	62°00'	4.5

In this connection we may refer to the observations of the density of the radiation belts made by the US Satellite Explorer VI. This had an elongated orbit extending out to 7.6 earth radii from the earth's centre; the orbital period is $12\frac{1}{2}$ hours. Observations of particular interest were made during the storm that occurred from 16 to 18 August 1959. During the earlier part of this disturbance, a notable decrease in the counting rate in the outer radiation belt was reported by Arnoldy et al. (1960). Moreover the same rocket revealed intense fluctuations of the rate between 5.5 and 7.5 earth radii from the center of the earth (Rosen et al. 1960). This may have been associated with much complexity of the outer geomagnetic field, as suggested by the study of the multiplicity of arcs.

The life time of each arc depends on the life of the irregular current layer. If there is some local action which invalidates the guiding center approximation the particles diffuse from one surface defined by $J = \int_{m'}^{m} w_s \, d\ell$ to another, and merge into the background ionization.

4.6 RAYED ARCS

4.61 Rayed arcs and high energy electrons

The most spectacular phase of auroral displays comes when the quiet form brightens and fine ray structure appears in it. Fig. 11 shows an all-sky camera photograph of an exceptionally fine example of a rayed arc. The photograph was taken at Kotzebue, Alaska (gm. lat. $63\overset{o}{.}6$ N) at $11^{h}19^{m}$ GMT, 23 September 1957 ($00^{h}19^{m}$ local time). A large polar magnetic disturbance (of order 1500 γ in the horizontal component) was recorded at College at the same time.

During this stage electrons make the major contribution to the auroral luminosity. This has been confirmed by balloon measurements (Winckler et al. 1958, 1959; Winckler 1960). The simultaneous appearance of the strong auroral-associated radio absorption might also indicate the precipitation of high energy electrons (Chapman and Little 1957; Little and Leinbach 1958; Reid and Collins 1959). It is thought that the energy of the typical auroral electrons is of order 30 Kev, and that their flux is of order $10^{11}/cm^2$ sec. The maximum radius of gyration of such electrons at the auroral level (taking the total intensity of the earth's field to be 0.6 gauss) is 7.1 m. We interpret the ray structure in the arc as an instability of the electron sheet-stream extending from the neutral line to the visible aurora. This is further discussed in § 4.7.

One of the outstanding facts to be explained is the extreme thinness of the rayed curtains and folds. Elvey (1957) estimated it to be not more than 250 meters. The two lines of force which in the auroral zone are separated by 250 meters in the meridian plane are only 6 km apart in the equatorial plane. This distance of 6 km may be contrasted with the width of the Van Allen radiation belts--of order at least 10,000 km. This suggests that the equatorial sources of auroral rayed forms are extremely local features in these immense belts. Similarly the width 6 km is far less than the radius of gyration (348 km) of the 130 Kev protons, or than their mean free path, or than the wave length of hydromagnetic waves (this is of order 200 km).

In § 4.32 we found that an eastward electric field can accelerate the electrons in a strip around the neutral line, of width $2X_{1e}$, and that it will produce an extremely large gradient of the magnetic field (see

also Fig. 4.6b). It seems likely that rayed arcs are produced by this strong constriction of electrons around the neutral line due to the electric field proposed in §4.32. The substantial increase of electron flux at this stage supports this view. As before in §4.53, taking H_M to be 150 γ , the width of the region traversed by the 30 Kev electrons drifting along the neutral line is

$$2X_{1e} = 2R_e = 5.6 \text{ km}$$

This agrees well with the above estimate of 6 km. The thickness of the corresponding arc would be 230 meters.

This thinness, of order less than 500 meters, may also be contrasted with the width of the zone in which there is a continual flux of high energy electrons. This zone is at least 1000 km wide (from geomagnetic latitude $65°$ to $75°$) (Van Allen 1957; Vernov et al. 1959). This continual flux may be connected with the high intensity of the 5577Å glow in the auroral zone (Roach and Rees 1960). But in the rayed arc there must be a far stronger concentration of electrons.

The width of the equatorial exit band (proton flow) decreases from 695 km during quiet arcs to 5.6 km at the time of the electron constriction. The motion of protons in a field with such a steep gradient may be unstable, and the constriction of protons there may be much less than that of electrons. An abrupt diminution of H_α radiation at the time of auroral break-up has in fact been reported by many workers (Dahlstrom and Hunten 1951; Fan and Schulte 1954; Romick and Elvey 1958; Galperin 1959; Fan 1958; Montalbetti 1959; Malville 1959a).

142

4.62 Runaway electrons near the neutral line

In § 4.32 we introduced the hypothesis of an electric field along the neutral line, that accelerates and constricts the electron flow. In § 4.61 we saw how rayed arcs can be explained by this electron flow. In their most active stage, the height of the lower border of the rays is decidedly less (from 70 km to 90 km; cf. Elvey 1957) than for quiet arcs (around 120 km); also the lower border of the rays is purplish-red. Auroras showing this purplish-red border are said to be of Type B. By using Bates' table 12 (1954, p. 625), Malville (1959b) inferred that Type B aurora is caused primarily by high energy electrons (of order 250 Kev). (This is because the atmospheric density rapidly increases downwards). Therefore a considerable acceleration of the electrons seems to accompany the sudden change of auroral form from quiet to the most active.

Furthermore, it has been shown by McIlwain (1960) that the flux of high energy electrons in an active aurora is as high as $10^{11}/cm^2$ sec. As has been shown in § 3.7, only a small fraction of the flux in the equatorial plane (1% of the total flux) can contribute to the auroral luminosity. The flux at the center of the outer radiation belt is of order $10^{11}/cm^2$ sec. Assuming an isotropic pitch-angle distribution (§ 3.4), even the center of the outer radiation belt can produce the flux of order only $10^9/cm^2$ sec for a few seconds, if there is no supply of such electrons. Arnoldy et al. (1960b) showed that the solar stream does not contain such a large flux of high energy electrons, so that there must be some mechanism which accelerates ambient electrons so as to produce a large flux of order $10^{11}/cm^2$ sec in the aurora.

143

In a magnetic field such as the outer geomagnetic field an electric field perpendicular to the field lines cannot accelerate the charged particles there, because such an electric field can produce only a drift motion perpendicular to both the field lines and the electric field (see § 3.31 (38)).

Suppose that a cloud of particles is injected from the solar stream around a region where the neutral lines are located. The protons drift westwards and electrons eastwards. There may arise a slight electric polarization field tending to prevent their independent motion, but it will be reduced in a short time. We show here that even an extremely weak electric field can accelerate both high energy electrons and ambient electrons to the required high energies.

It seems likely that the polarization electric field plays an important role in this process. As has been discussed in § 4.3, the direction of the electric field is eastward. The process must be a transient phenomenon, because the field will be reduced in a short time. We discuss this transient nature in Chapter 5.

In this section we associate the acceleration due to the electric field near the neutral line with the "runaway" phenomenon. When an electric field E is sufficiently weak (and the deviation from the Maxwellian velocity distribution is small), the electric current produced is proportional to the applied electric field. However, if an electric field exceeds a critical value, denoted by E_c, the electric current j increases more than proportionally to E, and there is no time-independent relation between them. This is called the "runaway" phenomenon.

144

The critical electric field E_c for which runaway can occur has been given by Dreicer (1959) as follows:

$$E_c = \frac{e}{\lambda_d^2} \ell n(\lambda_d/p_o) esu,$$ (63)

$$= 1.44 \times 10^{-6}/\lambda_d^2 \text{ volts/cm}$$

Here λ_d denotes the Debye length

$$\lambda_d = \left(\frac{\kappa T_e}{4\pi n_e e^2} \right)^{1/2} \text{cm;}$$ (64)

also $\ell n(\lambda_d/p_o)$ is the cut-off factor, here taken to be 10 for all conditions.

Even if we take the background thermal electrons (near the neutral line) to have energy as low as 1 ev (T = 7734° K) and if the density is as high as $10^2/cm^3$, the critical field E_c is only of order 3.9×10^{-10} volts/cm (λ_d = 61 cm). For more energetic electrons E_c will be still less.

4.7 INSTABILITIES OF AURORAS

4.71 Large-scale folded structure

In this section we discuss the large-scale wavy or folded structure of active auroral arcs. Waviness begins to develop when the rayed arc becomes fairly active, and as the activity increases the waves often develop into folded structures. The 'wave length' has a wide range, from 10 km up to 500 km. In their most developed form the folded structures or curtains often roll along. This stage is usually called 'auroral

145

drapery'. At such times a purplish-red color may appear at the lower border of the arc.

It is known that instability is one of the most common characteristics of strongly constricted electric currents. If strong constriction of an electric current occurs along the neutral line when the auroras become active, the current is likely to show such instability. Any distortion of the neutral line is immediately projected on to the auroral level, so that we regard wavy and folded structures of auroras as indicating a similar form for the associated neutral line or lines. If the purplish-red color mentioned above is due to high energy electrons of more than 100 Kev, as Malville (1959b) suggested, this supports the view that there is strong constriction and acceleration of electrons along the neutral line.

So far such a non-linear effect has been discussed only by perturbation methods (Lundquist 1951 ; Kruskal and Schwarzschild 1954; see also Pease 1958). Lundquist (1951) showed that kinks in a constricted cylindrical current in a free space develop when

$$H_\phi^2 > 2 H_z^2,$$

where H_ϕ denotes the azimuthal field produced by the current itself and H_z denotes the original axial field. In our case, $H_z = 0$. But the boundary conditions are quite different from those considered by Lundquist. Hence his result cannot be applied immediately. But we suspect that the kinks develop in essentially the same way when the constriction of the current exceeds some critical value.

4.72 The ray structure (the small-scale zigzag structure)

The auroral arc has another type of wave structure. Störmer gives a beautiful photograph showing this type (see Störmer 1955, his figure 83; the same photograph is reproduced in Chapman and Bartels (1940), plate 31a). A thin arc shows a small-scale zigzag structure when it becomes active. This produces an apparent inhomogeneity of the luminosity, vertical 'rays' or strips, as pointed out by Störmer (1955, pp. 325-327). Their width is less than 10 km.

This complicated feature can be most easily seen in an active corona such as appears when a rayed arc is seen at the magnetic zenith. In the most active coronas, extremely rapid and violent fluctuating motions of the zigzag structure are seen. Rapid changes of color usually appear there.

The thin electron sheet-stream from the neutral line may be unstable in the sense discussed by Webster (1955, 1957) and demonstrated by his experiments. This instability is essentially due to the electrostatic interaction of the electrons in the electron sheet stream. Small density fluctuations in the beam may produce the fluctuating electrostatic field E, which produces the drift motion of electrons in the direction determined by

$$\underline{v} = c \ (\underline{E} \times \underline{H})/H^2$$

The rate of growth of such an instability has been discussed by Gould (1959, p. 100), who treated the problem as a small perturbation. The rate of growth is largest for a wave length about eight times the beam thickness. In § 4.61 we have shown that the thickness of the rayed arc is less than 500 meters. Therefore the wave length of the fine ray

structure may be of order less than 4 km.

It may be noticed, however, that during the most active stage of the aurora there are various kinds of _apparent_ motions that have never yet been properly described or recorded. They may be regarded as instabilities of the aurora. Such motions are usually accompanied by rapid change of color, indicating quick changes in the exciting processes of various lines and bands of atoms and molecules at the auroral level.

4.73 The break-up of auroras

Auroral displays in the final phase are often fantastic. Isolated rays or patches are scattered over the sky, and there is no longer any arc structure. In § 4.71 we concluded that the wavy structures would develop into folded structures. We may regard this final display as the extreme case of the above instability. We may expect that when the folded form of the neutral line is completely developed, the configuration will be very complicated and tangled. High energy particles produced there may be stored in some way in this tangled field and be released first from one place and then from another. The projection of this condition on the auroral level may result in isolated rays or pulsating patches. Isolated rays fixed in the sky for a few minutes are also often seen. This stage is associated with rapid magnetic fluctuations with periods from 20 sec to 10 minutes. The ionospheric layers could not be the origin of these geomagnetic micro-pulsations (cf. Akasofu 1956), and we suggest that they correspond to irregular magnetic fluctuations around the neutral line. It should be noticed that at the same time strongly variable earth currents (Hessler and Wescott 1959), ionospheric absorption (Leinbach 1960)

148

and luminosity from the entire sky (Murcray 1959) have been recorded, e.g. at College, Alaska. Recently Campbell (1960) reported simultaneous fluctuations of the auroral luminosity (3914Å) and the magnetic pulsations.

This complicated stage may last until the irregular configuration of the field disappears and a rather simple neutral line is reformed. In fact, a quiet arc is often reformed after the break-up. An example is shown in Fig. 5.2, in which the quiet form is reformed between $01^h \, 30^m$ and $03^h \, 10^m$.
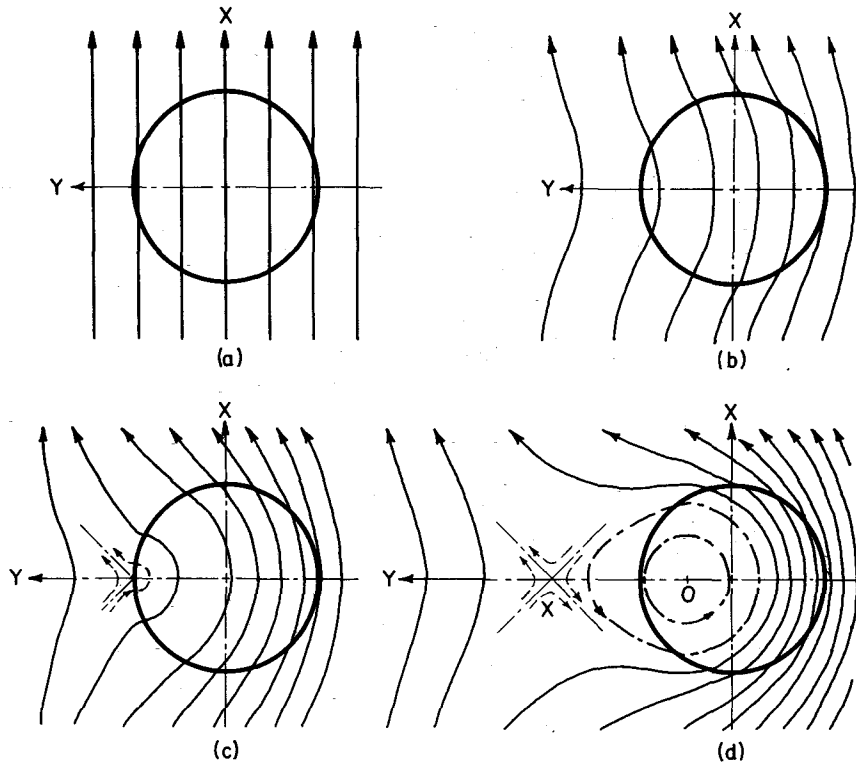
Fig.4.1. To illustrate the distortion of a uniform field by a uniform volume
electric current along and throughout a cylinder whose axis is normal to the
field. The volume current increases from zero in case (a) to a large value
in (d). The X- and)- type neutral lines are also shown (McDonald 1954).
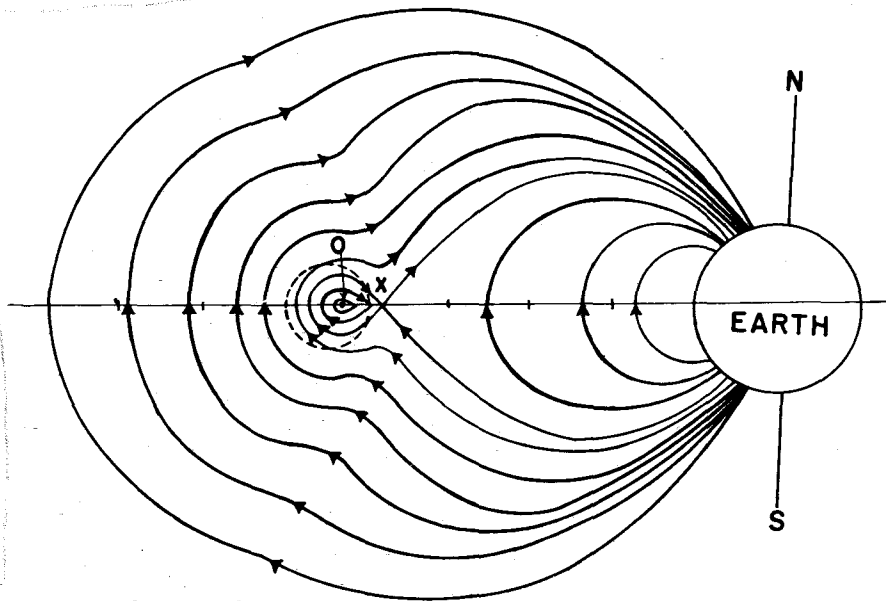
Fig.4.2. Schematic diagram of the magnetic field configuration in a meridian half-
plane,when a toroidal ring current is flowing round the earth. The boundary of
the cross section of the toroid is indicated by broken line. The X-and O-type
neutral lines are also shown.
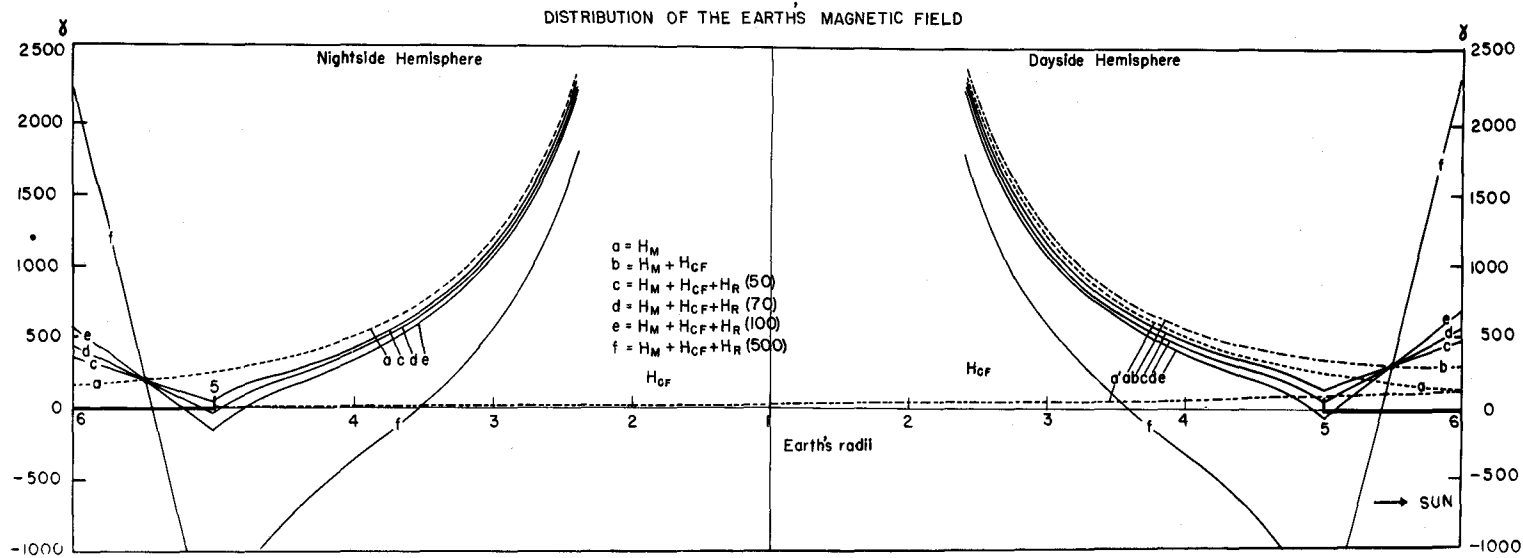
Fig. 4.3. Schematic diagram of the magnetic field intensity along the sun-earth line for various values of H_{RO}. Left, on the night side, right, on the day side, from the earth's surface to a distance of 6 earth radii. H_M, H_{CF} and ($H_M + H_{CF}$) are also shown.
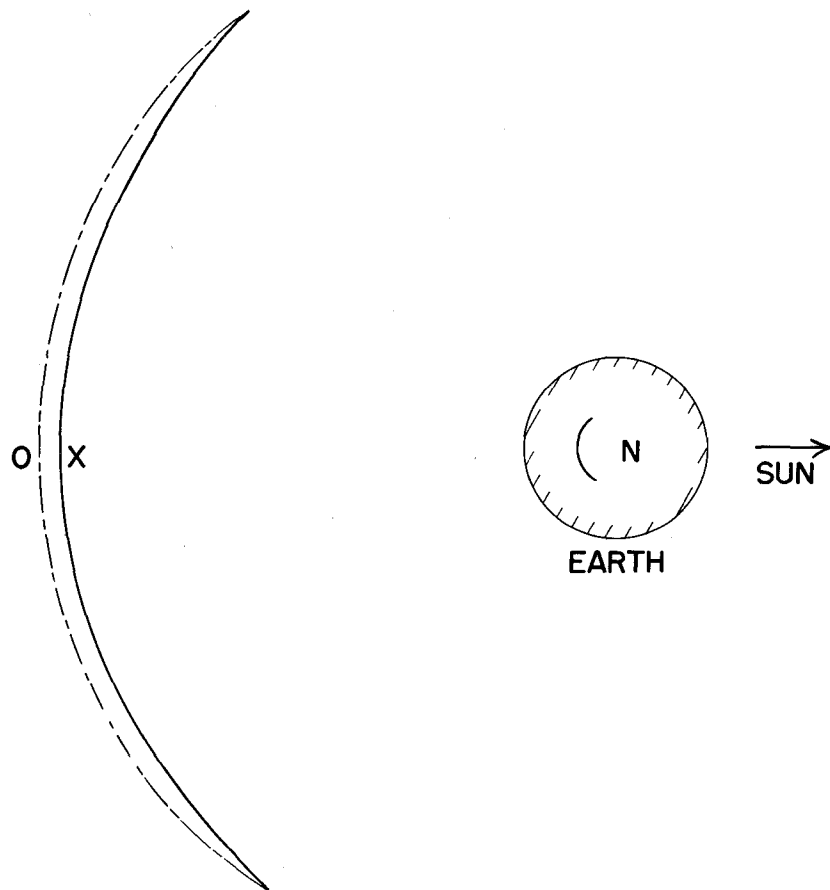
Fig. 4.4. Geometry of the X-type and O-type neutral lines in the equatorial plane. The projection of the X-type neutral line on the earth's surface is also shown.
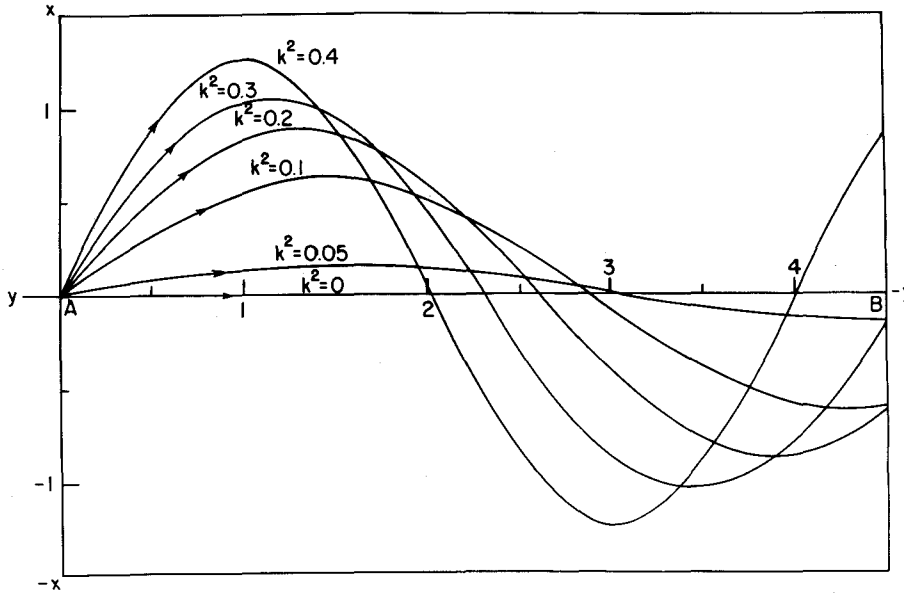
Fig.4.5. Paths of protons near the X-type line for various values of k^2.   The scale
unit of length is $(\,m\,w_p c/\,ef\,)^{1/2}$.   The paths lie in the equatorial plane; AB is
a part of the neutral line; the curvature of this line is too small to be shown
in this diagram.
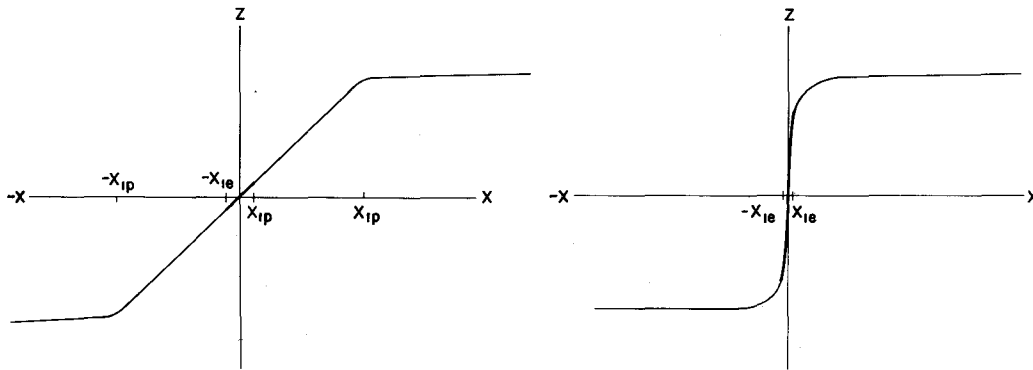
Fig.4.6a. Schematic distribution of the magnetic field intensity
near the X-type neutral line.   The protons (energy 130 Kev)
drift in the negative y direction (from the paper) with
oscillatory motion of amplitude X_{1p}.   The electrons (30 Kev)
drift in the positive y direction (into the paper) with
amplitude X_{1e}.

Fig.4.6b. Schematic distribution of the magnetic field intensity
near the X-type neutral line,when an electric field appears along
the positive y direction.   Note the increased gradient of the
field near the neutral line.
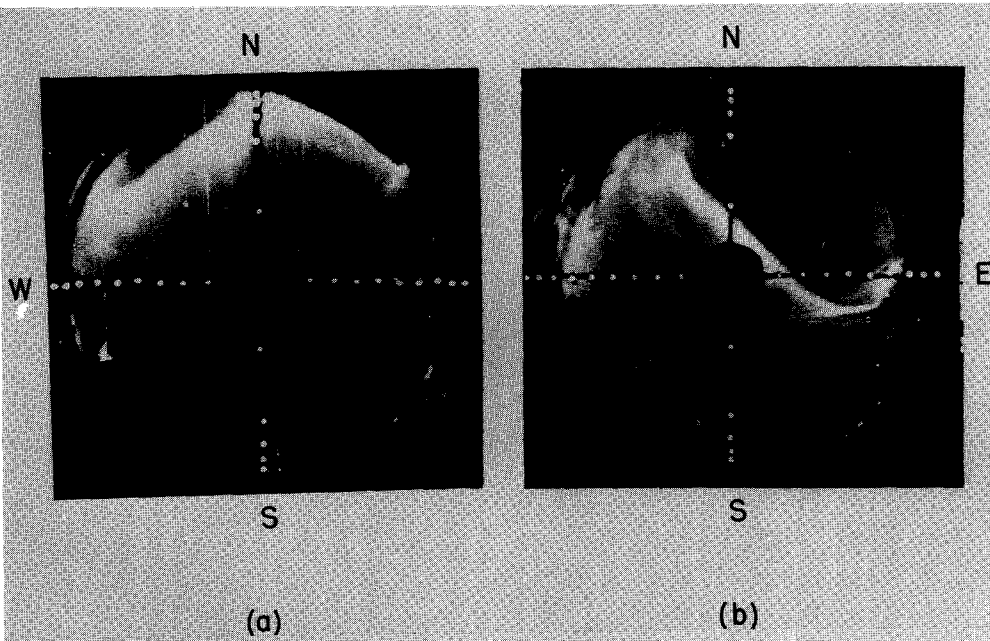
Fig.4.7. All-sky camera photographs of the aurora of 23 September 1957,from the US stations (a) Pullman (gm.lat. 5395N) at 10^h52^m GMT,and (b) Choteau (gm.lat. 55° N),about 400 km to the east of Pullman,at 10^h54^m GMT. The wavy rayed band here appears about 10° south of the auroral zone. A great magnetic storm was in progress at this time (see § 5).
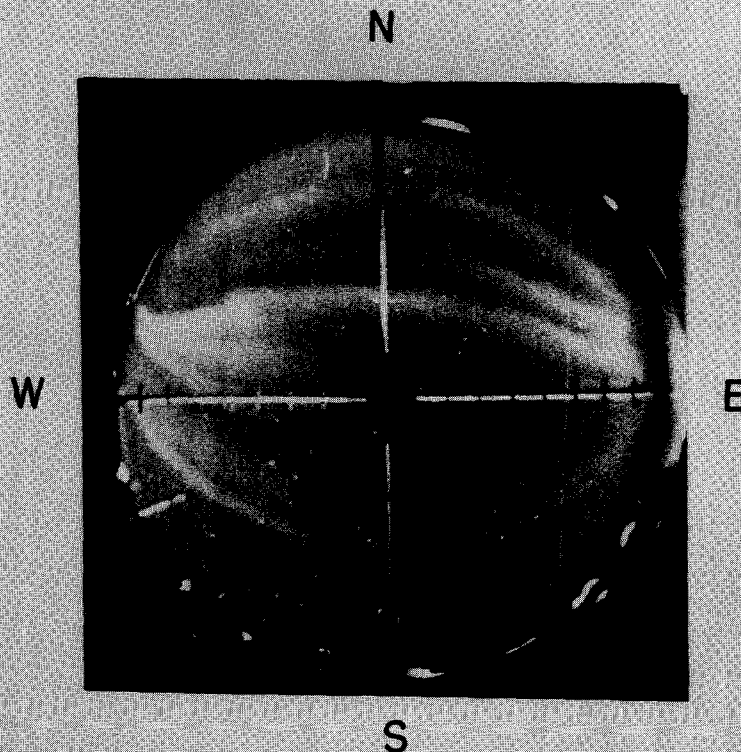
Fig.4.8. All-sky camera photograph taken from Fort Yukon,Alaska (gm.lat. 66.7N0 at 09^h37^m GMT on Februray 1958; the local time was 23^h37^m 15 Februray. The photograph shows at least five separate arcs.
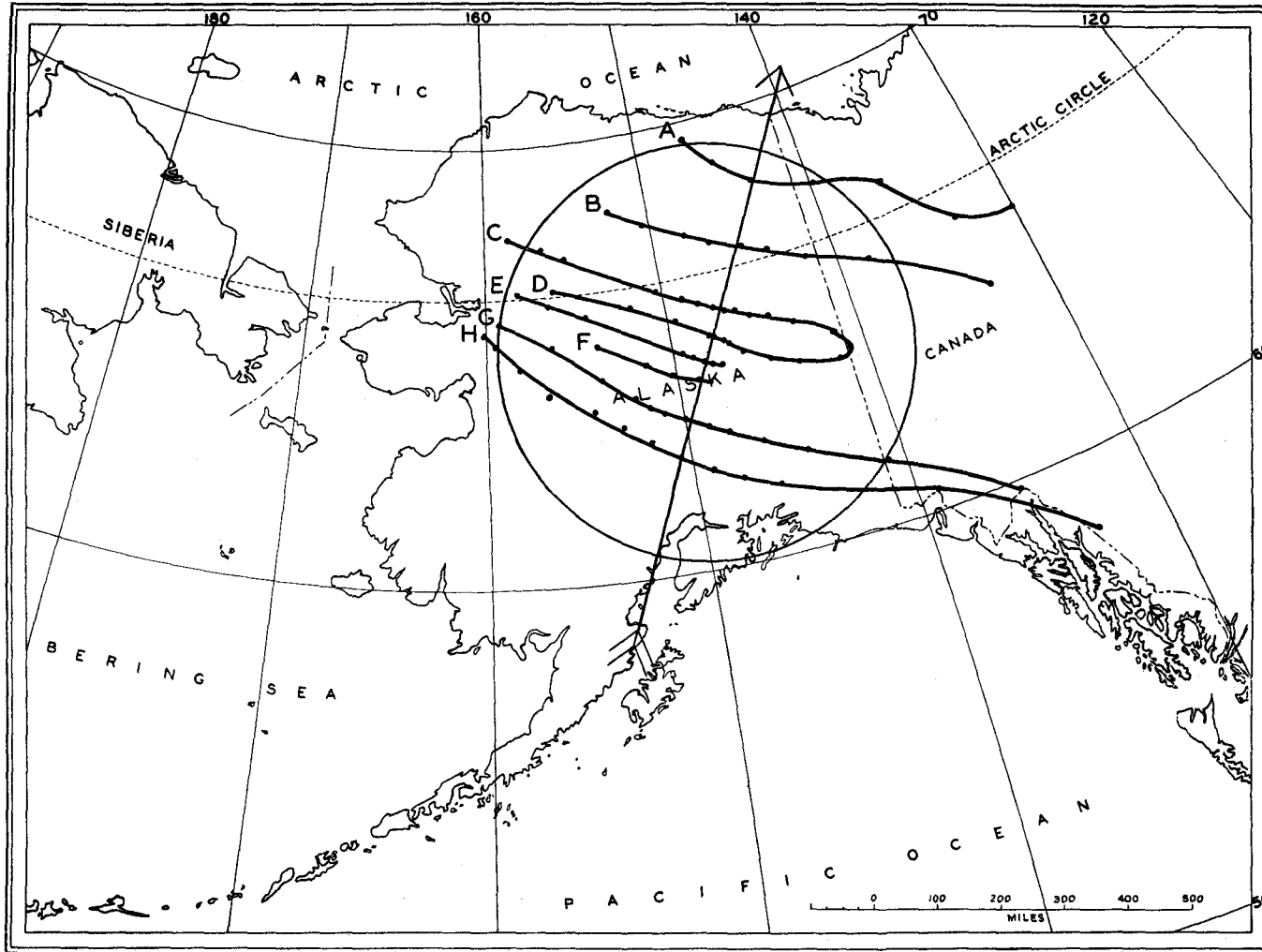
Fig.4.9. Ground projection of auroral draperies over Alaska at 07^h34^m GMT, 1 October 1954 (local time 21^h24^m 30 September 1954); from an all-sky camera photograph taken at College, Alaska (Elvey 1957).
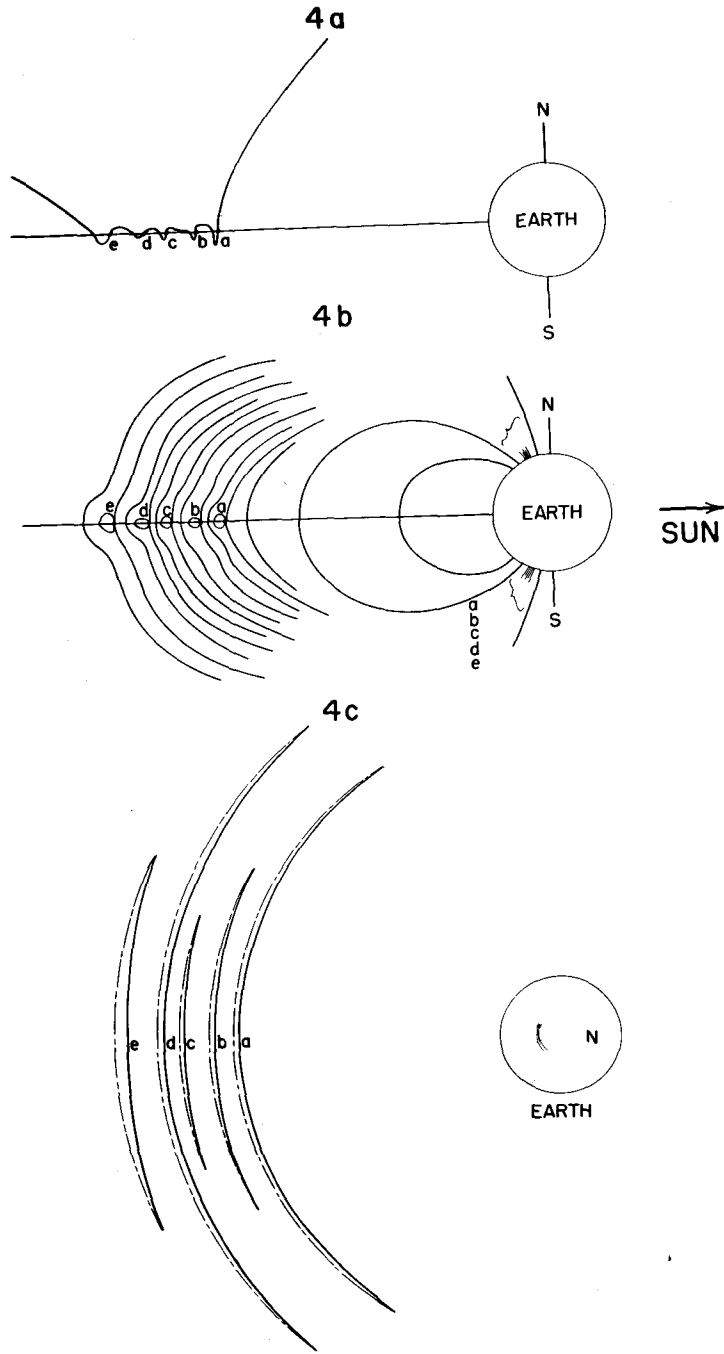
Fig.4.10. (a):Schematic graph of the intensity of the
disturbed magnetic field along an equatorial radius from
the earth,in the midnight meridian plane,during a magnetic
storm. The marked points a,b,c,d,e are the cross section
of the X-type neutral lines. (b): The corresponding
magnetic field lines. (c): The corresponding OX-loops
in the equatorial plane.
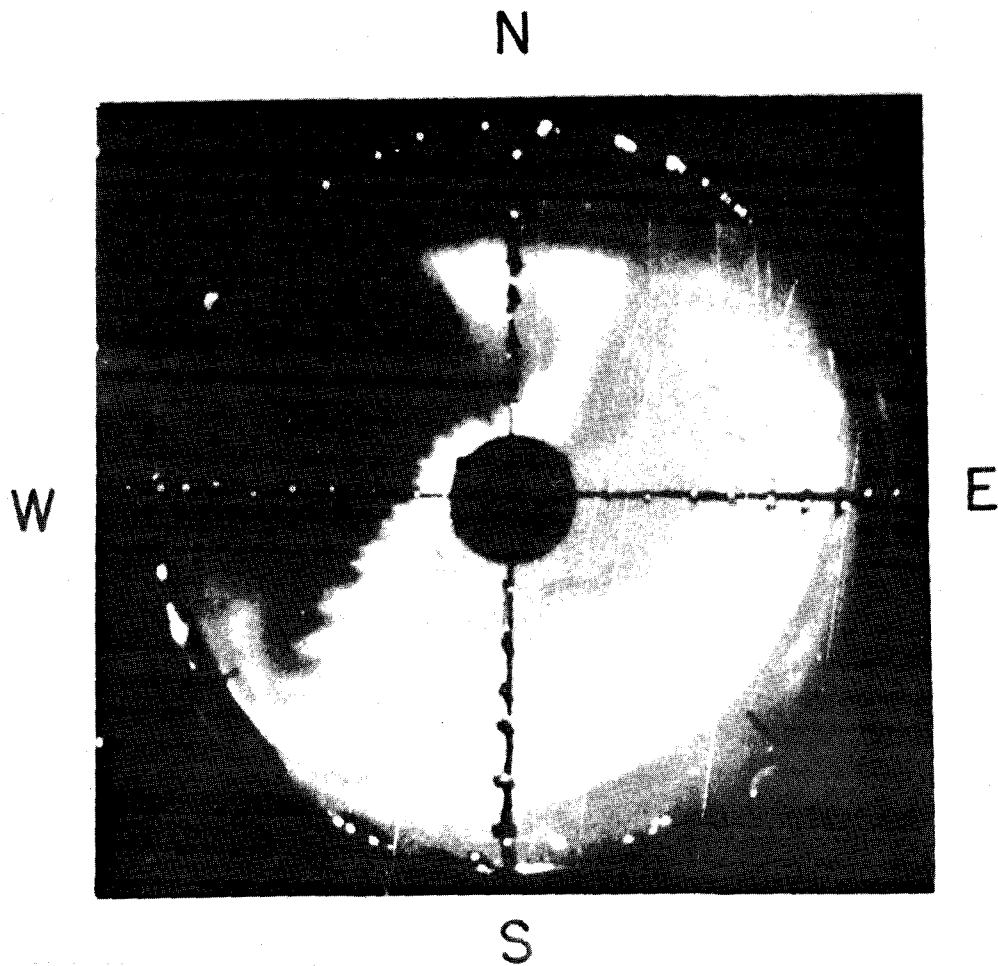
Fig. 4.11. All-sky camera photograph taken at Kotzebue, Alaska (gm.lat. $63°6N$) at 11^h19^m GMT 23 September 1957 (00^h19^m local time). It shows an exceptionally fine example of a rayed arc. A large polar magnetic disturbance of order 1500 gammas was observed at the same time at College, Alaska.

CHAPTER V

POLAR MAGNETIC DISTURBANCES[*]

5.1 INTRODUCTION

One of the most important associations with the sudden changes of

auroral form is the simultaneous appearance of polar magnetic disturbances

DP. Strong electric currents--auroral electrojets--appear at the ion-

ospheric E level along the auroral zone.

The auroral jet currents are limited to certain longitude sectors of

the auroral zone. They tend to set up a polarization field at their

eastern and western ends. This will cause the electric current to com-

plete its circuit over the polar cap, and also in lower latitudes. Thus

changes of electromagnetic condition in the auroral zone are communicated

even to the equatorial zone, without delay (within the time accuracy of

the observation). The DP disturbance, originating in the polar regions,

becomes a worldwide disturbance. Current diagrams for this kind of

disturbance have been drawn by Chapman (1935), Vestine (1940) and

Fukushima (1953). The DP currents are enhanced along the equatorial

electrojet in the ionosphere along the magnetic dip equator ($\S$ 2.6 and

Fig. 2.4). We interpret the daytime enhancement of sudden commencements

at Huancayo (gm. lat. 0.6 S), first noticed by Sugiura (1953), as a

consequence of this (Akasofu and Chapman 1961b).

Like active auroras, DP disturbances are intermittent and sporadic,

but their scale is more extensive, often worldwide. They are impulsive,

---

* Part of this Chapter covers the same ground as the papers: Akasofu and
  Chapman (1961a) and Akasofu (1960b).

150

and their life time is a few hours at most. Between the disturbances the magnetic condition is rather quiet. A quiet form of the aurora is often seen during this interval.

5.2 THE POLAR MAGNETIC DISTURBANCES OF 5 TO 6 DECEMBER 1958 (COLLEGE, ALASKA)

In this section we discuss in some detail two typical (though small) polar magnetic disturbances, which occurred during the night from 5 to 6 December 1958 (150° WMT). The data we here present are the magnetograms, all-sky camera photographs, spectrograms, VHF auroral radar and riometer data. They were mostly obtained by the Geophysical Institute, Alaska, and the Coast & Geodetic Survey Observatory as part of the IGY program.

Fig. 5.1 shows the College magnetograms of 5 to 6 December 1958 (Alaskan Standard Time, 150° WMT). Two polar magnetic disturbances began at 23^h56^m and 03^h15^m respectively. They are most easily seen in the H trace. It may be noticed how suddenly they began. Fig. 5.2 shows some of the all-sky camera photographs during this night. At 23^h50^m the all-sky photograph shows at least three rather quiet arcs. Rees et al. (1960) showed that the H_α emission layer had rapidly moved southward after a rather gradual daily southward motion in the early evening. The arcs slowly brightened between 23^h50^m and 23^h55^m. At 23^h57^m their intensity increased suddenly, and a polar magnetic disturbance began simultaneously. Until 01^h30^m the auroras were too bright for any detailed structure to be seen on the all-sky camera photographs. After 01^h30^m the auroras became quieter and the polar magnetic disturbance ceased. Between 01^h30^m and 03^h15^m several quiet arcs or bands are shown by the all-sky photographs.

At 03^h00^m a bright band is shown in the southern sky. At 03^h10^m the

aurora became active again and began to move northward. At 03^h16^m the

band crossed overhead, and a polar magnetic storm also began simulta-

neously. The auroral display lasted until dawn, when twilight obscured

it.

Fig. 5.3 shows the spectrograms taken at College on the same night

(Rees 1960). Their exposure time was 15 minutes. Before the break-up of

the aurora, H_α emission is shown in both spectrograms, taken at 23^h45^m -

00^h00^m(a) and at 03^h00^m - 03^h15^m(c). After the break-up, various lines

and bands are enhanced in (b) and (d), taken at 00^h15^m - 00^h30^m and 03^h30^m -

03^h45^m respectively. It should be noticed that there seems no particular

enhancement of the hydrogen emission after the break-up, although the

contamination due to the first positive band of N_2 obscures it. This

supports the view given in Chapter 4 that the major luminosity of the

aurora is produced by high energy electrons coming down to auroral levels.

Fig. 5.4 shows the VHF auroral radar data from Point Barrow (gm. lat.

$68^\circ.6$ N), College, and Farewell (gm. lat. $61^\circ.4$ N), from 23^h57^m to 00^h10^m on

the same night (Leonard 1960; see also Leonard 1959). Owing to the

geometrical complexity of the reflection of the radio waves, discussed

by Chapman (1952), detailed discussion must await further analysis of the

data. However, it may be said that at 00^h10^m the northernmost position

of the aurora was at least to the north of the Alaskan coast of the Arctic

Sea. Important data provided by ionospheric sounders on this occasion is

often intermittent because of a complete or partial blackout. This is

supposed to be due to the increase of ionization, especially in the lower

part of the ionosphere, which absorbs the sounding radio wave (cf. Chapman

and Little 1957). This absorption phenomenon has been demonstrated most clearly by the riometer observations (Little 1957).

Fig. 5.5 shows the absorption of 27.6 Mc cosmic radio noise measured by the riometer at College, Alaska (gm. lat. $64°7$ N) and Farewell, Alaska (gm. lat. $61°4$ N) during the night of 5 to 6 December 1958 (Leinbach 1960). It is interesting to note that the Z trace in Fig. 5.1 shows a negative excursion between 23^h37^m and 03^h00^m, indicating that the westward auroral jet appeared north of College during that time. This seems to correspond with the larger absorption of the cosmic radio noise at College than at Farewell during this interval.

From 03^h00^m to 03^h35^m the jet was south of College. Correspondingly the absorption was larger at Farewell than at College. The all-sky camera photographs in Fig. 5.2 during this interval suggest that the bright band was a seat of the electrojet when it became active. Between 03^h35^m and 03^h50^m the jet was north of College, and then until 04^h15^m it was south of College. After 04^h15^m the jet was north of College again. After 03^h45^m the absorption was larger at College than at Farewell. Hence it may be that except between 03^h50^m and 04^h15^m, when the absorption was larger at College than at Farewell, the jet was north of College or overhead there, and when the absorption was larger at Farewell than at College, the jet was south of College.

5.3 THE POLAR MAGNETIC DISTURBANCES OF 29 SEPTEMBER 1957 (WORLD-WIDE)

Fig. 5.6 shows the horizontal component magnetograms of 29 September 1957 from 12 observatories, fairly well spaced along the northern auroral zone. The mean distance between adjacent observatories is about 1300 km.

All the major DP's are likely to be recorded in the figure. The sudden commencement occurred at 00^h16^m GMT 29 September. The magnetic field along the auroral zone remained rather quiet for nearly 14 hours, until 14^h10^m. Then the first fairly large DP appeared (there was a small DP at about 06^h GMT). The second DP (one of the largest that occurred during the IGY) began at about 17^h10^m GMT. The third began at about 18^h05^m. It seems likely that active auroras were seen at these times along the dark part of the auroral zone, but data on this point are not yet available.

The horizontal disturbance vectors of the stations in the northern hemisphere at 15^h20^m GMT on that day are shown in Fig. 5.7. (For the stations of geomagnetic latitude below 60°, the Dst effect ($\S$ 3.6) is subtracted from the original vectors). It is seen that large DP currents (auroral electrojets) were located in the early morning sector in the auroral zone (Alaska) at that time.

It should be particularly noticed that even during an intense magnetic storm, like that of 29 September 1957, the magnetic disturbances in the auroral zone were intermittent, with quiet periods between. This is the major reason why we have introduced the hypothesis of an intermittent electric field that activates the neutral line, see $\S$ 4.32.

5.4 THE POLAR MAGNETIC DISTURBANCES OF 23 SEPTEMBER 1957

5.41 Introduction

One of the largest magnetic disturbances during the IGY began on 23 September 1957, at 0235 hours GMT. Various types of aurora were observed extensively during the storm, in the Northern American continent.

The magnetogram of Huancayo observatory indicated that the main phase (Dst variation) began at about 0300 GMT. Recovery there seemed to begin at about 1200 GMT. In addition to the Dst disturbance, there appeared several separate considerable magnetic disturbances in high latitudes in the Northern American continent with much shorter duration (less than 3 hr) accompanied by distinct and remarkable large-scale auroral displays. Table 5.41 shows the beginning times of this series of disturbances.

TABLE 5.41

List of polar disturbances, associated with auroras, observed in the Northern American Continent on 23 September 1957.

No.	Beginning time (GMT)
1	0438
2	0750
3	1046
4	1243

A detailed study of this interesting series of events has been made, and it is shown that all these distinct disturbances were accompanied by large-scale northward motion of the auroras. In the first part of this section, the study of the third disturbance, which began at 1046 GMT (no. 3 in Table 5.41), is reported in detail. The auroral electrojet, which was accompanied by the remarkable northward motion of the aurora, had developed between College ($64°.7$ geom. lat. N) and Sitka ($60°$ geom. lat. N) observatories, and the detailed development was almost completely recorded by both low-sensitive and rapid-run magnetographs (twelve records)

for about 25 min from the beginning. The observatories whose results have been used are listed in Table 5.42; see also Fig. 5.8.

In the second part of this section, the electric field associated with the auroral electrojet is discussed.

5.42 Auroras

The remarkable auroral display no. 3 began at 1040 GMT (0040 AST) on 23 September 1957 (Fig. 5.9). In the late evening on this day at Kotzebue in Alaska, all-sky camera films showed some auroral forms and a southward motion of several arcs; but 2 min before this particular display began, no trace of aurora was seen at Kotzebue. However, a rayed band with many folds was seen at Pullman ($53^\circ.5$ geom. lat. N) to the north (Gartlein, 1959) and at Farewell ($61^\circ.4$ geom. lat. N) to the south at that time, assuming that the arc extended nearly in east-west direction along geomagnetic latitudes. This indicates that the aurora lay somewhere along the geomagnetic latitudes between 60° and 55° just before the disturbance started.

At 1040 GMT apparent northward motion began at Farewell. The auroras crossed Farewell at about 1047 or 1048 GMT, and Kotzebue at about 1051 or 1052 GMT. However, the Pullman films clearly show that the aurora had also moved southward during this display.

Fig. 5.10 shows the approximate positions of the northernmost aurora along the geomagnetic meridian during this display (use is made of the distortion curve of the all-sky camera; Elvey and Stoffregen (1957), their Fig. 29).

156

TABLE 5.42

List of observatories and their results used in this paper

Observatory	θ	λ	ϕ	Λ	D	H_O	Results used
College	64°51 N	147°50 W	64.7N	256.5	+28°56	12,700	magnetograms
Sitka	57°03 N	135°20 W	60.0N	275.4	+28°55	15,600	magnetograms
Kotzebue	66°53 N	162°30 W	63.6N	242.2			all-sky camera
Farewell	62°32 N	153°54 W	61.4N	253.4			all-sky camera
Pullman	46°43 N	117°10 W	53.5N	300.6			all-sky camera

It is seen from Fig. 5.9 that the aurora covered the sky from the geomagnetic latitude $58°$ to $65°$ at 1100 GMT and the northernmost position was $65°$(geom.), so that the aurora was broadened there. Gartlein (1959), however, reports that there was no aurora between $55°$ and $59°$ but much between $50°$ and $55°$ in the geomagnetic longitudes between $280°$ and $325°$.

Accompanying these motions, there appeared also a rapid eastward motion of the auroras at Kotzebue and Farewell. This eastward motion cannot be easily recognized from the printed pictures taken every minute (Fig. 5.9). But it becomes very evident when the films are shown in a cine projector. The auroras were active for about 1 hr at Kotzebue and then had receded southward ($60°$ geom. lat.) just before the disturbance no. 4 began. Apart from these visible auroras, Roach and Marovich (1959) and Roach (1959) report that a great enhancement of monochromatic OI red (6300 Å) aurora appeared along the sub-auroral zone (at Fritz Peak; gm. lat. $49°$) on this night. The enhancement of the OI red line on the same night has been reported by Barbier (1958) at the Haute-Provence Observatory (geom. lat. 45°9 N).

5.43 Polar magnetic disturbances

The typical polar magnetic disturbance accompanying the above auroral display began at 1046 or 1047 GMT at Sitka. At that time there began a weak eastward current at College, which obscured the beginning of this particular event. At 1049 hours, the polar disturbance already in progress at Sitka began at College. Owing to the severe disturbance, the ordinary magnetographs were not usable. The rapid-run magnetographs (Fig. 5.11) were used together with the low-sensitive ones to construct the complete record of this disturbance (Fig. 5.12a,b,c). Horizontal disturbance vectors at College and Sitka were almost parallel and directed to geomagnetic south (S) or S by SE for about 25 min. Fig. 5.13 shows these vectors at 1055, 1100, 1105, and 1109 hours. They indicate that the primary ionospheric electric current flowed to the west (W) or W by SW. The disturbance reached its maximum (2000γ) at about 1130 hours, and almost completely subsided by 1240 GMT, just before the disturbance no. 4 started.

The earth current record obtained by Hessler and Wescott (1959a), Geophysical Institute College, Alaska, showed that the "earth current storm" began at about 1047 GMT (2 min earlier than the beginning time shown by the rapid-run magnetographs). It went off-scale at 1050 GMT (750 mV/km; north electrode positive) at College. At Point Barrow, Alaska ($68°.6$ geom. lat. N), only small earth current disturbance, of order less than 60mV/km, was recorded. This suggests that the disturbance no. 3 occurred far south of Point Barrow.

158

5.44 Auroral jet

It is assumed that the auroral and magnetic disturbances were located on the same geomagnetic latitude. Assuming that the current was at the auroral level and treating it as a line current, it is possible to find its position. This was first done by Birkeland (1913), but as Chapman (1935) pointed out, Birkeland's estimated heights are too great because no account was taken of the induced currents within the earth.

It is usually assumed that the external field is given by two-thirds of the horizontal disturbance vector and twice the vertical disturbance vector. However, these factors depend critically on the rate of the change of the field and on the electrical conditions within the earth. The above numbers are obtained from rather slow variations such as the solar daily variation Sq (with a rate of change of order 30 γ/6 hr $\sim$ 1.5 x 10^{-3} γ/sec) or Dst variation (80 γ/6 hr $\sim$ 4 x 10^{-3} γ/sec). This might be compared with the polar magnetic disturbance of order 600 γ/6 min $\sim$ 2 γ/sec.

Using the above numbers, $\frac{2}{3}$ for the horizontal vectors and 2 for the vertical vector, the estimated height of the auroral current had the improbably-high value 1000 km. The estimate may be partly because the auroral current may not be equivalent to a line current, but may have some definite width. Even so, calculation shows that the disturbance vectors cannot be explained properly with these numbers. Therefore, one may speculate that the above vertical force factor (2) is too small. This would correspond to a greater proportional reduction of the vertical force component, by induced currents, than in the case of the much slower variations. It will be shown in this section that it is possible to locate

159

the auroral jet from 100 km to 160 km in height by using the factors $\frac{2}{3}$

for horizontal vectors and 3 for vertical vectors. We take the geomagnetic north south cross-section (Fig. 5.8 line A-B), and project College and Sitka on this geomagnetic meridian plane (see Fig. 5.14).

In Fig. 5.14

$$< \text{JCS} = \phi_1 = 90^\circ - \tan^{-1} V_c/P_c \qquad (1)$$

$$< \text{JSC} = \phi_2 = 90^\circ - \tan^{-1} V_s/P_s \qquad (2)$$

where V and P denote the vertical and horizontal disturbance vectors and subscripts c and s refer to College and Sitka, respectively. The observed disturbance vectors are ΔH, $\Delta D'$ ($= \Delta D$ in gammas, that is, $H_o \Delta D'/3438$) and V.

ΔH = change of magnetic north component (northward positive);

ΔD = change in declination (eastward positive);

V = change of vertical component (downward positive);

H_o = mean horizontal intensity.

The geomagnetic north and east components X_m and Y_m can be obtained (Chapman and Bartels, 1940, p. 8; Fukushima, 1953, p. 307) from

$$\Delta X_m = \Delta H \cos (D - \psi) - \Delta D \sin (D - \psi) \qquad (3)$$

$$\Delta Y_m = \Delta H \sin (D - \psi) + \Delta D \cos (D - \psi) \qquad (4)$$

where D denotes the declination and ψ the angle made by the great circle joining the observatory and the geomagnetic pole with the geographic meridian line; it is given (Chapman and Bartels, 1940, p. 645) by

$$\sin \psi = - \sin \theta_1 \sin \Lambda / \sin \theta \qquad (5)$$

where $\theta_1 = 11°\!.5$ and Λ and θ denote the geomagnetic longitude and geographic co-latitude, respectively.

The magnitude of the horizontal vector P (Fig. 5.13) is given by

$$P = (\Delta X_m{}^2 + \Delta Y_m{}^2)^{1/2}. \tag{6}$$

The position of the auroral electrojet is obtained at each minute for three successive intervals (Fig. 5.15). The velocity of the first northward motion from 1047 to 1055 hours was about 1 km/sec and was the same as that of the auroras. At about 1051 hours, the all-sky camera films both at Kotzebue and Farewell showed some complex structures. It is difficult to trace them after the complete break-up of the auroras, but the magnetic records suggest that the auroral electrojet moved first southward and then northward.

Fig. 5.16 shows the growth of the electrojet current I given by

$$I = (P^2 + V^2)^{1/2} \cdot r/2 \tag{7}$$

where r denotes the distance from the jet to an observatory. The positions of the jet determined above give r at each minute and I can be calculated from the disturbance vectors obtained at College and Sitka. The fit of the two curves is rather poor, especially from 1100 hours. The tentative maximum current obtained from College data is 2.7×10^6 A at 1101 hours.

The treatment of the auroral jet as being a line current is, of course, an idealization. Neither a line current nor a sheet of uniform current can explain self-consistently the whole course of this disturbance. We infer that there may be several "strip" currents within a rather

161

uniform current sheet--pointing out the non-uniform auroral luminosity in all-sky camera films. In fact, the bright northern front of the aurora moved northward earlier than the jet did; at 1052 GMT, the bright front was almost right overhead at Kotzebue, but the jet was still 400 km south of College. From 1055 to 1101 hours, there appeared the southward motion of the jet, but the all-sky camera films at Kotzebue indicate that the bright northern front remained north of Kotzebue at that time, and was completely separated from the active auroras located south of Kotzebue (cf. 1100 hours picture).

The magnetograms cannot uniquely determine any such distribution of the complex current-system between Sitka and College, but they indicate that the auroral electrojet grew very quickly between 1047 and 1100 GMT. During this interval and during the recovery to normal, the current moved first northward, then broadened and moved southward and then again northward. The whole movement lay between College and Sitka[*].

It may be noticed that two large impulses observed at 1058 and 1110 hours at College (Fig. 5.12) were partially due to the approach of the auroral jet towards that observatory; they do not directly indicate the real growth of the current. Near the auroral zone the disturbance vector obtained at an observatory does not reliably indicate the intensity of overhead current (as is often assumed when drawing current diagrams).

---

[*] The magnetogram from Victoria Observatory (geom. lat. $54°1$, N; about 1240 km south-east of Sitka) shows the decrease of both horizontal and vertical components, indicating that this particular event occurred north of this observatory. The writer wishes to express his thanks to Messrs. R. G. Madill and E. I. Loomer, Dominion Observatory, Ottawa, Canada, for sending him the magnetogram.

5.5 THE EASTWARD MOTION OF AURORAS AND THE ELECTRIC
FIELD OF POLAR MAGNETIC DISTURBANCES

Taking the x and y axes in such a way that they coincide respec-
tively with geomagnetic south and east, the electric current equation in
the ionosphere may be written

$$I_x = K_{xx} E_x + k_{xy} E_y, \tag{8}$$

$$I_y = -K_{xy} E_x + K_{yy} E_y,$$

where K_{ij} is a tensor component of the height-integrated conductivity of
the ionosphere. Akasofu (1960b) has shown that the current intensity in
the westward auroral jet may be expressed by

$$I_y \approx -K_{xy} E_x, \tag{9}$$

One of the outstanding features of the break-up of the aurora is the
sudden brightening and the simultaneous appearance of the rapid eastward
motion of the auroras. A sudden considerable negative deviation of the
H component from its normal value (which is the most prominent feature
of most polar magnetic disturbances in the magnetograms) is generally
accompanied by a mainly eastward auroral motion. This has already been
studied by Kim and Currie (1958), using all-sky camera data, and by
Kaiser (1955), Bullough and Kaiser (1954, 1955), Bullough et al. (1957),
Dagg (1957) and Nichols (1959) by radio methods.

Assuming that the magnetic field is vertical (which is strictly true
only at the poles), Martyn (1953) gave the following horizontal drift
velocities of charged particles (v_e for electrons, v_i for ions) due to
an applied southward electric field

$$\left| v_e \right| = (c\ E_x/F)\ \sin \alpha_e \tag{10}$$

$$\left| v_i \right| = (c\ E_x/F)\ \sin \alpha_e \tag{11}$$

Here

$$\tan \alpha_{e,i} = \omega_{e,i}/v_{e,i} \tag{12}$$

$$\omega_{e,i} = F/m_{e,i} \tag{13}$$

where v_e and v_i are collision frequency of electrons and ions with neutral atoms, respectively; F denotes the total intensity of the magnetic field. Table 5.3 gives typical values of v_e, v_i and α_e, α_i.

From a reasonable estimate of the eastward speed of the aurora, obtained by radio methods (cf. Bullough et al. 1957; Nichols 1959), we may take the speed of the drifting electrons v_e to be 360 meters/sec, so that E_x is 6.67×10^{-7} esu (= 20 volts/km = 2×10^4 emu). Fig. 5.17 shows corresponding values of v_e and v_i due to the southward electric field of 6.67×10^{-7} esu. It is rather surprising that the eastward drift velocity of electrons is almost constant over the height range represented in Fig. 5.17.

TABLE 5.43

Typical values of v_i, v_e, α_e, and α_i at 110 km, 130 km and 200 km in height

Height	110 km	130 km	200 km
v_e (/sec)	3×10^4	5×10^3	10^3
v_i (/sec)	2×10^3	3×10^2	10
α_e	$89°50'$	$89°58'$	$90°$
α_i	$9°$	$48°$	$88°$

$\omega_e = 9.6 \times 10^6$/sec, $\omega_i = 3.3 \times 10^2$/sec

164

The electric current vectors are also shown in Fig. 5.17, and it is clear that the westward auroral electrojet discussed in the above section is mainly due to the eastward motion of electrons of order cE/F (= 360 m/sec) in the lower part of the ionosphere. This drift velocity of electrons is almost insensitive to the physical state in the ionospheric region because of the high gyrofrequency ω_e compared with the collision frequency ν_e. Therefore, this estimation has a great advantage compared with the discussion in the above section, which strongly depends on the conductivity of the ionosphere and so on the electron density.

Bullough et al. (1957), by a radio method, successfully observed the eastward drift motion of the auroras. They found speeds up to 500 m/sec during negative bays (polar disturbances). The radio observation measures the movement of electrons, and agrees fairly well with our estimation (their Fig. 15).

It is interesting to estimate the current density and the electron density in this aurora. Let us consider, as an example, the DP that began at $23^h 57^m$, 5 December 1958 (see Fig. 5.1). The maximum change $\Delta H'$ may be estimated to be 300 γ , so that the actual change ΔH due to the external field may be 200 γ (=(2/3) $\Delta H'$). Assuming that this disturbance is produced by current flowing in two (closely spaced) overhead arcs, and that each current sheet has the width 2 δ , ΔH is thus given by Chapman (1951)

$$\Delta H = 2x \left\{ 2 I_y c \tan^{-1} \frac{2 \delta/h}{1 - (\delta/h)^2} \right\} \tag{14}$$

Here I_y denotes the current density; h denotes the height of the jet, and is taken to be 120 km. As discussed above, we may take 2 δ (= 500 meters)

for the width of the rayed arc, so that the above equation is approximated by

$$\Delta H \simeq 2x \left\{ 2 I_y c (2 \delta/h) \right\}. \tag{15}$$

Putting $\Delta H = 2 \times 10^{-3}$ gauss (= 200 γ), 2 δ = 500 meters, and h = 120 km, I_y is estimated to be 3.6×10^9 esu/cm (= 1.2×10^{-1} emu/cm = 1.2 amp/cm). The total current J_y is, therefore, 1.2 amp/cm x 1 km = 1.2×10^5 amp.

Using the equatorward electric field $E_x = 6.67 \times 10^{-7}$ esu, the conductivity K_{xy} is

$$K_{xy} = \left| \frac{I_y}{E_x} \right| = 5.4 \times 10^{15} \text{ esu } (= 6.0 \times 10^{-6} \text{ emu}). \tag{16}$$

Chapman (1956b) gives the value of the Hall conductivity $k_2 = 4.54 \times 10^{-15}$ emu = 4.09×10^6 esu at the height 125 km. This corresponds to an electron density n_e of 1.5×10^5/cm^3. In the polar regions,

$$\int k_2 \, dh = K_{xy}, \tag{17}$$

Assuming a thickness of 30 km, K_{xy} is 4.09×10^6 esu x 3×10^6 cm = 1.23 x 10^{13} esu. From this we can infer the electron density of the arc. It is given by

$$1.5 \times 10^5 \left(\frac{5.4 \times 10^{15}}{1.23 \times 10^{13}} \right) = 6.6 \times 10^7/\text{cm}^3.$$

Several authors have discussed the electron density in the aurora (cf. Brown and Lovell 1958, p. 173; Chamberlain 1958, p. 191). It seems that the density of 7×10^7/cm^3 is possible in a narrow arc, where high energy electrons are entering at the rate 10^{10}/cm^2 sec.

5.6 THE ORIGIN OF THE ELECTRIC FIELD OF
POLAR MAGNETIC DISTURBANCES

5.61 Inadequacy of the dynamo theory of the DP

It has been already suggested that the electric field of order

6.67×10^{-7} esu (= 20 V/km) could not be produced by dynamo action in

the upper atmosphere. The dynamo theory of the DP has been developed

by Fukushima (1953), Vestine (1954), and Obayashi and Jacobs (1957).

They assumed a constant and fixed wind pattern over the earth (the same

as is responsible for the Sq variation), and assumed high conductive

belts in the ionosphere along the auroral zones. Therefore, their DP

current system is fixed relative to the sun, under which the earth rotates

once a day.

The auroral electrojet, its variability, its great concentration

and its intense current, and its rapid rise and fall, are facts difficult

to reconcile with a rather constant pattern of current system fixed over

the earth. It also seems scarcely possible that the winds responsible

for the dynamo e.m.f.'s could appear so abruptly and so simultaneously

over such a large range of at least 2500 km (from Kotzebue to Meanook)

and probably of 5000 km, such as indicated by the all-sky camera films.

The typical disturbance, discussed above, seems to suggest that the

auroral electrojet is caused by an electric field that varies rapidly

in time and place. It is shown in the above sections that the southward

electric field produces both the jet and eastward auroral motion.

The above statements are not new. Heppner (1954), pointing out the

change of forms of the auroras at the beginning of the polar disturbance,

questioned the dynamo theory of this phenomenon. He also stated that

the fairly abrupt decrease in the H-component coincides with a rapid southward movement of the southernmost auroral arc, and with the appearance of rayed structure north of the arc. In the storm of 23 September 1957, exactly the same thing happened, much more extensively, in its north-south and also east-west dimensions. It has also been pointed out by Maeda (1957, 1959) that the DP currents can be explained only by assuming an exceptionally-enhanced conductivity throughout the polar region, and a strong wind system quite different from that indicated by Sq, if the dynamo theory is adopted.

5.62 High-energy electrons and radio-wave absorption

The rather constant flux of electrons of energy as high as 100 keV was first detected by Van Allen and his co-workers (Meredith et al., 1955; Van Allen, 1957). Their data were obtained by rockets in the upper atmosphere in the auroral zone. What they observed was the X-ray photons generated by a small minority of such electrons. This is also recently confirmed by Vernov et al. (1959) by satellite observations. This is now supposed to be an outflow of electrons issuing from the tips of the radiation belt recently discovered by Van Allen and Frank (1959) and Van Allen et al. (1959).

These high-energy electrons have been also studied by radio absorption. Chapman and Little (1957) first suggested that the cosmic noise absorption is due to the high-energy electrons and their X-ray photons discussed above. It seems that a homogeneous arc and other quiet and stable types of aurora may be due to such constant inflow of protons and electrons.

Little and Leinbach (1958) and Reid and Collins (1959) later suggested that the strongest auroral-associated absorption corresponding to the break-up of the arc might be due to an increase in the number and/or energy of the X-ray photons produced by Bremsstrahlung from the above high-energy electrons.

Winckler et al. (1958) at Minneapolis observed an intense X-ray burst when the strong band structure moved across the station Choteau, which has exactly the same geomagnetic latitude as Minneapolis, 1050 GMT; this was at the fairly low geomagnetic latitude 55°. Therefore it is clear that the high-energy electrons appeared in quite a large area along a narrow band (from geom. lat. 55° to 65° and from geom. long. 260° to 330°) at about the same time (see also Winckler 1960).

The high energy electrons of order 100 keV (flux $10^{6}/cm^{2}sec$) can penetrate the atmosphere down to the upper part of the D-layer (80 km ~ 90 km) (Winckler et al., 1959). Malville (1959a) suggested that a short-lived purplish-red luminosity which appears at the lowest border level of the normal-type aurora (type-B aurora, Elvey, 1957) is caused by the high energy electrons of order 100 keV.

5.63 Extra-terrestrial protons

Many workers have reported that the auroral hydrogen emission diminishes abruptly at the time of break-up (Dahlstrom and Hunten 1951; Fan and Schulte, 1954; Romick and Elvey, 1958; Galperin, 1959; Fan, 1958; Montalbetti, 1959; Malville, 1959b).

It may be that there is an almost constant and equal flux of electrons and protons in homogeneous and quiet auroral arcs; and that there appears

suddenly a change of electrical state in the auroral level, which may
be expected to cause the auroral electrojet. The appearance of high-
energy electrons and the disappearance of protons seem to suggest this
change of electrical state.

5.64 Equations of motion of the auroral particles

Neglecting the displacement current ($\partial \underline{E} / \partial t$) in the ionized gas,
equation (40) in Chapter 3 is written by Parker

$$\frac{d\underline{v}}{dt} = - \nabla(p_n + p_m) + \left[(\underline{H} \cdot \nabla) \underline{H}/4\pi \right] \left[1 + (p_n - p_s)/2p_m \right], \quad (18)$$

and

$$\underline{v} = c \ (\underline{E} \times \underline{H})/H.^2 \qquad (19)$$

If there is any tendency towards a small charge separation, we must add
the term due to the electric polarization field $\underline{E}$. We may rewrite (18)

$$\rho \ \frac{d\underline{v}_p}{dt} = - \nabla(p_{np} + p_m) + \left[(\underline{H} \cdot \nabla)\underline{H}/4\pi \right] \left[1 + (p_{np} - p_{sp})/2p_m \right]$$

$$+ n_p \ e \ \underline{E} \ , \qquad (20)$$

$$\rho \ \frac{d\underline{v}_e}{dt} = - (p_{ne} + p_m) + \left[(\underline{H} \cdot \nabla)\underline{H}/4\pi \quad 1 + (p_{ne} - p_{se})2p_m \right]$$

$$- n_e \ e \ \underline{E} \ . \qquad (21)$$

Here we use the subscripts p and e for protons and electrons
respectively and,

$$\underline{E} = 4\pi \ e \ \int (n_p - n_e) \ dV \ . \qquad (22)$$

170

We have shown in § 3.21 that the electrons drift slowly eastward and the protons drift westward; both contribute to the westward ring current. We may suppose that the introduction of the electric polarization field $\underline{E}$ in the equations of motion (20) and (21) will slightly perturb the above steady eastward or westward motion of particles. The electric field must be eastward because the electrons move eastwards and the protons move westwards. Therefore the particles will be accelerated inward or outward from the earth, according to (19), (20) and (21).

We have seen that when ray structure appears in the arc the proton flux, of order $5 \times 10^5/cm^2$ sec, seems to be diminished by a large factor. At the same time the electron flux may be increased from a value such as $10^6 \sim 10^8/cm^2$ sec (cf. Van Allen 1957) to $10^{10}/cm^2$ sec. The great difference of the fluxes now becomes important, namely $10^{10}/cm^2$ sec for the electrons and perhaps $5 \times 10^3/cm^2$ sec for the protons. The electrostatic imbalance produced by the large increase of the electron flux and the large decrease of the proton flux can, however, be kept to a low value by motion of the electrons in the flux regions themselves, and by a differential motion of the background ionization along the lines of force. This can keep the electric potential along the lines of force nearly uniform.

Hence $(n_p - n_e)$ and the electric field in (22) must be much less than that expected from the large difference between the proton and electron fluxes. The degree of neutrality along the lines of force depends on many factors, such as the density of electrons in the electron flux (from 10^{-2} to $1/cm^3$), the density of the background ionization (from

1.8×10^5 to 2.7×10^{10} cm) or the collision interval (from 6×10^{-3} to 450 sec), and also the characteristic time involved (from 0.1 to 10 sec).

When the motion of the particles of the background is taken into account, another equation of motion must be added to (20) and (21). But the total amount of the background ionization is so large compared with the total number of particles in the fluxes that we may regard these as traversing nearly immobile background ionization. We also disregard any interaction between the fluxes and the background ionization. It is known, however, that an electron beam penetrating into a plasma produces plasma oscillation (cf. Gould 1959, p 107).

As shown in § 3.21 (Fig. 3.1), for the particles that can produce the aurora,

$$w_s \gg w_n \quad (ws \approx w) \tag{23}$$

$$u_2 \gg u_1 \tag{24}$$

Then the unperturbed east-west drift velocity due to the centrifugal force is given by

$$u_2 \approx -\underline{k} \, \frac{mc}{eH} \, \frac{w^2}{R_c} \tag{25}$$

Hence this motion is proportional to the individual energy of the particles. The ratio of the total energy of electrons in the electron flux to that of protons in the proton flux ($m_e \, n_e \, w_{se}^2 / m_p \, n_p \, w_{sp}^2$) is as large as 2×10^4. As a consequence the electron flux may be nearly unaffected by the protons and may drift eastward in accordance with (25).

172

But the proton flux may be affected by the eastward electric polarization field (associated with a very small decrease in the energy of the electrons). The unperturbed state is in balance between the inward Lorentz force and the outward centrifugal force. Therefore any small change of the velocity of the westward drift motion of the protons by the eastward electric field breaks this balance. The reduction of the westward motion diminishes the inward Lorentz force (because of the reduction of j), so that the protons are accelerated outward from the earth according to (19) and (20).

This acceleration will produce outward motion of the proton layer and will separate the proton layer slightly from the electron layer. However, such separation is checked by the new inward electric field (directed towards the earth) produced by this charge separation of the proton and the electron layers. If the westward motion of protons is completely halted by the eastward electric field, the outward centrifugal force must be balanced by this inward electric force, because the Lorentz force becomes zero and the motion of protons along the lines of force may not be affected by the eastward electric field (the centrifugal force is still operative). Thus, in this case the inward electric field between the proton and electron layers must satisfy

$$(e\ n_p)\ \frac{m_p\ w_{sp}^2}{e\ R_c}\ (\underline{j}\ \times\ \underline{h})\ -\ (n_p e)\underline{E}\ =\ 0 \tag{26}$$

Therefore the intensity of the electric field E is

$$E\ =\ m_p\ w_{sp}^2/eR_c\ . \tag{27}$$

173

When the protons and electrons descend to the auroral level, the protons appear just north of the rayed arc produced by the intense electron precipitation (but the reduction of the proton flux makes it difficult to observe the corresponding luminosity). Fig. 5.18 shows schematically this condition.

At the auroral level we take $\phi = 66°30'$. Then (3.14) gives $Rc = 1.87 \times 10^9$ cm. For 130 Kev protons, w_s is 4.99×10^8 cm/sec, so that the electric field is of order 2.3×10^{-6} esu. As mentioned earlier in § 5.5 we infer that the westward auroral electrojet is produced by an equatorward electric field E_x of order 6.7×10^{-7} esu (= 20 volts/km). (The conductivity K_{xy} is negative in the southern hemisphere). This number agrees with the above value of 2.3×10^{-6} esu within a factor of 3.

Therefore it seems that a strong equatorward electric field appears along the active rayed arc, which drives strong westward currents and causes ionospheric electrons to drift eastwards.

The opposite case might occur in a rather quiet arc, in which the proton flux exceeds the electron flux. In this case the electron layer is separated from the proton layer and moves outward from the earth, so that a northward electric field and an eastward auroral electrojet would be expected. Geomagnetic studies show that positive bays (caused by an eastward electrojet) appear sometimes in the early evening. But they are much more rare and less intense than westward jets.
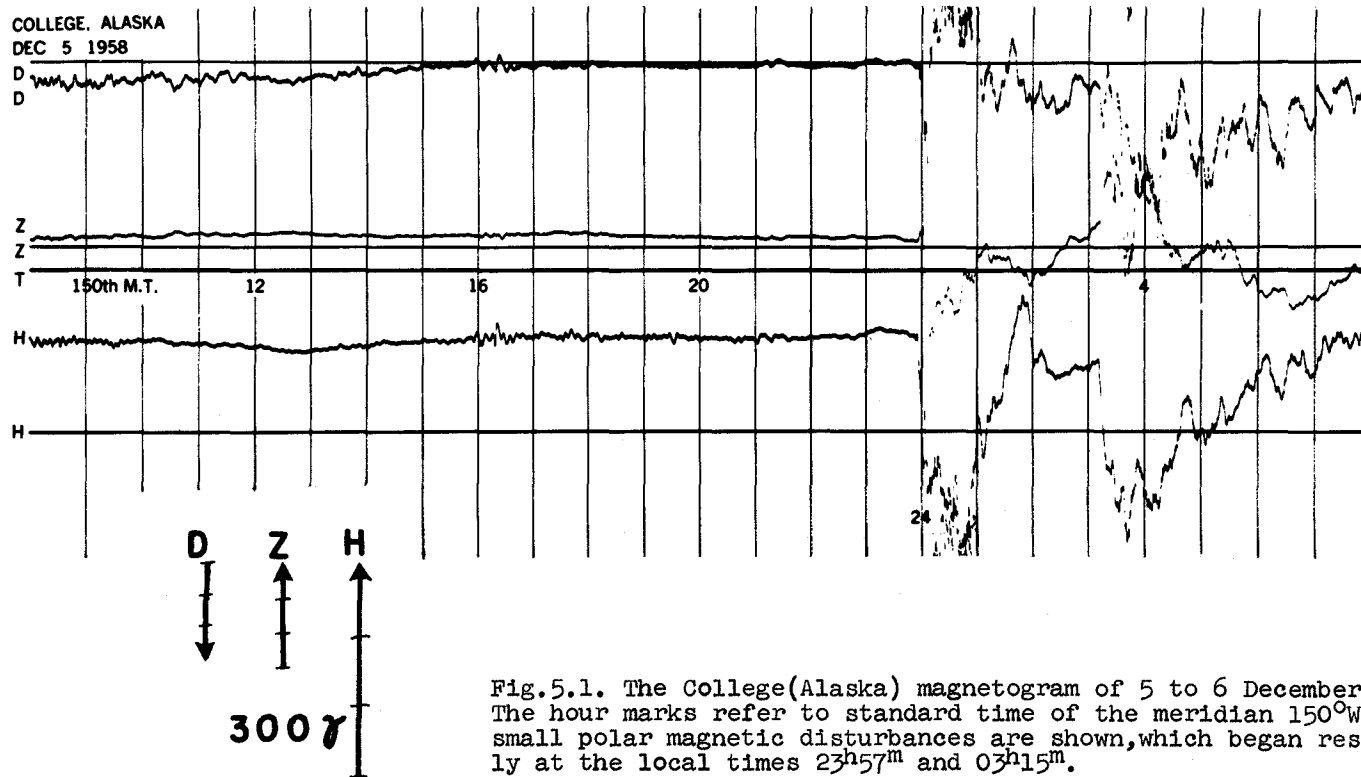
Fig.5.1. The College(Alaska) magnetogram of 5 to 6 December 1958. The hour marks refer to standard time of the meridian 150°W. Two small polar magnetic disturbances are shown,which began respectively at the local times 23^h57^m and 03^h15^m.

ALL-SKY CAMERA PHOTOGRAPHS (DEC. 5-6, 1958) COLLEGE, ALASKA
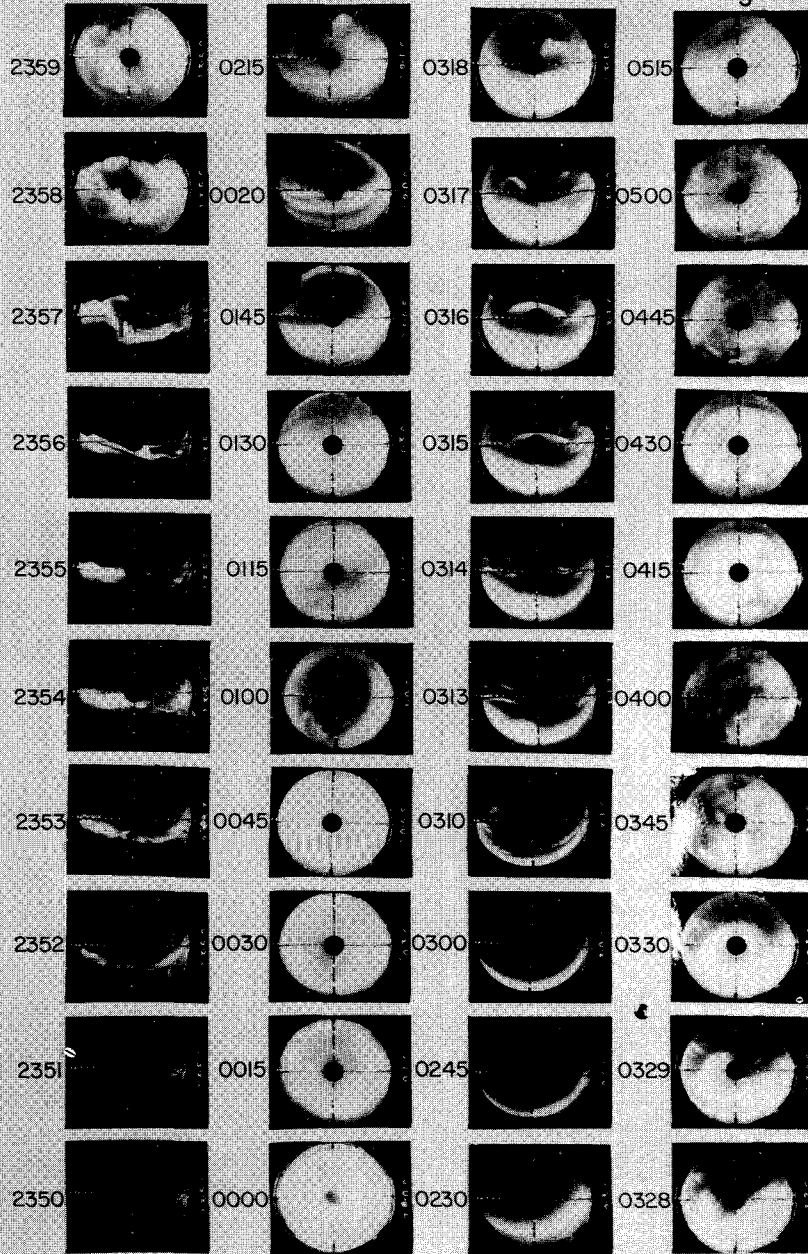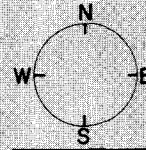
Fig. 5.2. The College (Alaska) all-sky camera photographs for the interval from 09^{h}50^m to 15^{h}15^m GMT 6 December 1958 (local time, from 23^{h}50^m 5 to 05^{h}15^m 6 December 1958). This interval includes the two break-ups (at 23^{h}57^m and 03^{h}15^m local time) associated with the two polar magnetic disturbances shown in Fig. 5.1.
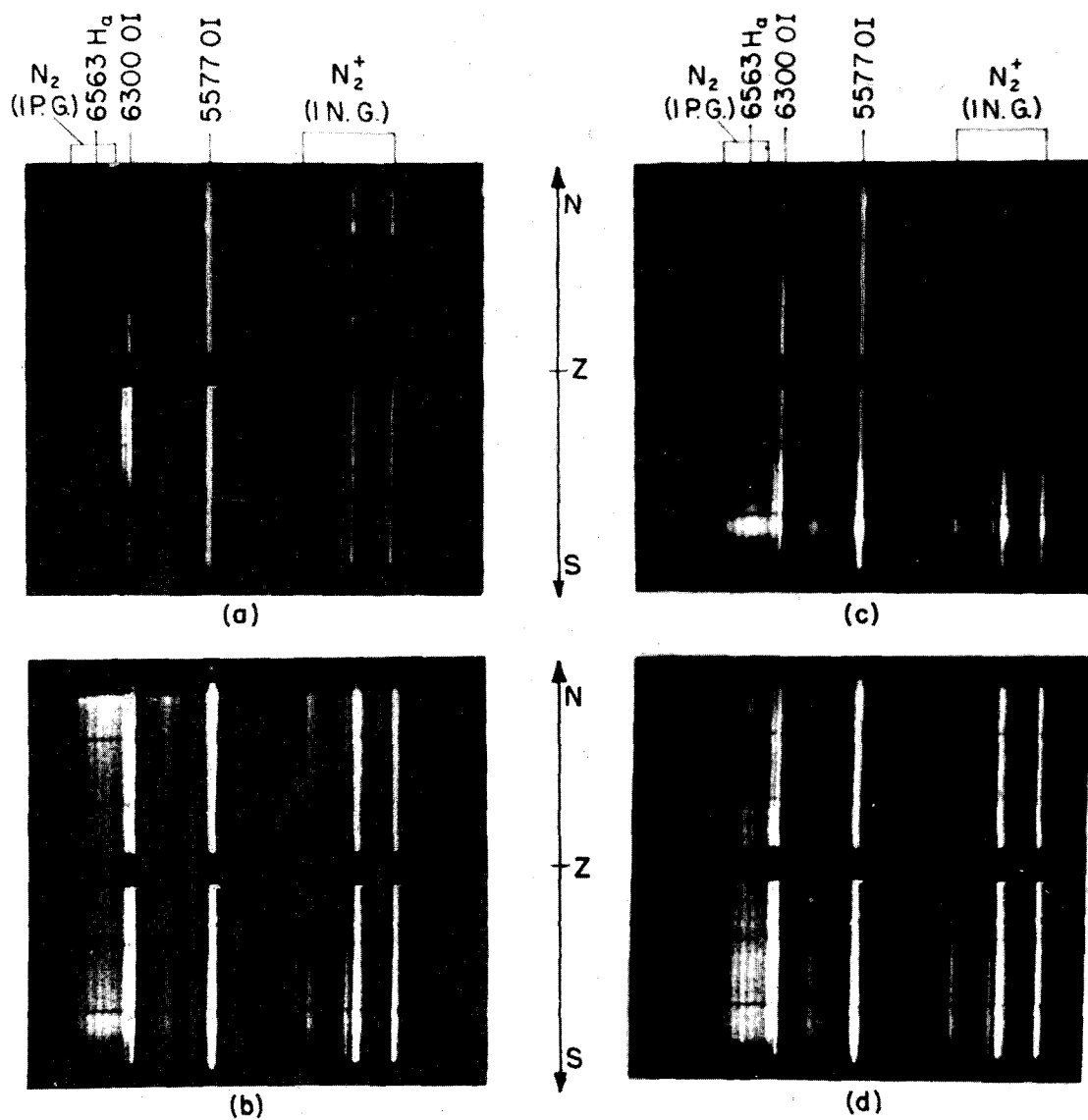
Auroral Spectrograms

Fig.5.3. Four spectrograms taken at College(Alaska) on the night of 5 to 6 December 1958.   Two of them,(a) and (c),were taken just before the auroral break-ups shown in Fig.5.2.   The others, (b) and (d),were taken just after the break-ups. (Rees 1960).

VHF Auroral Radar
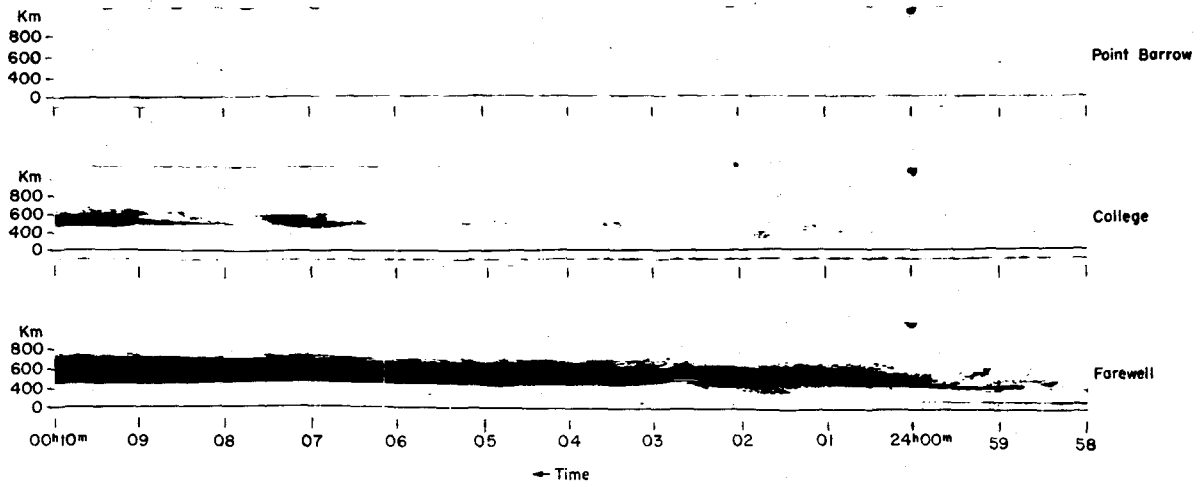
(Dec. 5-6, 1958) 150° WMT

Fig.5.4. VHF auroral radar data taken at Point Barrow(Alaska)(gm.lat.68.6 N),
College(Alaska)(gm.lat.64.7 N) and Farewell(Alaska)(gm.lat.61.4 N) on the
night of 5 to 6 December 1958. (Leonard 1960).
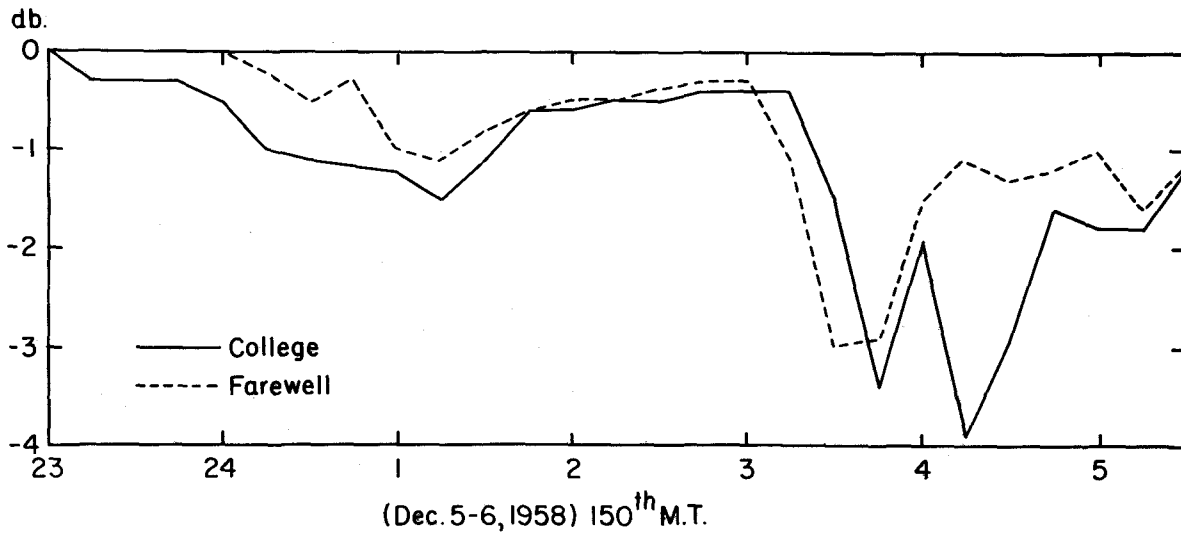
(Dec. 5-6, 1958) 150th M.T.

Fig.5.5. Absorption of 27.6 Mc cosmic radio noise at College,Alaska (gm.lat.64.7N)
and Farewell(gm.lat.61.4N),from 09h00m to 15h30m GMT December 1958 (local time
from 23h00m to 05h30m,5 to 6 December 1958) (Leinbach 1960).
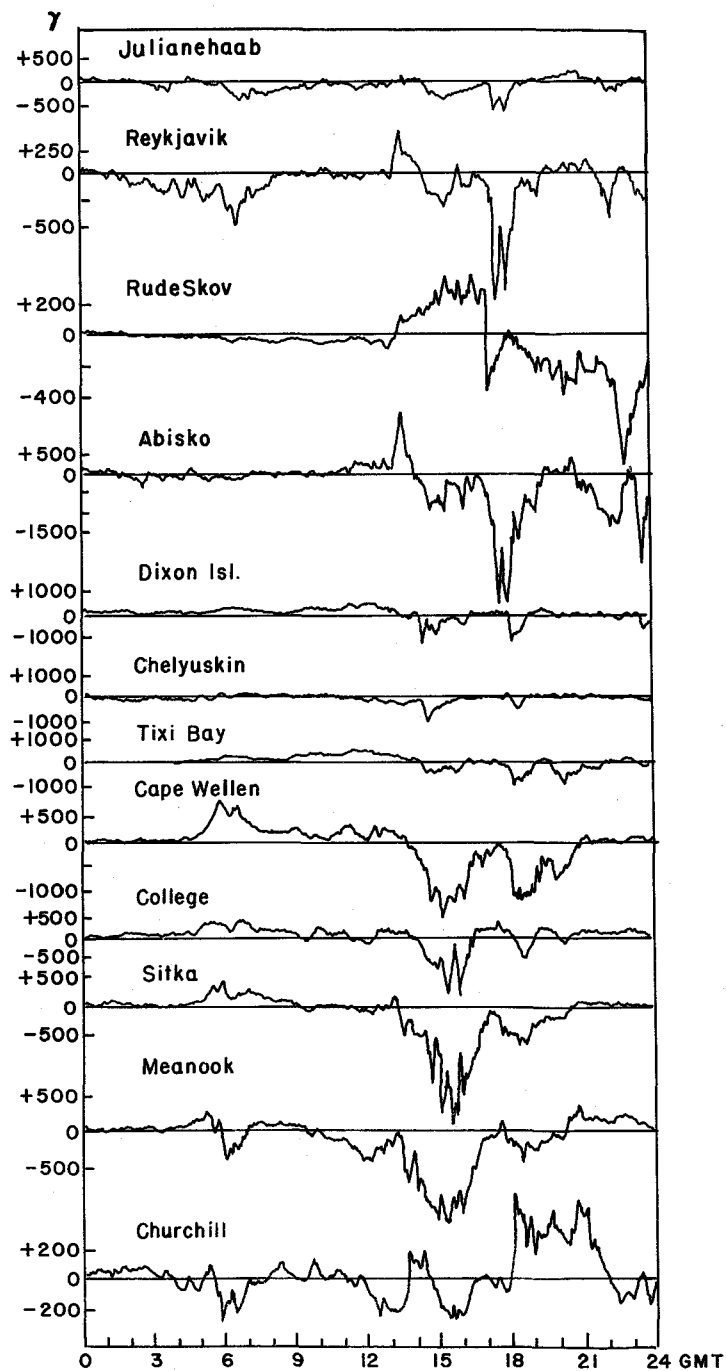
Fig.5.6. Horizontal component magnetograms of the storm of 29 September 1957 from twelve stations located along the northern auroral zone. The ssc occurred at 00^h16^m GMT,29 September 1957.
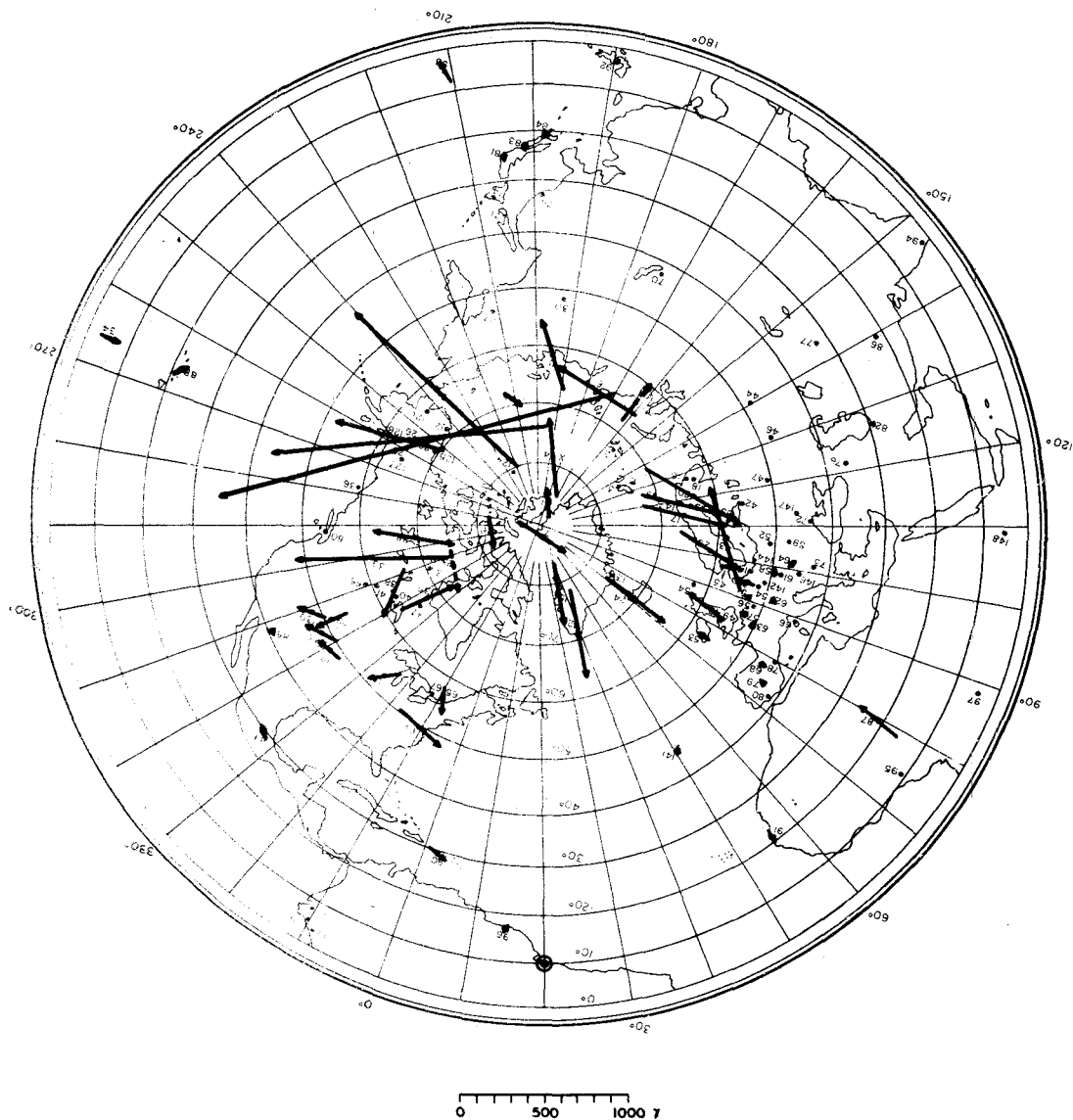
Fig.5.7. Horizontal disturbance vectors produced by one of the
DP-sub storms which occurred during the 29 September 1957
storm: Time, 15^{h}20^m GMT, 29 September 1957. The sub-solar
point is also shown.
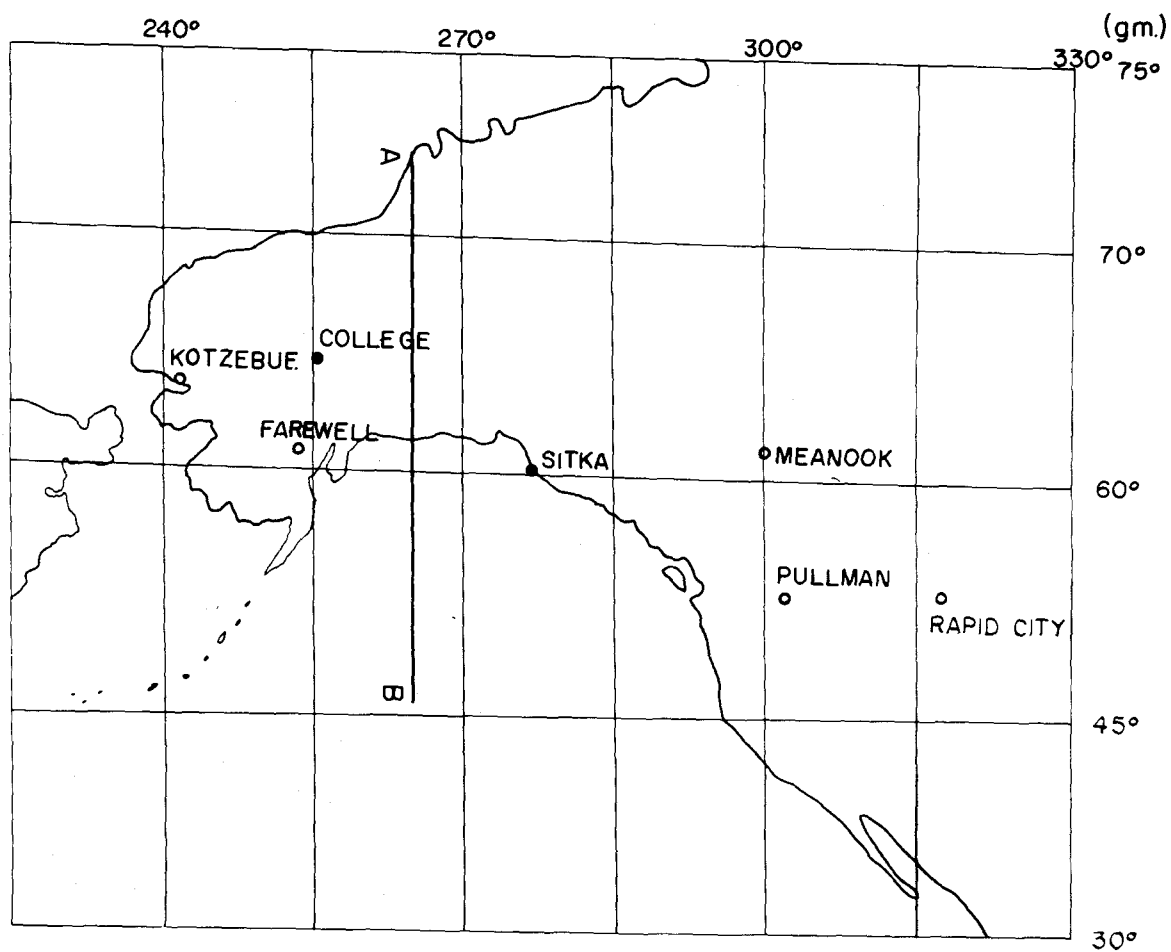
● Magnetograph
○ All Sky Camera

Fig.5.8. Map showing locations and instruments,whose results are used in
this chapter--(geomagnetic co-ordinates);   magnetograph;   all-sky camera.

ALL-SKY CAMERA PHOTOGRAPHS (SEPT. 23, 1957)
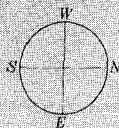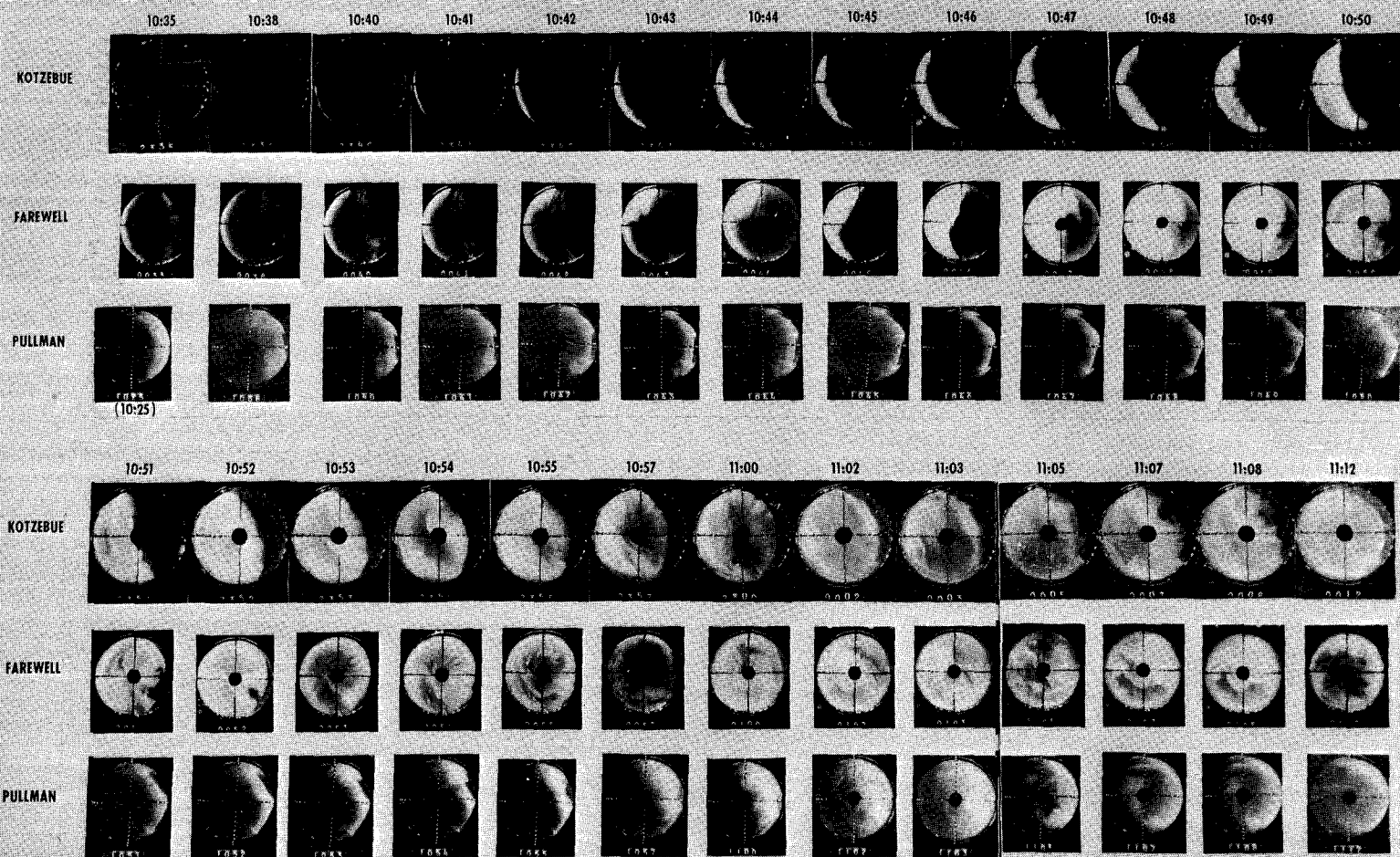
Fig.5.9. All-sky camera photographs of Kotzebue (gm.lat. 63°6N),Farewell(gm.lat. 61°4 N) and Pullman (gm.lat. 53°5N) from 10^h35^m to 11^h12^m 23 September 1957.
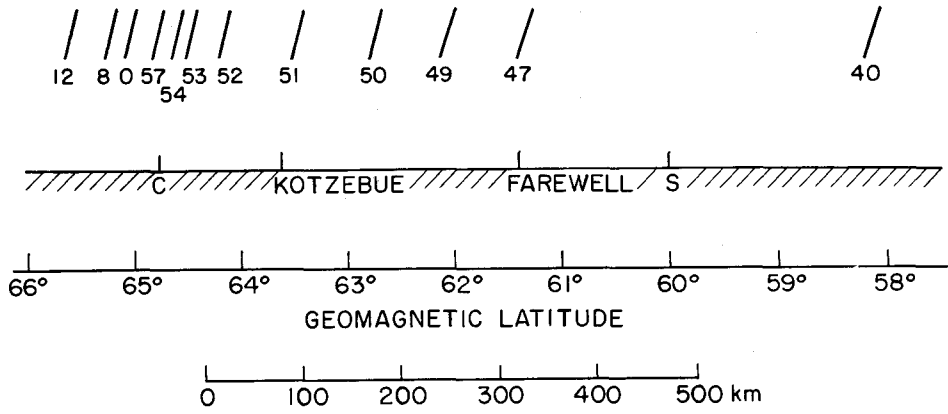
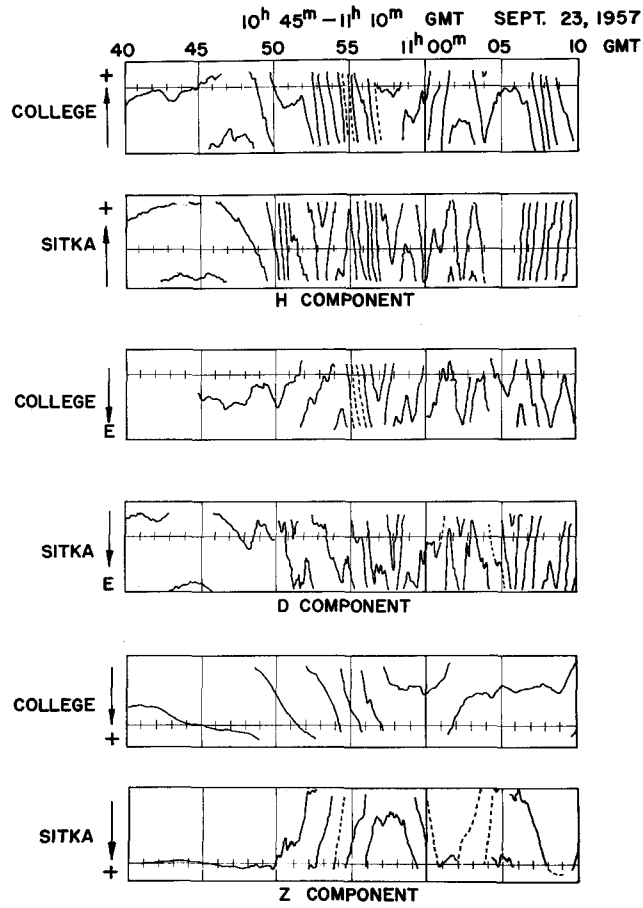Fig.5.10. Approximate positions of the northernmost aurora,10^h40^m-11^h12^m GMT, September 23,1957.

Fig.5.11. Rapid-run magnetograms at College and Sitka (three components), 10^h40^m-11^h10^m GMT,September 23, 1957.

(a) H COMPONENT   10^h 45^m – 11^h 10^m GMT SEPT. 23, 1957

(b) D COMPONENT   10^h 45^m – 11^h 10^m GMT SEPT. 23, 1957

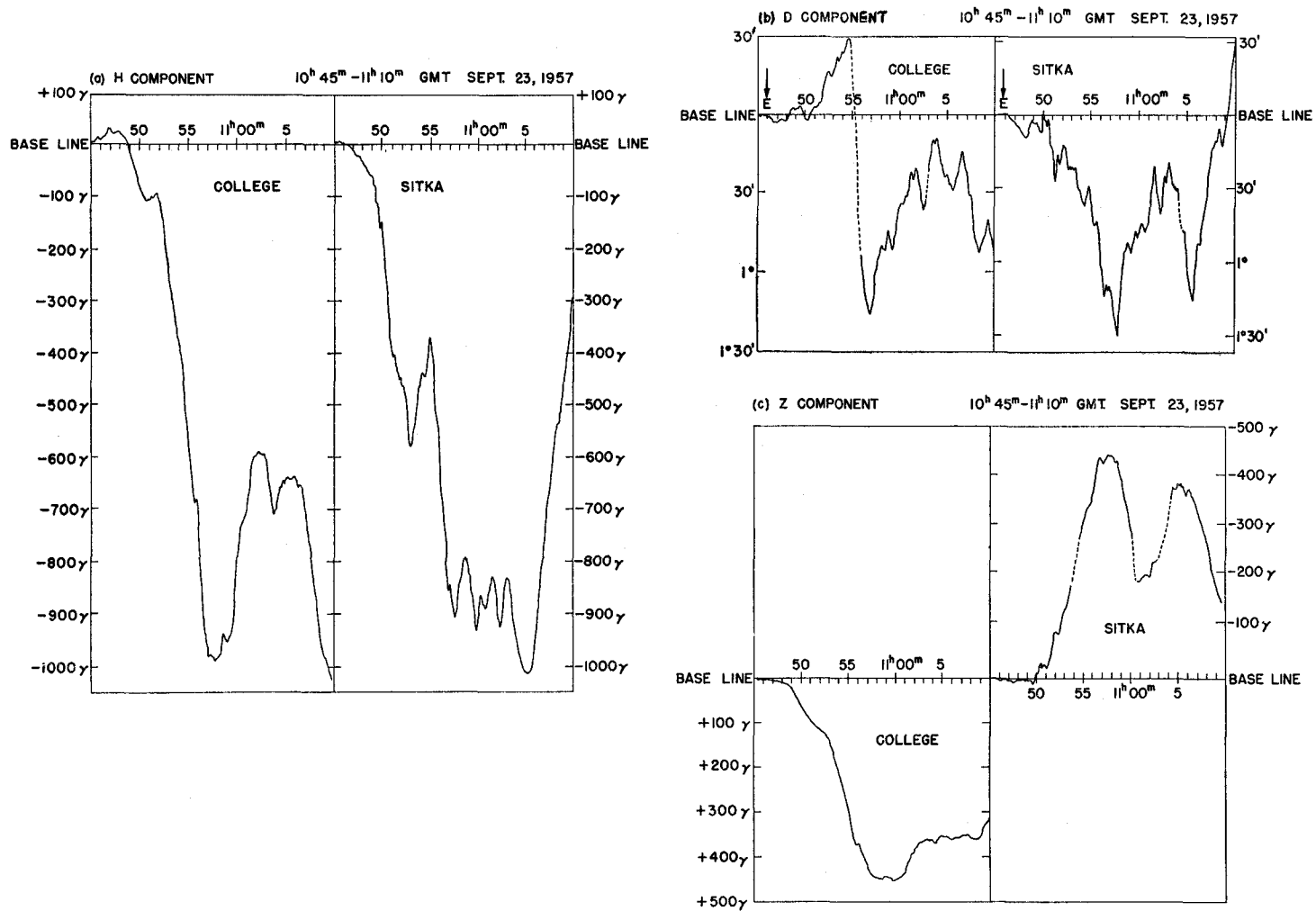(c) Z COMPONENT   10^h 45^m – 11^h 10^m GMT SEPT. 23, 1957

Fig.5.12. Magnetic records constructed from the rapid-run (Fig.5.11) and the low-sensitive magnetograms. Note the improved time resolution.
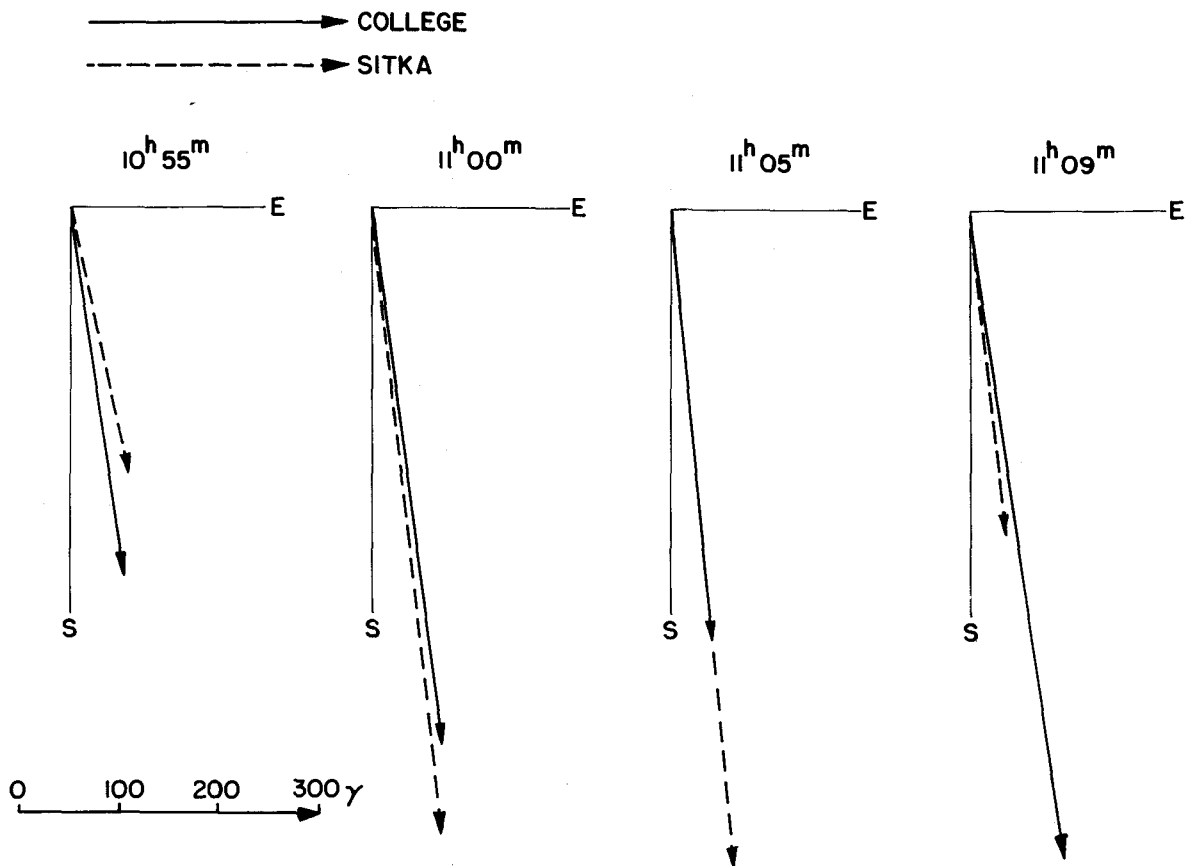
Fig.5.13 Horizontal disturbance vectors due to the external part of origin (two-thirds of original values), at $10^h55^m,11^h00^m,11^h05^m$ and 11^h09^m, at College and Sitka.
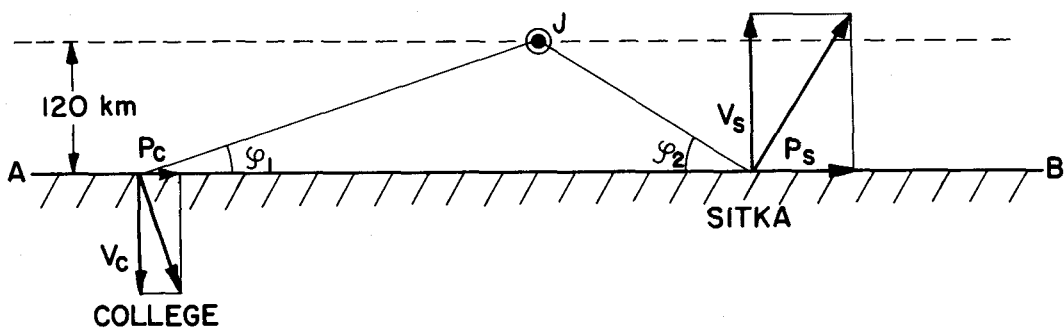

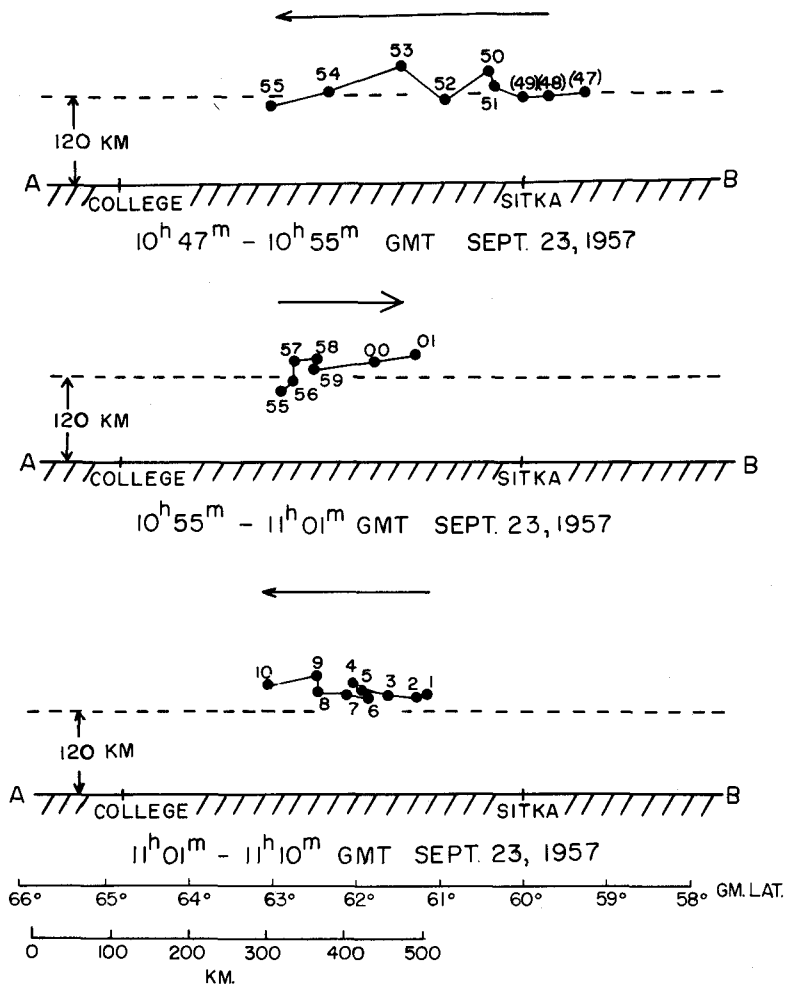Fig.5.14. Geometry showing parameters determining a position of auroral electrojet.

Fig.5.15. Positions of the auroral electrojet between College and
Sitka at each minute for three successive stages (10^h47^m-10^h55^m,
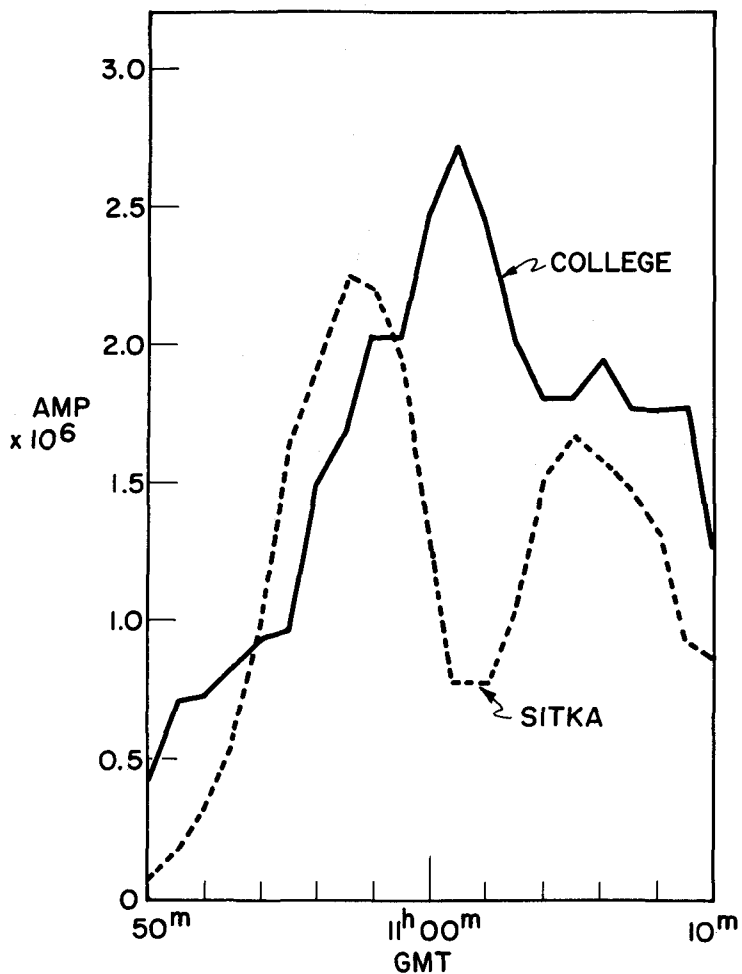10^h55^m-11^h01^m,11^h01^m-11^h10^m GMT,September 23,1957).

Fig.5.16. Variation of total current intensity of the auroral
electrojet obtained from equation (7) from College and
Sitka data.   Note that the fit is rather poor.

ELECTRON

ION

ELECTRIC CURRENT

$h_1 = 110$ km $h_2 = 130$ km $h_3 = 200$ km

Ve   Ve   Ve

Vi   Vi   J   Vi   J

J
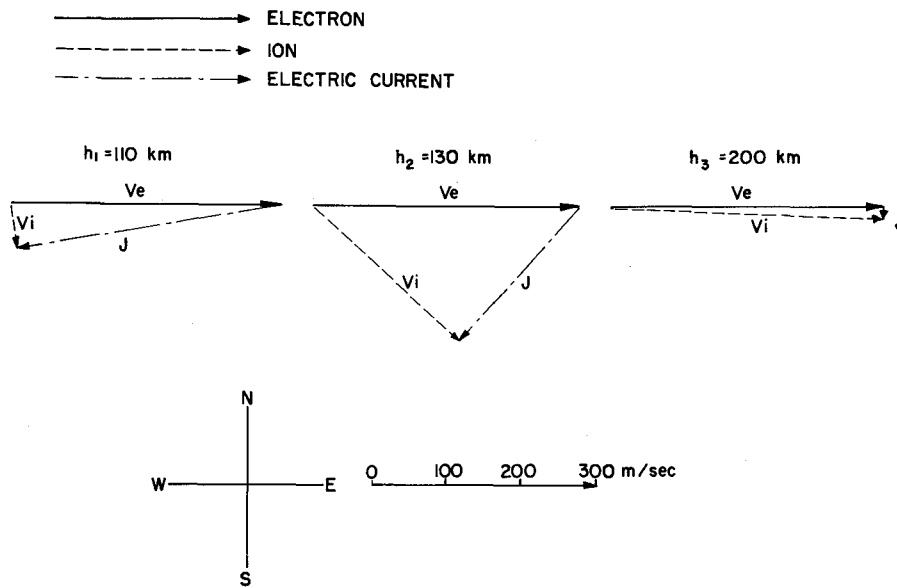
N

W ———————— E   0   100   200   300 m/sec

S

Fig.5.17. Electrons and ions drift velocity vectors at 110,130 and 200 km in height due to the southward electric field of 20 Volt/km in the polar region.

N

Westward Jet

EARTH
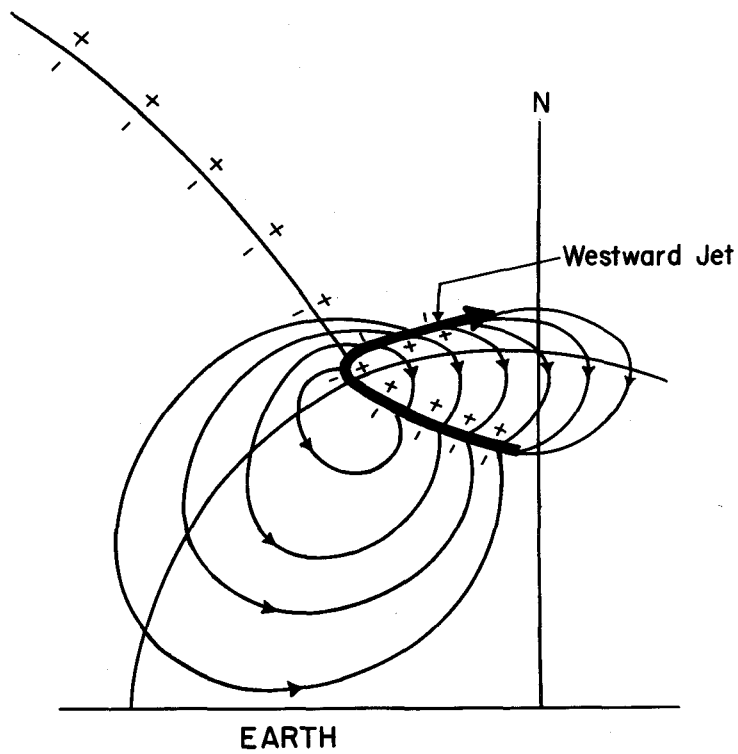
Fig.5.18. Schematic perspective representation of part of the DP current system associated with a westward auroral electrjet.   The electron and proton fluxes near a typical line of force ending on the electrojet are indicated.   All the current lines and the electrojet (thick line) are located in the ionosphere,that is, on a spherical surface concentric with the earth's surface.

CHAPTER VI

HYDROMAGNETIC WAVES IN THE IONOSPHERE[*]

6.1 INTRODUCTION

The earliest physical observation of geomagnetic micropulsations was made by Balfour Stewart in 1859. Since then sinusoidal traces on magnetograms have been extensively studied by many workers. Among these are Angenheister, Sucksdorff, Harang, Grenet, Kato (cf. 1959), Coulomb, Troitskaya. Kato and Watanabe (1957) summarized many of these studies. Here we discuss only a type of micropulsation that is supposed to be generated by the interaction between the solar stream and the outer atmosphere (Dungey 1954, Akasofu 1956). It is propagated through the ionosphere and is recorded by magnetographs. Recent workers in this field, theoretical and observational, include Campbell (1959), Dessler (1958a, b), Duffus and Shand (1958), Kato and his co-workers (cf. Kato 1959), Obayashi and Jacobs (1958), Piddington (1959), Fejer (1960).

Little is known as to how such micropulsations are produced, but some of them are thought to be generated in the far outer atmosphere. Thence they reach our magnetographs through the ionosphere (Dungey 1954, Akasofu 1956). The propagation of such low frequency waves in the ionosphere is decidedly complicated, mainly because of the presence there of a great number of neutral particles.

---

[*] Part of this Chapter covers the same ground as the paper Akasofu (1960c)

175

6.2 ON THE IONOSPHERIC HEATING BY HYDROMAGNETIC WAVES CONNECTED WITH GEOMAGNETIC MICROPULSATIONS

6.21 Introduction

Cowling (1956b) has shown that there may be large dissipation of magnetic energy in a partially ionized gas. Piddington (1956) has suggested that the high temperature in the solar corona is due to the dissipation of hydromagnetic energy.

The ionosphere is a partially ionized gas, but the physical conditions are quite different from those of the sun. It is the object of this section to show that in the F2-region the increase of temperature due to this process is less than 5°C in the most favourable conditions (Akasofu 1960c).

6.22 Fundamental equations

The ionosphere is treated as a ternary mixture composed of electrons, together with neutral particles and positive ions, each of one kind only. Subscripts e, n and p will indicate reference to these three kinds of particle.

The equation of motion of the ith gas in a mixture (Chapman and Cowling, 1953, pp. 415, 245) is

$$\rho_i \frac{D_i V_i}{Dt} = \rho_i F_i + N_i e_i v_i \times H - \text{grad } p_i + \sum_j \alpha_{ij} N_i N_j (v_j - v_i), \tag{1}$$

where

$$\alpha_{ij} = \frac{8}{3} \sigma_{ij}^2 \left[\frac{2\pi kT m_i m_j}{(m_i + m_j)} \right]^{1/2} \tag{2}$$

and

$\underline{v}_i$ = velocity;

N_i = particle number density;

m_i = mass;

ρ_i = particle mass density = $N_i m_i$;

$\underline{F}_i$ = force per unit mass;

T = temperature;

P_i = particle pressure = $kN_i T$;

k = Boltzmann constant = 1.38×10^{-16};

e_i = electronic charge = 1.6×10^{-20} e.m.u.

$$\frac{D_i}{D_t} = \frac{\partial}{\partial t} + \underline{v}_i \cdot \text{grad};$$

σ_{ij} = effective collision distance between particles i and j.

It should be noticed that α_{ij} $(=kT/N [D_{ij}]_1)$ relates to the collision frequency ν_{ij} in the following way (Chapman, 1956b, p. 12),

$$\nu_{ij} = \frac{\rho_i + \rho_j}{\rho_i \rho_j} N_i N_j \alpha_{ij} = \frac{8}{3} \rho \sigma_{ij}^2 \left[\frac{2\pi kT}{m_i m_j (m_i + m_j)} \right]^{1/2} \qquad (3)$$

Therefore, assuming that $\rho_n \gg \rho_p$ and $\rho_n \gg \rho_e$,

$$N_i N_j \alpha_{ij} = \frac{\rho_i \rho_j}{\rho_i + \rho_j} \nu_{ij},$$

$$\simeq \rho_p \nu_{pn} \text{ (for ions)}, \qquad \left. \begin{array}{c} \\ \\ \end{array} \right\}$$
$$\simeq \rho_e \nu_{en} \text{ (for electrons)}. \qquad (4)$$

v_{ij} calculated by Chapman (1956b) is given in Table 6.1 together with the model of the ionosphere adopted in this section

TABLE 6.1

Adopted model of the ionosphere (Chapman, 1956)

Height	$T(^{\circ}K)$	$N_n(cm^3)$	$N_e(cm^3)$	$\nu_{en}(sec)$	$\nu_{pn}(sec)$
80	205	4.38×10^{14}	10^3	3.39×10^6	2.11×10^5
90	220	8.53×10^{13}	10^4	6.38×10^5	4.12×10^4
100	280	1.78×10^{13}	10^5	1.61×10^5	8.59×10^3
125	430	1.23×10^{12}	1.50×10^5	1.38×10^4	6.16×10^2
150	580	2.16×10^{11}	2.00×10^5	2.81×10^3	1.12×10^2
175	730	6.03×10^{10}	2.00×10^5	8.80×10^2	3.20×10
200	880	2.23×10^{10}	2.00×10^5	3.57×10^2	1.21×10
225	1030	9.98×10^9	2.25×10^5	1.73×10^2	5.53
250	1180	5.12×10^9	2.50×10^5	9.50×10	2.90
275	1330	2.92×10^9	2.75×10^5	5.75×10	1.70
300	1480	1.80×10^9	3.00×10^5	3.74×10	1.08

Suppose that plane waves of frequency f $(= \omega/2\pi)$ travel in the direction of a uniform magnetic field parallel to the axis Oz of a Cartesian system, so that $\partial/\partial x = \partial/\partial y = 0$, $\partial/\partial z \neq 0$. Suppose also that each $\underline{v}_i$ $(v_{ix}, v_{iy}, 0)$ is proportional to exp $(i\omega t)$. Ignoring the body force $\underline{F}_i$ (e.g. gravity), (1) for neutral particles takes the form (Dungey, 1958, p. 169)

$$i\omega \rho_n \underline{v}_n = N_n N_p \alpha_{np} (\underline{v}_p - \underline{v}_n) + N_n N_p \alpha_{ne} (\underline{v}_e - \underline{v}_n). \qquad (5)$$

As $\alpha_{np}(10^{-32})$ is much larger than $\alpha_{ne}(10^{-35})$ and $\underline{v}_p \sim \underline{v}_e$ in the F2-region (Martyn, 1953), (5) gives

$$\frac{\underline{v}_p}{\underline{v}_n} = 1 + i\omega \frac{m_n}{N_p \alpha_{np}} .$$ (6)

Under the conditions of (4), equation (1) for positive ions and electrons is

$$\frac{D_i \underline{v}_i}{Dt} = \underline{F}_i + \frac{e_i}{m_i} \underline{v}_i \times \underline{H} - \frac{grad\ p_i}{\rho_i} + \nu_{in}(\underline{v}_n - \underline{v}_i).$$ (7a)

The dispersion equation, which results from (1) combined with Maxwell's equations, is given (Dungey, 1958, p. 170) by

$$K^2 = \frac{\omega^2}{(H^2/4\pi\rho_p)} \frac{1 - (i\nu_{pn}/\omega)}{\left[1 \mp (i\nu_{en}/\Omega_e)\right]\left[1 \pm (i\nu_{pn}/\Omega_p)\right]} ,$$ (7b)

where K denotes the wave number and Ω_e and Ω_p denote the gyro-angular frequency ($= eH/m_i$) of electrons and ions, respectively. The wave number K is <u>complex</u> and is expressed by

$$K = K_1 - iK_2.$$ (7c)

Therefore any varying field A is expressed by
(7d)

$$A \exp \left\{i\left[\omega t - (K_1 - iK_2)z\right]\right\} = A \exp(-K_2 z)\exp\left[i(\omega t - K_1 z)\right].$$

6.23 Interaction between ions and neutral atoms

A small harmonic motion of neutral atoms, as seen above, can certainly be generated by a harmonic motion of the ions. The result of the interaction between ions and neutral atoms is well shown by (6). A more general treatment gives the main features of the dispersion relation (the phase velocity vs. angular frequency). For the ionosphere this is illustrated in Fig. 6.1 (Akasofu, 1956). The theory of propagation of hydromagnetic waves in the ionosphere is an extension of the magneto-ionic theory to the case when the ions can move easily in response to field changes (Dungey, 1958, p. 170). The phase velocity varies markedly with frequency, and it is convenient to consider three ranges of frequency.

The highest frequency range $(\omega > 10^5/\text{sec})$, corresponding to ordinary radio waves, shows the familiar magneto-ionic behaviour of electrons in the almost immobile positive and neutral background. The middle part of the diagram (ω ranging from 10 to $10^5/\text{sec}$) is relevant to four distinct phenomena: (1) v.l.f. radio waves, (2) whistlers, (3) dawn chorus and (4) atmospherics ('sferics). The contribution of the motion of the ions becomes increasingly important (Hines, 1957) in this range.

The part of lowest frequency $(\omega < 10/\text{sec})$ shows the dispersion curves for those hydromagnetic waves which are recognized as geomagnetic micropulsations and the other very low frequency phenomena. This range is characterized by the dominant contribution of ions and of neutral atoms. The contribution of neutral atoms can be seen from the "lowering" of the phase velocity. The physical interpretation of this lowering becomes clear from (6), and will be shown by using numerical values for the

F-region. The velocity of hydromagnetic waves V is given by

$$V = \frac{H}{(4\pi\rho)^{1/2}} , \tag{8}$$

where ρ in the denominator is the _effective_ density.

(a) For the higher frequency range around the gyro-angular frequency ($\Omega_p = eH/m_p$) 2×10^2/sec, (6) gives

$$\frac{v_p}{v_n} = 1 + i \frac{2 \times 10^2 \times 2.7 \times 10^{-23}}{3 \times 10^5 \times 3.3 \times 10^{-32}} \sim i 5.4 \times 10^5 \tag{9}$$

or

$$\left|\frac{v}{n}\right| \ll \left|\frac{v}{p}\right| .$$

This indicates that the motion of the neutral atoms does not affect the propagation of such hydromagnetic waves, and so in (8) ρ is almost exactly the density of the ionized part of the gas, $\rho \sim \rho_p + \rho_e$.

(b) For frequency lower than $\omega = 10^{-5}$/sec, (6) gives

$$\frac{v_p}{v_n} = 1 + i2.7 \times 10^{-2} \tag{10}$$

or

$$\frac{v}{n} \simeq \frac{v}{p} .$$

This indicates that the motion of the neutral atoms fully contributes to the propagation of the waves, and in (8) we must take $\rho = \rho_p + \rho_e + \rho_n$. Therefore for these lower frequencies the velocity of hydromagnetic waves decreases from $H/(4\pi\rho_p)^{1/2}$ and finally converges to $H/\left[4\pi(\rho_p + \rho_n)\right]^{1/2}$.

181

We are particularly interested in hydromagnetic waves connected with geomagnetic micropulsations in the angular frequency range from $\omega = 6.38/\text{sec}$ to $\omega = 0.064/\text{sec}$ (or f from 1 c/s to 0.01 c/s; period from 1 sec to 100 sec). It is clear that in this range the approximate relation

$$\frac{v_p}{v_n} \sim i\omega \, \frac{m_n}{N_p \, \alpha_{np}} \tag{11}$$

is sufficiently accurate in the F2-region.

6.24 Joule heat loss

The propagation of hydromagnetic waves in a ternary mixture was first studied by Hines (1953). From (7a) he derived the current and the force equations for harmonic motion of the particles of the partially ionized gas. His current and force equations are

$$\underline{J} = \sum_i \left[\frac{N_i e^2 v_{in}'}{m_i (v_{in}'^2 + \Omega_i^2)} \right] \underline{E} + \sum_i \left[\frac{N_i e^3}{m_i^2 (v_{in}'^2 + \Omega_i^2)} \right] \underline{E} \times \underline{H} +$$

$$+ \sum_i \left[\frac{N_i e v_{in} v_{in}'}{(v_{in}'^2 + \Omega_i^2)} \right] \underline{v}_n + \sum_i \left[\frac{N_i e^2 v_{in}}{m_i (v_{in}'^2 + \Omega_i^2)} \right] \underline{v}_n \times \underline{H} , \tag{12}$$

$$\underline{F} = \sum_i \left[\frac{N_i e v_{in} v_{in}'}{(v_{in}'^2 + \Omega_i^2)} \right] \underline{E} + \sum_i \left[\frac{N_i e^2 v_{in}}{m_i (v_{in}'^2 + \Omega_i^2)} \right] \underline{E} \times \underline{H} -$$

$$- \sum_i \left[N_i m_i v_{in} \frac{i\omega v_{in}' + \Omega_i^2}{(v_{in}'^2 + \Omega_i^2)} \right] \underline{v}_n + \sum_i \left[\frac{N_i e v_{in}^2}{(v_{in}'^2 + \Omega_i^2)} \right] \underline{v}_n \times \underline{H} , \tag{13}$$

where $\underline{F}$ is exactly the right-hand side of (5) and $v_{in}' = v_{in} + i\omega$.

We now consider the rate of production of heat energy when hydro-magnetic waves pass through the ionosphere. Dr. Hines (1959) indicated to one of us (S.-I.A.) his formulae for a special case, but a more general formulation is presented here. It is seen from Table 1 that important parameters of the ionosphere vary by many orders of magnitude. In order not to limit the application of the equations throughout the ionosphere, we need to develop all the equations in numerical form without any initial approximation.

Substituting (13) in (5) and taking the co-ordinate system such that $\underline{v}_n$ lies in the x-direction, we obtain the algebraic simultaneous equations for E_x and E_y. In general, the electric field $\underline{E}$ is not perpendicular to $\underline{v}_n$, so that there are two components, E_x and E_y. Solving the simultaneous equations, we have

$$E_x = (a\omega^2 + ib\omega)v_n, \tag{14}$$

$$E_y = (a'\omega^2 + ib'\omega)v_n, \tag{15}$$

where a, a', b and b' are pure numbers calculated from Table 1 for each level of the ionosphere.

Putting (14) and (15) into (12), we have similar equations for the current components J_x and J_y. The Joule heat dissipation per unit volume per unit time is defined as half the real part of the scalar product $\left[\underline{E} \cdot \underline{\tilde{J}}\right]$, where $\underline{\tilde{J}}$ is the complex conjugate of $\underline{J}$. This gives the result:

$$Q = \frac{1}{2}\mathcal{R}\left[\underline{E} \cdot \underline{\tilde{J}}\right] = \frac{1}{2}\mathcal{R}\left[E_x \cdot \tilde{J}_x + E_y \cdot \tilde{J}_y\right], \tag{16}$$

where $\mathcal{R}$ signifies real part of $\left[\quad\right]$.

Substituting from (12), (14) and (15) in the above equation (16,) Q

is found to be given by

$$Q = (\alpha\omega^4 + \beta\omega^2) \, v_n^2, \tag{17}$$

where α and β are pure numbers. In the frequency range f from 1 to

0.01 c/s, $a\omega \ll b, a'\omega \ll b'$ and $\alpha\omega^2 \ll \beta$, so that we neglect a, a' and α in

the later developments.

The further relation we need for the determination of Q is one of

Maxwell's equations,

$$\text{curl } \underline{E} = -\frac{\partial \underline{h}}{\partial t}, \tag{18}$$

where $\underline{h}$ is the varying part of the magnetic field intensity. Recalling

that a varying field is expressed by $A \exp\left\{i\left[\omega t - (K_1 - iK_2)z\right]\right\}$, (18) gives

$$h^2 = \frac{(K_1^2 + K_2^2)}{\omega^2} \, E^2, \tag{19}$$

where K_1 and K_2 are already given in (7c), and

$$E^2 = (b^2 + b'^2) \, \omega^2 v_n^2 . \tag{20}$$

From (19) and (20), we have

$$v_n^2 = \left[\frac{1}{(K_1^2 + K_2^2) \, (b^2 + b'^2)}\right] h^2. \tag{21}$$

Substituting from (21) in (17), we finally obtain

$$Q = \left[\frac{\beta\omega^2}{(K_1^2 + K_2^2) \, (b^2 + b'^2)}\right] h^2. \tag{22}$$

6.25 The spectrum of geomagnetic micropulsations

In order to calculate from (22) the thermal energy Q produced in the ionosphere, we must know the intensity spectrum (intensity vs. angular frequency), and must have some information about the frequency of occurrence of micropulsations at each level of the ionosphere.

The spectrum of the geomagnetic micropulsations has been obtained by Campbell (1959) at California. His figure relates to the average amplitude for the daylight hours in a middle latitude during a moderately magnetically disturbed day. We assume that in the auroral zone the intensity will be increased by a factor of 10^2 during geomagnetic storms for the lower frequency end of the spectrum. Campbell's spectrum (1959, his Fig. 5) shows two distinct maxima; there is a transition from audio and sub-audio waves to geomagnetic micropulsations at frequencies between $0.2 \sim 2.0$ c/s. The intensity of geomagnetic micropulsations has a maximum at about $f = 0.05$ c/s.

Hydromagnetic waves may be generated far above the F-layer. Then a question arises as to whether there is some difference between the spectrum observed at the surface of the earth and that in or above the ionosphere. The dispersion equation involves the complex wave number K. Dungey (1958, p. 171; Table 4) gave K^2 for various heights for waves $\omega = 0.1/sec$. Similar calculations have been made for K^2 and K, (K_1, K_2), for frequencies $f = 1, 0.1$ and 0.01 c/s (see 7b, c). Then the transmission coefficient T at each level of the ionosphere is evaluated,

$$T = \exp(-dK_2),$$ (23)

where d is the thickness of each layer and is taken to be 10 km for a

height of 80 or 90 km and 25 km for 100 km and above. The results are shown in Fig. 6.3. Here, $1/K_2$ gives the damping length, in which the amplitude is decreased by the factor $1/e$. Table 6.2 gives the results of a rough numerical evaluation of the ratio exp $(-V)$ of the wave amplitude at the bottom of the ionosphere to that at the top: here

$$V = \int_{z_1}^{z_2} zK_2 \, dz \qquad (24)$$

and z_1, z_2 are taken to be 80 km and 300 km.

TABLE 6.2

The ratio of the amplitude of hydromagnetic waves at the bottom of the ionosphere to that at the top of the ionosphere for several frequencies

f(c/s)	0.01	0.1	1
ω(/sec)	0.0628	0.628	6.28
Period (sec)	100	10	1
Ratio	0.323	2.83×10^{-2}	8.22×10^{-6}

From Fig. 6.2 and Table 6.2, we can see that for frequencies less than 10^{-2} c/s the ionosphere is nearly transparent. But the E-layer is extremely opaque for higher frequencies around $f = 1$ c/s.

Table 6.3 shows the intensity h (γ) at the ground (taken from Campbell's diagram) and at 300 km calculated from the ratio discussed above. For $f = 1$ c/s,

TABLE 6.3

The tentative intensity spectrum of micropulsations at different levels

Frequency (c/s)	Period (sec)	Amplitude (γ) Ground level (middle lat.)	Amplitude (γ) 300 km (middle lat.)	Amplitude (γ) 300 km (auroral zone)
			(Inferred)	(Adopted)
1	1	5.0×10^{-3}*	6.1×10^{2} †	1
0.1	10	0.2	7.1	10
0.01	100	0.1	0.31	31.6

* Phillips (1960).   † See the following paragraph.

Phillips (1960) reports that in Alaska the maximum amplitude (at ground level) is about 0.02 γ . Using the ratio calculated above, we obtain $h = 2 \times 10^{-2} \gamma / 8.22 \times 10^{-6} = 2.43 \times 10^{3} \gamma$ as the intensity at 300 km. This would imply an enormous and improbable oscillation of the magnetic field at 7000 km above the ground. It seems more likely that such a sub-audio noise received at the ground is generated in the lower part of the E-layer (below the barrier at about 125 km in height; see Fig. 6.2).

We are particularly interested in the waves generated above the F2-region, for example, by the interaction between the outer atmosphere and the solar stream. The waves associated with sudden commencements of geo-magnetic storms are believed to be of this kind (Dessler, 1958). Their frequency is about f = 0.01 c/s or less. A typical amplitude is from 25 to 50 γ . Some inhomogeneity in the stream may produce additional wave motions in the outer atmosphere but probably with amplitude and frequency not so much different from the above values. Actually, it seems

more likely that their amplitude will be less than the above value[*].

Dessler (1959) assumed that during magnetic storms the high fre-
quency end of the wave spectrum will probably be important because of
the formation of hydromagnetic shocks. He considered an amplitude of
30 γ for waves of 1 c/s on quiet days, and that this may be increased
by a factor of at least 10 on disturbed days. But the amplitude of 30 γ
for 1 c/s cannot be attained even on disturbed days. Table 6.3 gives a
tentative model spectrum of the _average_ amplitude of geomagnetic micro-
pulsations at the top of the ionosphere in the auroral zone during
magnetic storms.

Furthermore, in the magnetograms from the polar regions, one can
often see two or three different superposed waves, which combine to give
a rather regular sinusoidal variation, except on very disturbed days.
At present, the only way to check the assumption made in Table 6.3 is
to examine the ionospheric data at times of intense geomagnetic activity.
This is done in the last section of this paper.

---

[*] Chapman and Ferraro (1931) showed in their theory of sudden
commencements of magnetic storms how solar corpuscular streams produce
a sudden change of the magnetic field when streams are stopped at sev-
eral earth radii. It is now believed that this sudden change is trans-
mitted towards the earth by hydromagnetic propagation into the outer
atmosphere, without any change in their basic idea. They also showed
how rapidly this happens. The rise time is shown to be about 100 sec
which agrees with the observations. A discontinuous change, such as a
sudden commencement, may be expressed by the Fourier series shown below.

$$f(t) = \frac{4}{\pi} \left(\frac{\sin t}{1} + \frac{\sin 3t}{3} + \frac{\sin 5t}{5} + \ldots \right).$$

This would imply that the amplitude of 1 c/s waves is of order 50 γ/100
= 0.5 γ, assuming that the amplitude of the first term is of order 50 γ
and the period of 100 sec.

6.26 Increase of temperature

The rate of production of thermal energy per unit volume per second is calculated from (22) for $h = 1\gamma$ at 300 km for frequencies $f = 1$, 0.1 and 0.01 c/s, taking into account the decrease of amplitude along the path, for vertical incidence. The results are shown in Fig. 6.3. For later use, some typical values of Q_0 in the F2-region and Q at 90 km are also given in Table 6.4. It is interesting to note that the rate of conversion of electromagnetic energy into heat attains its maximum at about 190-220 km, for the frequencies considered here. Below 170 km the rate of conversion decreases very steeply.

The only further relation we need to determine the change of temperature, which is our main concern, is the equation of thermal conduction. In the steady state the increase of the temperature ΔT at height z satisfies the equation

$$\lambda \frac{d^2 \Delta T}{dz^2} = -Q(z), \tag{25}$$

where λ denotes the thermal conductivity of the air and Q(z) the rate of heat production per unit volume per second, as above calculated.

Because of the complexity of Q(z), it is very difficult to infer the exact temperature distribution in the ionosphere. From Fig. 6.3 it seems reasonable to infer that below the level of maximum heat production, Q decreases rapidly downwards. Let it be taken to be approximately $Q_0 \exp(-az)$, measuring z positive downward; a can be calculated from Table 6.4.

189

TABLE 6.4

The adopted amplitude at 300 km above the auroral zone,
Q_o and ΔT in the F2-region and Q at 90 km

Frequency (c/s)	Period (sec)	$\underline{h}$ (γ)	Q_o (ergs/cm^3 sec)	ΔT ($^\circ$K)	Q (ergs/cm^3 sec)
			F2-Region		90 km
1	1	1	10^{-10}	0.21 (220 km)	2.08×10^{-22}
0.1	10	10	1.48×10^{-10}	0.83 (200 km)	1.81×10^{-14}
0.01	100	31.6	2.30×10^{-10}	1.18 (190 km)	2.10×10^{-13}

Hence assuming $d\Delta T/dz = 0$ at $z = 0$, where the maximum production

occurs, the integral of (25) has the form

$$\frac{d\Delta T}{dz} = \frac{Q_o}{\lambda a} \left[\exp(-az) - 1 \right].$$ (26)

Further integration gives

$$\Delta T(z) - \Delta T(0) = \frac{Q_o}{\lambda a} \left\{ \frac{1}{a} \left[1 - \exp(-az) \right] - z \right\},$$ (27)

where $\Delta T(z)$ and $\Delta T(0)$ denote the increase of temperature at z and

x = 0, respectively. We use the thermal conductivity λ given by Bates

(1951, p. 815), namely 2.4×10^3 for T = 500°K.

For the frequency f = 0.01 c/s at 190 km, we may take Q_o = 2.3 x

$10^{-13}h^2$ ergs/cm^3 sec (if h is expressed in γ). Taking h = 31.6 γ,

Q_o = 2.3 x 10^{-10} ergs/cm^3 sec at 190 km; as Q = 2.10 x 10^{-13} ergs/cm^3 sec

at 90 km (see Table 6.4), a is found to be 7 x 10^{-7}/cm.

Therefore (27) becomes

$$\Delta T(z) - \Delta T(0) = 1.37 \times 10^7 \left\{ \frac{1}{7 \times 10^{-7}} \left[1 - \exp(-7 \times 10^{-7} z) \right] - z \right\}.$$

$$(28)$$

The heating effect at 90 km is much less than at 190 km, so that, taking $z = 100$ km $= 10^7$ cm,

$$\Delta T(0) \simeq 1.18^\circ C.$$

$$(29)$$

A similar calculation for $f = 0.1$ and 1 c/s gives $\Delta T(0) \simeq 0.83^\circ C$ at 200 km and $\Delta T(0) \simeq 0.21^\circ C$ at 220 km, respectively.

In general, two or three particular frequencies superposed on higher frequency components are seen on the magnetograms in the auroral zone. Therefore, smoothing out the high-frequency waves, of which the heating effect is negligible (see Table 6.4), we can find these particular waves. However, as the contribution of each wave is at most $1.2^\circ C$, according to the above Table 6.4, the total contribution could not exceed $5^\circ C$.

6.27 Ionospheric disturbance on 11 February 1958

The magnetic storm on 11 February 1958 was accompanied by fluctuations of the magnetic field of a violence exceeding anything observed in the last decade. Therefore, it is of great interest to examine whether there was any appreciable heating of the upper atmosphere by hydromagnetic waves, as proposed by Dessler (1959). The magnetograms from College (gm. lat. 64°.7 N; insensitive recorder) and from Guam (gm. lat. 3°.9 N; sensitive recorder) are shown in Fig. 6.4 (a,b). Fig. 5(c) shows the ionospheric data (the electron density of the F2-layer) from Adak, Alaska (gm. lat. 47°.3 N).

Intense and rapid magnetic fluctuations, of order 100 γ, began simultaneously with the sudden commencement at 0126 GMT on 11 February 1958. They were active at least until 0600 GMT. The very abrupt ionospheric storm began at 0215 GMT at Adak, and f_oF2 reached its minimum at 0330. The ionospheric storm quickly subsided at about 0515, while intense fluctuations of the magnetic field were still continuing. Fig. 6.5 shows the daily variation of the electron density of the F2-layer at Adak on the same day. Except for the above mentioned remarkable "bite" out of the normal curve, the ionosphere was rather normal. The same phenomenon was observed at several other places, including Delhi, Singapore, Okinawa, Yamagawa, Kokubunji, Akita, Wakkanai, Maui (Hawaii) and Stanford.

The first difficulty in trying to explain such a phenomenon by hydromagnetic heating is its abrupt beginning. Furthermore, it is altogether impossible to expect such a quick recovery if the upper atmosphere expanded upward as a whole by heating. Such an expansion would change the density distribution so as to alter the ion production rate and electron density distribution, although the F2-layer may not be an independent ionized layer.

It is interesting to note that at about the commencement of the ionospheric storm, the College magnetogram showed a large polar magnetic disturbance, of order 1000 γ or more (see Fig. 6.4a). It is shown in § 5.64 that such a negative polar disturbance could be produced by a southward electric field of order 4×10^4 e.m.u. (40V/km). If such an electric field appeared at the same time in the ionosphere over Adak,

192

it would produce a vertical upward drift motion of ions and electrons of order 15 m/sec at 210 km there. It may be that only the ions and electrons moved upwards by electric drift, while the neutral background air was little affected; then a new F2-layer was formed by solar ultraviolet radiation, after the strong drift ceased.

6.28 Conclusion

Dessler (1959), in a recent paper, discussed ionospheric heating by hydromagnetic waves. He concluded that the increase of h'F2 at the time of ionospheric disturbances in the auroral zone may be explained by hydromagnetic heating. It is shown in this chapter that the increase of temperature is at most $5^{o}C$ in the F2-region. It seems unlikely that such a small increase of temperature can produce violent upward movement of the upper atmosphere.
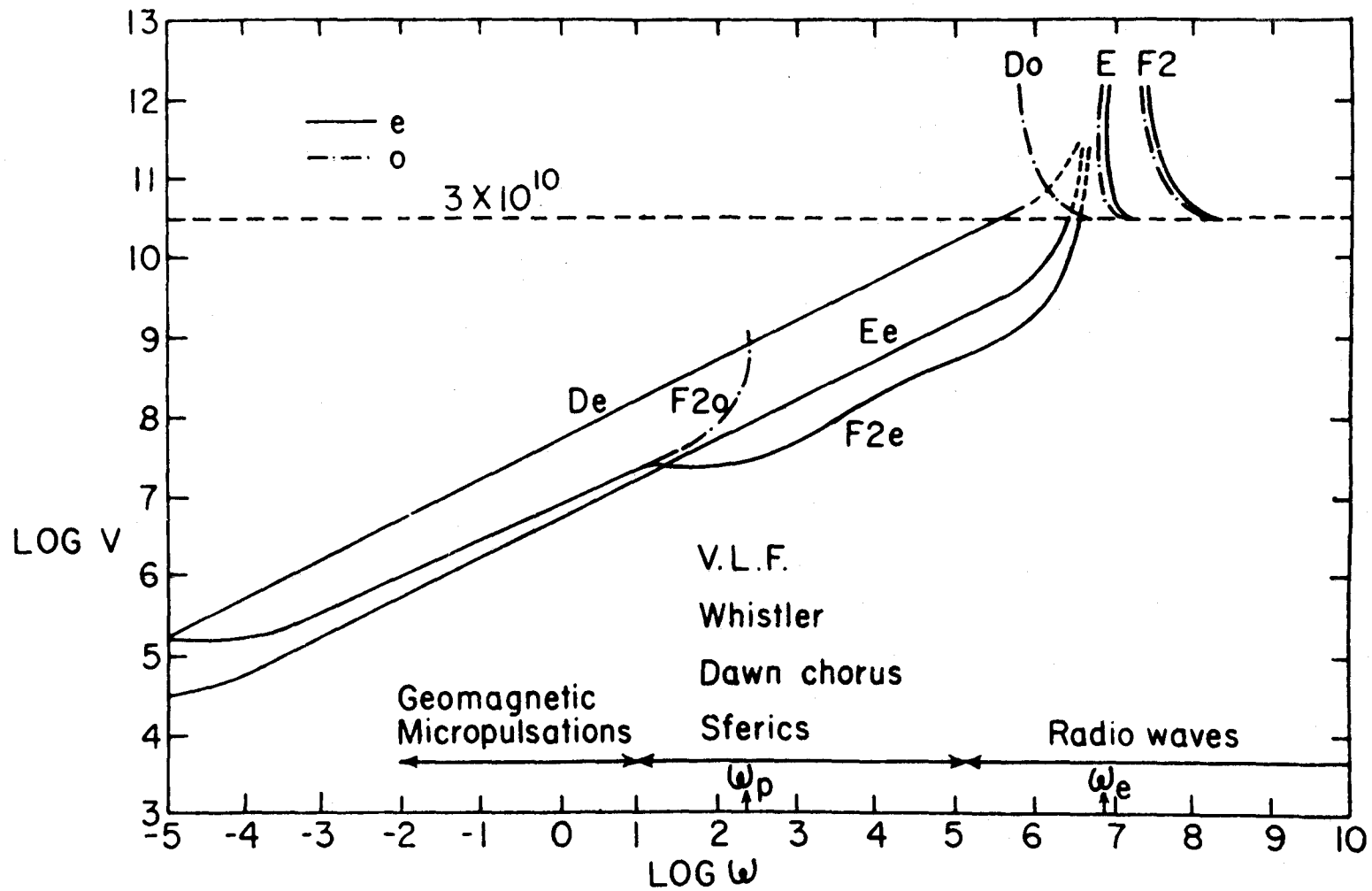
Fig.6.1. Dispersion relation (the phase velocity V vs. angular frequency ω) of hydromagnetic waves in the F2-,E- and D-regions of the ionosphere. Subscripts o and e refer to ordinary and extraordinary waves,respectively; ω_p and ω_e denote the gyrao-frequencies of ions and electrons,respectively (Akasofu 1956).
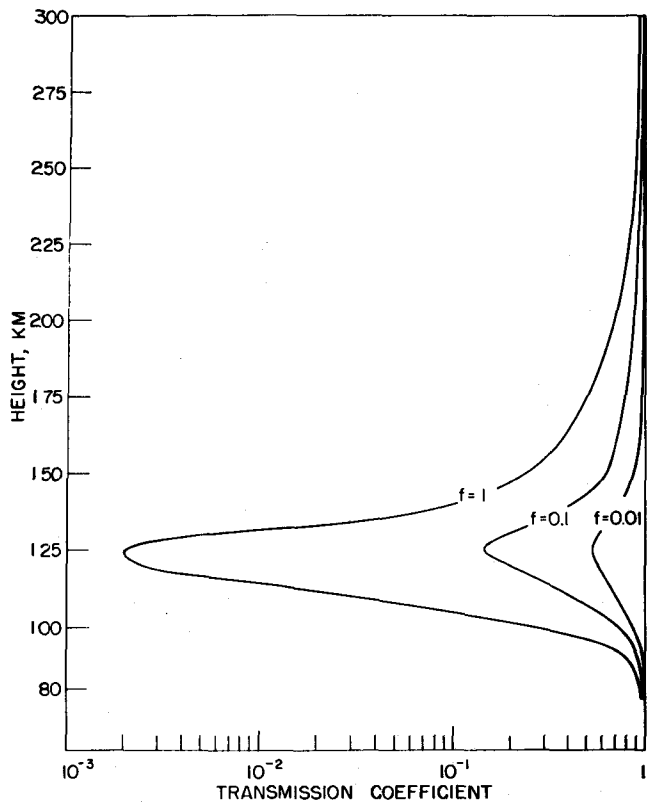
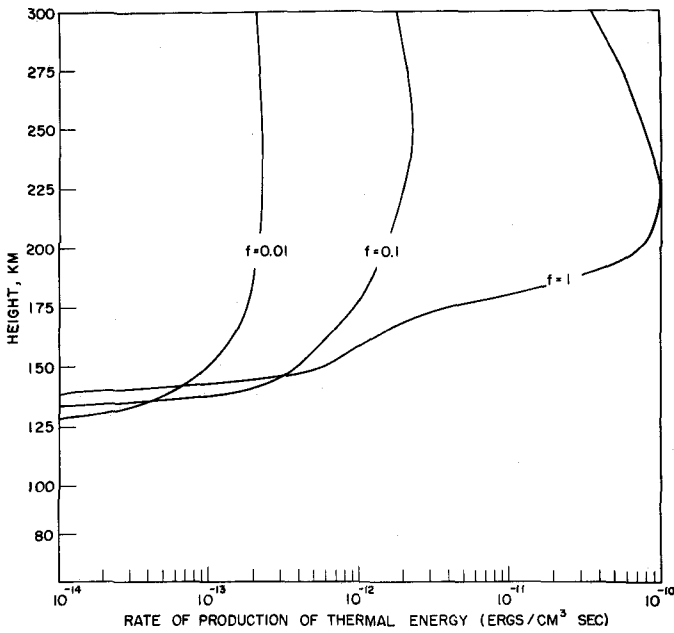Fig.6.2. Transmission coefficient of the ionosphere for frequencies f=1,0.1 and 0.01 c/s.

Fig.6.3. Thermal energy production rate in the ionosphere (ergs/cm^3 sec), for frequencies f= 1, 0.1 and 0.01 c/s, for waves of amplitude h = 1 gamma at 300 km (vertical incidence).
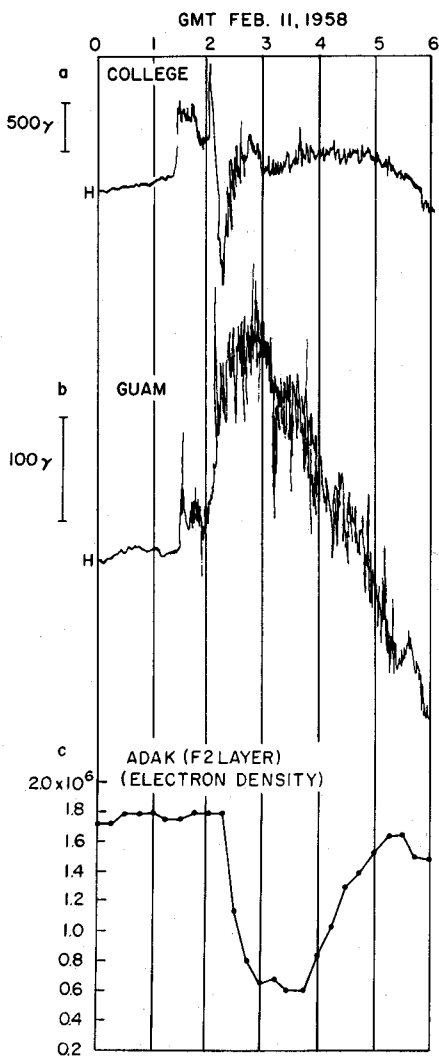
Fig.6.4. a: Magnetogram (Insensitive recorder),College, Alaska(gm.lat. 64°7N). b: Magnetogram (Sensitive recorder),Guam (gm.lat. 3°9N). c: Change of electron density of the F2 layer,Adak,Alaska(gm.lat.47°3N).
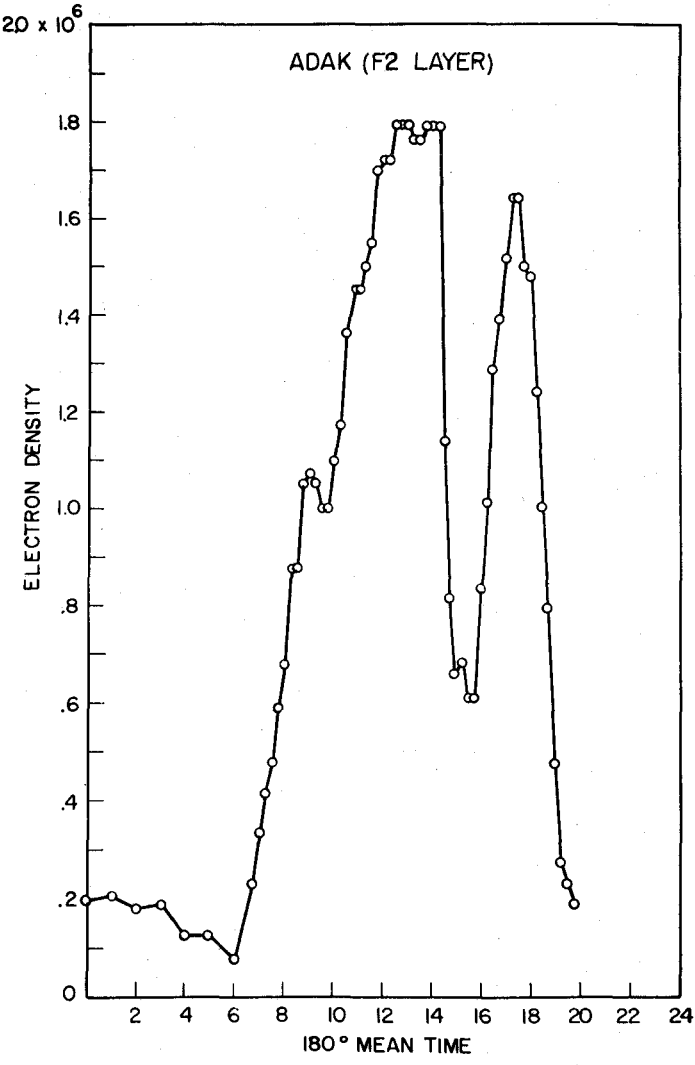
Fig.6.5. Daily variation of electron density of the F2 layer,
Adak,Alaska(gm.lat. 47?3N), on February 10,1958.

ACKNOWLEDGEMENTS

REFERENCES

Adams, W. G., Comparison of simultaneous magnetic disturbances at several observatories, Phil. Trans. Roy. Soc., A, 183, 131-140, 1892.

Akasofu, S.-I., On the geomagnetic micropulsations, Rep. Ionosphere Res. Japan, 10, 227-249, 1956.

Akasofu, S.-I., Hydromagnetic relationships between the sun and the earth, Sci. Rep. Tohoku Univ. ser. 5, 8, 133-145, 1957.

Akasofu, S.-I., The ring current and the outer atmosphere, J. Geophys. Res., 65, 535-543, 1960a.

Akasofu, S.-I., Large-scale auroral motions and polar magnetic disturbances - I., J. Atmosph. Terr. Phys., 19, 10-25, 1960b.

Akasofu, S.-I., On the ionospheric heating by hydromagnetic waves connected with geomagnetic micropulsations, J. Atmosph. Terr. Phys., 18, 160-173, 1960c.

Akasofu, S.-I. and S. Chapman, Some features of the magnetic storms of July 1959, and tentative interpretations, UGGI Chronicle, 1960.

Akasofu, S.-I. and S. Chapman, A neutral line discharge theory of the aurora polaris, Phil. Trans. Roy. Soc. A, 253, 359-406, 1961a.
***
Akasofu, S.-I. and S. Chapman, The sudden commencement of magnetic storms, Annals of IGY, Pergamon Press, 1961c.

Alfvén, H., A theory of magnetic storms and of the aurorae, Kungl. Sv. Vet.-Akademiens Handl. 18, No. 3, 1939.

Alfvén, H., On the motion of a charged particle in a magnetic field, Ark. f. Mat. Astr. o. Fysik, 27A, No. 22, 1940.

Alfvén, H., Cosmical Electrodynamics, Oxford Univ. Press, 1950.

Alfvén, H., On the electric field theory of magnetic storms and aurorae, Tellus, 7, 50-64, 1955.

Alfvén, H., The sun's general magnetic field, Tellus, 6, 1-12, 1956.

Alfvén, H., On the theory of magnetic storms and aurorae, Tellus, 10, 104-116, 1958.

Angenheister, G., Propagation velocities of magnetic disturbances and pulsations, Nachrichten Ges. Wiss. Göttingen, Math.-Phys. Klasse, 4, 565-581, 1913.

***Akasofu, S-I. and S. Chapman, The ring current, geomagnetic disturbance, and the Van Allen radiation belts, J. Geophys. Res., May, 1961b.

Allcock, G.McK., The electron density distribution in the outer ionosphere derived from whistler data, J. Atmosph. Terr. Phys., 14, 185-199, 1959.

Arnoldy, R. L., R. A. Hoffman, and J. R. Winckler, Observations of the Van Allen radiation regions during August and September 1959, Part I, J. Geophys. Res., 65, 1361-1376, 1960a.

Arnoldy, R. L., R. A. Hoffman, and J. R. Winckler, Solar cosmic rays and soft radiation observed at 5,000,000 kilometer from the earth, J. Geophys. Res., 65, 3004-3007, 1960b.

Ashour, A. A. and A. T. Price, The induction of electric currents in a non-uniform ionosphere, Proc. Roy. Soc., A, 195, 198-224, 1948.

Aström, E., Electron orbits in hyperbolic magnetic fields, Tellus, 8, 260-267, 1956.

Babcock, H. D., The sun's polar magnetic field, Astrophys. J., 130, 364-365, 1959.

Babcock, H. W., and H. D. Babcock, The sun's magnetic field, 1952-1954, Astrophys. J., 121, 349-366, 1955.

Baker, W. G., and D. F. Martyn, Electric currents in the ionosphere, I. The conductivity, Phil. Trans. Roy. Soc., A, 246, 281-294, 1953.

Barbier, D., L'activite aurorale aux basses latitudes, Ann. de Géophys., 14, 334-346, 1958.

Bates, D. R., The temperature of the outer atmosphere, Proc. Phys. Soc. B, 64, 805-821, 1951.

Bates, D. R., The Earth as a Planet, (ed. G. P. Kuiper), Univ. Chicago Press, 1954.

Bates, D. R., Physics of the Upper Atmosphere, (ed. J. A. Ratcliffe), Academic Press, New York, 1960.

Bauer, L. A., Beginning and propagation of the magnetic disturbance of May 8, 1902, and of some other magnetic storms, Terr. Mag., 15, 9-20, 219-232, 1910.

Biermann, L., Solar corpuscular radiation and the interplanetary gas, Observatory, 77, 109-110, 1957.

Birkeland, Kr., The Norwegian Aurora Polaris Expedition, 1902-1903, Vol. I, Ascehoug, Christiania, Norway.

Blackwell, D. E., A study of the outer corona from a high altitude aircraft at the eclipse of 1954 June 30, I. Observational Data, Mon. Not., R. Astr. Soc., 115, 629-649, 1955.

Blackwell, D. E., A study of the outer corona from a high altitude aircraft at the eclipse of 1954 June 30, II. Electron densities in the outer corona and zodiacal light regions, Mon. Not., R. Astr. Soc. 116, 56-68, 1956.

Bond, F. R. and F. Jacka, Distribution of auroras in the southern hemisphere, Aust. J. Phys., 13, 610-612, 1960.

Brown, R. H. and A. C. B. Lovell, The Exploration of Space by Radio, John Wiley & Son, Inc., New York, 1958.

Bullard, E. C., The magnetic field within the earth, Proc. Roy. Soc. A, 197, 433-453, 1949.

Bullard, E. C. and H. German, Homogeneous dynamo and terrestrial magnetism, Phil. Trans. Roy. Soc., A, 249, 213-278, 1954.

Bullough, K. and T. R. Kaiser, Radio reflections from aurorae, J. Atmosph. Terr. Phys., 5, 189-200, 1954.

Bullough, K. and T. R. Kaiser, Radio reflections from aurorae, II. J. Atmosph. Terr. Phys., 6, 198-214, 1955.

Bullough, K., T. W. Davidson, T. R. Kaiser, and C. D. Watkins, Radio reflections from aurorae-III, The association with geomagnetic phenomena, J. Atmosph. Terr. Phys., 11, 237-254, 1957.

Cahill, L. Jr., Investigation of the equatorial electrojet by rocket magnetometers, J. Geophys. Res., 64, 489-503, 1959.

Campbell, W. H., Studies of magnetic field micropulsations with periods of 5 to 30 seconds, J. Geophys. Res., 64, 1819-1826, 1959.

Campbell, W. H., Micropulsations in the earth's magnetic field simultaneous with pulsating aurora, Nature, 185, 677, 1960.

Chakrabarty, S. K., 'Sudden commencements' in geomagnetic field variations, Nature, 167, 31, 1951.

Chamberlain, J. W. and A. B. Meinel, The Earth as a Planet (ed. G. P. Kuiper), Univ. Chicago Press, 1954.

Chamberlain, J. W., The Airglow and the Aurorae, (ed. E. B. Armstrong & A. Dalgarno), Pergamon Press, 1956.

Chamberlain, J. W., Advances in Geophysics, (ed. H. E. Landsberg and J. Van Mieghem) Vol. IV, Academic Press Inc., New York, 1958.

Chamberlain, J. W., Interplanetary gas II, Expansion of a model solar corona, Astrophys. J., 131, 47-56, 1960.

Chapman, S., On the time of sudden commencement of magnetic storms, Proc. Phys. Soc., 30, 205-214, 1918.

Chapman, S., An outline of a theory of magnetic storms, Proc. Roy, Soc. A, 95, 61-83, 1919.

Chapman, S., The electric current-systems of magnetic storms, Terr. Mag., 40, 349-370, 1935.

Chapman, S., The equatorial electrojet as detected from the abnormal electric current distribution above Huancayo, Peru, and elsewhere, Arch. Met., Wien, 4, 368-390, 1951.

Chapman, S. The geometry of radio echoes from aurorae, J. Atmosph. Terr. Phys., 3, 1-20, 1952.

Chapman, S., The morphology of geomagnetic storms. An extension of the analysis of DS, the disturbance local-time inequality, Annali de Geofisica, 5, 481-499, 1952.

Chapman, S., The morphology of geomagnetic storms and bays, A general general review,Vistas in Astronomy, II, 912-928, (ed. A. Beer), Pergamon Press, 1956a.

Chapman, S., The electrical conductivity of the ionosphere: a review, Nuovo Cimento, 4, Suppl., 1385-1412, 1956b.

Chapman, S., Notes on the solar corona and the terrestrial ionosphere, Smithsonian Contributions to Astrophysics, 2, 1-12, 1957a.

Chapman, S., Speculations on the atomic hydrogen and the thermal economy of the upper ionosphere, The Threshold of Space, (ed. M. Zelikoff) Pergamon Press, 1957b.

Chapman, S., The solar corona and the interplanetary gas, Space Astrophysics, McGraw-Hill Co., New York, 1961a.

Chapman, S., Dynamical and other aspects of cosmic gases of low density, Second International Symposium on Rarified Gas Dynamics, Berkeley 1960, Academic Press, 1961b.

Chapman, S., Scale times and scale lengths of variables with geomagnetic and ionospheric illustrations, Proc. Phys. Soc., 1961c.

Chapman, S. and J. Bartels, Geomagnetism, Oxford Univ. Press, 1940.

Chapman, S. and T. G. Cowling, Mathematical Theory of Non-Uniform Gases, 2nd ed. Cambridge Univ. Press, 1953.

Chapman, S. and V. C. A. Ferraro, A new theory of magnetic storms, Terr. Mag., 36, 77-97, 1931a; 171-185, 1931b.

Chapman, S. and V. C. A. Ferraro, A new theory of magnetic storms, Part II, the main phase, Terr. Mag., 38, 79-96, 1933.

Chapman, S. and V. C. A. Ferraro, The theory of the first phase of a geomagnetic storm, Terr. Mag., 45, 245-268, 1940.

Chapman, S. and P. C. Kendall, An idealized cylindrical problem of plasma dynamics that bears on geomagnetic storm theory; oblique projection, to be published.

Chapman, S. and C. G. Little, The nondeviative absorption of high-frequency radio waves in auroral latitudes, J. Atmosph. Terr. Phys., 10, 20-31, 1957.

Chew, G. F., M. L. Goldberger, and F. E. Low, Series of Lectures on Ionized Gas, Los Alamos Scientific Laboratory, Univ. California, 1956.

Chree, C., Time measurements of magnetic disturbances, Proc. Phys. Soc., 23, 49-57, 1910.

Coleman, P. J. Jr., L. Davis, and C. P. Sonett, Steady component of the interplanetary magnetic field: Pioneer V, Phys. Rev. Letters, 5, 43-46, 1960.

Cowling, T. G., The Sun (ed G. P. Kuiper), Univ. Chicago Press, 1956a.

Cowling, T. G., The dissipation of magnetic energy in an ionized gas, Mon. Not., R. Astr. Soc., 116, 114-124, 1956b.

Dagg, M., The correlation of radio-star-scintillation phenomena with geomagnetic disturbances and the mechanism of motion of the ionospheric irregularities in the F region, J. Atmosph. Terr. Phys., 10, 194-203, 1957.

Dahlstrom, C. E. and D. M. Hunten, O_2^+ and H in the auroral spectrum, Phys. Rev., 84, 378-379, 1951.

Davis, L. Jr., Interplanetary magnetic fields and cosmic rays, Phys. Rev., 100, 1440-1444, 1955.

Davis, T. N. and D. S. Kimball, Incidence of auroras and their north-south motions in the northern auroral zone, Geophys. Inst. Univ. Alaska, R-100, 1960.

Dessler, A. J., The propagation velocity of worldwide sudden commencements of magnetic storms, J. Geophys. Res., 63, 405-408, 1958a.

Dessler, A. J., Large-amplitude hydromagnetic waves above the ionosphere, Phys. Rev. Letter, 1, 68-69, 1958b; J. Geophys. Res., 63, 507-511, 1958b.

Dessler, A. J., Ionospheric heating by hydromagnetic waves, J. Geophys. Res, 64, 379-401, 1959.

Dessler, A. J. and E. N. Parker, Hydromagnetic theory of geomagnetic storms, J. Geophys. Res., 64, 2239-2252, 1959.

Dessler, A. J., W. F. Francis, and E. N. Parker, Geomagnetic storm sudden-commencement rise time, J. Geophys. Res., 65, 2715-2719, 1960.

Dreicer, H., Electron and ion runaway in a fully ionized gas. I. Phys. Rev. 115, 238-249, 1959.

Duffus, H. J. and J. A. Shand, Some observations of geomagnetic micropulsations, Can. J. Phys., 36, 508-526, 1958.

Dungey, J. W., Conditions for the occurrence of electrical discharges in astrophysical systems, Phil. Mag., 44, 725-738, 1953.

Dungey, J. W., Electrodynamics of the outer atmosphere, Ionosphere Res. Lab. The Pennsylvania State Univ. Sci. Rep., No. 69, 1954.

Dungey, J. W., Cosmic Electrodynamics, Camb. Univ. Press, 1958.

Dungey, J. W., Interplanetary magnetic field and the auroral zones, Phys. Rev. Letters, 6, 47-48, 1961.

Elliot, H., Cosmic-ray intensity variation and the interplanetary magnetic field, Phil. Mag., 5, 601-619, 1960.

Ellis, W., On the simultaneity of magnetic variations at different places on occasions of magnetic disturbance, and on the relations between magnetic and earth current phenomena, Proc. Roy. Soc. A, 102, 191, 1892.

Elsasser, W. M., Induction effects in terrestrial magnetism, Phys. Rev., 69, 106-116, 1946.

Elsasser, W. M., Some dimensional aspects of hydromagnetic phenomena, Magnetohydrodynamics (ed. R. K. M. Landshoff), Stanford Univ. Press, 1957.

Elvey, C. T., Problems of auroral morphology, Proc. Nat. Acad. Sci., 43, 63-75, 1957.

Elvey, C. T. and W. Stoffregen, Auroral photography by all-sky camera, Annals of IGY, V, Part II, 121-151, Pergamon Press, 1957.

Fan, C. Y., Time variation of the intensity of auroral hydrogen emission and the magnetic disturbance, Astrophys. J., 128, 420-427, 1958.

Fan, C. Y. and D. H. Schulte, Variations in the auroral spectrum, Astrophys. J., 120, 563-565, 1954.

Fejer, J. A., Semidiurnal currents and electron drifts in the ionosphere, J. Atmosph. Terr. Phys., 4, 184-203, 1953.

Fejer, J. A., Hydromagnetic wave propagation in the ionosphere, J. Atmosph. Terr. Phys., 18, 135-146, 1960.

Fermi, E., Galactic magnetic fields and the origin of cosmic radiation, Astrophys. J., 119, 1-6, 1954.

Fermi, E. and Chandrasekhar, S., Magnetic fields in spiral arms, Astroph. J., 118, 113-115, 1953.

Ferraro, V. C. A. and W. C. Parkinson, Sudden commencements in geomagnetism: their dependence on local time and geomagnetic longitude, Nature, 165, 243-244, 1950.

Ferraro, V. C. A., W. C. Parkinson, and H. W. Unthank, Sudden commencements and sudden impulses in geomagnetism, Cheltenham (MD), Tucson, San Juan, Honolulu, Huancayo and Watheroo, J. Geophys. Res., 56, 177-195, 1951.

Ferraro, V. C. A., On the theory of the first phase of a geomagnetic storm, J. Geophys. Res., 57, 14-49, 1952.

Ferraro, V. C. A., Electromagnetic Theory, The Athlone Press, London, 1954.

Ferraro, V. C. A., Some remarks on recent notes by Drs.Sugiura and Vestine, J. Geophys. Res., 59, 309-311, 1954.

Forbush, S. E. and E. H. Vestine, Daytime enhancement of size of sudden commencements and initial phase of magnetic storms at Huancayo, J. Geophys. Res., 60, 299-316, 1955.

Francis, W. E., M. I. Green, and A. J. Dessler, Hydromagnetic propagation of sudden commencements of magnetic storms, J. Geophys. Res., 64, 1643-1745, 1959.

Fritz, H., Das Polarlicht, Leipzig, 1881.

Fukushima, N., Polar magnetic storms and geomagnetic bays, J. Faculty of Sci. Tokyo Univ. 8, 293-412, 1953.

Galperin, G. I., Hydrogen emission and two types of auroral spectra, Planet. Space Sci., 1, 57-62, 1959.

Gartlein, C. W., Auroral spectra showing broad hydrogen lines, Trans. Amer. Geophys. Union, 31, 18-20, 1950.

Gerard, V. B., The propagation of world-wide sudden commencements of magnetic storms, J. Geophys. Res., 64, 593-596, 1959.

Gold, T., Gas Synamics of Cosmic Clouds, (ed. Van de Hulst and J. M. Burgers) North-Holland Pub. Co. Amsterdam, 1955.

Gould, R. W., The dynamics of electron beams, Plasma dynamics (ed F. H. Clauser), Addison-Wesley Pub. Co., Reading, Mass., 1960.

Green, M. I., W. E. Francis, and A. J. Dessler, The refraction of hydromagnetic waves in the geomagnetic field, Bull. Amer. Phys. Soc., 4, 360, 1959.

Heppner, J. P., Time sequences and spatial relations in auroral activity during magnetic bays at College, Alaska, J. Geophys. Res., 59, 329-338, 1954.

Hewish, A., The irregular structure of the outer regions of the solar corona, Proc. Roy. Soc., A, 228, 238-251, 1955.

Hewish, A., The scattering of radio waves in the solar corona, Mon. Not., R. Astr. Soc., 118, 534-546, 1958.

Hiltner, W. A., Interstellar polarization, Vistas in Astronomy, (ed. A. Beer), 1956.

Hiltner, W. A., Polarization of the Crab nebula, Astrophys. J., 125, 300-305, 1957.

Hessler, V. P. and E. M. Wescott, Rapid fluctuations in earth currents at College, Alaska, Geophys. Inst. Univ. Alaska, R87, 1959.

Hiltner, W. A., Photoelectric polarization observations of the Jet in M87, Astrophys. J., 130, 340-343, 1959.

Hines, C. O., Generalized magneto-hydroynamic formulae, Proc. Camb. Phil. Soc., 49, 299-307, 1953.

Hines, C. O., On the geomagnetic storm effect, J. Geophys. Res., 62, 491-492, 1957.

Hines, C. O. and L. R. O. Storey, Time constants in the geomagnetic storm effect, J. Geophys. Res., 63, 671-682, 1958.

Hirono, M., A theory of diurnal magnetic variations in equatorial regions and conductivity of the ionosphere E region, J. Geomag. Geolect., 4, 7-21, 1952.

Hoyle, F., Some Recent Researches in Solar Physics, Camb. Univ. Press, 1949.

Jackson, W., 'Sudden commencements' in geomagnetism, Nature, 166, 691-692, 1950.

Jackson, W., World-wide simultaneous magnetic fluctuations and their relation to sudden commencements, J. Atmos. Terr. Phys., 2, 160-172, 1952.

Johnson, F. S., The structure of the outer atmosphere including the ion distribution above the F2 maximum, Lockheed Tech. Rep., April 1959.

Kaiser, T. R., The Airglow and Aurorae, (ed. E. B. Armstrong and A. Dalgarno), Proc. Symposium, Belfast, 1955, Pergamon Press, 1955.

Kato, Y., Investigation on the geomagnetic rapid pulsation, Sci. Rep. Tohoku Univ. ser. 5, 11, suppl. pp. 28, 1959.

Kato, Y. and T. Watanabe, Studies on geomagnetic micropulsations, Sci. Rep. Tohoku Univ., ser. 5, 8, 111-132, 1957.

Kim. J. S. and B. W. Currie, Horizontal movements of aurora, Canadian Phys., 36, 160-170, 1958.

Kruskal, M. and M. Schwarzschild, Some instabilities of a completely ionized plasma, Proc. Roy. Soc. A, 223, 348-360, 1954.

Kupperian, J. E. Jr., E. T. Byram, T. A. Chubb, and H. Friedman, Far ultraviolet radiation in the night sky, Planet. Space Sci., 1, 3-6, 1959.

Leinbach, H., Private communication, 1960.

Leonard, R. S., A low power VHF radar for auroral research, Proc. IRE, 47, 320-322, 1959.

Leonard, R. S., Private communication, 1960.

Lindemann, F. A., Note on the theory of magnetic storms, Phil. Mag., 38, 669-684, 1919.

Little, C. G., The measurement of ionospheric absorption using extra-terrestrial radio waves, Annals of IGY, III, Part II, p. 207, Pergamon Press, 1957.

Little, C. G. and H. Leinbach, Some measurements of high-latitude ion-ospheric absorption using extraterrestrial radio waves, Proc. IRE, 46, 334-348, 1958.

Livingston, M. S., High-energy Accelerators, Interscience Pub. Inc., New York, 1954.

Lundquist, S., On the stability of magneto-hydrostatic fields, Phys. Rev., 83, 307-311, 1951.

Maeda, H., The vertical distribution of electrical conductivity in the upper atmosphere, J. Geomag. Geoelec. 5, 94-104, 1953.

Maeda, H., Wind systems for the geomagnetic Sd field, J. Geomag. Geoelec., 9, 119-121, 1957.

Maeda, H., On the geomagnetic Sd field, J. Geomag. Geoelec., 10, 66-68, 1959.

Malville, J. M., Antarctic auroral observations, Ellsworth Station, 1957, J. Geophys. Res., 64, 1389-1393, 1959a.

Malville, J. M., Type B aurora in the Antarctic, J. Atmosph. Terr. Phys., 16, 59-66, 1959b.

Martyn, D. F., The theory of magnetic storms and auroras, Nature, 167, 92-94, 1951.

Martyn, D. F., Electric currents in the ionosphere, III Ionization drift due to winds and electric fields, Phil. Trans. Roy. Soc. A, 246, 306-320, 1953.

Matsushita, S., On sudden commencements of magnetic storms at high latitudes, J. Geophys. Res., 62, 162-166, 1957.

Mayer, P., E. N. Parker, and J. A. Simpson, Solar cosmic rays of Feb. 1956 and their propagation through interplanetary space, Phys. Rev., 104, 768-783, 1956.

McDonald, K. L., Topology of steady current magnetic fields, Amer. J. Phys., 22, 586-596, 1954.

McIlwain, C. E., Direct measurement of protons and electrons in visible aurorae, Dept. Phys. Astr., State Univ. Iowa, SUI 59-29, 1959.

McIlwain, C. E., Direct measurements of particles producing visible auroras, J. Geophys. Res., 65, 2727-2747, 1960.

McNish, A. G., Sudden commencements at Watheroo, Comptes Rendus Assemblée de Lisbonne, 1933, IATME (now IAGA) Bull. No. 9.

Meinel, A. B., On the entry into the earth's atmosphere of 57 kev protons during auroral activity, Phys. Rev., 80, 1096-1097, 1950.

Meredith, L. H., M. B. Gottlieb, and J. A. Van Allen, Direct detection of soft radiation above 50 kilometers in the auroral zone, Phys. Rev., 97, 201-205, 1955.

Meredith, L. H., L. R. Davis, J. P. Heppner, and O. E. Berg, Rocket auroral investigations, IGY Rocket Rep. No. 1, Nat. Acad. Sci. USA, 1958.

Montalbetti, R., Photoelectric measurements of hydrogen emissions in aurorae and airglow, J. Atmosph. Terr. Phys., 14, 200-212, 1959.

Moos, N. A. F., Colaba Magnetic Data; Part II, The phenomenon and its discussion, Bombay, 1910.

Morrison, P., Solar origin of cosmic-ray time variations, Phys. Rev., 101, 1397-1404, 1956.

Morrison, P., On the origin of cosmic rays, Rev. Mod. Phys., 29, 235-243, 1957.

Murcray, W. B., Some properties of the luminous aurora as measured by a photoelectric photometer, J. Geophys. Res., 64, 955-959, 1959.

Nagata, T., Distribution of SC^* of magnetic storms, Rep. Ionosphere Res. Japan, 6, 13-30, 1952.

Nagata, T. and S. Abe, Notes on the distribution of SC^* in high latitudes, Rep. Ionosphere Res. Japan, 9, 39-44, 1955.

Newton, H. W., "Sudden commencements" in the Greenwich magnetic records (1879-1944) and related sunspot data, Mon. Not. R. Astr. Soc. Geophys. Suppl., 5, 159-185, 1948.

Nichols, B., Auroral ionization and magnetic disturbances, Proc. IRE, 47, 245-254, 1959.

Northrop, T. G. and E. Teller, Stability of adiabatic motion, Phys. Rev., 117, 215-225, 1960.

Obayashi, T. and J. A. Jacobs, Sudden commencements of magnetic storms and atmospheric dynamo action, J. Geophys. Res., 62, 589-616, 1957.

Obayashi, T. and J. A. Jacobs, Geomagnetic pulsations and the earth's outer atmosphere, Geophys. J., 1, 53-62, 1958.

Oguti, T., Notes on the morphology of SC, Rep. Ionosphere Res. Japan, 10, 81-90, 1956.

Omholt, A., Photometric observations of rayed and pulsating aurorae, Astrophys. J., 126, 461-462, 1957.

Onwumechilli, C. A., A study of the equatorial electrojet-II. A model electrojet that fits H-observations, J. Atmosph. Terr. Phys., 13, 235-257, 1959.

Oort, J. H. and Th. Walraven, Polarization and composition of the Crab nebula, Bull. Astr. Inst. Netherlands, 12, 285-308, 1956.

Oort, J. H., F. J. Kerr, and G. Westerhout, The galactic system as a spiral nebula, Mon. Not., R. Astr. Soc., 118, 379-389, 1958.

Parker, E. N., Hydromagnetic dynamo models, Astrophys. J., 122, 293-314, 1955.

Parker, E. N., On the goemagnetic storm effect, J. Geophys. Res., 61, 625-637, 1956.

Parker, E. N., Newtonian development of the hydromagnetic properties of ionized gases of low density, Phys. Rev., 107, 924-933, 1957.

Parker, E. N., Interaction of the solar wind with the geomagnetic field, Phys. Fluid, 1, 171-187, 1958a.

Parker, E. N., Dynamics of the interplanetary gas and magnetic fields, Astrophys. J., 128, 664-676, 1958b.

Parker, E. N., Origin and dynamics of cosmic rays, Phys. Rev., 109, 1328-1344, 1958c.

Parker, E. N., Plasma dynamical determination of shock thickness in an ionized gas, Astrophys. J., 129, 217-223, 1959a.

Parker, E. N., The hydrodynamic treatment of the expanding solar corona, Astrophys. J., 132, 175-183, 1960.

Pease, R. S., Electrodynamic Phenomena in Cosmic Physics, (ed. Lehnert,B.) Camb. Univ. Press, 1958.

Petschek, H. E., Aerodynamic dissipation, Rev. Mod. Phys., 30, 966-974, 1958.

Piddington, J. H., Solar atmospheric heating by hydromagnetic waves, Mon. Not., R. Astr. Soc., 116, 314-324, 1956.

Piddington, J. H., Interplanetary magnetic field and its control of cosmic-ray variations, Phys. Rev., 112, 589-596, 1958.

Piddington, J. H., The transmission of geomagnetic disturbances through the atmosphere and interplanetary space, Geophys. J., 2, 173-189, 1959.

Piddington, J. H., Geomagnetic storm theory, J. Geophys. Res., 65, 93-106, 1960.

Pope, J. H., An estimate of electron densities in the exosphere by means of nose-whistlers, J. Geophys. Res., 65, 67-75, 1961.

Rees, M. H., Private communication, 1960.

Rees, M. H. and G. C. Reid, The aurora, the radiation belt and the solar wind: A unified hypothesis, Nature, 184, 539-540, 1959.

Rees, M. H., A. E. Belon, and G. J. Romick, The systematic behaviour of hydrogen emission in the aurora, I. Planet. Space Sci., (in publication).

Reid, G. C. and C. Collins, Observations of abnormal VHF radio wave absorption at medium and high latitudes, J. Atmosph. Terr. Phys., 14, 63-81, 1959.

Reid, G. C. and M. H. Rees, The systematic behaviour of hydrogen emission in the aurora, II., Planet. Space Sci., (in publication).

Roach, F. E. and E. Marovich, A monochromatic low-latitude aurora, J. Res. Nat. Bureau of Standards (D), 63D, 297-301, 1959.

Roach, F. E. and M. H. Rees, The absolute zenith intensity of (OI) 5577 at College, Alaska, J. Geophys. Res., 65, 1489-1493, 1960.

Rodes, L., Periodo diurno--an les perturbaciones subitas, Terr. Mag., 37, 273-277, 1932.

Romick, G. J. and C. T. Elvey, Variations in the intensity of the hydrogen emission line H$_\beta$ during auroral activity, J. Atmosph. Terr. Phys., 12, 283-287, 1958.

Rosen, A., T. A. Farley, and C. P. Sonett, Soft radiation measurements on Explorer VI Earth Satellite, IGY Satellite Rep. No. 11, Nat. Acad. Sci. USA, 1960.

Rosenbluth, M. N. and C. L. Longmire, Stability of plasma confined by magnetic fields, Ann. Phys., 1, 120-140, 1957.

Rothwell, P. and C. E. McIlwain, Magnetic storms and the Van Allen radiation belts: Observations from Satellite 1958 (Explorer IV), J. Geophys. Res., 799-806, 1960.

Schmidt, A., Erdmagnetismus, Enzyklopädie der mathematischen Wissenschaften, Band VI, Leipzig, 1917.

Shain, G. A., The inclination to the galactic equator of the general magnetic field of the Galaxy in the solar vicinity, Soviet Astronomy, 1, 1-8, 1957.

Shklovski, I. S., The interplanetary medium and some problems of the physics of the upper atmosphere, Soviet Astronomy, 2, 516-527, 1958.

Siedentopf, H., A. Behr, and H. Elsässer, Photoelectric observations of the zodiacal light, Nature, 171, 1066-1067, 1953.

Singer, S. F., A new model of magnetic storms and aurorae, Trans. Amer. Geophys. Union, 38, 175-190, 1957.

Sonett, C. P., E. J. Smith, D. L. Judge, and P. J. Coleman, Jr., Current systems in the vestigial geomagnetic field: Explorer VI, Phys. Rev. Letter, 4, 161-163, 1960.

Spitzer, L. Jr., Equations of motion for an ideal plasma, Astrophys. J., 116, 299-316, 1952.

Störmer, C., The Polar Aurora, Oxford Univ. Press, 1955.

Storey, L. R. O., An investigation of whistling atmospherics, Phil. Trans. Roy. Soc., A, 246, 113-141, 1954.

Stratton, J. A., Electromagnetic Theory, McGraw-Hill Book Co., Inc., New York, 1941.

Sugiura, M., Electromagnetic induction in the ionosphere, Rep. Ionosphere Res. Japan, 3, 65-72, 1949.

Sugiura, M., The solar diurnal variation in the amplitude of sudden commencements of magnetic storms at the geomagnetic equator, J. Geophys. Res., 58, 558-559, 1953.

Sugiura, M. and S. Chapman, The average morphology of geomagnetic storms with sudden commencement, Abhandlungen der Akad. Wiss. in Göttingen, Math.-Phys. Klasse, 1960.

Thomas, J. O. and A. Robins, The electron distribution in the ionosphere over Slough, J. Atmosph. Terr. Phys., 13, 131-139, 1958.

Van Allen, J. A., Direct detection of auroral radiation with rocket equipment, Proc. Nat. Acad. Sci. Wash., 43, 57-62, 1957.

Van Allen, J. A., The geomagnetically-trapped corpuscular radiation, J. Geophys. Res., 64, 1683-1689, 1959.

Van Allen, J. A. and F. A. Frank, Survey of radiation around the earth to a radial distance of 107,400 kilometers, Nature, 183, 430-434, 1959.

Van Allen, J. A., C. E. McIlwain, and G. H. Ludwig, Satellite observations of electrons artificially injected into the geomagnetic field, J. Geophys. Res., 64, 877-891, 1959.

Van Allen, J. A. and W. C. Lin, Outer radiation belt and solar proton observations with Explorer VII during March-April, 1960.

Van de Hulst, H. C., The electron density of the solar corona, Bull. Astr. Inst. Netherlands, 11, 135-160, 1950.

Vegard, L., Hydrogen showers in the auroral region, Nature, 144, 1089-1090, 1939.

Vernov, S. N., A. E. Chudakov, E. V. Grochakov, J. L. Logadiev, and P. V. Vakulov, Study of the cosmic-ray soft component by the 3rd Soviet earth satellite, Planet. Space Sci., 1, 86-93, 1959.

Vernov, S. N., A. E. Chudakov, P. V. Vakulov, and Yu. I. Logachev, Study of terrestrial corpuscular radiation and cosmic rays during flight of the cosmic rocket, Dokalady Akad. Nauk SSSR, 125, 304-307, 1959.

Vestine, E. H., Disturbance field of magnetic storms, Trans. Wash. Assem. 1939. Pub. IATME Bull. No. 11, 360-381, 1940.

Vestine, E. H., The geographic incidence of aurora and magnetic disturbance, northern hemisphere, Terr. Mag., 49, 77-102, 1944.

Vestine, E. H. and E. J. Snyder, The geographic incidence of aurora and magnetic disturbance, southern hemisphere, Terr. Mag., 50, 105-124, 1945.

Vestine, E. H., Winds in the upper atmosphere deduced from the dynamo theory of geomagnetic disturbance, J. Geophys. Res., 59, 93-128, 1954.

Vestine, E. H. and W. L. Sibley, Remarks on auroral isochasms, J. Geophys. Res., 64, 1338-1339, 1959.

Vestine, E. H. and W. L. Sibley, The geomagnetic field in space, ring currents, and auroral isochasms, J. Geophys. Res., 65, 1967-1979, 1960.

Watson, K. M., Use of the Boltzmann equation for the study of ionized gases of low density I, Phys. Rev. 102, 12-19, 1956.

Watson, R. A. and D. H. McIntosh, Sudden commencements in geomagnetism, Nature, 165, 1018, 1950.

Webster, H. F., Breakup of hollow electron beams, J. Appl. Phys., 26, 1386-1387, 1955.

Webster, H. F., Structure in magnetically confined electron beams, J. Appl. Phys., 28, 1388-1397, 1957.

Wentworth, R. C., W. M. MacDonald, and S. F. Singer, Lifetimes of trapped radiation belt particles determined by Coulomb scattering, Phys. Fluid, 2, 499-509, 1959.

Wild, J. P., Radio observations of solar flares, Trans. IAU, 9, 661-663, 1955.

Wild, J. P., Spectral observations of solar activity at meter-length, Radio Astronomy, IAU Symposium No. 4, (ed. Van de Hulst), Camb. Univ. Press, 1957.

Winckler, J. R., L. Peterson, R. Arnoldy, and R. Hoffman, X-rays from visible aurorae at Minneapolis, Phys. Rev., 110, 1221-1231, 1958.

Winckler, J. R., L. Peterson, R. Hoffman, and R. Arnoldy, Auroral X-rays, cosmic rays, and related phenomena during the storm of February 10-11, 1958, J. Geophys. Res., 64, 597-610, 1959.

Winckler, J. R., Balloon study of high-altitude radiations during the International Geophysical Year, J. Geophys. Res., 65, 1331-1359, 1960.

Wulf, O. R., On the relation between geomagnetism and the circulatory motions of the air in the atmosphere, Terr. Mag., 50, 185-197, 259-278, 1945.

Wulf, O. R., On the production of glow discharges in the ionosphere by winds, J. Geophys. Res., 58, 531-538, 1953.

Yamaguchi, Y., Si phenomenon, Mem. Kakioka Mag. Obs., 8, 33-40, 1958.